Riadh Dhaou
André-Luc Beylot
Marie-José Montpetit
Daniel Lucani
Lorenzo Mucchi (Eds.)

123

Personal Satellite Services

LNICST

5th International ICST Conference, PSATS 2013
Toulouse, France, June 2013
Revised Selected Papers

Lecture Notes of the Institute
for Computer Sciences, Social Informatics
and Telecommunications Engineering 123

Riadh Dhaou André-Luc Beylot
Marie-José Montpetit Daniel Lucani
Lorenzo Mucchi (Eds.)

Personal Satellite Services

5th International ICST Conference, PSATS 2013
Toulouse, France, June 27-28, 2013
Revised Selected Papers

Springer

Volume Editors

Riadh Dhaou
IRIT-ENSEEIHT, 31071 Toulouse, France
E-mail: riadh.dhaou@enseeiht.fr

André-Luc Beylot
IRIT-ENSEEIHT, 31071 Toulouse, France
E-mail: beylot@enseeiht.fr

Marie-José Montpetit
MIT, Cambridge, MA 02139, USA
E-mail: mariejo@mit.edu

Daniel Lucani
Instituto de Telecommunicações, Porto 4200-465, Portugal
E-mail: daniel.lucani@fe.up.pt

Lorenzo Mucchi
University of Florence, 50139 Florence, Italy
E-mail: lorenzo.mucchi@unifi.it

ISSN 1867-8211 e-ISSN 1867-822X
ISBN 978-3-319-02761-6 e-ISBN 978-3-319-02762-3
DOI 10.1007/978-3-319-02762-3
Springer Heidelberg New York Dordrecht London

Library of Congress Control Number: 2013950911

CR Subject Classification (1998): C.2, H.4, J.1, J.2, C.4

Typesetting: Camera-ready by author, data conversion by Scientific Publishing Services, Chennai, India

Printed on acid-free paper

Springer is part of Springer Science+Business Media (www.springer.com)

Preface

It is our pleasure to welcome you to the 5th International Conference on Personal Satellite Services (PSATS) held in Toulouse, France during 27–28 June 2013.

Technology advances in communications together with changes in the regulatory framework are paving the way for next generation satellite systems. Broadband on the move, improved spectrum efficiency, flexible payloads are the keywords. These evolutions foster advances both for the end-users and the satellite operators, yielding opportunities for new value-added services including those that blur the frontiers between Earth observation, telecommunications and positioning. The legacy role of satellite communication as bearer of broadband and broadcast services is also confirmed as the need for global multimedia distribution rises.

In addition to that, the gap between terrestrial and the so-called space communication technologies is getting narrower. The space segment is now the natural bridge among heterogeneous networks providing flexible capacity wherever and whenever needed.

The Personal Satellite Service conference, confirms through its 5th edition that there is a need for a scientific forum where these evolutions are prepared. The conference provides a multifaceted floor for technology and networking where all R&D actors including academic and industrial researchers, practitioners, and students can meet and discuss. In organizing PSATS 2013, we were delighted to work with a dedicated team of volunteers whose efforts ensured a strong two day programme. The tireless work of these volunteers helped to ensure that PSATS continues to be a reputed conference in the area. We are grateful to the TPC chairs Dr Marie-Josée Montpetit (Cambridge MA, USA) and Dr. Daniel Lucani (Instituto de Telecommunicacoes Porto, Portugal). Thanks to their efforts, PSATS has a strong and focused technical programme. PSATS 2013 has 18 regular papers, 3 tutorials and 3 demos in diverse topics under Personal Satellite Services. The Technical Programme Committee of PSATS 2013 deserves a special mention, since their efforts have lead to a selective and strong technical programme. We thank the industrial chair Mr. Nicolas Chuberre (Thales Alenia Space, France), publicity chair Prof. Laurent Franck (Télécom Bretagne, Institut Mines Télécom, France), demos and tutorial chairs Dr. Emmanuel Dubois (CNES, France) and Dr. Fabrice Arnal (Thales Alenia Space, France), publications chair Dr. Lorenzo Mucchi (University of Florence, Italy), local organising chair Dr. Emmanuel Chaput (IRIT-ENSEEIHT, France). We are grateful to the web chair Dr. Julien Fasson (IRIT-ENSEEIHT, France) for a high quality and superb website. We are particularly grateful to the conference coordinator Ms Erica Polini (EAI, Italy). Her timely feedback and suggestions has ensured the organization of this two day program. We thank the venue manager and conference coordinator Ms. Elisa Mendini (EAI, Italy). Lastly, we are grateful to

the Steering Committee and the Advisory Committee for their support to the conference.

PSATS 2013 is proud to welcome Mr. Hugo Gonzales Perez, the programme officer for broadband and mobile initiatives at CNES (Centre National des Etudes Spatiales, France), as our keynote speaker. He will set the tone of the topic during the two days of the conference, with a special focus on new challenges for satellite communications.

PSATS 2013 includes three tutorials by experts in the area. The first tutorial, in the networking domain, entitled "Emergency Communications" is offered by Prof. Laurent Franck, Telecom Bretagne, France. The second tutorial, in the telecommunication domain, entitled "Advanced Techniques for Foward Error Correction for Future Satellite Systems" is presented by Prof. Jérôme Lacan, ISAE, France. The third tutorial entitled "Advanced Access & Networking Techniques for Future Aeronautical Systems Aided by Satellite" is offered by Mr. Christian Kissling, scientific researcher working in the Institute of Communications and Navigation at the German Aerospace Center (DLR), Germany. We sincerely hope that the delegates will find the state-of-the-art tutorials useful.

PSATS 2013 also included a panel discussion session of the topic: "Hybrid Satellite/Terrestrial Networks". This session aims at discussing the most interesting scenarios combining satellite and terrestrial network technologies in the context of the future 5G network infrastructure. This session will bring in the view of the satellite operators, satellite research centres, SMEs and universities on the future role of satellite communications in our everyday life. We would also like to thank all the members of the panel session, and all the student volunteers of PSATS 2013.

PSATS has traditionally received strong support from industry over the years. This year as well, our corporate sponsors, have generously supported us with funds that enable us to hold a high quality conference. We thank our sponsors: ICST, Centre National des Etudes Spatiales (CNES, France), Institut National Polytechnique de Toulouse (INPT, France), Institut National de Recherche en Informatique (IRIT, France) and ASI, Italy. for their generous financial support. We thank Thales Alenia Space (TAS, France) for the technical support.

We thank all the authors and speakers for their technical contributions and the attendees for their participation. Given the excellent technical program and the hard work put in by all the organizers, we are sure that you will all have an intellectually stimulating and enjoyable PSATS 2013. We wish you a pleasant stay in Toulouse, France and we hope you will greatly enjoy the conference!

June 2013

Riadh Dhaou
André-Luc Beylot

Organization

Program Committee

Carlos Aguilar	XLIM, France
Paolo Barsocchi	ISTI-CNR, Italy
Matteo Berioli	German Aerospace Center (DLR), Germany
Carlo Caini	University of Bologna, Italy
Nedo Celandroni	ISTI-CNR, Italy
Bernhard Collini-Nocker	University of Salzburg, Austria
Michaël Crosnier	ASTRIUM, France
Haitham Cruickshank	University of Surrey, UK
Philip A. Dafesh	The Aerospace Corporation, USA
Franco Davoli	CNIT, Italy
Vincent Deslandes	EADS-Astrium, France
Roberto Di Pietro	University of Rome, Italy
PFabio Dovis	Politecnico di Torino, Italy
Alban Duverdier	CNES, France
Benoit Escrig	IRIT, France
Gorry Fairhurst	University of Aberdeen, UK
Julien Fasson	IRIT, France
Carles Fernandez-Prades	CTTC, Spain
Alberto Gotta	ISTI-CNR, Italy
Gentian Jakllari	IRIT, France
Igor Kotenko	SPIIRAS, Russia
Ajay Kulkarni	Cisco Systems, USA
Michele Luglio	University of Roma2, Italy
Muriel Medard	Cambridge MA, USA
Maria Luisa Merani	University of Modena & Reggio Emilia, Italy
Gabriele Oligeri	ISTI-CNR, Italy
Athanasios Panagopoulos	ICCS-NTUA, Greece
Charly Poulliat	IRIT, France
Anand Prasad	NEC Corporation, Japan
Jose Radzik	ISAE, France
Patrice Raveneau	IRIT, France
Cesare Roseti	University of Rome, Italy
Renaud Sallantin	IRIT, France
Raffeallo Secchi	University of Aberdeen, UK
Aaditeshwar Seth	IIT Delhi, India
Petia Todorova	Fraunhofer Institut FOKUS, Germany
Alexey Vinel	SPIIRAS, Russia

Conference Organization Credits

Steering Committee

Imrich Chlamtac	Create-Net, Italy
Kandeepan Sithamparanathan	RMIT, Australia
Agnelli Stefano	ESOA/Eutelsat, France
Mario Marchese	University of Genoa, Italy

Advisory Committee

Giovanni Giambene	University of Siena, Italy
Fun Hu	University of Bradford, UK
Vinod Kumar	Alcatel-Lucent, France

General Chairs

Riadh Dhaou	IRIT-ENSEEIHT, France
André-Luc Beylot	IRIT-ENSEEIHT, France

Industrial Chair

Mme Isabelle Buret	Thales Alenia Space, France

Publicity Chair

Laurent Franck	Telecom Bretagne, France

Demos and Tutorial Chairs

Emmanuel Dubois	CNES, France
Fabrice Arnal	Thales Alenia Space, France

Publications Chair

Lorenzo Mucchi	University of Florence, Italy

Local Organising Chair

Emmanuel Chaput	IRIT-ENSEEIHT, France

Conference Coordinators

Erica Polini	EAI, Italy

Website Chair

Julien Fasson	IRIT-ENSEEIHT, France

TPC Chairs

Marie-Josee Montpetit	Cambridge MA, USA
Daniel Lucani	Instituto de Telecommunicacoes Porto, Portugal

Technical Program Committee

Carlos Aguilar	XLIM, France
Paolo Barsocchi	ISTI-CNR, Italy
Matteo Berioli	German Aerospace Center (DLR), Germany
Carlo Caini	University of Bologna, Italy
Nedo Celandroni	ISTI-CNR, Italy
Bernhard Collini-Nocker	University of Salzburg, Austria
Michaël Crosnier	ASTRIUM, France
Haitham Cruickshank	University of Surrey, UK
Philip A. Dafesh	The Aerospace Corporation, USA
Franco Davoli	CNIT, Italy
Vincent Deslandes	EADS-Astrium, France
Roberto Di Pietro	University of Rome, Italy
Fabio Dovis	Politecnico di Torino, Italy
Alban Duverdier	CNES, France
Benoit Escrig	IRIT, France
Gorry Fairhurst	University of Aberdeen, UK
Julien Fasson	IRIT, France
Carles Fernandez-Prades	CTTC, Spain
Alberto Gotta	ISTI-CNR, Italy
Gentian Jakllari	IRIT, France
Igor Kotenko	SPIIRAS, Russia
Ajay Kulkarni	Cisco Systems, USA
Michele Luglio	University of Roma2, Italy
Muriel Medard	Cambridge MA, USA
Maria Luisa Merani	University of Modena & Reggio Emilia, Italy
Gabriele Oligeri	ISTI-CNR, Italy
Athanasios Panagopoulos	ICCS-NTUA, Greece
Charly Poulliat	IRIT, France
Anand Prasad	NEC Corporation, Japan
Jose Radzik	ISAE, France
Patrice Raveneau	IRIT, France
Cesare Roseti	University of Rome, Italy
Renaud Sallantin	IRIT, France
Raffeallo Secchi	University of Aberdeen, UK
Aaditeshwar Seth	IIT Delhi, India
Petia Todorova	Fraunhofer Institut FOKUS, Germany
Alexey Vinel	SPIIRAS, Russia

Table of Contents

Satellite for Emergency and Aerocommunication

Satellite for networking

Resource Management

Air Interface

DTN LEO Satellite Communications through Ground Stations and GEO Relays

Pietrofrancesco Apollonio[1], Carlo Caini[1], and Martin Lülf[2]

[1] DEI, Department of Electrical, Electronic, and Information Engineering "Guglielmo Marconi", University of Bologna, Italy
[2] Department of Electrical Engineering and Information Technology, Technische Universität München, Germany
pietro.apollonio@studio.unibo.it, carlo.caini@unibo.it, martin.luelf@tum.de

Abstract. LEO satellites are characterized by intermittent connectivity with their ground stations. Contacts are short and separated by long intervals, which with urgent data can become a critical factor. To solve this problem, the use of GEO satellites as relay has recently been suggested. This solution is appealing, but has some limits, especially with polar orbits, as the link between the LEO satellite and the GEO relay is affected by long disruptions over polar regions. Moreover, the bandwidth available may be limited and difficult to fully exploit. In this paper, we show that GEO relays are complementary rather than alternative to ground stations, and that the enabling technology for their combined use is DTN (Delay-/Disruption- Tolerant Networking) architecture and related protocols, including CGR (Contact Graph Routing). To demonstrate this, a series of experiments carried out on a testbed running ION, the NASA implementation of the DTN protocols and CGR, is discussed in the paper.

Keywords: Delay-/Disruption- Tolerant Networking (DTN), Satellite Communications, GEO relays, Earth Observation, Bundle Protocol, CGR.

1 Introduction

LEO (Low Earth Orbit) satellites are characterized by a much shorter distance from Earth than GEOs have (LEOs 160 - 2000 km; GEOs, 36000 km). This short distance is essential in Earth observation and it offers the additional advantages of lower path loss and shorter propagation delay. However, because of the low orbital height, LEO satellites move fast in the sky, as seen by a terrestrial observer, and can be in Line Of Sight (LOS) with a ground station for only a few minutes each contact. While a LEO satellite moves along its orbit, the Earth rotates around its polar axis, which is an advantage for Earth observation, as different regions are covered by the same satellite at each orbital period, but also implies that a LEO satellite does not pass over the same ground station every orbital period.

To quantify the time connectivity of a LEO, let us focus on a typical Earth observation satellite. Assuming an orbital height of 700 km, we have a period of about 100 min and contact lengths of roughly 10 min. Although the minimum time interval between consecutive contacts is one orbital period, it is generally longer,

R. Dhaou et al. (Eds.): PSATS 2013, LNICST 123, pp. 1–12, 2013.

depending on the orbit of the satellite and the latitude of the ground station. In order to provide a global coverage, the orbit has to be polar or close to polar. In such a case, for a ground station close to the pole we have a contact each orbit, while moving towards the equator we have groups of a few consecutive contacts (one at each orbit), separated by much longer intervals.

By contrast to GEO satellites, which have usually continuous connectivity, the link between a LEO and a ground station is characterized by short contacts separated by long intervals. The channel is therefore intermittent, but known a priori, because related to the deterministic satellite and Earth motion. This kind of connectivity, which can be suitably classified as scheduled intermittent, cannot be tackled by ordinary TCP/IP protocols, but can be easily handled by DTN (Delay-Disruption-Tolerant Networking) [1], [2], [3], [4]. In fact, apart from the much shorter propagation delay, it is the same kind of intermittent connectivity as in deep space networks, for which DTN was conceived [5]. Using DTN architecture and protocols in LEOs was actually suggested in the original DTN standardization document [1] and some preliminary experiments on a real LEO constellation have been successfully carried out [6]. This has also been investigated by some of the present authors [7], [8], [9], and is also suggested here, where, however, a more complex scenario is involved.

For some applications (e.g. disaster monitoring, military observation) the variable but generally long delay between data creation and data availability at the LEO control centre is a clear disadvantage. A partial remedy is the use of multiple ground stations. A more radical and innovative solution is using a GEO satellite, or a GEO constellation, as a relay, as suggested in [10], [11], [12]. In particular, in [12] Inmarsat promotes the use of its Inmarsat-4 GEO satellite constellation and the BGAN ground network to establish bi-directional near-continuous IP connectivity between a LEO satellite, its control centre and remote users. Although appealing, this solution too is not problem free: LEO-GEO connectivity is not continuous, but more precisely scheduled intermittent, at least for LEOs on polar orbits, because of the GEOs well-known inability to cover polar regions.

In this paper, after carefully examining the pros and cons of the two connectivity solutions (ground station or GEO relay), we conclude that they are complementary rather than alternative. The aim of this paper, and its most important contribution, is thus to show that this cooperative use is possible and that the enabling technology is that of DTN and its related protocols, including CGR (Contact Graph Routing) [13].

To this end, after two introductory sections devoted to DTN and ION (the BP and CGR implementation developed by NASA) [14], [15], we study the concurrent transmission of both bulk data (e.g. images) and “streaming-like” data (e.g. telemetry) from a LEO satellite connected via both one ground station and a GEO relay. The results of a series of tests on a virtual testbed, running the GNU/Linux operating system and ION, are then presented and thoroughly analyzed.

2 A Brief Overview of the DTN Architecture

The BP DTN architecture is based on the introduction of the new “Bundle layer” [1] between Application and lower layers (usually Transport). The corresponding protocol (the BP) [2] is in charge of the transmission of “bundles” (large packets of data) between DTN nodes. The BP layer is inserted on not only source and

destination, but also on some intermediate nodes, as shown in Fig. 1, thus dividing the end-to-end path into many DTN hops (three in the figure). The BP interfaces with lower layers through "Convergence Layer Adapters" (CLAs), such as those for TCP, UDP, the Licklider Transmission Protocol (LTP) [16], [17] or Saratoga [18]. In the DTN architecture, transport protocol end-to-end features are now confined to one DTN hop, while end-to-end communication through multiple DTN hops is provided by the bundle layer, which acts as a store-and-forward overlay.

2.1 DTN Overlay

In a heterogeneous network, the intermediate DTN nodes are usually chosen at the border of each homogeneous network segment (A, B and C in Fig. 1) [7]. In this way on each DTN hop it is possible to use the best suited transport protocol (or more generally, protocol stack). For example, LTP can be used on a satellite segment and TCP on terrestrial ones. In this respect, DTN recalls TCP splitting PEPs, widely used on commercial GEO systems to cope with the long RTT. In [7] it was shown that the DTN architecture, applied to GEO satellite communications, can be actually be considered as an evolution of TCP-splitting PEPs.

2.2 BP Store-and-Forward and Custody Option

The transmission of bundles is based on store-and-forward. If the link to the next "proximate" node is not available, bundles received must be locally stored even for relatively long periods of time. This is essential to cope with disruption and intermittent connectivity.

To make bundle delivery still more reliable, the custody option can be set. In this case the application on the source node asks the bundle protocol of all DTN nodes on the path to take "custody" of the bundle by setting a bit in the bundle header. A DTN node may or may not accept custody of the incoming bundle, i.e. the task of bundle retransmission and reliable delivery to another "custodian" or to destination. If it accepts, it must notify the previous custodian and store bundles on persistent memory (e.g. on hard disks), to increase robustness in case of reboots or hardware failure.

2.3 Scheduled Links and Licklider Transmission Protocol

Scheduled links allow the convergence layer to open and close connections at exactly the beginning and end of known contacts, thus maximizing link usage efficiency. They are particularly useful when contacts are short, as here between the LEO sat and the ground station. Note, however, that at present this feature is supported in ION only by the LTP convergence layer. LTP provides retransmission-based reliability over point-to-point links with extremely long RTT and/or frequent disruption, and so is suitable as DTN convergence layer in space environments [16], [17]. Here, we will use LTP on the satellite links for the following reasons: resilience to long RTTs (useful for the connection via the GEO relay), possibility of matching the available bandwidth (LTP is rate controlled), and compatibility with scheduled links and CGR. Saratoga, which could be used in alternative to LTP as in [6], has not been considered here because it has not been openly released yet.

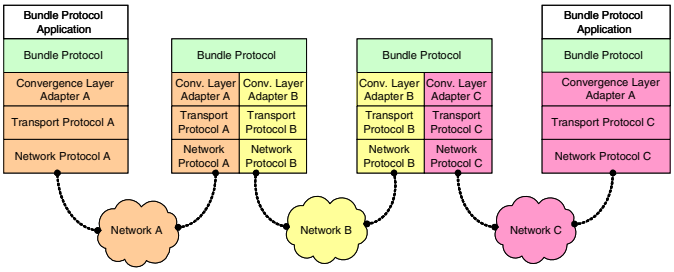

Fig. 1. DTN Bundle Protocol architecture and protocol stack

3 ION (Interplanetary Overlay Network)

ION is the DTN BP implementation developed by NASA JPL (Jet Propulsion Laboratory), with the contributions of Ohio and other Universities [14]. It is open source, available for GNU/Linux (and other platforms) [15], and is partially interoperable with DTN2, the BP reference implementation [19]. ION has been preferred here because it includes CGR, LTP and scheduled links.

3.1 Contact Graph Routing

CGR is a dynamic routing algorithm for DTN networks characterized by intermittent scheduled connectivity [13]. In these environments communication between DTN nodes is possible only during "contact windows". Each contact offers the opportunity to transfer a limited amount of data. Its maximum is the "contact volume", given by the product of the Tx rate and the contact window. Contact periods and Tx rates are summarized in a "contact plan", assumed to be known a priori, because dependent on either DTN node motion or scheduled bandwidth allocation. On each node the CGR uses the information contained in the contact plan to find the most suitable path from source to destination, following a complex algorithm, which has recently been updated. The key points are the following.

- Each node implementing CGR has in principle a global knowledge of contacts; however, in practice it may be useful (as will be shown later), to eliminate superfluous information in the contact plan for a specific node.
- For each bundle, CGR computes the full route to destination and selects "the best" path; however, this only determines the most suitable "proximate" DTN node.
- The route is computed at each node implementing CGR, either at bundle creation (for the source) or at bundle arrival (for intermediate nodes).
- Routes are always recomputed for each new bundle, or in case of re-transmission, to cope with network dynamics.
- There are backoff mechanisms in case a bundle cannot be transferred because of some sort of impairment.
- Static routes may integrate CGR, but only if CGR is unable to find a route (either because no suitable contacts or no information about a node in the contact plan).

- CGR can compute route to destination for nodes included in the contact plan, while non-included nodes can be reached through gateway nodes.
- The criteria for "best" route selection may vary. In the latest ION releases the "best" path is that which provides the shortest "expected delivery time" [15].
- CGR takes bundle priorities into account.
- CGR path computation considers data already scheduled for transmission to "proximate" nodes (like seats booked on a flight), but not on successive hops. More generally, congestion control in DTN is a complex problem [20].

4 LEO Communications through a GEO Constellation and a Ground Station

In our scenario, a LEO satellite for Earth observation is connected to its control centre by two possible paths: via one ground station, or via a GEO satellite constellation, acting as a relay. The two solutions are not alternative, but complementary, as we want to show. More specifically, our aim is to prove that, thanks to the ION CGR, the two paths can be pooled and shared dynamically by different kinds of BP traffic. In particular, we will show that it is neither necessary nor advantageous to reserve one path statically for a single kind of traffic (e.g. telemetry vs. images).

4.1 DTN Topology and Protocol Stack

Our satellite communications scenario consists of five DTN nodes (Fig. 2): a LEO satellite, a ground station used by LEO, a LEO Control Centre, a GEO control centre and a final user. Note that the GEO relay is not in the figure because it is transparent to BP traffic (it is not a DTN node). Intermittent satellite links are denoted by dotted lines, terrestrial wired links by continuous ones. To cope with intermittency, the LTP convergence layer is used on both satellite links. By contrast, as terrestrial hops are continuous, the TCP convergence layer is more suitable. We consider the transfer of both telemetry data and image files. The source for both is the LEO satellite, while the destination is LEO control centre for telemetry and the final user for images.

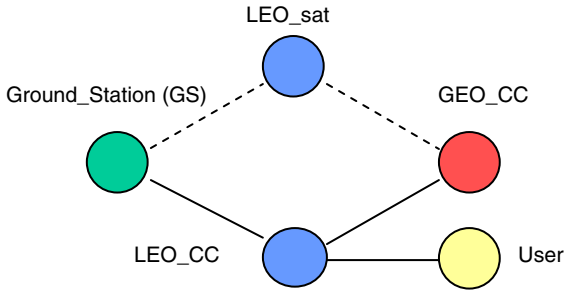

Fig. 2. Topology of the LEO-GEO scenario. Dotted lines: intermittent sat links (LTP); continuous lines: continuous terrestrial links (TCP).

4.2 Dual Characteristics of Satellite Sops: Time Availability and Bandwidth

For LEO and GEO satellites we want to adhere as closely as possible to [12]. For the LEO we consider the same orbital data (a height of 720 km and a quasi-polar sun-synchronous orbit, an orbital period of 100 min). A few integrations are however necessary, regarding the connection via the ground station, which was not considered there. We will also emphasize the duality of the two satellite hops.

LEO_sat-GEO_CC hop. In this case, the time availability is relatively high, roughly 70% of every orbital period, with two disruptions of approximately 15 min in correspondence to the poles (see Figure 7 of [12]). By contrast, the Tx rate is relatively low. We have the choice between two kinds of service. The "Standard IP" is best effort with a maximum of about 470 kb/s in each direction. However, the bandwidth is shared among all users of the same spot and, probably worse, variable in time, which could be problematic at Transport layer. The "Streaming IP", offers fixed rates in a range from 8 to 128 kb/s. We will use it assuming a fixed rate of 128 kbit/s.

LEO_sat-GS hop. This hop has opposite characteristics. Here, we assume a ground station far from the polar regions, with a contact window of 10 min. Moreover, for the sake of simplicity, we consider just one orbital period, in which we have one contact. We also assume a Tx rate of 10 Mbit/s, thanks to the low path loss.

4.3 CGR and Contact Plans

The characteristics of DTN hops are summarized in the LEO_sat contact plan given in Table I. The first row of the table, and the following three, represent also the only contact plan information that must be provided to GEO_CC and GS, respectively. Dummy contacts (i.e. contacts longer than the experiments) have been inserted for continuous links. Finally, no information about the LEO_CC-User link is given because irrelevant for LEO_sat (all bundles to the user must be routed to LEO_CC).

Table 1. LEO_sat Contact Plan. LEO_sat Contact Plan.

Link	*Contact#*	*Start-stop time (min)*	*Speed*	*Contact Volume*
LEO_sat-GS	1	45-55	10Mbit/s	750 MB
LEO_sat-GEO_CC	1	1-20	128kbit/s	19.2 MB
	2	35-70	128kbit/s	33.6 MB
	3	85-100	128kbit/s	14.4 MB
GS–LEO_CC	Dummy (TCP cont.)	1-200	10Mbit/s	
GEO_CC-LEO_CC	Dummy (TCP cont.)	1-200	10Mbit/s	

5 Experiments

All tests were carried out on a testbed consisting of five GNU/Linux virtual machines running ION 3.0.2. The experiments are presented in ascending order of complexity. For easier test execution, while link speeds are left unaltered, actual contact durations are scaled down by a factor 60 (s instead of min), and so contact volumes.

5.1 Streaming Traffic Only (TMTC)

We start by considering the transfer of "streaming" data generated at regular intervals on board the satellite, e.g. telemetry. We assume that a new bundle of 5 kB is generated every 5m in the real world, i.e. every 5s in our experiments. These bundles have a very high priority (more than "expedited", 2.2 in ION priority settings) and should be delivered to the LEO control centre as soon as possible, either through the GEO relay or through the ground station, the faster the better. The transfer must be reliable; therefore, the custody option is set. Results are presented in Fig. 3, which gives the time series of bundle generated ("src") and delivered ("dlv via GEO"). At the bottom of the graph the LEO_sat contacts are also shown.

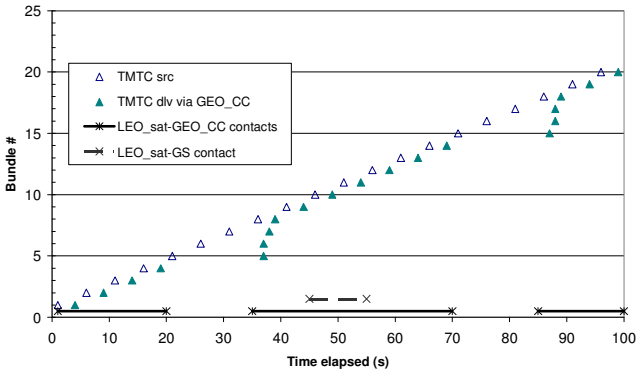

Fig. 3. Bundle Telemetry traffic (from LEO_sat to LEO_CC). Both GS and GEO links available.

At the beginning of the experiment, the LEO_sat-GEO_CC first contact is open and bundles are promptly delivered through it, as expected, until the first polar disruption occurs at 20s. Bundles generated during this disruption (bundles 5-7) cannot immediately be forwarded because there are no more contacts available. They are safely kept in custody on a local database, waiting for the next contact. After 15s the second LEO_sat-GEO_CC opens, and these bundles are promptly delivered to destination followed by new ones. Note that as the BP protocol (by contrast to TCP) does not enforce an ordered bundle delivery, waiting bundles are transmitted by LTP CL in parallel to reduce delay and to more efficiently exploit the bandwidth available.

As a result, bundles can be delivered slightly out of order (i.e. with minimal differences in delivery time). This sort of jitter is not relevant and has been deliberately filtered here, in the interest of result readability. Bundle transfer goes on regularly until the second polar disruption, and then until the end of the orbital period (100s). Note that for bundles generated during the LEO_sat-GS contact this additional path is also available, but never selected. This is because in case of parallel contacts CGR gives priority to the contact that starts first (and this even when both the contacts are already open, as here). Results show that DTN BP is able to promptly recover from disruption, as bundles generated during disruption are sent immediately after.

5.2 Data Only (Images)

We continue our analysis by considering the transfer of images data bundles from LEO_sat to User. In this case we assume that a burst of 20 bundles of 100 kB is generated during the first polar disruption, at 25s. They have low priority ("bulk", i.e. 0 in ION priority settings) and are addressed to the User node, which, however, can be reached only through LEO_CC, as before. After 5s, these bundles are followed by a high priority ("expedited", i.e. 2.1 in ION priority settings) bundle always of 100 kB, representing urgent sensor data (e.g. a high value target).

GS link only; both bulk and expedited bundles. Let us temporarily assume that the GEO relay is not present and that the only possibility is to use the LEO_sat-GS contact. Results are given in Fig. 4. All bundles are timely delivered through the LEO_sat-GS contact, which is the only one available, as soon as it opens. The relevant information for future comparisons is: the expedited bundle is delivered first, although generated last (apart from the usual jitter due to LTP parallel transfers); then, all bundles fit in this contact.

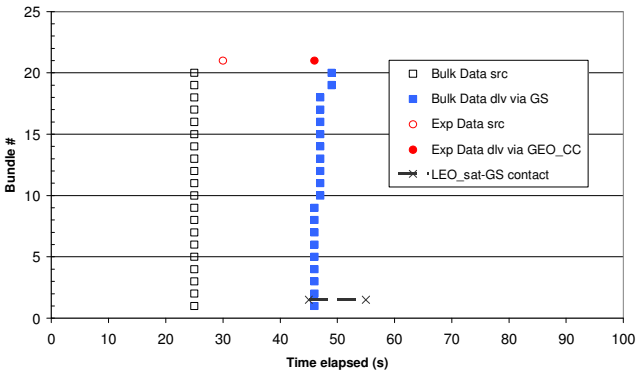

Fig. 4. Bundle Data traffic (from LEO_sat to User). GS link only; both bulk and expedited bundles.

GS and GEO links; bulk bundles only. We now re-insert the GEO-relay, so that all contacts are available again. However, we remove the expedited bundle. Results are given in Fig. 5, and are not as intuitive as before; it is necessary first to consider the peculiarities of DTN CGR routing. When a bundle is generated, CGR is invoked to find the "best" route for it, which can differ for each bundle to cope with link intermittency. To highlight this crucial point, we deliberately generated 20 bundles at the same time, addressed to the same destination, and with the same priority. Looking at results, we can see that the first 6 bundles are routed through the GEO-relay, the others through the ground station. This is due to the fact that the routing decision is taken bundle by bundle and that CGR gives priority to the contact that open first, i.e. the second LEO_sat-GEO_CC contact. However, when its residual volume has finished, this contact is no longer considered (like a "fully booked" flight), and the next bundles are routed on the next contact available, i.e. LEO_sat-GS. This very reasonable policy is however disturbed by the presence of nested contacts, as here. Although the overall result is satisfactory, as CGR has allowed the pooling of the two paths and all bundles are delivered in a reasonable time, we observe two sub-optimal results. First, the order of delivery is scrambled on a large scale (bundles 1 and 2 are delivered first; then 7-20, with 3 in parallel, finally 4-6); although this is compliant with BP rules, is not optimal. Second, bundles 4-6 could have been delivered earlier through the LEO_sat-GS contact.

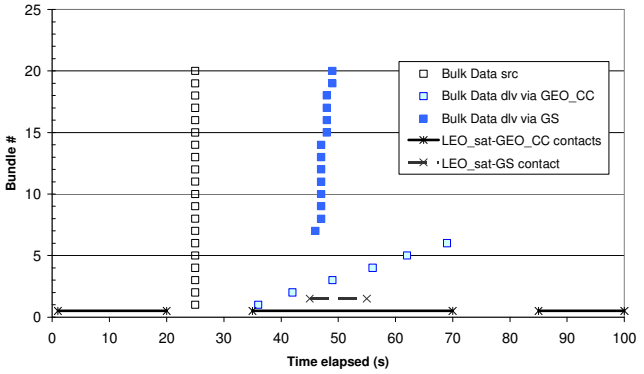

Fig. 5. Bundle Data traffic (from LEO_sat to User). Both GS and GEO links available; bulk bundles only.

Both GS and GEO links available; both bulk and expedited bundles. By re-inserting the expedited bundle into the latest scenario, we obtain the results given in Fig. 6. The good news is that the expedited bundle is delivered first, on LEO_sat-GEO_CC, although this contact was already "fully-booked" when it was routed. This positive result is expected, as CGR deliberately does not consider the volume allocated to lower priority bundles in checking the residual capacity. The bad news is that because of the insertion of the expedited bundle, bundle 6 cannot be transmitted, as it was supposed to be, before the closure of the second LEO_sat-GEO_CC contact,

and must be deferred to the third, after the second polar disruption. The sub optimality here is that when CGR "overbooks" the second LEO_sat-GEO_CC contact, the LEO_sat-GS contact still has a lot of residual capacity, and bundle 6 could have been re-allocated to it. Ironically, this bundle would have arrived earlier than expected! This suggests the insertion in CGR of an "overbooking" check, with a forced re-routing of lower priority bundles waiting to be forwarded on an "overbooked" contact.

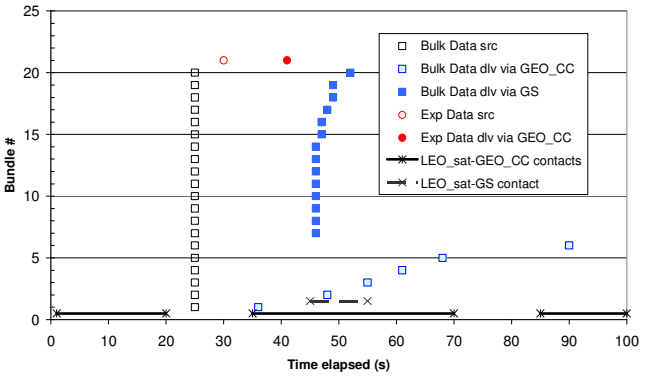

Fig. 6. Bundle data traffic (from LEO_sat to User). Both GS and GEO links available; both bulk and expedited bundles.

5.3 Telemetry and Images

In this last experiment, telemetry and images are generated in parallel, with all contacts available. Results are given in Fig. 7. The complexity of the results make it clear that the experiments presented so far were a necessary pre-requisite to the interpretation of these last results. There are few differences with respect to the merging of results for telemetry alone (Fig. 3) and images alone (Fig. 6). The most apparent is that now not only bundle 6, but bundle 5 too has also been deferred to the last contact; second, that telemetry bundle 14 has also been deferred; last, that telemetry bundle 20 is not delivered in the orbital period, but it is however delivered immediately after (not in the graph), so this last difference is of little significance. All can be explained on the basis of CGR behavior, as already discussed. The contact volume of the second LEO_sat-GEO_CC contact is allocated first to image bundles 1-6, which, however, have the lowest priority; then we have the allocation of the image expedited bundle, of higher priority; finally, we have the allocation of telemetry bundles generated during the first polar disruption and during the contact itself, with the highest priority. This double "overbooking" explains the deferred delivery of bulk bundles 5 and 6 and the deferred delivery of telemetry bundle 14, generated immediately before the closure of the contact, when LTP was already fully busy in the attempt to complete transfer of previous bundles.

From a general point of view, results are encouraging. They show that the two possible connections (via GEO relay and via ground station) can be pooled thanks to CGR (no need to reserve a path for a specific kind of traffic) and that priorities are easily enforced and generally respected. In fact, all high priority bundles are routed via GEO-relay not as a result of a fixed assignment, but because this route offers to them the fastest delivery in the scenario considered; conversely, bulk bundles can exploit the GEO-relay, but only when there is residual capacity available, otherwise are routed to the ground station.

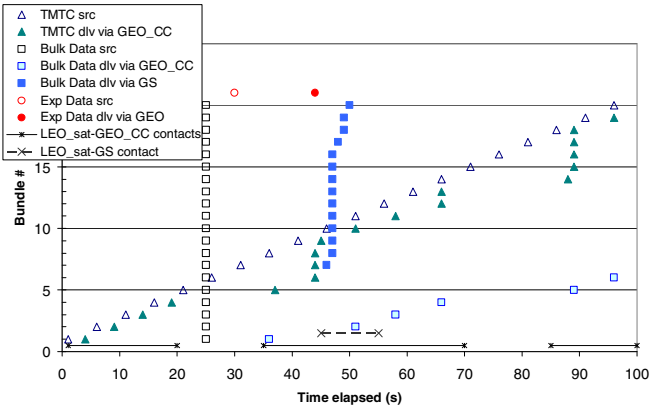

Fig. 7. Overall bundle traffic. Bundle telemetry (from LEO_sat to LEO_CC, always via GEO_CC) and Bundle data (from LEO_sat to User, either via GEO_CC or GS).

6 Conclusions

In this paper we have shown that GEO relays and ground stations complement each other and that DTN protocols and CGR routing are the enabling technology for their use in tandem. Considering the complexity of the scenario, the results are more than satisfactory. They show in particular that DTN BP is able to recover promptly from disruption, present on both satellite links, and that CGR allows different kinds of traffic, with different priorities, to share the paths dynamically, thus avoiding any fixed assignment. The comments to the results suggest some possible improvements to CGR congestion control. They also provide a comprehensive explanation of why the features peculiar to DTN so greatly contribute to the positive results achieved.

References

1. Cerf, V., Hooke, A., Torgerson, L., Durst, R., Scott, K., Fall, K., Weiss, H.: Delay-Tolerant Networking Architecture. Internet RFC 4838 (April 2007)
2. Scott, K., Burleigh, S.: Bundle Protocol Specification. Internet RFC 5050 (November 2007)

3. McMahon, A., Farrell, S.: Delay-, Disruption-Tolerant Networking. IEEE Internet Computing 13(6), 82–87 (2009)
4. Fall, K., Farrell, S.: DTN: an architectural retrospective. IEEE J. Select. Areas in Commun. 26(5), 828–836 (2008)
5. Burleigh, S., et al.: Delay-tolerant networking: An approach to interplanetary internet. IEEE Commun. Mag. 41(6), 128–136 (2003)
6. Ivancic, W., Eddy, W.M., Stewart, D., Wood, L., Northam, J., Jackson, C.: Experience with Delay-Tolerant Networking from Orbit. Int. J. Satell. Commun. Netw. 28(5-6), 335–351 (2010)
7. Caini, C., Cruickshank, H., Farrell, S., Marchese, M.: Delay-, Disruption-Tolerant Networking (DTN): An Alternative Solution for Future Satellite Networking Applications. Proceedings of IEEE 99(11), 1980–1997 (2011)
8. Caini, C., Firrincieli, R.: Application of Contact Graph Routing to LEO satellite DTN Communications. In: Proc. of IEEE ICC 2012, Ottawa, Canada, pp. 1–5 (June 2012)
9. Caini, C., Firrincieli, R.: DTN, satellite communications. In: Vasilakos, A., Zhang, Y., Spyropoulos, T. (eds.) Delay Tolerant Networks: Protocols, Applications, pp. 283–318. CRC Press, New York (2011)
10. Greda, A., Knupfer, B., Knogl, J.S., Heckler, M.V.T., Bischl, H., Dreher, A.: A multibeam antenna for data relays for the German communications satellite Heinrich-Hertz. In: Proc. of EuCAP 2010 Conf., pp. 1–4 (April 2010)
11. Katona, Z.: GEO Data Relay for Low Earth Orbit Satellites. In: Proc. of ASMS 2012 Conf., Baiona, Spain, pp. 81–88 (September 2012)
12. Johnston, B., Haslam, M., Trachtman, E., Goldsmith, R., Walden, H., McGaugh, P.: SB-SAT- Persistent Data Communication LEO Spacecraft via the Inmarsat-4 GEO Constellation. In: Proc. of ASMS 2012 Conf., Baiona, Spain, pp. 21–28 (september 2012)
13. Burleigh, S.: Contact Graph Routing, Internet-Draft (July 2010) (work-in-progress), http://tools.ietf.org/html/draft-burleigh-dtnrg-cgr
14. Burleigh, S.: Interplanetary Overlay Network (ION) an Implementation of the DTN Bundle Protocol. In: The Proc. of 4th IEEE Consumer Communications, Networking Conference, pp. 222–226 (2007)
15. ION code: http://sourceforge.net/projects/ion-dtn/
16. Ramadas, M., Burleigh, S., Farrell, S.: Licklider Transmission Protocol – Motivation. Internet RFC 5325 (September 2008)
17. Ramadas, M., Burleigh, S., Farrell, S.: Licklider Transmission Protocol – Specification. Internet RFC 5326 (September 2008)
18. Wood, L., Eddy, W., Smith, C., Ivancic, W., Jackson, C.: Saratoga: A Scalable Data Transfer Protocol. Internet draft, work-in-progress draft-wood-tsvwg-saratoga-12 (October 2012)
19. Internet Research Task Force DTN Reseach Group (DTNRG) web site: http://www.dtnrg.org/
20. Bisio, I., Cello, M., de Cola, T., Marchese, M.: Combined Congestion Control, Link Selection Strategies for Delay Tolerant Interplanetary Networks. In: IEEE GLOBECOM 2009, pp. 1–6 (2009)

Airborne Base Stations for Emergency and Temporary Events

Alvaro Valcarce[1], Tinku Rasheed[2], Karina Gomez[2], Sithamparanathan Kandeepan[3], Laurent Reynaud[4], Romain Hermenier[5], Andrea Munari[5], Mihael Mohorcic[6], Miha Smolnikar[6], and Isabelle Bucaille[7]

[1] TriaGnoSys GmbH, Wessling, Germany
alvaro.valcarce@triagnosys.com
[2] Create-Net, Trento, Italy
tinku.rasheed/karina.gomez@create-net.org
[3] RMIT University, Melbourne, Australia
kandeepan.sithamparanathan@rmit.edu.au
[4] Orange, Lannion, France
laurent.reynaud@orange.com
[5] German Aerospace Center, Germany
Romain.Hermenier/Andrea.Munari@dlr.de
[6] Jozef Stefan Institute, Ljubljana, Slovenia
miha.mohorcic/miha.smolnikar@ijs.si
[7] Thales Communications & Security, France
isabelle.bucaille@thalesgroup.com

Abstract. This paper introduces a rapidly deployable wireless network based on Low Altitude Platforms and portable land units to support disaster-relief activities, and to extend capacity during temporary mass events. The system integrates an amalgam of radio technologies such as LTE, WLAN and TETRA to provide heterogeneous communications in the deployment location. Cognitive radio is used for autonomous network configuration. Sensor networks monitor the environment in real-time during relief activities and provide distributed spectrum sensing capacities. Finally, remote communications are supported via S-band satellite links.

Keywords: Emergency, LTE, sensor networks, altitude platform.

1 Introduction

The rapid growth of bandwidth-hungry communication applications has put network operators under pressure to exploit the radio spectrum as efficiently as possible. Furthermore, recent events have shown that in the aftermath of an unexpected event, communication infrastructures play an important role in supporting critical services such as emergency recovery operations, infrastructure restoration, post-disaster surveillance, etc [1].

In this context, this paper considers the provision of rapidly deployable and resilient networks to provide Broadband access in large coverage areas. Current mission critical systems, including Public Protection and Disaster Relief (PPDR)

R. Dhaou et al. (Eds.): PSATS 2013, LNICST 123, pp. 13–25, 2013.

communication systems, are limited in terms of network capacity and coverage. They are not designed for or suitable to address large scale emergency communication needs in a disaster aftermath. PPDR systems are also limited by interoperability barriers, the technological gap with commercial technologies and evolving standards. Further, the terminals of first responders are getting smarter thanks to the introduction of new applications with integrated sensors and to the availability of multi-mode transceivers for supporting for example video conferencing, near-real-time video streaming and push-to-talk. Such improvements lead to an increase in capacity and energy demands at the terminals. Moreover, some events with large aggregation of professional and consumer users such as e.g. big sporting events or concerts require high capacity and/or dedicated coverage that the legacy terrestrial network infrastructure cannot rapidly provide.

Airborne communication networks have been recently studied for the provision of wireless communication services and have continually attracted interest from government, industry and academia [2]. Most of the original efforts focused on long endurance High Altitude Platforms (HAPs) [3] operating at altitudes of about 17-25 km. However, other types of airborne platform including aerostats and aerodynes, have been recently developed to fly at altitudes between a few dozen and a thousand meters. Those platforms, gathered under the denomination of Low Altitude Platforms (LAPs), are increasingly believed to complement conventional satellite or terrestrial telecommunications infrastructure. For example, the Deployable Aerial Communication Architecture (DACA) architecture proposed by the FCC in the US explores the feasibility of LAPs to be employed during emergency situations to restore critical communications [4].

In this paper, a holistic and rapidly deployable mobile network is presented. This is composed of a LAP-based airborne communications segment combined with a satcom-enabled Portable Land Rapid Deployment Unit (PLRDU). The solution, developed within the framework of the ABSOLUTE project [5], attempts to demonstrate the high-capacity, low-latency and large coverage capabilities of LTE-A for the provision of broadband emergency communications. In addition, the system integrates heterogeneous radio access technologies (i.e. LTE-A, TETRA, WLAN, S-band satellite links, etc) to fulfill coverage, data rate and latency requirements. Finally, technical challenges and methods for autonomous network reconfiguration in such scenarios are discussed.

2 Scenarios and Use Cases

The architecture described here is applicable to the event types described next.

2.1 Public Safety Communications

In the wake of a disaster, multiple PPDR agencies need to operate collaboratively on the rescue site using reliable and interoperable communication systems [6]. In this context, prominent services include first responder communications, critical infrastructure restoration support systems, post-disaster surveillance, medical

service networks, etc. However, preexisting networks may have been damaged or destroyed. For instance, base stations from cellular networks may have been hit by an earthquake or tsunami, as well as affected by power outages induced by multiple causes such as severe weather events, including floods and hurricanes [7].

Some disasters or emergency events may, to some extent, be anticipated. However, the degree of anticipation varies greatly, and generally remains very limited [8]. In any case, first responders rely on communication devices, equipped with multiple sensors and heterogeneous transceivers to support increasingly bandwidth-demanding applications, including real-time video streaming or exchanges of large amounts of data (e.g. high resolution images, environmental or medical monitoring). This puts a strong demand on the PPDR community for reliable and scalable communication infrastructures to provide network coverage, low delay and high capacity, as well as interoperability with legacy radio technologies. In the proposed system architecture, typical public safety applications can be supported such as Half-duplex video conferencing, near-real-time video streaming, bulk file transfer, e–mail, web, LTE Push-to-talk and VoIP [9].

2.2 Capacity Enhancements during Temporary Events

In recent years, mobile network access has grown in coverage and capacity, especially in densely populated regions. However, in less populated areas, access to high-speed mobile networks did not follow this trend. In fact, Mobile Network Operators (MNOs) now face the task of defining economically viable network architectures for the deployment of high-speed services in suburban or rural zones. Such architectures are not necessarily permanent and could be deployed only during demand peaks.

As a result, the organizers of mass events to take place in areas with limited network capacity need affordable solutions to provide connectivity to the temporary users, such as attendees and the organizers themselves. Such temporary service can be deployed to accommodate different events including outdoor gatherings, conference and seminars, construction sites, festivals and sporting events [10]. Communication solutions for these cases could lean upon temporary networks, such as the LAP-based one proposed in this paper, thus replacing or complementing preexisting network infrastructure.

3 Architecture

Figure 1 illustrates the proposed deployment architecture to provide emergency and temporary communications. This network needs to be resilient, supportive of broadband applications and secure. In addition, network service shall be tailored to the type of disaster or temporary event. Moreover, the architecture must support rapid configuration and deployment of the broadband network. This is achieved through the design of two tightly interconnected segments: an air segment, which consists of LAPs, and a terrestrial segment, enabled by multiple cooperating terrestrial equipments.

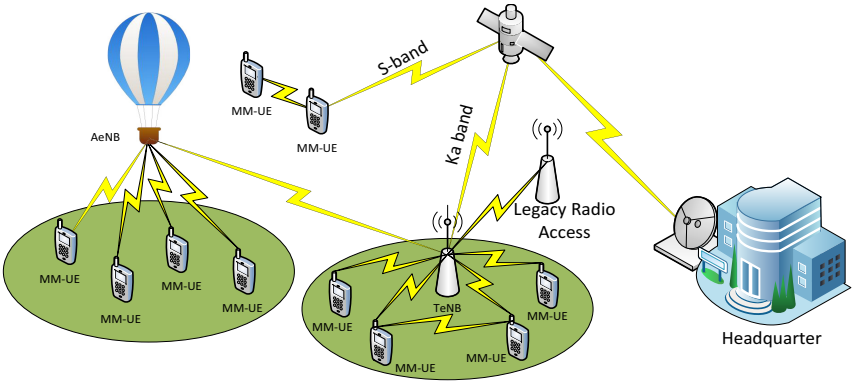

Fig. 1. Rapid deployment architecture for broadband access provision

(a) Airborne Helikite.

(b) Helikite resting on a Helibase.

Fig. 2. Low Altitude Platform

Several radio access technologies can be offered from the LAP. These shall be chosen based on the required coverage and capacity, as long as LAP payload constraints are respected (i.e. size, power consumption and weight, etc). Recent approaches were based on the use of IEEE 802.11 access points and on femtocells [11] to support communications with terrestrial User Equipments (UEs) and surviving Base Stations (BSs). In this project [5], the design and deployment of low-complexity eNodeBs is analyzed. In particular, the so-called Airborne eNodeB (AeNB) is embedded in each LAP's communications payload, with includes inter-LAP links, thus supporting reliable communications for emergency or temporary events. The air segment also supports dynamic spectrum access, therefore to gain awareness of existing terrestrial networks and provide seamless network reconfigurability and scalability. The terrestrial segment consists of nodes such as the PLRDUs and the Multimode User Equipments (MMUEs), which are explained in the next section.

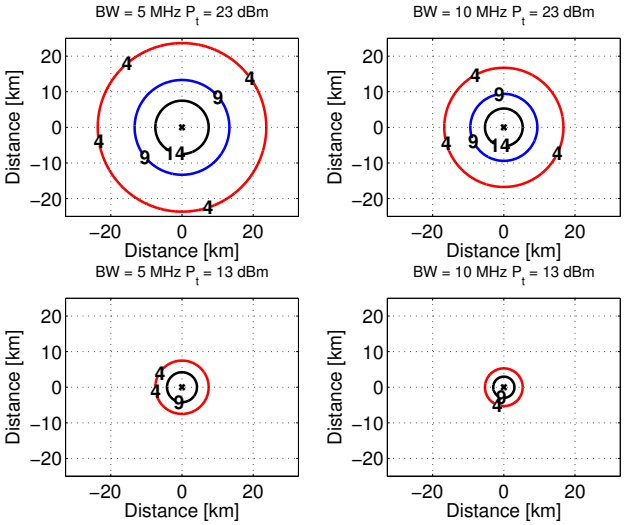

Fig. 3. Ground-level downlink SNR (dB) contours for an airborne LTE cell at 795.5 MHz and 300 m height. System parameters for these estimations are given in Table 1.

4 Subsystems

4.1 Low Altitude Platform (LAP)

The capabilities of the various interoperable nodes, which is explained next, turns the proposed network into a system that is more than the sum of its parts. As opposed to HAPs [3], a LAP is an airborne system capable of lifting communications equipment off the ground to heights between 300 m and 4 km. In the architecture described in this paper, the LAP is a lighter-than-air kite manufactured by Helikites [12] and known as a *Helikite* (see Figure 2(a)). The Helikite is an aerostat, thus relying on aerostatic lift to achieve buoyancy. It uses a helium-filled balloon to provide lift power, while the more aerodynamic kite provides stability against wind-caused drift. Additionally, the Helikite is tethered, which provides stability in changing winds. The Helikite has a lifting capacity of 10 kg and it can remain airborne for several days. However, climatological conditions may reduce its lifting capacity as well as its time aloft. When on the ground, the Helikite rests on an inflatable platform known as the *Helibase* (see Figure 2(b)) to prevent accidental punctures and to facilitate safe and rapid deployments.

When lifting an eNodeB, RF signals overcome most ground-level obstacles such as trees, buildings, hills, etc. This enables nearly all UEs to enjoy a line-of-sight (LOS) to the AeNB, thus increasing the coverage area. For example, considering LOS free space propagation, Figure 3 shows the cell sizes than can be achieved from an AeNB in the absence of cochannel interference. This is illustrated with SNR isolines, where the SNR is calculated in dB as

Table 1. System Parameters

Parameter	Fading margin	AeNB antenna gain	UE noise figure	UE antenna gain
Symbol	F	G_t	F_{UE}	G_{UE}
Value	4 dB	3 dBi	7 dB	0 dBi

$$SNR = P_r - N_{th} - F_{UE}, \tag{1}$$

being P_r the DL power received by the UE and calculated as

$$P_r = P_t + G_t - L_{fs} + G_{UE} - F. \tag{2}$$

Similarly, N_{th} is the thermal noise for a given system bandwidth BW in Hz at the standard temperature $T = 293.15$ K and calculated as $N_{th} = 10{*}\log_{10}(k_B{\cdot}T{\cdot}BW)$, where k_B is Boltzmann's constant in joules per kelvin. Furthermore, F_{UE} is the noise figure of the UE, P_t is the AeNB transmit power, G_t the antenna gain of the AeNB, L_{fs} the free space RF propagation losses, G_{UE} the UE antenna gain and F a fading margin. Finally, the calculations of Figure 3 use the values summarized in Table 1 and inspired by [13] for downlink LTE link budgets.

4.2 Portable Land Rapid Deployment Unit (PLRDU)

The PLRDU is a standalone and self-sufficient communications platform. It takes the form of a rugged suitcase (see Figure 4(a)) to accommodate systems such as a WLAN access point, a Terrestrial eNodeB (TeNB), a sensors gateway, an IP router, an interface to a TETRA system and a Ka band satellite modem. Additionally, the PLRDU also includes subsystems that support its main role as a communications platform. These are: batteries, power supply and a PC that controls all of the PLRDU functions. The PLRDU is designed to be easily transported to locations where a communications network is required. This enables wireless transmissions in the destination area, where local communications are piped through a router and remote communications through a satellite link.

Despite its ability for self sustainment and independence from the other subsystems, the PLRDU plays an integrating routing role within the larger system architecture. This is achieved through the Ka band satellite modem and the local IP router, that provide remote connectivity to the systems on board of the LAP. IP traffic is exchanged between the PLRDU and the LAP through means such as cabling (through the Helikite tether), WLAN or even optical radio links. The "LAP modem" in Figure 4(b) illustrates the heterogeneous nature of this link. Using the PLRDU to provide Internet and PSTN connectivity through satellite backhauling avoids the need for satellite modems on the LAP, whose lifting capacity is limited. Besides, orienting a satellite antenna from a balloon platform is more challenging than relaying the LAP traffic to the ground-based PLRDU.

4.3 Multimode User Equipment

As illustrated in Figure 1, MMUEs support LTE and TETRA radio interfaces for communicating within TeNB or AeNB coverage. In addition, direct reception of

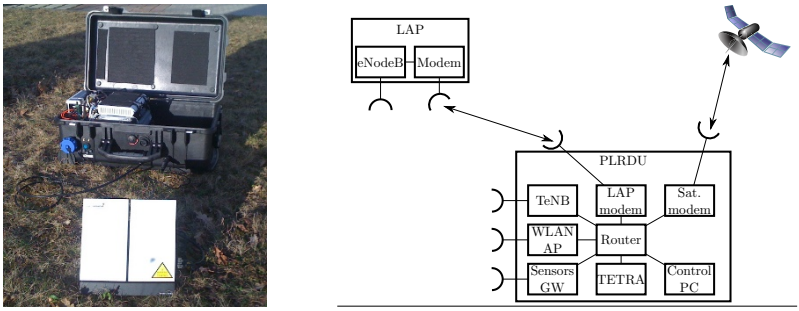

(a) Rugged suitcase. (b) Subsystems architecture.

Fig. 4. Portable Land Rapid Deployment Unit

narrowband broadcast satellite services in S-band are supported to guarantee the resilience of the network infrastructure. To meet the requirements of emergency recovery situations, the interoperability between infrastructure and proximity communications exploits the dynamic service discovery as well as the imposed energy constraints to maximize the overall system lifetime.

Apart from supporting the ubiquitous multi-mode high speed wireless broadband coverage, MMUEs also feature functionalities of sensor data fusion, localization and identification. In this respect sensors embedded in the handheld UE provide to the user and other members of the rescue team with context about the environment (e.g. temperature, humidity, luminosity, concentration of toxic or hazardous gases, etc). This information is mapped to the relative and/or absolute MMUE location (by means of GPS or ad hoc established infrastructure for localization exploiting triangulation principles), and movement (e.g. by means of accelerometer, electronic compass and gyroscope sensors). With respect to identification the capabilities of the system allow users to combine different parts in a virtual network. The main interfaces used for these purposes are RFID, NFC or special biometric sensors.

Wireless sensors in the form of body area networks can also be used in emergency scenarios to monitor the status of first responders. In such case a mobile sensor node can be used as a personal gateway between the UE and the body sensors. These can be used for monitoring heart beats, blood pressure, breathing, sweating, stress, presence and concentration of various gases, ambient temperature, spot temperature, radiation, etc. All of these can be embedded in the first responder's equipment or clothing.

Various radio interfaces in the MMUE can also be used for distributed monitoring of the radio environment and complemented by externally distributed spectrum sensing nodes (see section 5). This could be used to build radio environment maps and spectrum occupancy tables.

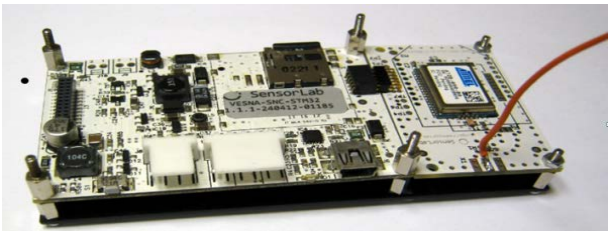

Fig. 5. VESNA wireless sensor gateway to be integrated into the PLRDU

4.4 Sensors Network

In a disaster-hit area, first responders rely on previously existing reports (if available) and on their own senses. In order to support planning activities and actions in the field, ad-hoc self-organizing sensor networks could play a role in monitoring the environmental conditions. Such networks would diminish risks for members of the rescue teams and gather real-time data to monitor the evolution of the disaster-relief activities.

The need for monitoring critical infrastructure and the operating environment where first responders work is addressed in this project by the development of scenario-tailored sensor modules. For example, specific modules are foreseen for flooding scenarios where water levels and flows need to be monitored. Similarly, earthquake scenarios would require of aftershock monitoring, sensing of infrastructure cracks. In nearly all disaster-hit scenarios, environmental conditions (weather, gas presence, etc) need to be monitored. Additionally, wireless sensors can be used for distributed spectrum sensing, which would support the constructions of environmental radio maps. This would support the set up of emergency communication systems in interference-free frequency bands.

The modules described above take the form of application specific expansion boards for sensor nodes based on the VESNA platform [14]. These sensor nodes are equipped with a radio interface, a battery and if necessary an energy harvesting module. They set up ad-hoc sensor networks and connect them to the sensor gateway in the PLRDU (see Section 4.2). Scenario-specific sensor modules thus represent the building blocks of the various scenario-specific VESNA deployments. Figure 5 illustrates the core module and radio boards of the VESNA gateway, which is to be integrated in the PLRDU.

It is important to note that this paper aims to present the overall concept of supporting emergency and temporary events in which also sensor networks play an important role, on one hand serving as environmental sensors supporting safe operation of rescue teams, and on the other hand when used as spectrum sniffers supporting operation of cognitive radio enabled communication equipment. Clearly, both uses will also affect the system capacity, the extent of this affect depending also on the number and type of sensors, and need to be taken into account in future work when we will look deeper into capacity issue.

4.5 Satellite Backhauling

One key feature of the presented architecture is its capacity for seamlessly resorting to satellite backhauling when necessary. Such an approach brings multifold benefits. On the one hand, the most cost effective User Plane (UP) traffic backhauling means can be dynamically chosen when the terrestrial communication infrastructure is unavailable (e.g. thus enabling communications with the safety operations control centre in case of disaster), or insufficient to cover traffic peaks(e.g. satisfying increased internet network demand during temporary events). On the other hand, the routing data through satellite links paves the way for the investigation and design of solutions which dynamically switch the backhauling strategy so as to maximize network capacity and performance.

The IP-based satellite link will provide UP traffic backhauling connectivity between the TeNBs, the Internet and the Public Switched Telephone Network (PSTN). This is achieved through a geostationary satellite operating in Ka band. The availability of satellite communications can also be exploited to establish Internet connections for the users. In this perspective, although resorting to LTE links when located in a LTE cell, MMUEs will use direct messaging services over satellite in S-band when outside of AeNB or TeNB coverage. Moreover, S-band enabled mobile terminals shall be used as relays in both forward and return link directions to provide limited services to citizens in the disaster area where the regular terrestrial networks are disrupted: broadcast (alert and information) in the forward link and messaging in the return link (for example distress).

5 Cognitive Communications in PPDR

There, where the existing communications infrastructure is damaged or malfunctioning, scalable and adaptable network architectures are needed. Cognitive radio technology [15] is regarded here as a candidate to provide such flexibility in temporary deployments. In cognitive radio, wireless nodes learn about the radio environment and adapt their transmissions to maximize spectral efficiency. This is done by implementing the cognitive cycle (see Figure 6).

The cognitive cycle includes the mapping of the radio environment, in which nodes learn about and create a radio map of their surroundings. This allows the nodes to take intelligent decisions at the radio level such as Dynamic Spectrum Access and Energy Efficient Communications. The environmental radio mapping includes *spectrum sensing* and the *localization* of nearby radio users.

Though multiple *spectrum sensing* techniques exist, it is generally challenging because other radios need to be reliably detected. This is especially difficult when radio users are far from the sensing node or undetectable, thus leading to the 'hidden node problem'. To address this, cooperative spectrum sensing is considered, in which various cognitive radio nodes share the collected information. *Localization* is even more challenging since the radio to be located does not necessarily cooperate. Therefore no prior knowledge exists to find it satisfactorily. To cope with this, blind techniques have also been proposed [17].

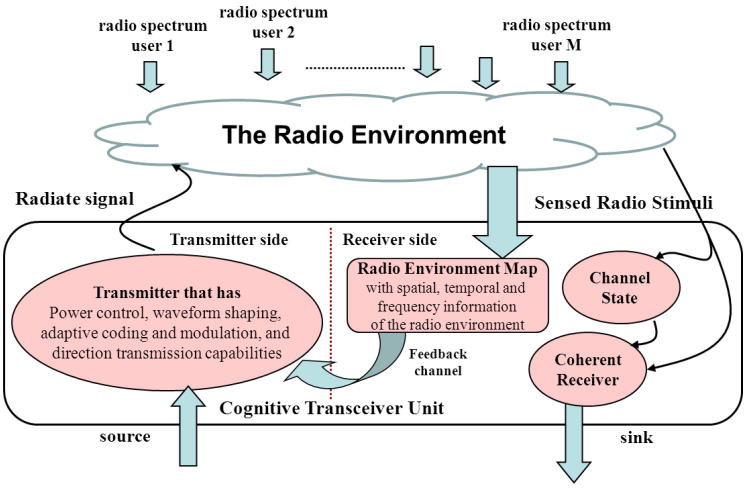

Fig. 6. Cognitive Cycle, as initially described by Mitola [15] and Haykin [16]

5.1 Cooperative Spectrum Sensing

Let there be K cognitive radio nodes, where each node senses alone and creates a test statistic ξ_k with $k = 1, 2 \dots K$ to detect the presence of a radio user. A local decision can be made based on a binary decision making criteria as,

$$d_k = \begin{cases} 1, & \text{if } \xi_k \geq \mu \\ 0, & \text{if } \xi_k < \mu \end{cases} \tag{3}$$

where, μ is the detection threshold. In cooperative sensing, the local decisions d_k or the test statistics ξ_k are sent to a central Cognitive Base Station (CBS), which collects the data and makes global decisions on behalf of the distributed radios and reports it to them. Through cooperative sensing the hidden terminal problem is greatly addressed. Let us consider next a cooperative sensing example based on local energy detection [18]. Let us assume the cognitive radio nodes send the local decisions d_k to the CBS where d_k are derived using energy test statistics ξ_k. If the CBS performs a fusion strategy $\Lambda(u_1, u_2 \dots u_k, \dots u_K)$ on the received data, and $u_k = d_k$, then the miss detection and false alarm probabilities for the corresponding detection mechanism are respectively given by,

$$P_{M,c} = \sum_{j=0}^{K-1} \frac{K!}{(K-j)!j!} P_D^j (1 - P_D)^{K-j} \tag{4}$$

$$P_{FA,c} = 1 - \sum_{j=0}^{K-1} \frac{K!}{(K-j)!j!} P_{FA}^j (1 - P_{FA})^{K-j}, \tag{5}$$

where P_D and P_{FA} are the detection and the false alarm probabilities for the local sensing performed at every cognitive radio node, assuming all the cognitive radio nodes have the same P_D and P_{FA} values, and $\Lambda(.)$ is a logical 'OR' function.

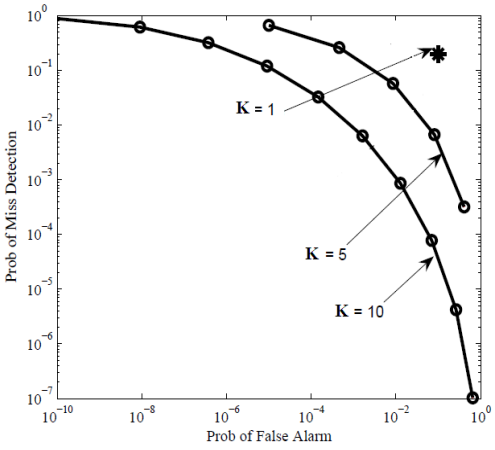

Fig. 7. Performance of a cooperative sensing scheme based on energy detection

Figure 7 depicts the Receiver Operating Characteristic (ROC) curves of the sensing scheme described above for various numbers of cooperative nodes. This illustrates that the detection performance increases with the number of cooperating nodes. This is also compared with the non-cooperative scheme (i.e one single node or $K = 1$). ABSOLUTE will research cooperative sensing schemes taking into account the features of the various radios (e.g. sensors and UEs).

5.2 Dynamic Spectrum Access and Management

Based on the collected information about the radio environment, the nodes can utilize the radio spectrum dynamically and opportunistically by either reducing interference to other radios or by avoiding interference themselves. The spectrum access strategies adopted in the network can be tailored to the specific requirements set by the network policies. In essence two types of dynamic access are considered in this project, 1) underlay spectrum access where cognitive radios share the spectrum simultaneously whilst keeping interference to any radio below the levels assigned by the regulatory bodies, 2) overlay spectrum access where cognitive radios utilize the spectral gaps opportunistically to transmit.

6 Conclusions

It has been highlighted, that during disasters or temporary events, communication networks play a supporting role and that new architectures are needed to provide flexible, scalable, resilient and secure broadband access.

Based on a rapidly deployable airborne platform with an embedded eNodeB, the ABSOLUTE system will quickly deploy mobile networks with large *local* coverage. This is thanks to the combination of multiple airborne, terrestrial and

satellite systems. The system can be deployed to support first responders communications, to support the restoration of critical infrastructure and to serve as temporary (main or complementary) high-capacity communication infrastructure for large-scale events. The architecture described is well suited for public safety applications and it will also allow operators to increase their capacity during specific events such as the Olympic Games. In this context, the following challenges still remain to be solved in order to achieve the above listed goals:

- Development of a standalone eNodeB that can be embedded in an a platform. Factors such as weight, size, temperature range of the 4G components as well as the antenna need to be considered in these aeronautical systems.
- Cooperative spectrum sensing techniques that guarantee network resilience.
- Design of a satellite backhauling solution capable of providing the necessary capacity while keeping the system's mobility.

Moreover, as future work, we are currently evaluating the impact of LAP altitude on the network performance, in terms of capacity and delay, for several services running on parallel such as half-duplex video conferencing and LTE Push-to-talk. Besides, we are also evaluating the most suitable techniques in order to optimize the ABSOLUTE system capacity for the network infrastructure deployed for supporting disaster-relief activities and extending capacity during temporary mass events.

Acknowledgement. This document has been produced in the context of the ABSOLUTE project. ABSOLUTE consortium wants to acknowledge that the research leading to these results has received funding from the European Commissions Seventh Framework Programme (FP7-2011-8) under the Grant Agreement FP7-ICT-318632.

References

1. Information and Communications in the Aftermath of the Great East Japan Earthquake, Ministry of Internal Affairs and Communications, Tech. Rep. (2011)
2. Reynaud, L., Rasheed, T.: Deployable Aerial Communication Networks: challenges for futuristic applications. In: 9th ACM International Symposium on Performance Evaluation of Wireless Ad Hoc, Sensor, and Ubiquitous Networks, PE-WASUN (October 2012)
3. Thornton, J., Grace, D., Spillard, C., Konefal, T., Tozer, T.: Broadband communications from a high-altitude platform: the European HeliNet programme. Electronics & Communication Engineering Journal, 138–144 (June 2001)
4. The Role of Deployable Aerial Communications Architecture in Emergency Communications and Recommended Next Steps, Federal Communications Comission (FCC), Tech. Rep., Washington (September 2011)
5. ABSOLUTE (Aerial Base Stations with Opportunistic Links for Unexpected and Temporary Events), `http://www.absolute-project.eu/`
6. Reinforcing the Union's Disaster Response Capacity, COM(2008) 130, European Commission Communication, Tech. Rep. (March 2008)

7. Reynaud, L., Rasheed, T., Sithamparanathan, K.: An integrated Aerial Telecommunications Network that supports emergency traffic. In: 14th Symposium on Wireless Personal Multimedia Communications, WPMC (October 2011)
8. Talbot, D.: 80 Seconds of Warning for Tokyo. MIT Technology Review (March 2011), http://www.technologyreview.com/news/423274/80-seconds-of-warning-for-tokyo/
9. Public Safety LTE, http://enterprise.alcatel-lucent.com
10. Hunter, J.: Telecommunications delivery in the Sydney 2000 Olympic Games. IEEE Communications Magazine (2001)
11. Goddemeier, N., Rohde, S., Pojda, D., Wietfeld, C.: Evaluation of Potential Fields Strategies for Aerial Network Provisioning. In: 2nd Workshop on Wireless Networking for Unmanned Autonomous Vehicles, Wi-UAV (December 2011)
12. Allsopp Helikites Limited, http://www.helikites.com
13. Holma, H., Toskala, A. (eds.): LTE for UMTS - OFDMA and SC-FDMA Based Radio Access. Wiley (2009)
14. VESNA (2011), http://sensorlab.ijs.si/hardware.html
15. Mitola, J., Maguire, G.Q.: Cognitive Radio: Making Software Radios More Personal. IEEE Personal Communications 6(4), 13–18 (1999)
16. Haykin, S.: Cognitive Radio: Brain-Empowered Wireless Communication. IEEE Journal on Seleted Areas of Communications 23(2), 201–220 (2005)
17. Mariani, A., Kandeepan, S., Giorgetti, A., Chiani, M.: Cooperative Weighted Centroid Localization for Cognitive Radio Networks. In: IEEE International Symposium on Communications and Information Technologies (ISCIT) (October 2012)
18. Kandeepan, S., Giorgetti, A.: Cognitive Radio Technqiues: Spectrum Sensing, Interefrence Mitigation and Localization. Artech House (October 2012)

A Realization of Integrated Satellite-Terrestrial Communication Networks for Aeronautical Services via Joint Radio Resource Management

Yongqiang Cheng, Kai J. Xu, Anju Pillai, Prashant Pillai,
Yim Fun Hu, Muhammad Ali, and Adeel Ahmed

Schools of Engineering Design and Technology, University of Bradford
Bradford, UK
{y.cheng4,k.j.xu,a.pillai,p.pillai,y.f.hu,m.ali70,
a.ahmed84}@bradford.ac.uk

Abstract. Despite air travel has not grown as predicted, air travel is still expected to rise to just less than doubling the current figure by 2030. This creates an urging need to develop more efficient Air Traffic Management (ATM) solutions. Around the globe, research and development initiatives have been launched to modernize the air traffic control infrastructures. These modernized infrastructures will be built around continuous information gathering, sharing and transferring of data between aircraft and air navigation service providers and airports ground infrastructure, which will be difficult for current aeronautical communications systems to handle. As a result, new communication infrastructures are required to manage future aeronautical communication traffic demand. This paper proposes an integrated aeronautical communication architecture consisting of four radio access technologies for communications between aircrafts and ground Aeronautical Telecommunication Network (ATN). The design and implementation of a Joint Radio Resource Management (JRRM) framework to manage these radio resources are discussed. The design is verified by a proof-of-concept JRRM prototype which is developed for the management of radio resource between the Inmarsat Broadband Global Area Network (BGAN) and the Aeronautical Mobile Airport Communication System (AeroMACS).

Keywords: Aeronautical Communication, Satellite-Terrestrial Communication, JRRM, Integrated Modular Radio.

1 Introduction

The continuous growth in air travel has resulted in an increasingly congested airspace. According to the EUROCONTROL forecast [1], the Instrument Flight Rules (IFR) flights in Europe will increase to 22 million in 2030, which is equivalent to 18 to 33 thousand more flights in the European network in one day than it is now. Despite air traffic has not grown as predicted since 2010 due to the economic recession, the impact of this short-term traffic downturn on the long term air traffic forecast is expected to be marginally down by 6% [2]. This prompts an urging need to develop more efficient Air Traffic Management (ATM) solutions around the globe. Research and development initiatives such as the EU

R. Dhaou et al. (Eds.): PSATS 2013, LNICST 123, pp. 26–37, 2013.

Single European Sky ATM Research (SESAR) project and the US Next Generation Air Transportation System (NextGen) have been launched to modernise the air traffic control infrastructure. It is envisaged that advanced ATM techniques and operations, automated airspace concept and intelligent decision support tools will be deployed in different stages between the next few years and the year 2020 and beyond. These advanced methods and tools will be built around continuous information gathering, sharing and transferring of data between aircraft and air navigation service providers and airports ground infrastructure.

However current aeronautical communications systems will be insufficient to handle the vast amount of information transfer created by these advanced ATM systems. As a result, new communication infrastructures are required to manage future aeronautic communication traffic demand and to provide an always-connected infrastructure for air-ground communication. According to the technology investigations carried out under the Action Plan 17 (AP17) of the EUROCONTROL-FAA Memorandum of Cooperation, the following three datalink systems are proposed as the air-ground communications [3] infrastructures:

1. A ground-based, high-capacity, airport surface datalink system, referred to as the Aeronautical Mobile Airport Communications System (AeroMACS);
2. A ground-based datalink system for continental airspace in general, referred to as the L-band Digital Aeronautical Communications System (LDACS);
3. A satellite-based datalink system for the oceanic, remote (deserted) and continental environment (in the latter case complementing the terrestrial systems).

While AeroMACS will be based on the IEEE802.16 WiMAX mobile communications standard in order to benefit from commercial general telecom developments and minimise the required development resources, further investigations have yet to be carried out to select and standardise the other two proposed systems.

To complement the study carried out by AP17, the EU FP7 project SANDRA (Seamless Aeronautical Networking through integration of Data links Radios and Antennas) [4] started in 2009 aims to design, specify and develop an integrated aircraft communication system that consists of VDL2, AeroMACS and two candidate satellite technologies, namely, Inmarsat BGAN and DVB-S2. The goal is to demonstrate the communication technologies and the flexibility, scalability, modularity and reconfigurability offered by the SANDRA system.

As a ‘system of systems’, SANDRA examines four integration levels, including:

1. Service integration of aeronautical communication service provision through the development of a middleware layer;
2. Network integration using the Internet Protocol (IP) as a unification technology;
3. Radio integration using software defined radio (SDR) technology to realise the physical and data link layers radio;
4. Antenna integration for the realisation of a dual L-Band and Ku-Band antenna.

From the communication architectural point of view, SANDRA spans across three segments, namely, the Ground Segment, the Transport Segment and the Aircraft Segment as shown in Figure 1.

The Aircraft segment consists of three main physical components: the Integrated Router (IR), the Integrated Modular Radio (IMR) and the Antennas. These three components form the SANDRA terminal.

In the Transport Segment, four different radio transport technologies are considered: VDL mode 2 [5] in VHF band, BGAN [6] in L-band, DVB-S2 [7] in Ku-band and AeroMACS[8].

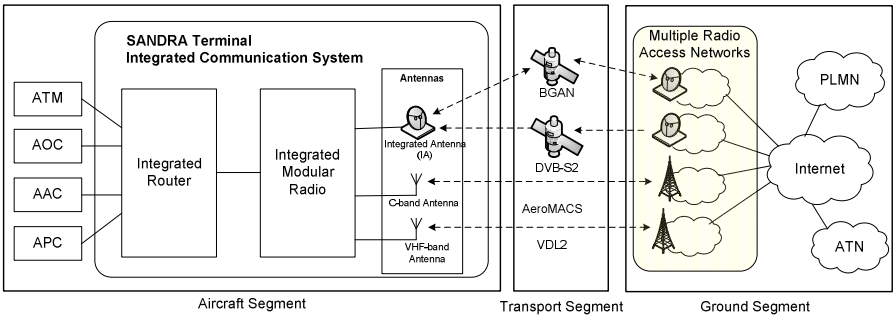

Fig. 1. SANDRA Communication Network Architecture

The Ground Segment consists of multiple Radio Access Networks (RANs) and their corresponding core networks of the radio transport technologies, the Aeronautical Telecommunication Network (ATN), the Internet and possibly the Public Land Mobile Network (PLMN), for passenger communications. The RANs can also be connected directly to the ATN and the PLMN on the ground. In order to provide mobility service and security services for aeronautical communications, functional components such as the mobility server, security and authentication server are required in the ground segment to provide corresponding mobility information services as well as security services. These components will be provided by the ATS, AOC, AAC and APC service providers of the ATN on ground.

The SANDRA scope focuses on the aircraft segments while making use of the existing transport and ground segments facilities. Authorities, such as the FAA, specify a minimum level of redundancy of equipment that must be operational before an aircraft is allowed to take off. The design should avoid single point of failure to meet the minimum level of the aeronautical aircraft equipment requirements; the size, complexity and cost in aircraft avionics equipments are highly constraint; the system should be able to manage radio resources whose availabilities will depend on different flight phases, i.e. AeroMACS will only be available when the airplane is on ground and taxing speed is less than a certain amount, e.g. 50 knot; the BGAN system will have the always available coverage but limited bandwidths.

To enable interoperability and to manage radio resources among heterogeneous radio links, this paper proposed a realization of joint radio resource management (JRRM) framework to allocate radio resources of the heterogeneous radio transport networks to different applications taking into consideration QoS and routing related parameters and in conjunction with the real-time link conditions and characteristics. A unified cluster of interface primitives[9] between different link layer technologies and the JRRM are defined by extending the MIH framework[9, 10]. Hence, the JRRM monitors and manages the resources available in the different radio links via the

unified interface to ensure that the application QoS/SLA requirements are met during connection establishment and the handover process. Sitting on top of the data link layer, the JRRM framework also provides the interface between the IP based network layer and lower layer protocol stacks.

In addition, the proposed JRRM is designed to have Master-Slave (1+1) redundancy capability which meets the minimum level of the aeronautical aircraft equipment requirements.

The primary focus of this paper is to report on the functional design, and software realization of the JRRM. A prototype implementation of the JRRM interfacing with AeroMACS and Inmarsat BGAN lower layer stacks and higher layer stacks is described and results obtained from the prototype are analysed.

The rest of the paper is organised as follows: Section two recalls the system architecture design from our previous work; Section three is the detailed design of the proof-of-concept test bed; experiment results and analysis are discussed in Section four. Our conclusion is given in section five.

2 JRRM System Architecture Design

Figure 2 shows the architecture of the JRRM described in [11, 12]. The JRRM, with its provision of adaptation functions and together with the link management functions, forms an Adaptation Layer between the higher network layer and the lower link layer. This Adaptation Layer is primarily required for RRM purposes. It hides the underlying complexities due to multiple radio protocol stacks from the network layer and provides a uniform interface to control the multiple radios.

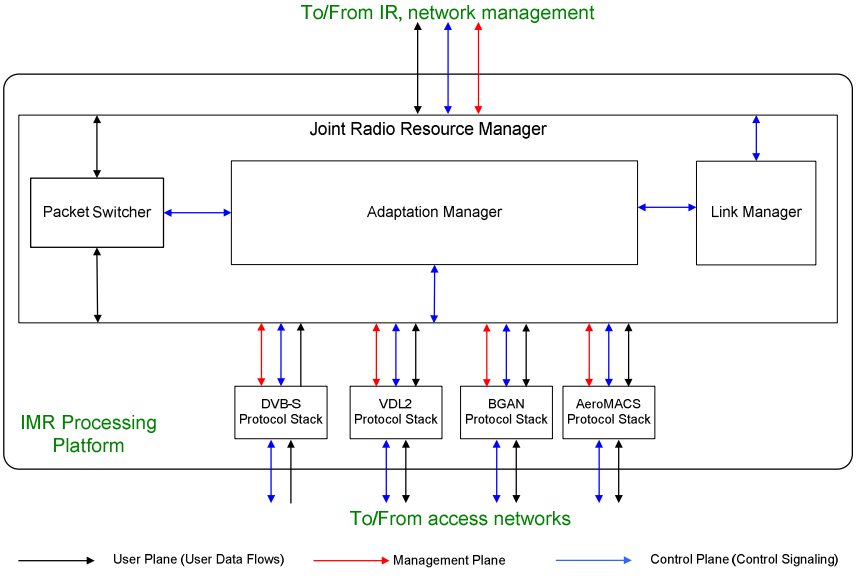

Fig. 2. JRRM Functional Architecture

The JRRM functional entities are further described below from the protocol stack perspective:

- *Link Manager (LM):* the Link Manager is a cross-layer entity performs network layer and link layer connection management, QoS management and mobility management in relation to admission control, packet scheduling and handover functions together with the Resource Manager (RM) in the IR.
- *Adaptation Manager (AM)*: The adaptation manager is primarily responsible for providing the various adaptation functions required for proper interfacing between the IR and the radio stacks.
- *Packet Switcher (PS):* The PS is responsible for switching data packets received from the IR in the user plane to the destined radio modules according to a packet switching table generated and passed by the address resolver in the AM during connection establishment. Sessions established between the higher layer IR and the Link layers are identified by Queue Identifiers (QIDs) which are mapped onto Link IDs and the link's specific connection IDs. And the mapping is synchronized and stored in PS. As a result, each data packet can be switched directly to the radio modules without passing through the AM in the user plane.

3 Proof of Concept Testbed Software Design

3.1 Software Architecture Design

Figure 3 depicts the proposed software architecture of the SANDRA terminal down to the Radio Stacks which makes use of the JRRM to integrate different radio technologies. Hardware nodes are represented by the grey boxes. As shown in the miniature figure of the SANDRA terminal, the IMR is built up by two identical IMR processing platforms. The JRRMs on the two platforms work in a Master-Slave configuration, whereby a hot swap can take place if the current master JRRM fails due to any hardware or software failure. These provide the reliability and redundancy feature that is critical for the aeronautical communication systems. The Master JRRM controls and manages the various radio links and control which radio link is loaded onto the processing platform. It can then establish connection over the links according to the various QoS requirements. Handover of connections from one link to another can then be performed if a radio link is lost.

The JRRM software consist several modules: the JRRM Manager module, the Link Manager module, the Packet Switcher module, the Adaptation Manager module, the JRRM health checker module, the Waveform Status Servo module and the Flight Status Detector module. The ***JRRM Manager Module*** reads and sets system settings of the radio technologies which can be used, handover strategies and policies etc.; Information fusion, radio link control, synchronizations between JRRMs and decisions making are carried out in the ***Link Manager Module***; the ***Packet Switcher Module*** is responsible for switching data packets between the radio technologies and the IR via tunnels created by the Virtual tunnel Manager application; the ***Adaptation Manager Module*** is primarily responsible for providing the various adaptation functions required for proper interfacing between the IR and different radio technologies; the ***Health Checker Module*** responses and monitors keep alive messages of the system to prevent itself being killed by the Supervisor application

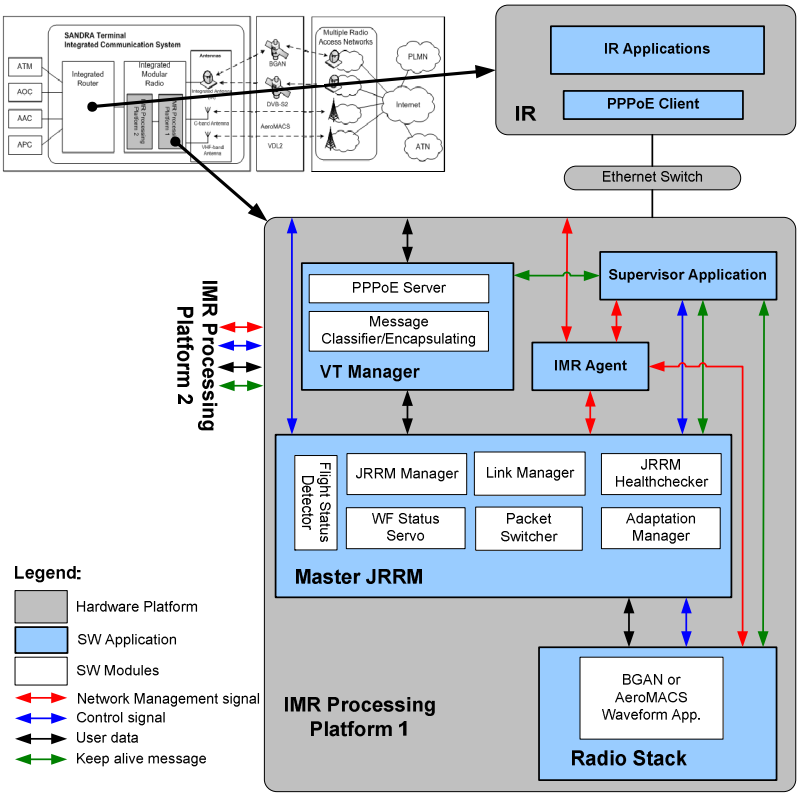

Fig. 3. Testbed Software Architecture

and decide whether a Master-Slave swap should be triggered; the ***WFStatus Servo Module*** is dedicated for managing the various waveform related processes such as loading or unloading of a waveform upon different flight status detected by the ***Flight Status Detector Module***.

In addition to the JRRM application, there are four other applications running on each IMR process platform to supporting the integration of the radio technologies:

- The Supervisor Application: This is responsible for launching the JRRM and the various waveforms. The JRRM can then tell the Supervisor Application which application to launch. If a waveform application goes down, the supervisor will inform the JRRM.
- The Virtual Tunnel (VT) Manager: This is a user plane entity responsible for carrying user traffic between the IR and the IMR. The IMR works as PPPoE server and the IR behaviour as PPPoE client. On one hand, the VT Manager receives and opens the user plane PPPoE packets sent by the IR and encapsulates the extracted IP packets in the SANDRA specific SAP messages and passes to the JRRM PS; on the other hand, the VT Manager processes the SANDRA messages and packets them as PPPoE session data to the IR.
- The Waveform application: In this paper, it can be either the BGAN or the AeroMACS radio protocol stacks.

- The IMR agent: This is a network management application which is responsible for collecting network management related information. It consists of three main parts: a management interface, a Management Information Base (MIB), and the core agent logic.

3.2 Detailed Design of JRRM Modules

To process multiple requests in parallel, the Link Manager is designed with multiple sub-link managers which are separate working threads, dedicated to process individual sessions. One session is identified by a queue identifier (QID). In case for the waveforms which do not support parallel requests, a mutex mechanism is designed. One type of radio has one mutex lock to keep all sub-link managers synchronized when processing link specific messages. Each sub link manager has a state machine as shown in Figure 4.

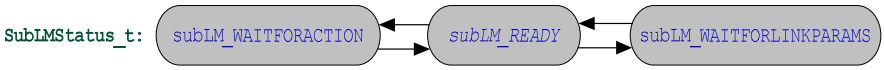

Fig. 4. Sub link manager state machine

When the sub-link manager is in the READY state, it can start processing new requests. When the sub link manager starts processing a request, it will enter the ACTION state and wait for confirmation messages. Either a timeout event or a confirmation can drive the sub link back to the READY state.

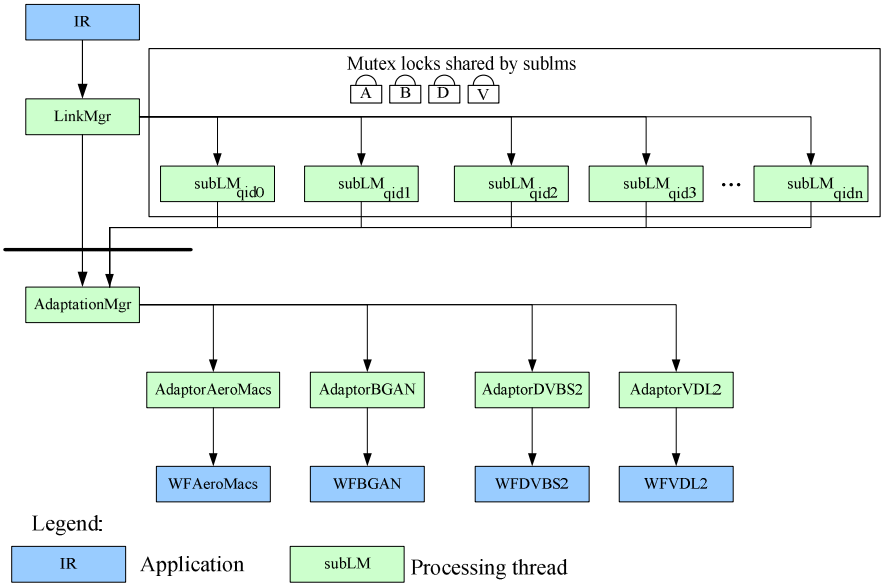

Fig. 5. JRRM return signal handling design

As shown in Figure 5, when the general Link Manager receives messages from the higher layer entity, the IR, it will forward all requests to the related sub-link managers. The sub-link manager will first try to get the locks of its links and perform the requests accordingly. As an exception, the sub-link manager 0 is not related to any connections. It is reserved for the Link Manager to process non-connection specific messages. For example if the Link Manager receives a Close request from the IR but the QID does not exist, then QID 0 will handle this message and sends an Error code to the IR.

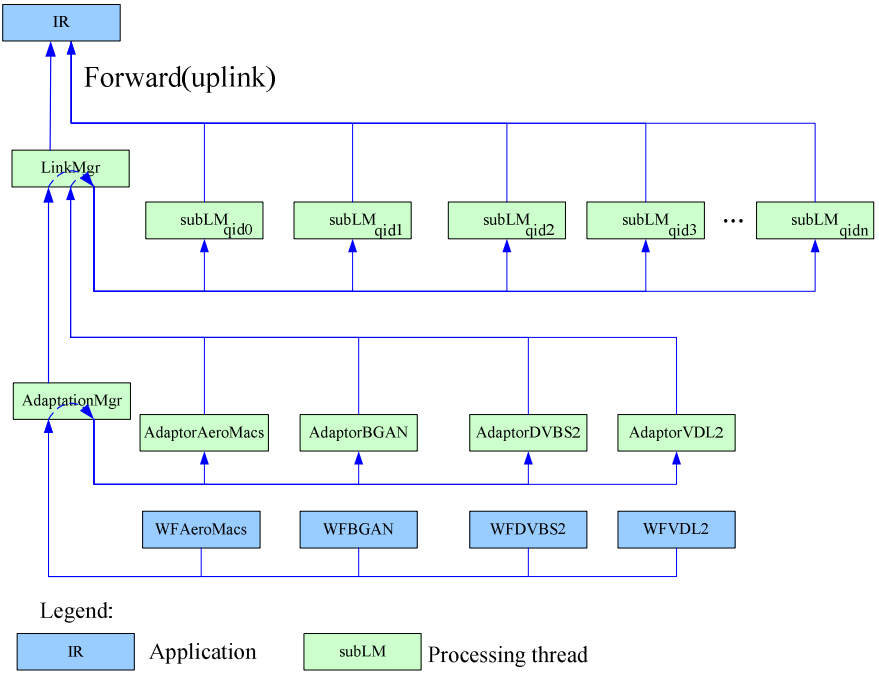

Fig. 6. JRRM forward signal handling design

Figure 6 shows the forward signal handling design of the JRRM. There are different waveform adaptors controlled by the Adaptation Manager, where each of them is dedicated for one kind of link. When the adaptors received messages from the waveforms, the messages will be processed and translated by the adaptors and then sent to the Link Manager for further processing. If the messages are related to connections, then sub-link managers will process them, otherwise the Link Manager will handle the messages directly (e.g. link up events).

4 Experiments Results

4.1 Testbed Configurations

The testbed is consisted of four Dell Vostro 430, Interl® Core™ i5 CPU, 2x2.67GHz, 2.00GB Memory PCs, with one performing as the IR, two working as IMR processing

platforms and one working as a application workstation. In supporting the JRRM core software, one AeroMACS Emulator and one BGAN Emulator software from Future Ubiquitous Network (FUN) Lab, University of Bradford are deployed. Testing software includes iperf [13] and Wireshark [14] are used to collect results.

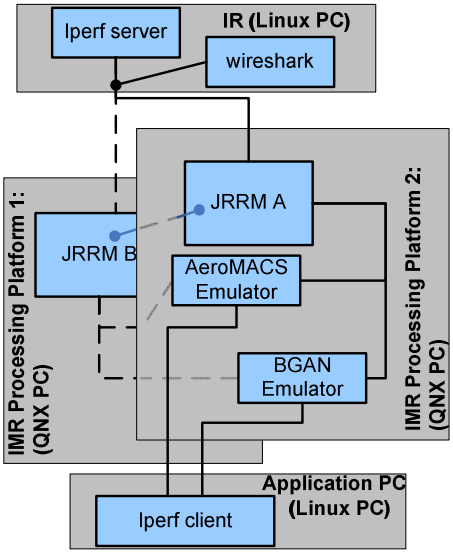

Fig. 7. Settings of the experimental environment

As shown in Figure 7, iperf server and client are running on two Linux PCs to stream TCP packets. The JRRM software runs on each QNX PC as 1+1 redundancy. One JRRM is active as the Master to process all the traffic whilst the other JRRM is inactive as the Slave but keeps synchronization with the Master. Connections will be established by the Master JRRM to carry data between the applications on the two Linux PCs.

Two sets of experiments are collected from the testbed:

1. Master-Slave JRRM hot swap during data transmission via the established AeroMACS connections.
2. Sessions handover from AeroMACS to BGAN.

4.2 Master-Slave Swap

The parameters used in iperf server and client are listed as below:

server	-s –P 0 –i 1 –p 5001 –f k
client	-c server_ip_addr –P 1 –i 1 –p 5001 –f k –t 100 –T 1

Upon receipt of a connection request from the IR, a Sub Link Manager is created by the Link manager. The Adaptation Manager translates the request from the Sub Link Manager to AeroMACS waveform to start the session. User TCP packets sent

from the iperf server to the client is collected by wireshark network protocol analyzer. The JRRM process is terminated by a shell script on each QNX PC every 30 seconds during data transmission. From Figure 8, we can see the connection established successfully hence the TCP data can pass through the JRRM. Because the connection information are synchronized between the two JRRMs, one is killed, another JRRM takes over the tasks immediately (300ms delay due to the keep alive health check interval). When the JRRM and the AeroMACS are on the same processing platform, the average throughputs are, as can be observed in Figure 8, 9500000B/s * 8/1024/1024 = 72.4Mbps. If the JRRM and the AeroMACS emulator are running on different processing platforms; the average data rate is 1000000B/s * 8/1024/1024 = 7.6Mbps. The data rate is limited by the QNX Neutrino Inter-Process Communication across platform POSIX messages.

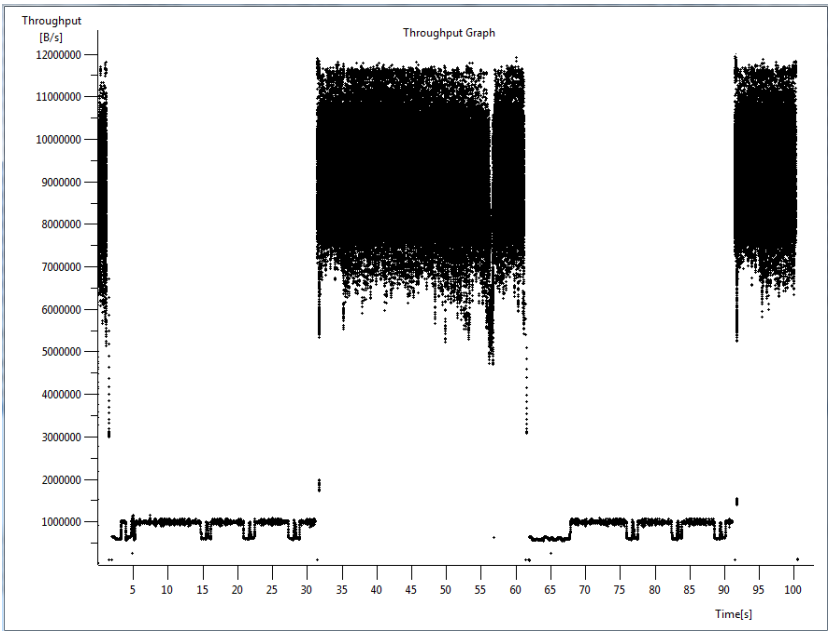

Fig. 8. Master-Slave swap throughput graph

Another observation from Figure 8 is when the Master-Slave switchover happens from JRRM/waveform co-located platform to across platforms, the instantaneous throughput varies between 1000000B/s and 950000MBps, for example, at time 5, 15, 22, 28 etc.. This is caused by the processing congestions when TCP retransmissions occurred.

From the experiment, the hot swap feature of the JRRM has avoided single point of failure successfully and maintained the continuity of service in the case of Master JRRM being terminated.

4.3 Handover

A twenty seconds transmission of data is sent from the iperf client, on the user application PC, to the iperf server running on the IR. This is shown in Figure 9. During the first ten seconds, data were sent via the AeroMACS link. The average data rate is 73Mbps. On 10th second, AeroMACS stack is torn down due to flight phase changes [15]. The connections then switch to the available BGAN link. There is around three seconds' interruption of data transmission due to the link establishment of BGAN. The data transmission resumed at 13th second, and the average data rate is now about 300kpbs (the maximum date rate is set to 320kbps for BGAN Emulator) and the waveform loading delay causes the connections handed over to available BGAN link.

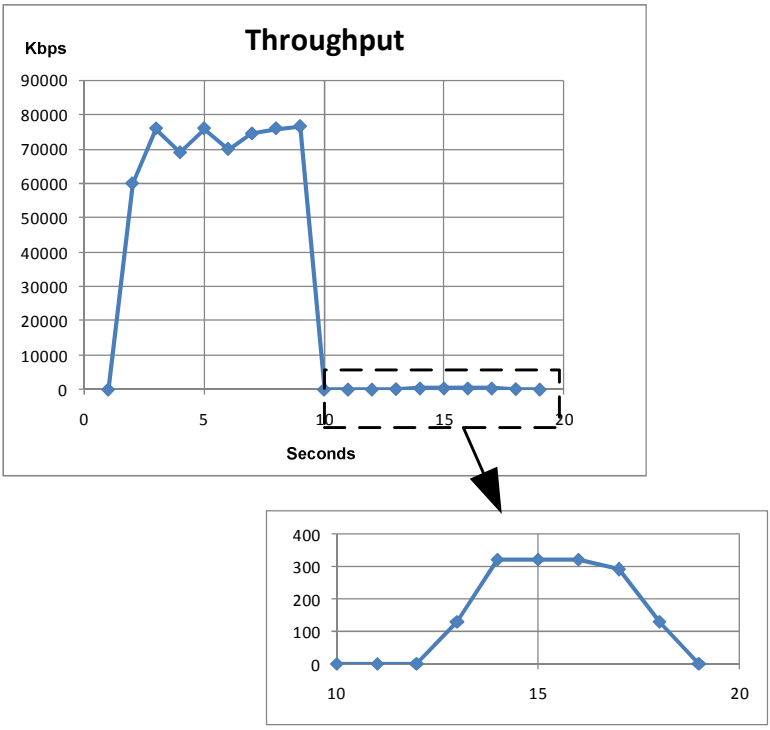

Fig. 9. Handover from AeroMACS to BGAN

The JRRM approach implemented in the testbed has demonstrated the benefit of integrating AeroMACS and BGAN links, namely, the high availability of BGAN link with the high bandwidth of the AeroMACS link and the successful inter-technology handover from one link to another.

5 Conclusion

This paper presents a realization of the integrated satellite-terrestrial communication networks for aeronautical services via JRRM approach. Details of the software design

are described. The integrated modular radio shares a common radio resource management which minimized the level of the size, complexity and cost of aeronautical on board communication system as well as increased the availability of links by introducing multiple radio technologies. The results collected from the proof-of-concept JRRM prototype verified the validity of the design.

Acknowledgment. The research leading to these results has been partially funded by the European Community's Seventh Framework Programme (FP7/2007-2013) under Grant Agreement No. 233679. The SANDRA project is a Large Scale Integrating Project for the FP7 Topic AAT.2008.4.4.2 (Integrated approach to network centric aircraft communications for global aircraft operations).

References

[1] EUROCONTROL, Long-Term Forecast: IFR Flight Movements 2008-2030. 1(v1.0) (2008)
[2] EUROCONTROL, Traffic Demand in Europe: Short-Term Falls But Modest Rises in the Long Term. SkyWay, p. 13 (Winter 2012)
[3] EUROCONTROL/FAA Memorandum of Cooperation, Action Plan 17 Future Communications Study, Final Conclusions and Recommendations Report, November 2007.
[4] SANDRA. Seamless Aeronautical Networking through integration of Data links Radios and Antennas, http://www.sandra.aero
[5] ICAO, Manual on VHF Digital Link (VDL) Mode 2. Doc 9776 AN/970 (2001)
[6] INMARSAT, http://www.inmarsat.com/Services/Land/Services/High_speed_data/BGAN.aspx?language=EN&textonly=False
[7] ETSI, Digital Video broadcasting (DVB) 2nd generation framing structure, channel coding & modulation systems for broadcasting, interactive services, news gathering and other broadbands satellite applications (DVB-S2). ETSI EN 302 307 V1.2.1 (August 2009)
[8] EUROCONTROL, http://www.eurocontrol.int/communications/public/standard_page/AeroMACS.html
[9] Xu, K., et al.: Interoperability Among Heterogeneous Networks for Future Aeronautical Communications. In: Plan, S. (ed.) Future Aeronautical Communications. InTech (2011)
[10] IEEE, Media Independent Handover Services. IEEE Std. 802.21 (2009)
[11] Ali, M., Xu, K., Pillai, P., Hu, Y.F.: Common RRM in satellite-terrestrial based Aeronautical communication networks. In: Giambene, G., Sacchi, C. (eds.) PSATS 2011. LNICST, vol. 71, pp. 328–341. Springer, Heidelberg (2011)
[12] Baddoo, J., et al.: Integration and Management of Multiple Radios in Satellite-Terrestrial based Aeronautical Communication Networks. ICST Transactions on Ubiquitous Environments 12(1-3), e4 (2012)
[13] http://sourceforge.net/projects/iperf/
[14] Wireshark Foundation: http://www.wireshark.org/
[15] Hu, Y.F.: SANDRA WP4.1.2 D4.1.1.2 Resource Management Design Report (September 2010)

On the Impact of Link Layer Retransmissions on TCP for Aeronautical Communications

Nicolas Kuhn[1,2], Nicolas Van Wambeke[3], Mathieu Gineste[3], Benjamin Gadat[3], Emmanuel Lochin[2], and Jérôme Lacan[2]

[1] NICTA, Sydney, Australia
firstname.lastname@nicta.com.au
[2] University of Toulouse, ISAE, TeSA, Toulouse, France
firstname.lastname@isae.fr
[3] Thales Alenia Space (TAS), Toulouse, France
fistname.lastname@thalesaleniaspace.com

Abstract. In this article, we evaluate the impact of link layer retransmissions on the performance of TCP in the context of aeronautical communications. We present the architecture of aeronautical networks, which is manly driven by an important channel access delay, and the various retransmission strategies that can be implemented at both link and transport layers. We consider a worst case scenario to illustrate the benefits provided by the ARQ scheme at the link layer in terms of transmission delay. We evaluate the trade-off between allowing a fast data transmission and a low usage of satellite capacity by adjusting link layer parameters.

Keywords: aeronautical communications, ats/aoc services, retransmissions strategies, tcp, link-layer.

1 Introduction

According to recent evolutions in the aeronautical communications domain, advanced safety aeronautical communications are composed by two kinds of service: Air Traffic Services (ATS) and Air Operations Control (AOC), most of these novel services being supported by the SWIM communication paradigm. The goal of such services is to ensure safety and regulate the needs of aeronautical services through the use of binary communication, *i.e.* transmitting messages between pilots and control centers, instead of actual voice-to-voice communication. ATS/AOC services are small and sporadic, making their transmission over satellite links of interest. In the context of aeronautical communications, the transmission of ATS/AOC services data might be critical and some applications require a reliable transmission with important delay constraints for 95% of the application data.

When channel codes implemented at the physical layer cannot rebuild packets and forward them to the link layer, retransmissions can be introduced to overcome this problem. The multiple retransmission at different layers might decrease the transmission delay and ensure the reliability of the transmission.

R. Dhaou et al. (Eds.): PSATS 2013, LNICST 123, pp. 38–48, 2013.

However, the satellite resource is expensive and must be equally shared among the users.

In this article, we illustrate the trade-off between (1) increasing the reliability and decreasing the transmission delay by introducing link layer retransmissions and (2) using more satellite link capacity. We propose simulations in NS-2 conjointly with a realistic model for the plane-satellite channel. We assess the performance of TCP with and without link layer retransmissions on the return link of the plane in terms of transmission delay and capacity utilization.

The rest of the article is organized as follows: in Section 2, we present the aeronautical communication networks and retransmission strategies that can be introduced at different layers. In Section 3, we present the tools used to simulate the whole protocol stack of elements of such complex network. We consider specific scenarios detailed in Section 4. We present and comment the results of the simulations in Section 5 and then conclude this study in Section 6.

2 Link and Transport Layers Retransmissions in Aeronautical Communications

In this section, we present the aeronautical communications network in terms of structure and traffic carried out. We detail the different delays encountered during the transmission of packets. We list available retransmission strategies specifying at which level they can occur.

2.1 Satellite, Plane and Gateway

In Figure 1, we present the network and highlight the difference between up (also called forward) and down (also called return) links.

On the return link (from the plane to the satellite gateway), the average useful throughput is 260 bps, which is enough to transmit the small and sporadic data exchanges required by ATC and AOC services. Each application has specific

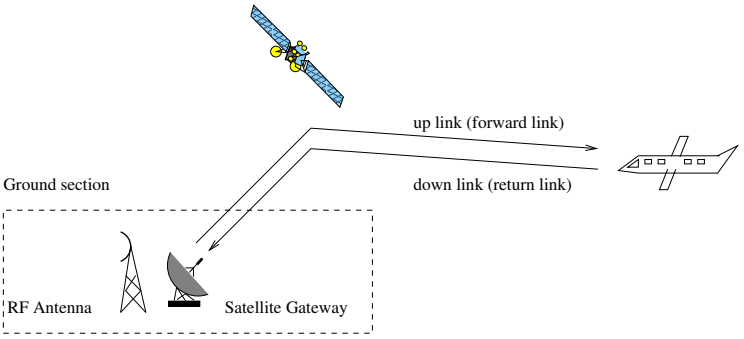

Fig. 1. Plane, satellite and satellite gateway

requirements in terms of capacity, delay constraint (for 95% of the packets) or availability[1]. The bounds of these requirements are: (1) the size of data packets is ranging from 70 to 2500 bytes; (2) the inter-packet time for each application varies from 1000 s to 3000 s; (3) some applications might have delay constraints.

2.2 Channel Access Delays

The network presented in Section 2.1 is complex due to important delays and medium shared between an important number of users. As a result, we present in this section how we model the channel access delays.

The time needed by an applicative data packet to be transmitted from the client to the server (denoted T_{data}) is the sum of the propagation delay (denoted T_{prop}), the channel access delay (T_{acc}) and retransmission delays (T_{ret}):

$$T_{data} = T_{prop} + T_{acc} + T_{ret}$$

The propagation time is set to $T_{prop} = 250$ ms, which is a standard value for satellite transmissions.

Table 1. Channel access delay (in ms)

	Forward link	Return link
Data packets	$\in [10; 100]$	$\in [500; 1300]$
TCP Ack.	55	900

We detail in Table 1 the values of T_{acc} for both up and return link.

Forward link
At the physical layer of the satellite gateway, the transmission is scheduled by frames. The important size of the antenna enables the gateway to transmit frames of 90 ms gathering data for different users. Depending on when the data packet reaches the gateway (will the packet be sent straight away or after 90 ms) and considering the 10 ms necessary for the processing of the frame, we explain the value presented in Table 1 for the forward link. We choose an average delay of 55 ms for the TCP acknowledgements. The channel access delay can be up to 100 ms: as a result, it cannot be neglected compared to the propagation delay for both acknowledgements and data packets.

Return link
In order to obtain capacity, a user terminal on the plane requests for capacity following DAMA VBDC access method. Indeed, the medium is fairly shared between the users as the satellite gateway manages to allow dedicated slots (in terms of transmission date and frequency) for each user. As a result, on

[1] Unfortunately, this list is confidential and cannot be communicated.

the return link, we consider a delay for the request to be sent to the gateway (between 0 ms and 800 ms), propagation delay for the transmission of the capacity request from the plane to the gateway (250 ms), propagation delay for the resource allocation plan from the gateway to the users (250 ms). We neglect the time needed by the gateway to compute this plan which is very low compared to the propagation delays. We consider an average delay of 900 ms for the TCP acknowledgments.

2.3 Link and Transport Layers Retransmissions

The coding schemes introduced at the physical layer might not be suitable to recover the data when the signal-to-noise ratio is low. As a result, we present in this section the retransmissions schemes introduced at both link and transport layers to ensure a reliable transmission.

At the link layer, there are different retransmission techniques which are presented in [1,2]. We denote by LLDU the Link Layer Data Unit. Among the different existing techniques, we focus on the two following:

Automatic Repeat reQuest (ARQ)
Automatic Repeat reQuest family can be defined by a subset of retransmission strategies (Stop-and-Wait ARQ, Go-Back-N ARQ or Selective-Repeat ARQ). We consider here SR-ARQ mechanism at the link layer level: it consists in the retransmission of the LLDUs that have been lost during the transmission. We denote SR-ARQ by ARQ.

HARQ
Forward Error Correction (FEC) is a scheme where the sender sends a combination of data and repair LLDUs. Let N_D (resp. N_R) be the number of data (resp. repair) LLDUs and $N = N_D + N_R$. The process to recover data LLDUs is successful if at least N_D LLDUs are received, otherwise (if the number of erasures is strictly greater than N_R) no correction is possible. The FEC scheme does not enable the retransmission of LLDUs. Hybrid-Automatic Repeat reQuest (HARQ) mechanism is a combination of the FEC and ARQ mechanisms previously described: after the first transmission of a FEC block, including data and repair LLDUs, HARQ allows the sender to transmit additional repair LLDUs when a recovery is not possible at the receiver side. In other words, if no correction is possible, the transmission of additional repair LLDUs is requested by the receiver. Also, if the receiver requests M LLDU, HARQ can send $M + M'$, where M' is the number of supplementary LLDU that can be transmitted, to potentially reduce the number of retransmissions. In the rest of this article, we consider that HARQ does not transmit a first block FEC but still only transmits repair packets to recover the useful data (*i.e.*, $N_R = 0$).

At the transport layer, reliable Transmission Control Protocol (TCP) [3] is considered for on-board applications executing in a SWIM like context while the no retransmission User Datagram Protocol (UDP) [4] is considered for COCR

like traffic. There are different variants of TCP [5]. Most of them mostly adapt the congestion window size in the congestion avoidance phase, however, based on the application sizes detailed in Section 2.1 and the requirements in terms of delay, we focus on TCP New Reno [6] to model the retransmission behaviour as its RFC describes the currently base-line version for TCP. Due to the inter-packet delays considered, TCP never exits the slow-start phase, making the choice for different congestion avoidance mechanism irrelevant.

2.4 Discussion

For safety reasons, reliability is compulsory in both kind of environments and different retransmission strategies can be introduced at both link and transport layers (Section 2.3). The transmission delay (including channel access) of retransmissions can be important for both layers (Section 2.2) and some applications have delay constraints (Section 2.1). Moreover, if not properly tuned, introducing retransmissions at multiple layers can lead to counter productive interactions, highly increasing the use of the limited satellite capacity.

In Sections 3,4 and 5, we argue that a trade-off must be found between (1) introducing link layer retransmissions and reducing the transmission delay by using FEC that uses more capacity and (2) no link layer retransmissions, thus leading to a higher end to end transmission delay but using less capacity.

We denote by A the set of applications of each plane, P the set of planes, D one data packet, $C(D)$ and $T_{data}(D)$ the exploited capacity and transmission delay of D, and $T_{MAX}(a)$ the maximum transmission delay authorized for the application $a \in A$.

$$\forall a \in A,\ \forall p \in P,\ min(C(D), T_{data}(D)) \tag{1}$$

Equation (1) expresses the problem we seek to optimize with the constraint:

$$T_{prop}(D) + T_{acc}(D) < T_{data}(D) < T_{MAX}(a),$$

i.e.

$$T_{ret}(D) < T_{MAX}(a) - T_{prop} - T_{acc}$$

The objective is thus to adapt the retransmission strategies to reduce $T_{ret}(D)$ and $C(D)$ for each data packet D.

3 Simulation

In this section, we present the model and simulation of the network.

The work presented herein uses TDM simulators from CNES[2]. This simulator takes into account realistic satellite links characteristics, such as satellite orbits or recent correcting codes to generate physical layer traces [7]. As a result,

[2] CNES is the french government agency responsible for shaping and implementing France's space policy in Europe, see `http://www.cnes.fr/`.

each packet transmitted by the physical-layer is characterized by an transmission timestamp and a decoding time. Additionally, its probability to be lost is determined by the physical layer codes and the model of the channel used in the simulation scenario.

Based on the physical layer traces, an simulation of the ARQ or HARQ schemes effects have been derived by the use of the Trace Manager Tool (TMT) [8] that produces link layer traces. These link layer traces are then loaded into the NS-2 network simulation, extended with a Cross-Layer InFormation Tool (CLIFT) [9] to schedule the transmission of applicative packets through the protocol stack (particularly using a specific transport layer) and simulating the behavior of the link and physical layers.

Therefore, with these tools, it is possible to simulate the full protocol stack including link layer FEC, ARQ and HARQ mechanisms to conduct realistic simulations in order to evaluate the impact of retransmissions at the link layer on end to end performances.

4 Scenario

In this section, we present the different retransmissions approaches, the traffic and the metrics that we consider to assess the impact of retransmissions at the link layer when the plane transmits data to the satellite gateway.

Retransmissions

As we detail in Section 2.3, retransmissions can be introduced at different layers of the protocol stack. For compatibility with the SWIM architectures, we argue that the transport layer protocol should be TCP [6]. As a result, we consider the combination of 3 different configuration by varying the link layer reliability mechanism configuration: no retransmission scheme, ARQ at the link layer or HARQ at the link layer.

Traffic

The traffic is generated with exchanges taking place between a plane and a ground system through a satellite gateway (*i.e.*, no air to air communication considered). Applications transmit packets of various sizes ($\in [70; 2500]$ bytes), depending the content carried out and the inter-packet time is different for each application ($\in [1000; 3000]$ s) (more details can be found in Section 2.1). We consider that there is one TCP connection for each application executing on-board.

Metrics

The transmission of data at the application level is ensured by a reliable transport layer protocol. Therefore, for each $Eb/N0 \in (1.05\,dB; 1.3\,dB; 1.8\,dB)$ (*i.e.* LER (Link layer data unit Error Ratio) $\in 2.3e^{-1}; 6e^{-2}; 2e^{-4}$) and for each applicative packet size, we measure the transmission delay for 95% of the packets and the mean transmission delay as most applications are delay-sensitive. We also measure the effective coding ratio (defined by the ratio between the applicative data byte transmitted and the total number of byte transmitted on the air interface) to assess the impact of link layer retransmissions on the usage of the available capacity.

5 Results

In this section, we present the metrics of the simulations defined in Section 4. We focus on the benefits that ARQ can provide when used together with TCP and illustrate a worst-case scenario where HARQ is of interest compared to ARQ.

5.1 On the Benefits of ARQ on TCP Performance

In this subsection, we present the evolution of the metrics when $Eb/N0 \in (1.05\,dB; 1.3\,dB; 1.8\,dB)$. We plot in Figure 2, the mean delay for the transmission of one packet, in Figure 3, the transmission delay of 95% of the packets and in Figure 4, the effective coding ratio.

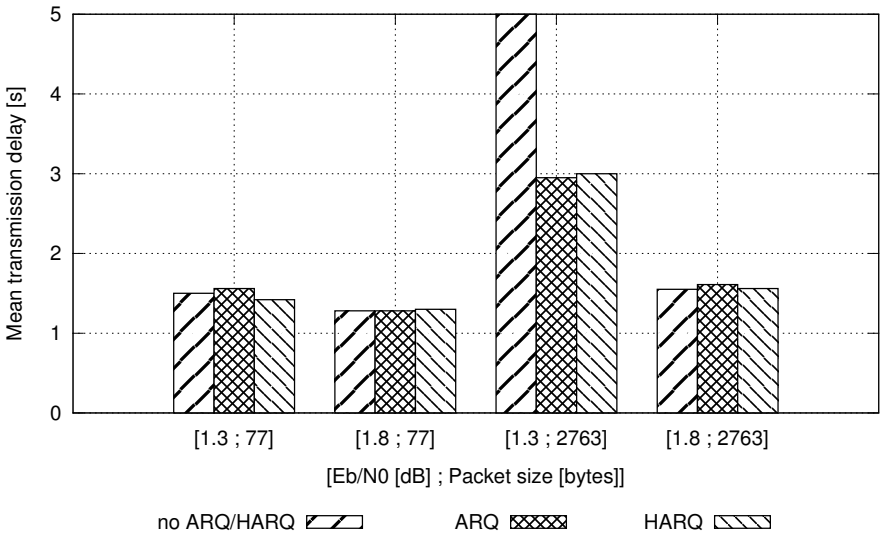

Fig. 2. Mean delay

In Figures 2 and 3, we can see that the benefits provided by ARQ at the link layer is not clear in most of the cases. Indeed, as it can be seen, the use of ARQ brings absolutely no benefit for most of the simulations. However, we can see that when the size of the application packets is high (i.e. 2763 bytes) the average delay necessary to transmit a packet is more than 5 s (around 200 s, note that we do not represented this value in order to let the figure readable). We argue that this specific case is enough to justify the need for retransmission at the link layer when dealing with high PER at link layer.

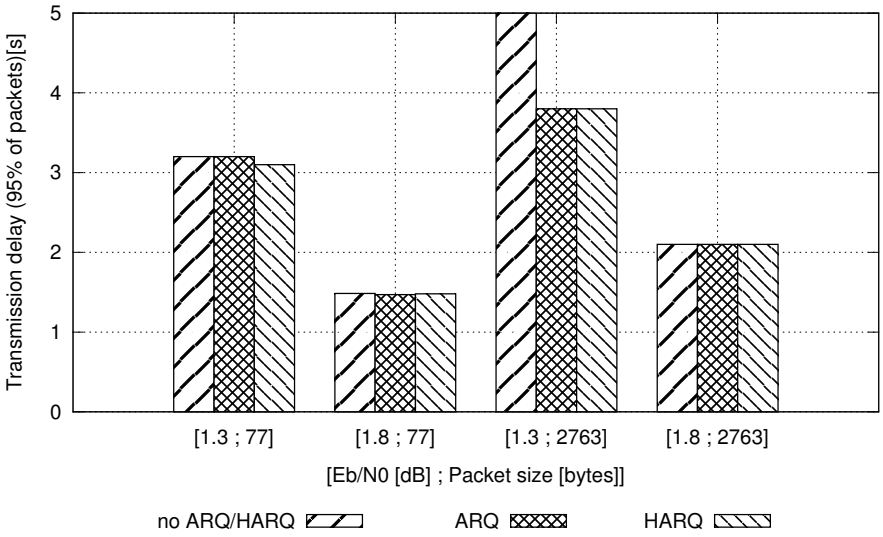

Fig. 3. Transmission delay of 95% of the packets

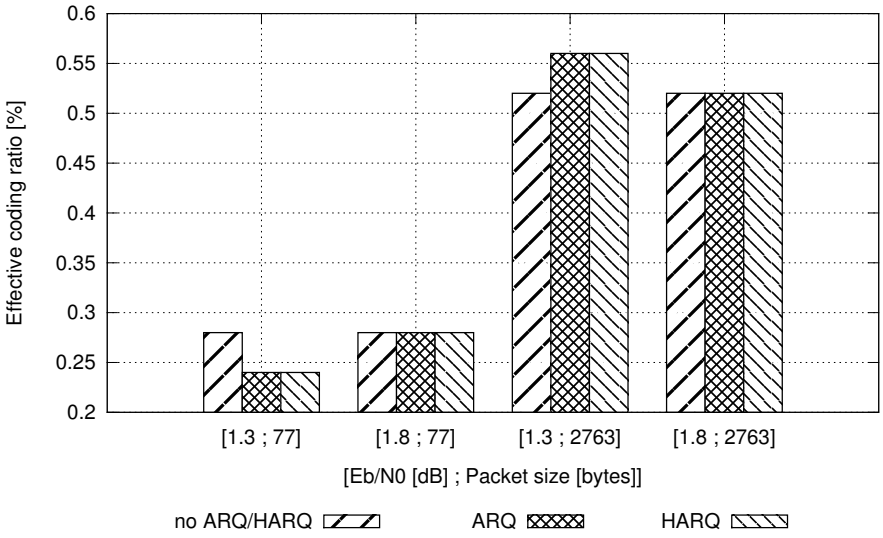

Fig. 4. Effective coding ratio

However, as we discussed in Section 2.4, Figure 4 shows that in this example (large packets in high PER conditions), in order to decrease the transmission delay, more capacity is exploited to transmit one single data packet thus increasing the risk of jamming the system in high load conditions.

As shown, in some specific use cases, link layer retransmissions are beneficial. This experiments also show that this link layer retransmissions have a cost in terms of capacity usage. However, results of this section do not highlight differences between ARQ and HARQ link layer retransmissions schemes, which we focus on in Section 5.2.

5.2 Comparison of ARQ and H-ARQ on TCP Performance

The results presented in Section 5.1 do not reveal any advantage for or against ARQ and HARQ implementations at the link layer. We present additional simulations in this section, with a higher PER at physical layer and considering various size of applicative packets. We plot in Figure 5 the transmission delay of 95% of the packets and in Figure 6, the effective coding ratio. As we compare ARQ and HARQ, we focus on a specific implementation of HARQ. HARQ does not transmit a first FEC block, but introduce more additional retransmission packets than ARQ (more details can be found in Section 2.3).

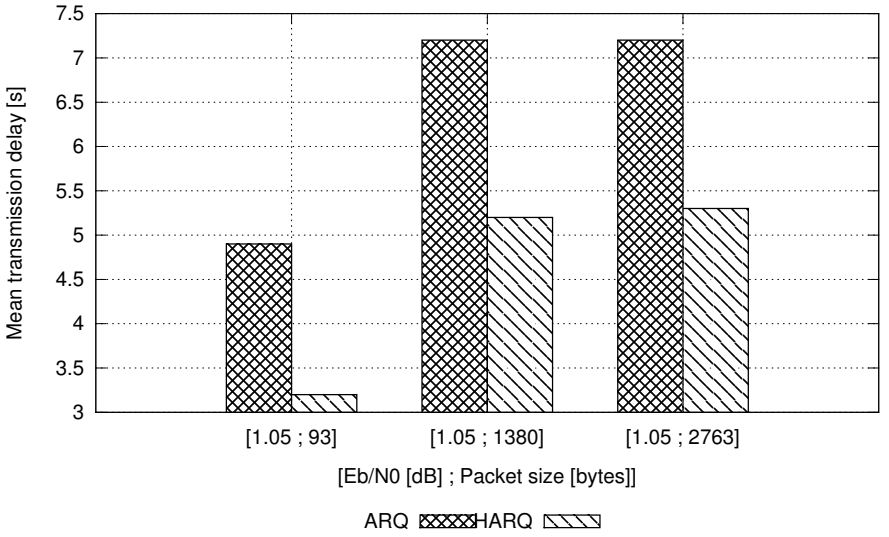

Fig. 5. Transmission delay of 95% of the packets

We measure that HARQ can reduce the transmission delay of ARQ on several cases (in Figure 5), making their use of interest in case of a very noisy channel. However, this improvement has a cost in terms of capacity usage as illustrated in Figure 6.

Considering a specific HARQ reduces the scope of our results, but we highlight the need for deeper studies on the impact of the parameters of HARQ on the TCP performance in the context of critical aeronautical communications. We illustrate

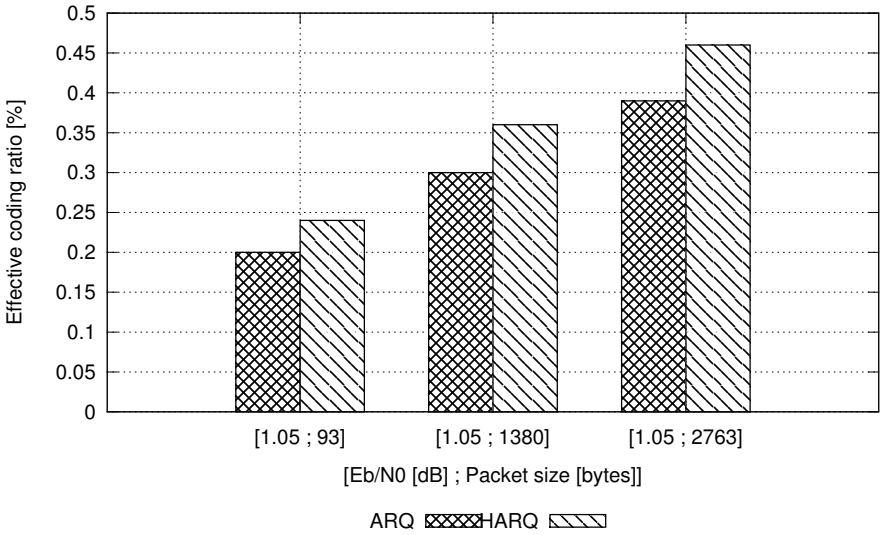

Fig. 6. Effective coding ratio

that different link layer retransmission schemes have different performances in terms of delay and capacity utilization, illustrating the discussion presented in Section 2.4.

5.3 Limits of Interpretations

The considered physical layer performances are located well below the currently defined targets for satellite communication systems used in aeronautical communications. For systems which are well designed, and for which the physical layer performances meet the established criterion, the use of ARQ and HARQ at the link layer does not provide any improvement when compared to the use of TCP without any link layer retransmissions.

Furthermore, the use of SWIM like communication paradigms, heavily relying on protocols such as HTTP and SOAP make the use of TCP a natural choice. In these contexts, although the introduction of ARQ and HARQ can improve the performance in high PER contexts, the overall transmission delays observed (even in a fully optimized context) are not compliant with the application requirements. Finally, the presence of timeout values in protocols executing above TCP have not been considered in this study.

6 Conclusion

In this article, we argue for the introduction of link layer retransmissions schemes in the context of aeronautical communications. We make use of link layer simulation traces on which we simulate link layer retransmissions to assess the impact

on ARQ and HARQ on the performance of TCP. We show that, in worst cases with regards to the propagation channel conditions, link layer retransmissions enable to transmit applicative data in acceptable delays for the safety of aeronautical communications. We also illustrate that a trade-off must be found between having a low transmission delay and a good channel capacity usage.

Acknowledgments. This work presented in this article documents part of the simulation scenarios and results obtained in a study funded by CNES in which TéSA and Thales Alenia Space took part.

References

1. Lin, S., Costello, D.J.: Error control coding: fundamentals and applications, ch. 15. Prentice-Hall (1983)
2. Berlekamp, E., Peile, R., Pope, S.: The application of error control to communications. IEEE Communications Magazine 25, 44–57 (1987)
3. Kurose, J., Ross, K.: A top-Down Approach. In: Computer Networking, p. 284. Addison Wesley (2008)
4. Postel, J.: User Datagram Protocol, RFC 768, RFC Editor (August 1980)
5. Callegari, C., Giordano, S., Pagano, M., Pepe, T.: Behavior analysis of tcp linux variants. Comput. Netw. 56, 462–476 (2012)
6. Allman, M., Paxson, V., Blanton, E.: TCP Congestion Control, RFC 5681, RFC Editor, Fremont, CA, USA (September 2009)
7. Chauvet, W., Amiot-Bazile, C., Lacan, J.: Prediction of performance of the dvb-sh system relying on mutual information. In: 2010 5th Advanced Satellite Multimedia Systems Conference (ASMA) and the 11th Signal Processing for Space Communications Workshop (SPSC), pp. 413–420 (September 2010)
8. Kuhn, N., Lochin, E., Lacan, J., Boreli, R., Bes, C., Clarac, L.: Enabling realistic cross-layer analysis based on satellite physical layer traces. In: PIMRC 2012, pp. 285–290 (2012)
9. Kuhn, N., Lochin, E., Lacan, J., Boreli, R., Bes, C., Clarac, L.: Clift: a cross-layer information tool to perform cross-layer analysis based on real physical traces. CoRR, abs/1206.5459 (2012)

Satellite and Wireless Links Issues in Healthcare Monitoring

Rahim Kacimi[1] and Ponia Pech[2]

[1] University of Toulouse, IRIT-UPS, 118 route de Narbonne, 31062 Toulouse, France
[2] TéSA Association Lab., 14-16, Port Saint-Etienne, 31000 Toulouse, France
rahim.kacimi@irit.fr, ponia.pech@tesa.prd.fr

Abstract. Thanks to the facilities offered by telecommunications, telemedicine today allows physicians and clinicians to access, monitor and diagnose patients remotely. Telemedicine includes several applications such as remote monitoring of chronically ill patients, monitoring people in their everyday lives to provide early detection and intervention for various types of diseases, computer-assisted physical rehabilitation in ambulatory settings, and assisted living for the elderly at home. These new applications require a reliable, wireless communication link between the devices implanted in the patient's skin and a clinician. In this article, this issue is discussed and a list of performance criteria for the different communication links used is addressed, especially focusing on the satellite link.

Keywords: Vital sign monitoring, health-care monitoring, wireless sensor networks, wireless body networks, satellite, telemedicine.

1 Introduction

Nowadays, remote health-care is becoming increasingly attractive due to several advantages it brings: extending the health system coverage to rural and isolated areas, ensuring autonomy to chronic patients by letting them stay at home, allowing the clinicians to remotely diagnose and monitor their patients, ensuring real-time monitoring for critical illnesses, etc. Moreover, advances in key areas such as Wireless Sensor Networks (WSN) and Body Sensor Networks (BSN) are enabling technologies for the application domain of unobtrusive medical monitoring [1]. This field includes cable-free continuous monitoring of vital health signs in intensive care units, remote monitoring of chronically ill patients, monitoring people in their everyday lives to provide early detection and intervention for various types of diseases, computer-assisted physical rehabilitation in ambulatory settings, and assisted living for the elderly at home.

These innovative applications, where a pacemaker communicates the patient's health state and performance data to a base station, or a BSN integrating a number of devices, require a reliable wireless communication link between the sensing devices implanted in the patient's skin and a physician. Otherwise, the wireless link can be used to interrogate the implant at either irregular intervals, or on a regular basis, or to provide near permanent communication. A one-way wireless link may be used to

R. Dhaou et al. (Eds.): PSATS 2013, LNICST 123, pp. 49–64, 2013.

obtain the patient's health information or performance data from the implanted device, while a two-way link allows external reprogramming of an implanted device [1]. Due to the critical and sensitive nature of the medical information transmitted through the wireless network, reliable data transfer for BSNs and network reliability are of paramount importance. In addition to wireless terrestrial networks, satellite link can (or have to) be used in some cases. For example, when the patient is outside of the cellular network coverage, the satellite network can be used to transmit data to the medical call center or to contact the patient for further information.

Network reliability directly affects the quality of the patient's monitoring, and in a worst-case scenario can be fateful when a life threatening event has gone undetected. However, due to the constraints on communication bandwidth and power consumption, traditional network reliability techniques such as the retransmission mechanism for TCP (Transmission Control Protocol) may not be practical for BSN applications, whereas they are used in satellite links despite their drawbacks (as in the OURSES [18] and URSAFE [17] projects that will be described later on below). With similar constraints on WSNs, researchers have proposed several methods for improving their reliability. One simple approach is to use limited retransmission where packets are retransmitted for a fixed number of times until an acknowledgment is received; however, retransmission often induces significant overhead to the network. Another approach is to form a multi-path network and exploit the multiple routes to avoid disrupted links. It is expected that this will be an area that will raise significant research interest in the coming years, particularly in exploring the autonomic sensing paradigm for developing self-protecting, self-healing, self-optimizing, and self-configuring BSNs.

Unlike typical wired or wireless network architectures in which the network configuration is mostly static and there are limited constraints on resources, the BSN architecture is highly dynamic, placing more rigorous constraints on power supply, communication bandwidth, storage and computational resources.

The remainder of this paper is organized as follows: the context of this work and its critical problems are discussed in section 2. Section 3 states the reliability problem and performance criteria for WBAN (Wireless Body Area Networks) and WSN links. Section 4 focuses on satellite link issues in telemedicine applications. In section 5, the main conclusions of our work are summarized, and a set of open issues and future directions is presented.

2 Context and Problem

TeSA laboratory conducted with its partners two projects in the context of remote health-care. These two projects are UR-Safe (Universal Remote Signal Acquisition For hEalth) and OURSES (Offer of Services using Satellite for Rural Usage).

2.1 UR-Safe Project Description

The UR-Safe project [18] aimed at creating a mobile telemedicine care environment for the elderly, thus helping mitigate the problems of health care provision observed in

the Western societies caused by an aging population and the associated increasing costs. The adopted technological solution maximizes the concepts of autonomous living and quality of life for the patient, in alignment with the emerging models of health care provision, while at the same time addressing safety and alarm detection issues. The technological solution consists in placing medical sensing devices on the patient's body, all of them being connected via a short range Wireless Personal Area Network (WPAN) to a central, portable electronic unit called Personal Base Station (PBS). These wearable sensors enable to record electrocardiograms (ECG) and oxygen saturation level for instance, while a shock/fall detector sends an alarm when the patient falls or presses a button. Thanks to speech recognition algorithms, the PBS allows the exchange of simple spoken sentences with the patient in order to better analyze the patient's health condition. The pieces of information coming from the different sensors and from the shock/fall detector are gathered. Based on these data, preliminary computer-aided diagnosis is performed by the PBS. The data are then sent to a medical call center.

2.2 OURSES Project Description

The OURSES project [17] proposed three telemedicine applications related to services offered to elderly people. It focused on the use of satellites as a complement to terrestrial communication technologies to ensure the deployment of teleservices in areas where telecommunication infrastructure is lacking. These three telemedicine applications are described in the following.

A typical architecture of a remote telemedicine solution conjugates tree or four different communication technologies according to different wireless architecture links:

- The first link: the first link connects the medical nodes and the coordinator, in order to form a WBAN mainly using a star topology. The WBAN is often composed of a limited number of medical nodes (body sensors) connected to a coordinator (that may be a normal sensor node or a PDA (Personal Digital Assistant)).
- The second link: a second link exists between coordinators and a base station collector (local PC). The routing of information between the coordinators and the base station can be done in various ways and with different communications technologies: on the one hand, a WSN can be formed with all coordinators. The coordinators are also associated with environmental sensors that monitor the physical environment surrounding the patients (temperature, humidity, light,...). The information is then transmitted to the base station via a WSN mesh topology. On the other hand, centralized WiFi technology can replace the WSN by setting direct links between coordinators and access points to collect information.
- The third link: a last link is used to transmit data from the base station (local PC) to a remote physician. In the absence of wide-coverage terrestrial networks, a satellite link is used in this case.

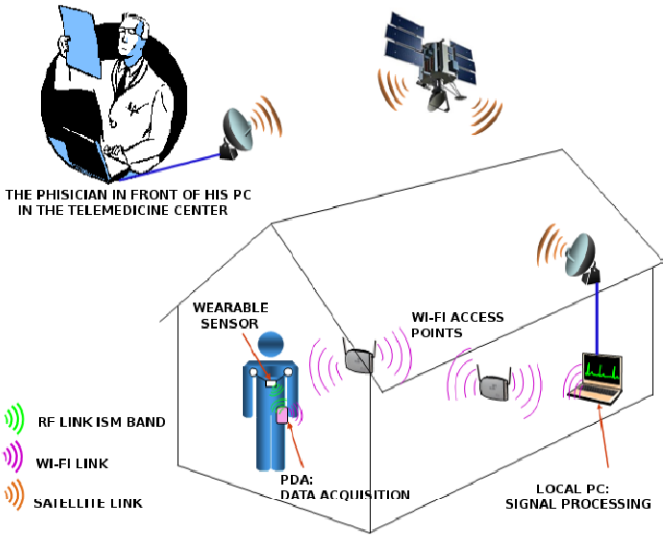

Fig. 1. Global scheme of ECG monitoring in OURSES project

Figure 1 shows a usage scenario on wireless vital sign monitoring using different technologies. This solution is based on a wireless wearable sensor which transmits ECG to a portable device in real time. The latter is then connected to a local PC which is located in the patient's house through a Wi-Fi link. ECG signals are then sent to the physician's office using a satellite link. When an abnormal event during an ECG analysis is detected by a specific automatic signal-processing-based diagnosis application running on the PC, an alarm is raised and sent to the physician's office.

2.3 Position of the Problem

The purpose of this paper is to join together different scientific communities involved in such challenging projects as telemedicine and biomedical vital signs remote monitoring, namely, the medical end-users (physicians, medical experts), the digital signal processing scientists from academia, and the telecommunication scientists and engineers from both academia and industry. Indeed, telemedicine projects include so wide and multidisciplinary technical and scientific expertise fields that a minimum of dialogue between the different disciplines should be sought for the sake of a better mutual understanding and a more unified and integrated approach.

More precisely, one peculiar problem arose in the experiments carried out in the framework of the aforementioned telemedicine projects: packet loss was observed at the physician's PC side on the satellite return channel downlink, which manifested itself in "hole" periods, that is, missing samples in the received ECG signal. In other words, a few ECG samples were missing due to undetected causes occurring somewhere in the wireless/satellite transmission chain that are attributed to the fact that the different links involved (fixed access network, mobile access network and satellite

DVB-RCS interfacing) are liable to inducing errors or loss on the transmitted data. Such data corruption/loss can occur anytime and anywhere. The timeout of several ARQ (Automatic Repeat Request) procedures was shown to induce packet loss: 1-2% for GPRS, and 8% for the satellite [24]. To cope with that problem, TeSA devised a recovering method which hybridized Papoulis-Gerchberg (PG) algorithm and an Auto-Regressive (AR)-based reconstruction algorithm.

The principle of the PG exact reconstruction algorithm lies in an interpolation of the missing samples using the band-limited property of the ECG signal, via an iterative process which allows to replace the missing part of the signal with the result of the Inverse Fast Fourier Transform (IFFT). The PG algorithm performs well with a reduced number of missing samples, but its drawback lies in the long convergence time of its iterative process. Therefore another ECG missing sample reconstruction method was proposed, namely, an audio signal reconstruction method based on AR modeling [24]. This method is used to predict forward and backward signal samples. The final step in the proposed reconstruction algorithm is to jointly use the two PG and AR methods, the AR algorithm being executed at initialization phase to be followed by the PG algorithm. The reconstruction performance was measured using the local signal to reconstruction error (noise) ratio given by:

$$SNR = 10log\left(\frac{\sigma^2_{xgap}}{\sigma^2_{(x-\hat{x})gap}}\right) \text{ in dB}$$

where σ^2_{xgap} represents the variance of the original signal in the missing part and $\sigma^2_{(x-\hat{x})gap}$ represents the variance of the reconstruction error also restricted in the missing part. Tested on the MIT-BIH Arrhythmia Database, the combined method yielded better performance than the PG and AR algorithms for missing parts of up to 30 consecutive samples (120 ms).

The paper aims at identifying and qualitatively surveying all the different factors related to the wireless and satellite links that may be a cause of packet error or loss, and thus undermine the reconstruction performance of TeSA's algorithm, without any quantitative assessment at this stage. Packet errors and loss can be traced back to mainly three different sources: (i) general performance criteria of the transmission system; (ii) wireless issues; (iii) satellite link issues.

2.4 Performance Criteria

The performance criteria of wireless network links which have significant implications in the healthcare domain include the number of collisions, the energy consumption at the nodes, the network throughput, the number of unicast packets delivered, the number of packets delivered to each node, the signals received and forwarded to the Medium Access Control (MAC) layer, and the change in energy consumption with variation in transmission range, etc. Some of these criteria are described hereafter:

- ***The delay:*** The delay for data packets delivery is of paramount importance in health-care monitoring and its criticality depends on the way data traffic is transmitted. Indeed, the data can be transmitted on either a periodical basis or a non-periodical basis. A periodic transmission mode corresponds to the case where the traffic data packets collected by the body sensors are sent periodically, while a non-periodic transmission mode refers for instance to the case where an alarm is sent by a body sensor every time it detects an anomaly.
- ***The Packet Received Rate (PRR):*** In a health-care network solution, a high PRR is necessary so that the physician can make a good diagnostic. For instance, it may sometimes be difficult for him to interpret ECG data, which makes a diagnostic completely impossible.
- ***The Quality of Service (QoS):*** loss of data is more significant in BSNs, and may require additional measures to ensure QoS and real-time data interrogation capabilities.

3 Wireless Sensors and Body Networks in Vital Signs Monitoring

The advent of smart wireless sensors that are able to form a BSN would not be possible without the availability of appropriate and inexpensive low power short-range transceivers for low to moderate data rates. These are capable of transmitting real-time data with a latency of typically less than one second within a range of up to five meters.

Current standardization efforts affect most of the layers of a communication stack, starting from the Physical (PHY) layer, including the Medium Access Control (MAC) layer and reaching the higher layers, such as network or routing layers, and even sometimes the data representation and application layers. Different standardization bodies may work in a cooperative fashion, as is the case with ZigBee and IEEE 802.15.4.

The problems encountered in BSNs involved respectively on the first and the second links listed above are summarized as follows:

Energy Consumption: It is widely recognized that limiting energy is an inescapable issue in the design of wireless BSNs due to the strict constraints which it imposes on the network operations. In fact, the energy consumption is a crucial factor impacting the network lifetime that has become the prevailing performance criterion in this area. If the network is to operate as long as possible, these energy constraints require make a trade-off between various activities at both the node and network levels, so that the less energy consumed by the nodes, the longer the network lifetime to satisfy the running application [15].

Scalability: Scalability is an important factor in designing efficient WSN solutions. A good solution has to be scalable in the sense of being adaptable to future changes in the network topology. Thus scalable protocols should perform well as the network grows larger or as the workload increases.

Congestion: In healthcare WSN applications (particularly for medical emergencies or closely monitoring critically ailing patients), it is obviously desirable in the first place to avoid congestion, and should it occur, to reduce data loss due to congestion.

Mobility Issues: The wireless network solution must manage the mobility of equipments and mobility of persons in order to maintain a good connectivity.

3.1 IEEE 802.15.4 Solution

Although a wireless BSN is not always a lowest duty cycle application (such as continuous ECG streaming), the ZigBee/IEEE 802.15.4 framework appears to be the most intriguing and suitable protocol suite for it. The IEEE 802.15.4 MAC offers a number of valuable ingredients for BSNs: the MAC is optimized for low power and short messages and includes peer-to-peer network support, guaranteed time slots, etc. IEEE 802.15.4 is also likely to be chosen as the radio layer basis for IEEE P1451.5-based wireless sensors [27]. Highly integrated single-chip IEEE 802.15.4-compliant transceivers are already available from a number of IC manufacturers, yet they are a bit more power hungry than simple FSK (Frequency Shift Keying) transceivers because of DSSS (Direct Sequence Spread Spectrum), but they offer better robustness and better interoperability compared with FSK. Of course, the data rate is not sufficient to carry video data in ambient applications, but it could well convey pre-processed data, e.g. from a camera system that detects when a person is moving or falling. The IEEE 802.15.4a alternate PHY may add another interesting flavour to BSNs in the not-too-distant future. Worldwide interest in ZigBee-/IEEE 802.15.4-compliant products will inspire global creativity and keep costs down.

In [27], the authors present a usage scenario on wireless vital sign monitoring using IEEE802.15.4a standard. The 15.4a piconet is composed of one piconet controller (PNC) and a number of vital-sign sensors attached to the patient. The PNC, which plays the role of a data aggregator, is located at bedside; thus, the distances between the PNC and the sensors are generally shorter than 2 meters. Vital signs typically monitored in a patient's body can be categorized into two types: one type corresponds to continuous data, that is, data information (such as ECG) continuously transmitted from a sensor, and the other type corresponds to routine data, which is generated sporadically from the sensors including body temperature (BT), oxygen saturation (SpO2), and blood pressure (BP). For the continuous data type, wireless transmission which supports delay QoS maintenance is required because ECG waveform is a streamed data signal.

4 Satellite Issues in Telemedicine Applications

A satellite link raises several issues in a network deployed for telemedicine applications. Some of them may have a multifold impact on the biomedical signal in terms of: receive signal quality; signal reconstruction algorithm performance; quality of service (QoS) performance.

In the following, the focus will be placed upon, (i) the satellite channel itself in relation with propagation impairments in high frequency bands, and the nature of errors occurring in a satellite link; (ii) QoS issues with a special emphasis on performance requirements related to the transmitted IP-based traffic usable in telemedicine applications, (iii) and quite significant issues related to the TCP (Transmission Control Protocol) over the satellite link. The discussion is limited to geostationary satellites.

4.1 The Satellite Channel Issue

The satellite channel is a sensitive link in two respects:

- with regards to atmospheric impairments in high frequency bands, which can cause severe link outages;
- with regards to the error behavior, bit errors tending to cluster in bursts. An analysis and a thorough characterization of error patterns are required in order to assess the impact of bit errors on higher layers protocols.

These two aspects are detailed in the following.

Channel Impairments in High Frequency Bands: In high frequency bands above the Ka band, tropospheric effects in the satellite propagation channel may be strong, and thus detrimental to communications. Two categories will be considered [19]:

- Atmospheric attenuation due to gas, water vapor, clouds, the melting layer, and rain, the rain component being the prevailing factor for percentages of time lower than 1% (cf. figure 2). The rain attenuation component results in slow signal fading variations and can yield a magnitude of 20 dB for 0.05 % of an average year in Ka band. It represents the most serious limitation to the performance of satellite communication links in the millimeter wave domain. In addition, second order statistics of rain attenuation should also be taken into account in the design of a satellite communication system, since they directly relate to outage durations.
- Amplitude scintillation manifesting itself in the form of rapid signal fluctuations. Scintillation may impact the long term system availability (time percentages higher than 1%).

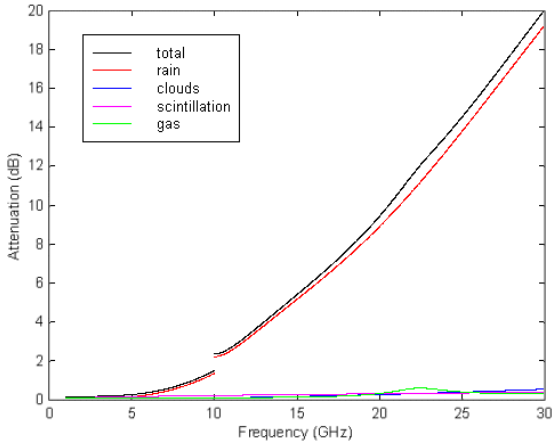

Fig. 2. Components of the atmospheric attenuation versus the frequency for 0.01% of the time

Channel Error Behavior Modeling: The numerous statistical propagation models that exist today for Ku band and above enable to estimate the degradation on a given link in terms of signal-to-noise ratio (SNR) C/N_0. Nevertheless, for new SatCom systems, C/N_0 loss does not directly relate to the degradation of the QoS offered to the end user. Thus, in

order to be able to obtain a sound estimation of the QoS information, it becomes necessary to resort to methods that link the channel with higher layers mechanisms or more QoS-oriented parameters. In this perspective, an analysis and a modeling of the satellite channel error behaviour are also required.

a) Parametric analytical models: A first approach in that direction lies upon parametric analytical models. Most of the models built for the wireless fading channel use discrete-amplitude and discrete-time Markov chains, among which the two-state Gilbert model is a well-known one [33]. It was demonstrated that the error pattern can have a considerable impact on the performance of protocols at higher layers such as TCP or any ARQ-typed retransmission protocols [29], especially when errors occur in bursts. Combined with a broadened definition of outage events, different from the conventional definition as the exceeding of a threshold by a first order statistical parameter (such as the BER [Bit Error Rate] or the PER [Packet Error Rate] [35]), or with a peculiar framing strategy (for instance interleaving) [33], N-state Markov models enable to capture the intrinsic bit errors correlation and derive accurate predictions of the system performance when N increases.

b) Error performance methodology for ATM (Asynchronous Transfer Mode) by satellite after the ITU-R Rec. S.1062-1 WP-4B: The ITU-R Rec. S.1062-1 WP-4B constitutes a second approach towards the goal expounded above, that is, linking higher layers performance parameters to the physical layer parameters [3]. The recommendation defines a specific methodology to be applied when designing a satellite system using ATM with the purpose of satisfying the G.826 recommendation which addresses physical layer performance. The S.1062-1 WP-4B recommendation also links ITU I.356 QoS parameters at ATM layer with higher layers QoS parameters. It can be considered that the ITU-R S.1062-1 WP-4B recommendation provides a fruitful methodological framework for linking performance parameters located at different levels. These relations have been exploited in other contexts and studies [7, 8]. A same type of methodology should also be applied to assess the error performance of satellite links, and their deep and maybe subtle impacts on higher layers protocols such as TCP, which will directly translates into a level of biomedical signal restitution quality in our case of interest.

- *Errors model:* In order to properly study error performance in a satellite link, a valid model of error statistics is required. The most common model is that of random errors in which a sequence of statistically independent bits is observed from two possible Bernoulli outcomes: “errored” or “non-errored”. The number of errors during the observation period then follows a binomial distribution, but if the observation period is quite long and the bit error probability is very low, it can also be characterized by a Poisson distribution.
- *Statistical characterization of error bursts using lattice diagrams:* The random errors model is inappropriate when errors occur in bursts mainly because of the memory introduced by signal processing techniques in communication systems. It is possible to statistically characterize the patterns of the errors bursts (times and inter-arrival times of the bursts) at the output of the decoder by means of the lattice diagram of the coder, by invoking the concept of transfer function (Viterbi) of the convolutional code, and using an algorithm

that systematically and exhaustively collects all patterns of burst errors. The approach can be extended so as to characterize the effects of the scrambler, the descrambler, the interleaver and the concatenated coding, which are processes that are commonly used in DVB-RCS satellite communications.

- *Generic models of burst errors:* The characterization methods presented previously are specific to a particular coding scheme. Consequently their interest is limited for globally evaluating the performance parameters of digital satellite links. Therefore more generic models are based on a small number of statistical quantities such as typically the average length L of the bursts and the average number of errors per burst. Burst errors are generally assumed to follow a Neyman-A contagion distribution.

4.2 QoS Issues

For satellite communications, one of the most critical requirements is to provide the desired QoS level to the different services. The discussion will focus on IP applications. The QoS issue should be dealt with addressing the diverse network layers and the QoS architecture, and assessing the application and network behaviour. In addition to classic QoS metrics [16], subjective metrics should also be introduced in order to evaluate the IP applications from a user point of view, such as PSNR (Peak Signal to Noise Ratio) and MOS (Mean Opinion Score) [28]. The data to be transmitted is characterized mainly in terms of bit rate, overhead, error rates (BER [Bit Error Rate], or PER [Packet Error Rate]), delay, jitter, average and maximum packet sizes. In the following, two types of services are considered and their salient QoS features will be presented along with a number of constraints from higher layer protocols [20, 21, 22]: real-time applications; data-like loss-sensitive, but not or very little delay-sensitive applications.

QoS Requirements for Basic Applications

a) Real-time applications: A first typical real-time commonly required service is VoIP, which is a delay-sensitive but very little loss-sensitive application. A VoIP call is expected to be intelligible. A strictly minimum bit rate of 5.3 kbps (assuming ITU H.323 G.723.1 ACELP [Algebraic Code Excited Linear Prediction] codec) is required. It has been shown however that optimal bandwidth occupation for VoIP over satellite is around 12 kbps. VoIP bit rate also varies depending on the codec, on whether RTP (Real-Time Protocol) is compressed, and on the redundancy introduced by the headers of the protocol suite (Ethernet, IP, UDP [User Datagram Protocol], RTP). The bit rate can thus be considered to range between 5.3 and 13 kbps. A minimum MOS requirement of 3.5 ensures a good voice quality. Moreover, ITU-T G.114 Recommendation [12] specifies a maximum latency value of 150 ms for one-way VoIP communications. Lastly, in terms of packet corruption and loss, some experiments have shown that the satellite link is quite robust to packet corruption in clear sky or moderately degraded channel environment up to a BER of 10^{-5} (that is, Frame Erasure Rate or FER of 2%) [25].

A second type of real-time services concern video applications. These applications range from real time communications to surveillance, Internet video streaming, as well as collaborative scene visualization, broadcasting and virtual meetings. Although QoS constraints are strongly dependent on the application considered, the following QoS specifications can be used as a baseline for video services [23]: the variable average bit rate allocated to a video application shall not be lower than 256 kbps in the two ways. Critical applications such as telemedicine require a fairly good video quality. The maximum transmission delay should be lower than 400 ms. The video codec which is used (for instance H.323) should be able to provide a good picture quality for telemedicine applications. A video connection should be established in less than 30 s for high priority applications.

c) Data-like loss-sensitive, but not or very little delay-sensitive applications: In this category are for instance SMS (Short Message Service) / MMS (Multimedia Messaging System), email applications, file exchange and Internet browsing. The transmitted mean bit rate must be at least 32 kbps for Web browsing and file exchange, and 200 kbps for email applications [31]. BER values of up to 10^{-6} can be supported [31]. Moreover, the time interval between the sending of an SMS and its reception by the receiver must be between 6 and 8 s in average, given that actually 98% of sent SMSs are successfully delivered by a mobile user to a fixed network within a 5-s time period, according to some telecom operators [4, 5]. Since the integrity of SMS messages is 100%, it is obvious that SMSs are well fitted to telemedicine communications, especially in emergency situations [20, 21, 22], where there is a need to transmit an alarm.

c) Other QoS issues: Another crucial QoS optimization method consists in properly handling and managing data traffic, especially when different services are aggregated. Differentiated services QoS architecture has received much attention these last years as traffic flows are of mixed categories (TCP flows and UDP flows for instance). By assigning each IP packet a specific traffic class, a more optimized management buffer is made possible resulting in improved bandwidth resource utilization. In particular, if excess TCP and excess UDP were both treated equally, TCP flows would reduce their rates on packet drops while UDP flows would not change, and instead monopolize the entire excess bandwidth [2]. All this leads to proper buffer management associated with efficient dropping strategies.

4.3 Issues Related to TCP over the Satellite

TCP is the most widely used Internet transmission protocol located at the OSI transport layer. TCP allows an end-to-end flow control mechanism between a sender and a receiver on the Internet with acknowledgments (ACKs) being sent back by the receiver to the sender, and to vary the transmission packet rate based on the rate at which acknowledgements are received back from the receiver. This mechanism enables to verify the correct delivery of data between a client and a server. TCP supports error or data loss detection, and implements a retransmission technique until the packets sent

are correctly and completely received [26]. It also implements a network congestion control. All these TCP features make it a reliable and efficient transport protocol over the Internet stack, independently from the applications above it and the Internet below it. Moreover, the Internet is quite a particular network because it consists of different network topologies, bandwidth, delays and packet sizes. The satellite link possesses inherent characteristics that may have negative impacts on the TCP. Two of them are mentioned here:

- Transmission errors: satellite channels are much more prone to bit errors than typical terrestrial networks. A characterization of the burst errors in satellite links has been given in section §IV.A.2. TCP assumes that all packet drops are caused by network congestion to avoid congestion collapse [27].
- Latency: latency is due to propagation delay, transmission delay, and queuing delay [9]. Of course, the round trip time (RTT) propagation delay of about 275 ms in geostationary links is the prevailing term. The dominant addition to the end-to-end one way latency will be roughly 300 ms of fixed propagation delay [9]. This delay mainly impacts some of the TCP congestion control algorithms. Originally, the TCP protocol suite was designed for a terrestrial environment with short transmission delays that seldom exceed 250 ms [1]. When applied to a geostationary satellite link, TCP performs poorly due to the long latency introduced between a ground Earth station and the satellite. Latency calls for protocol-specific acceleration.

Hence, the use of TCP over the satellite raises important issues to be pondered. Two of them deserve special attention and are tackled in the following [6, 9].

Capacity, Latency and Congestion: TCP is responsible for flow and congestion control, ensuring that data is transmitted at a rate consistent with the capacities of both the receiver and the intermediate links in the network path. Since there may be multiple TCP connections active in a link, TCP is also responsible for ensuring that a link capacity is responsibly shared among the connections using it. As a result, most throughput issues are associated to TCP. Four congestion control mechanisms exist in TCP: slow start, congestion avoidance, fast retransmit before the RTO (Retransmission Time-Out) expires, fast recovery to avoid slow start [26].

The basic principle of the TCP protocol congestion mechanism can be summarized as follows [9]: a congestion window is initialized to a value of one segment upon connection startup. It determines the TCP sending rate. During the slow start phase, the congestion window doubles every round trip time (RTT), until congestion is experienced due to a data packet loss. The congestion avoidance phase is entered upon detection of congestion. Then TCP retransmits the missing segment, and the window is emptied down to its half content. If retransmitted packets happen to be lost again, the TCP sender is forced to retransmit the missing packets, but this is done with an imposed timeout where slow start is resumed and the window is reduced to one segment [26]. Consequently, the throughput becomes very low. Congestion control mechanisms in TCP thus degrade the performance of individual TCP connections over satellite links because the algorithms slowly probe the network for additional capacity, which in turn wastes bandwidth. Indeed, the satellite latency which can easily exceed 2000 ms is seen as evidence of a congested network or packet loss and thus TCP will not increase the rate at which it sends packets, even though there is no actual congestion or packet loss across the satellite link [1].

TCP Acceleration and the Security Issue: Several techniques to accelerate TCP exist. Performance Enhancing Proxies (PEPs) are one of them and basically involve an alteration of the TCP header data before and after the satellite link in order to hide the high latency of the satellite link from the TCP session [1]. Examples of PEP techniques are TCP spoofing and TCP multiplexing (also known as cascading TCP or split TCP). TCP spoofing consists in shortening the delay path and thus bypassing slow start, by adding a spoofing device/software (e.g. a rooter near the satellite link) which is in charge of returning ACKs to the sender, and in the meantime suppressing the ACKs from the receiver [1, 26]. The spoofing device also retransmits any segments lost and contains storage buffers. The TCP multiplexing technique accelerates data transfer rates across the satellite link by converting a single TCP sessions into several parallel TCP sessions. At the receive side, all TCP sessions are recombined into a single session [1].

Problems arise when TCP acceleration is achieved simultaneously with security by means of a VPN (Virtual Private Network) in the tunnel mode. Assuming that the data packets enter the VPN tunnel before TCP is accelerated, one is left with TCP packets entirely encrypted and the header of which cannot be altered anymore, or otherwise the authentication safeguards would be violated [1]. TCP multiplexing technique alone is compatible with VPN, but the processing must not take place inside the satellite modem. In addition, a number of performance degradation factors appear with the technique.

All these performance and security issues associated with TCP acceleration have led to the development of a number of proprietary solutions to optimize the bandwidth resource and utilization for TCP over satellite. Among these, the End II End's patent-pending Broadband Network Optimization (BNO) [1] and UDcast solutions are worth to be mentioned [3].

With the revised, mobile version of the DVB-RCS standard, called DVB-RCS+M [6] as well as with the recent DVB-RCS2 standard, which both use the DVB-S2 waveform and ACM feature for the return channel, other optimization issues over a satellite link would also need to be discussed. In particular, IP encapsulation efficiency depending on the encapsulation technique employed, whether it be MPE, GSE or ULE, should be investigated for the return link as for the forward link [11].

5 Conclusion

In this paper a reflection on some issues related to the use of hybrid wireless / satellite links in the field of telemedicine was conducted. At the starting point of our reflection, was our interest in the analysis of the performance of a combined PG-AR signal reconstruction algorithm we proposed to apply in order to remedy the problem of missing ECG samples at the user-end side. We started from the crude observation that along the transmission chain there were data errors and/or loss that could occur anywhere and anytime, and that was our motivation to investigate more thoroughly the multiple causes of such errors and loss from a pure network and telecommunication point of view.

First, the context was presented with telemedicine projects (U-R-SAFE and OURSES) which enabled us to highlight some issues still open with respect to performance criteria having significant implications in health-care applications, in terms of, for example, packet error rate, energy consumption at the nodes, bandwidth occupation, etc.

Furthermore, due to the multifold impact of the telecommunications and networking issues on biomedical signals, a special emphasis was laid on design constraints in a wireless network architecture, then on the satellite channel itself which can be strongly impaired in high frequency bands, and causes errors of a particular kind. QoS issues such as that of performance requirements as to the transmitted IP-based traffic usable in telemedicine applications, and quite significant issues related to the TCP (Transmission Control Protocol) protocol over the satellite link were also surveyed. Indeed, strong propagation channel impairments requiring efficient adaptive strategies, transmission errors occurring in bursts, and high latency due to the geostationary Round Time Trip (RTT) are the three main drawbacks of the satellite path in high frequency bands. These factors combine together making data errors or packet loss very likely, which we know to be quite critical in telemedicine applications, in that human lives closely depend on high quality biomedical signal reception, and correct diagnoses.

This paper only explored a few well known networking and telecommunication issues from a qualitative point of view for telemedicine applications. The complex connections between the two worlds of telemedicine on one side, and networking and telecommunications on the other side still remain to be investigated in more details from a quantitative perspective. This will be carried out in a forthcoming paper.

References

1. Anderson, T.J.: TCP/IP over Satellite: Optimization vs. Acceleration, End II End Communications, Inc. White Paper (April 2005)
2. Durresi, Kota, S., Goyal, M., Jain, R., Bharani, V.: Achieving QoS for TCP traffic in Satellite Networks with Differentiated Services. Journal of Space Communications 17(1-3), 125–136 (2001)
3. Brandão, J.C., Pinto, E.L., Maia, M.A.G.: A Review of Error Performance Models for Satellite ATM Networks. IEEE Communications Magazine, Broadband Satellite Network Performance 37(7), 80–85 (1999)
4. ETSI, Digital cellular telecommunications system (Phase 2+); Universal mobile telecommunications system (UMTS); Technical realization of short message service (SMS) (3GPP TS 23.040 version 5.8.1 Release 5) (October 2004)
5. ETSI, TR 102 444 V1.1.1: Analysis of the short message service (SMS) and cell broadcast service (CBS) for emergency messaging applications; emergency messaging; SMS and CBS (February 2006)
6. ETSI, EN 301 790 V1.5.1: Digital Video Broadcasting (DVB); Interaction channel for satellite distribution systems (May 2009)
7. Hashimoto, A.: Outage Probability Analysis in Relocatable Wireless Access Systems under Line-of-Sight Non-Rayleigh Fading. IEICE E80-B(5), 746–754 (1997)

8. Hashimoto, A.: Error Performance and ATM Cell Transfer Characteristics in Relocatable Wireless Access Systems. Proceedings of the IEICE E81-B(6), 1213–1223 (1998)
9. Henderson, T.R., Katz, R.H.: Transport Protocols for Internet-Compatible Satellite Networks. IEEE Journal on Selected Areas of Communications (1999)
10. Inigo, P., Durin, B., Girault, N., Verelst, G.: OURSES: Medical assistance over Satellite. In: IWSSC 2008 (2008)
11. Jegham, N., Girault, N., Le Guern, C., Roussel, G., Lohier, S., Beylot, A.-L.: VoIP over a DVB-S2 ACM link. In: IWSSC 2008 (2008)
12. ITU-T, G.114 Recommendation: Transmission systems and media, general recommendations on the transmission quality for the entire Internet telephone connection: One-way transmission time, number 114 in G. ITU-T (2000)
13. Ganesan, D., Govindan, R., Shenker, S., Estrin, D.: Highly-resilient, energy efficient multipath routing in wireless sensor networks. Mobile Computing and Communication Review 1(2), 28–36 (2002)
14. Girault, N., Jegham, N., Lerouge, N., Le Guern, C., Beylot, A.-L.: OURSES: Efficiency of IP Encapsulation over DVB-S2 Links. In: IWSSC 2008 (2008)
15. Kacimi, R., Dhaou, R., Beylot, A.-L.: Load-Balancing Strategies for Lifetime Maximizing in Wireless Sensor Networks. In: IEEE International Communications Conference (IEEE ICC 2010), Cape Town, South Africa, May 23-27 (2010)
16. Kota, S., Marchese, M.: Quality of service for satellite IP networks: a survey. International Journal of Satellite Communications and Networking 21, 303–349 (2003), doi:10.1002/sat.765
17. Mailhes, Castanié, F., Henrion, S., Lareng, L., Alonso, A.: The URSAFE telemedicine project: improving health care of the elderly. In: European Federation for Medical Informatics (MIE 2003), Saint Malo, France (2003)
18. Mailhes, Prieto-Guerrero, A., Comet, B., De Bernard, H., Campo, E.: Telemedicine Applications in OURSES Project. In: International Workshop on Satellite and Space Communications (IWSSC 2008), Toulouse, France (2008)
19. Pech, P.: Incidence de la prise en compte des effets de techniques de mécanismes de lutte contre les affaiblissements (FMT) en bande Ka sur la gestion des ressources dans un système d'accès multimédia par satellite géostationnaire, Ph.D dissertation, Supaero, Toulouse, France (Décembre 19, 2003)
20. Pech, P., Huang, P., Bousquet, M., Robert, M., Duverdier, A.: Simulation of an Adaptive Strategy Designed for Low Bit Rate Emergency Satellite Communications Links in Ku/Ka/Q/V Bands. In: International Workshop on Satellite and Space Communications 2009 (IWSSC 2009), Siena-Tuscany, Italy, September 10-11 (2009)
21. Pech, P., Huang, P., Bousquet, M.: Low Bit Rate Satellite Link for Emergency Communications. In: International Workshop on Satellite and Space Communications 2008 (IWSSC 2008), Toulouse, France, October 1-3 (2008)
22. Pech, P., Robert, M., Duverdier, A., Bousquet, M.: Design and Simulation of a DVB-S2-like Adaptive Air interface Designed for Low Bit Rate Emergency Communications Satellite Link in Ku/Ka/Q/V Bands. In: Diodato, N. (ed.) Satellite Communications, ch. 9. Sciyo, Rijeka (September 2010), http://sciyo.com/articles/show/title/design-and-simulation-of-a-dvb-s2-like-adaptive-air-interface-designed-for-low-bit-rate-emergency-co
23. Pech, P.: Liaison bas débit par satellite pour les situations d'urgence. Study report for work package 2, release 2.1, TeSA/CNES, June 8 (2009)

24. Prieto-Guerrero, A., Mailhes, C., Castanié, F.: Lost Sample Recovering of ECG Signals in e-Health Applications. In: Proceedings of the 29th Annual International, Conference of the IEEE EMBS, Cité Internationale, Lyon, France, August 23-26 (2007)
25. Nguyen, T., Yegenoglu, F., Sciuto, A., Subbarayan, R.: Voice over IP Service and performance in satellite. IEEE Communications Magazine 39, 164–171 (2001)
26. Sun, Z.: Satellite Networking. Principles and Protocols. John Wiley & Sons (2005)
27. Takizawa, K., Li, H.-B., Hamaguchi, K., Kohno, R.: Wireless Vital Sign Monitoring using Ultra Wideband-Based Personal Area Networks. In: IEEE EMBS, Lyon, France (2007)
28. Tou, Gineste, M., Gayraud, T., Berthou, P.: Quality of Service Evaluation in Satellite Systems. In: IWSSC 2008 (2008)
29. Web site of UDcast, http://www.udcast.com/
30. Wang, Wang, L., Huang, B.-Y., Wu, D., Lin, S.-J., Zhang, Y.-T., Chen, W.: A Low-Complexity Medium Access Control Framework for Body Sensor Networks. In: IEEE EMBS, Minnesota, USA (2009)
31. WISECOM – Deliverable 1.1-1: Survey of use cases, contract number 034673 (August 9, 2007), http://www.wisecom-fp6.eu/deliverables/D1.1-1_Survey_of_Use_Cases.pdf
32. Yang, G.Z.: Body Sensor Networks. Springer, London (2006)
33. Zorzi, M., Rao, R.R.: Impact of Burst Errors on Framing. In: PIMRC 1998, Boston, U.S.A. (September 1998)
34. Zorzi, M., Rao, R.R.: Performance of ARQ Go-Back-N protocol in Markov channels with unreliable feedback. Wireless Networks 2, 183–193 (1997)
35. Zorzi, M.: Outage and Error Events in Bursty Channels. IEEE Transactions on Communications 46, 349–356 (1998)

Content Delivery in Hybrid Networks Using SatTorrent

Bernd Klasen*

SES ASTRA TechCom, Chateau de Betzdorf, Luxembourg
research@berndklasen.de

Abstract. The global Internet traffic is constantly increasing and consistently reaching the limits of capacity. Commonly this is challenged by upgrading the infrastructure. Alternatively this can be achieved by utilizing existing facilities more efficiently. Using a hybrid network that efficiently combines unicast and broadcast delivery can reduce Internet traffic, server loads and download durations significantly. In order to substantiate this paper introduces and evaluates the payload broadcasting facility of SatTorrent, a peer-to-peer protocol optimized for hybrid networks. The results show that it fulfills our expectations while inducing only a comparatively small amount of additional broadcast traffic.

Keywords: content distribution, peer-to-peer protocols, sattorrent, distributed systems, network performance.

1 Introduction

The degree to which the Internet and online services pervade our every day life reached a high level and is still increasing. Contemporaneously the bandwidth demand is rapidly growing. If no measures are taken, this leads to congestion and to delayed or failed transfers [11] [6]. One possibility to encounter this problem is to constantly extend the infrastructure. However, this is economically and ecologically not an optimal solution. Much better would be to use the existing infrastructure more efficiently, if possible. The most important traffic drivers in todays Internet usage are—according to studies by [12] and [2]—mainly video content and peer-to-peer (P2P) downloads. Both share common properties: The files transmitted are rather big in size and the same data is often repeatedly transferred to numerous recipients [4], [5], [9] and [8]. For delivering the same content so many recipients broadcast networks such as satellites are well suited. Additionally they provide scalability and great geographical coverage. This work will show that using a hybrid network of satellites and Internet in combination with SatTorrent, a peer-to-peer protocol optimized for hybrid networks—which is presented in section 3. Thereby knowledge of the BitTorrent protocol (see [7], [16]) is postulated.

* Funded by *National Research Fund* (FNR) of Luxembourg.

R. Dhaou et al. (Eds.): PSATS 2013, LNICST 123, pp. 65–76, 2013.

2 Content Distribution Model

The content distribution model relies on the existence of a hybrid network which is composed of a unicast and broadcast network. Precisely, we assume these two networks to be the terrestrial Internet infrastructure and a satellite network. In principle also other broadcast channels can be used with this approach. The decision for satellites has been taken because they combine good scalability, high bandwidth and outstanding geographical coverage. Most satellite reception hardware currently on the market—e.g. set-top-boxes, television sets with integrated satellite receivers—already provides Internet connectivity and thus the required infrastructure is already in place. However,currently both networks are utilized either in an mutually exclusive manner—watch e.g. either YouTube videos via Internet or HD movies via satellite—or in a way that the Internet channel is used to provide additional information to the broadcasted content. In contrast to these existing solutions, the proposed hybrid network approach uses both networks in conjunction, where delivery of arbitrary content can be dynamically assigned to either of them.

Due to the large fraction of P2P Internet traffic, a P2P protocol is a natural choice to implement our model. This selection is amplified by the ability for substitution of video streaming traffic by P2P streaming even for real time delivery [17] [13]. Among the numerous P2P protocols, BitTorrent was chosen as a basis. This decision has been taken not only because it is the most successful P2P protocol in use, it further employs a tracker as a central entity that obtains an overview of the number of active downloaders. This exactly matches SatTorrent's need for a global entity that is able to decide on what files respectively pieces should be broadcasted and which not. Further details are explained when we introduce SatTorrent in section 3. A more exhaustive description of the content distribution model and exemplary usage scenarios can be found in previous work [9].

3 SatTorrent Protocol

The SatTorrent protocol is an extension of the popular BitTorrent protocol. This paper first provides an overview about the basic protocol functioning and those aspects that have been previously introduced in [10] and then concentrates on the newly developed features.

SatTorrent utilizes broadcast networks—e.g. satellites—as additional distribution channel for P2P data. Thereby it supports two operation modes: Broadcasting metadata only and broadcasting payload, the latter being a superset of the former. The metadata broadcast approach is capable to reduce the number of messages in the unicast network while at the same time consuming only a minor amount of satellite bandwidth. This is achieved by broadcasting those messages that contain information that is needed by a large number of peers, such as bitfield and have messages or tracker responses to GetRequests. Not only does this save messages but further increases the information each individual peer

is provided with. As a result peers gain a global knowledge about the overlay network and thus are able to choose the best exchange partners. The notable reduction of message complexity and Internet traffic that can be achieved by this approach has been analyzed and the result been presented in [10].

This paper proceeds this work and sheds light on the payload broadcast mode. Since the payload transmission—which is carried by peer wire messages of type *piece*—makes up the largest fraction of the overall traffic, shifting the corresponding piece-messages to the satellite broadcast can be assumed to lead to a much more significant traffic reduction in the unicast network (Internet) than they have already been observed for metadata broadcasts in [10]. As already mentioned in section 2, the tracker plays an important role in the SatTorrent operation. On the one hand it is the central entity where information about peers is aggregated, on the other hand it has to initiate the message broadcasts. The following paragraph introduces the procedural method that is applied in order to conform to this role.

As its ancestor—the *BitTorrent tracker*—the SatTorrent tracker is the first contact point for peers starting a download before they are able to connect to a P2P overlay network and it keeps track of all active peers, which are downloading those files it is responsible for. Let the number of files managed by the tracker be N and the the aforementioned set of files F be defined as $F = \{f | f \text{ is handled by this tracker }\}$. Each file $f \in F$ consists of a specific number of pieces (or chunks) so that $f = \{c | c \text{ is a piece of } f\}$. Further for each $f \in F$ the corresponding tracker holds a list of peers which is defined as $P^f = \{p | p \text{ is currently downloading } f \in F\}$. Further, for each peer known by the tracker, it stores a vector V^p containing the necessary information about peer p. This information includes the peer's IP address, the port it is listening on and its ID. So far, this is identical to the information that the BitTorrent tracker stores. For a SatTorrent tracker each V^p contains additional information about the corresponding peer. This is stored in the fields *location*, *sat-enabled* and *bitfield* which are explained in the following.

The *location* information is used for the location awareness feature of the SatTorrent protocol as well as to allow the tracker to identify the corresponding satellite that can be used in order to reach a specific peer. The latter is needed since one satellite can not reach all locations on earth. However, to avoid unnecessary complexity which would hinder the understanding of the concept, in this paper we speak of a *broadcast* even in cases where the same content needs to be broadcasted over more than one satellite in order to reach all nodes. In fact the results presented in [14], [3] and [1] show that content popularity tends to be rather geographically localized and thus in the majority of cases one broadcast using a single satellite is supposed to be sufficient.

The *sat-enabled* entry is a boolean value reflecting the ability of a peer to receive satellite broadcasts. Even if it might be desirable to have all participating peers equipped with the satellite reception hardware, this can not be expected. Therefore the SatTorrent protocol must support heterogeneous peer configurations with peers that can not receive broadcasts. As we will see in section 4,

Algorithm 1. Determining piece broadcasts

```
1: for all f ∈ F do
2:     for all c ∈ f do
3:         counter ← 0
4:         for all p ∈ P^f do
5:             if b(f, p, c) = 0 & s(p) = 1 then
6:                 counter ← counter + 1
7:             end if
8:         end for
9:         if counter ≥ BT then
10:            Broadcast piece c
11:        end if
12:    end for
13: end for
```

also non sat-enabled peers take profit of the SatTorrent protocol by means of a reduced download duration even for low ratios of sat-enabled peers.

In this context we define the following function:

$$s(p) = \begin{cases} 1, & \text{if peer } p \text{ is sat-enabled} \\ 0, & \text{otherwise} \end{cases} \tag{1}$$

The last additional entry stored by the tracker is the *bitfield*. This is a list of bitfield information for every file downloaded by a specific peer. We define B_p^f as the bitfield of peer p for file f and the function

$$b(f, p, c) = \begin{cases} 1, & \text{if } p \in P \wedge p \text{ has piece } c \in f \\ 0, & \text{otherwise} \end{cases} \tag{2}$$

Having this information, a tracker will trigger a broadcast for piece c of file f only if

$$\sum_{i=0}^{|P^f|-1} (b(f, p_i, c) \cdot s(p_i)) \geq BT \tag{3}$$

BT is a threshold which must be exceeded in order to trigger a piece broadcast. It denotes the required number of peers that potentially have a demand for the specific piece. The exact value of BT depends on numerous parameters such as for example the available satellite bandwidth, the cost comparison between Internet delivery and broadcast and whether there is a competitive situation of several broadcast attempts that can not all be served within an acceptable time frame. Narrowing down this threshold for a specific scenario is not subject of this paper. Instead we evaluate the performance of SatTorrent under varying values of BT and present the corresponding results in section 4. The procedure that a tracker periodically executes in order to determine the pieces that are suitable for a broadcast is illustrated as pseudo code in algorithm 1. For each piece of

every file it counts the number of peers that are downloading the corresponding file but still do not possess that piece. After this has been evaluated for all files, those pieces where the number of demanding peers exceeds BT are passed to the uplink station for broadcast. In current implementation there is no bound for the amount of data that the tracker is allowed to send to the uplink. However, the latter has only a limited satellite bandwidth at its disposal. Currently we just monitor the broadcast queue in order to detect congestion or under utilization. Future implementations will have a feedback mechanism that triggers an adjustment of BT at the tracker according to the satellite load.

Before we examine how peers handle broadcast messages we must clarify how the information vectors V^p respectively is the information that is used by algorithm 1 is maintained? Most of it is sent from a peer to the tracker with the initial GetRequest when it starts downloading a file and is seldom changed afterwards. *ID*, *IP address*, *port* and *sat-enabled* do not change frequently. Also the *location* does only change for mobile clients. However, the *bitfield* entry must be updated immediately when a peer's bitfield changes, as becomes obvious by its central role in the piece broadcast algorithm presented above. In order to achieve this, whenever a peer receives a *piece message*—besides of updating its own local bitfield—it also sends an extra *have message* to the tracker, who in turn updates the corresponding bitfield. It is worth noting that although this puts additional messages on the unicast network, the total number of *have messages* is much smaller compared to BitTorrent as we will show in section 4. This is due to the *have message suppression* feature of SatTorrent which does not only avoid *have messages* to peers that are known for already possessing this piece—as the equally named BitTorrent feature does. It further is able to eliminate *have messages* whose recipient is sat-enabled. The have messages to sat-enabled peers are substituted by metadata broadcasts (see [10]).

A peer that receives file pieces by broadcast stores them and immediately cancels all potentially pending requests for these pieces and sends updated interest status messages to the connected peers accordingly. Since each sat-enabled peer can potentially receive all piece broadcasts, no matter whether it is downloading the corresponding file or not, different modes for handling this data are provided. Either a peer can only store data for files it is downloading or it might store all data for potential future downloads. Another possibility is to apply collaborative filters, use recommendations, ratings and personal preferences in order to identify those files that might be interesting and in consequence probably will be requested in the near future. Based on this the peer can make a decision on whether the data should be kept or withdrawn in case the file is not being downloaded. However, this feature is not implemented yet and subject of future work.

4 Evaluation

In order to evaluate SatTorrent's performance under varying conditions in comparison to BitTorrent and how parameters should be adjusted to obtain the best attainable results for a specific purpose, the protocol has been implemented

in a simulator. In order to ensure reproducibility of the achieved results, each simulation is unambiguously specified by a configuration file.

The scalability of the simulator is mostly limited by the memory consumption, which primarily depends on two factors, the number of peers and the size of the files that are to be exchanged. The former is obvious, the latter is due to the fact that every peer has to save the bitfields for all connected peers, while the size of that data structure is determined by the number of pieces a file is partitioned into and the number of files that are being downloaded. However, the piece size can not arbitrarily be increased since this causes performance degradation and thus quantity depends on the filesize. In order to increase the maximum number of peers and the size respectively the count of files that can be simulated, measures must be taken in order to reduce the memory demand as much as possible. One is the geographical limitation of the simulation. This means an assumption is made that all nodes reside within the same satellite footprint and thus when a broadcast is made, potentially all nodes can receive it (in case they are sat-enabled). Further an abstraction for the location awareness is made in a way that it determines the distance by means of autonomous system (AS) membership. In case two nodes are within the same AS they are considered being nearby, otherwise they are distant. We argue that the traffic within one AS—which in the majority of cases means that is also is within the same Internet service provider (ISP) network—comes with low cost and little delay. In contrast, traffic that is crossing AS boundaries is expensive for ISPs and has a higher probability for an increased delay. This coherence has also been highlighted in [15] who further find that the inter ISP network traffic is limiting the performance of P2P approaches since ISPs tend to throttle P2P traffic. Thus using location awareness to keep traffic within one AS as much as possible is reasonable.

Another measure to limit the simulation's complexity and its memory demand is a reduction of message granularity. In real SatTorrent traffic the peer wire messages of type *piece* do not carry a complete piece but a block of data of a piece. Thus one piece is submitted by several piece messages. However, using such a fine granularity for the simulation further increases the memory consumption and thus decreases the number of network nodes that can be simulated. Thus in the simulation a piece message always carries a complete piece. For a better distinction between real world piece messages carrying blocks and those in the simulator, we refer to the former as *block messages*. The rate in which piece messages are being sent has been adjusted accordingly. Further, since each peer wire message comes with a certain overhead, the number of blocks a piece is partitioned into must be considered in order to calculate the real bandwidth consumption of a piece message. The common block size used in most current BitTorrent client implementations is 16 kByte per block. Considering a piece size of 512 kByte, this results in 32 blocks per piece. The overhead per block message is 72 bit = 9 Byte. This means each piece message in the simulation generates a network traffic of $512kByte + 32 \cdot 9Byte = 524,576Byte$. Since the simulator counts only the number of piece messages, the results presented in this paper are adapted accordingly.

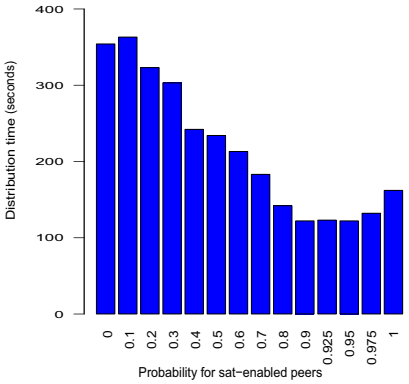

Fig. 1. Distribution time under different proportions of sat-enabled peers

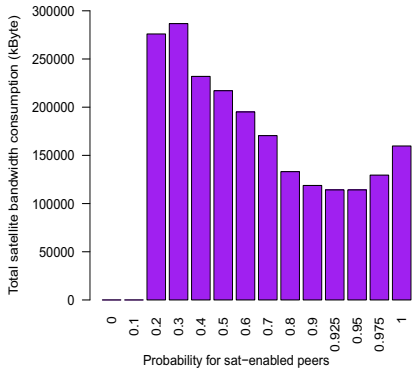

Fig. 2. Satellite bandwidth consumption for varying SSP

4.1 Specific Simulation Settings

Since it is not possible to describe each simulation parameter in detail, we will shortly discuss those settings which remain unchanged during all simulations but are important for the assessment of the results in this section. The parameters that are subject of the evaluation are described later in section 4.2. One of the parameters that are statically assigned is the satellite transponder bandwidth. Here we use a conservative value of 36Mbit. This is what even the older operational geostationary television satellites are capable of after deducting error correction (net bandwidth). Further, as already indicated above, a piece size of 512 kByte has been used. According to [16] this is a common value for BitTorrent and represents a good trade off between torrent-file size and efficiency for that protocol. In order to provide an equitable comparison between BitTorrent and SatTorrent—respectively the solely unicast delivery and a satellite broadcast aided approach—it is vitally important to apply the best possible settings for BitTorrent.

4.2 Results

As a first performance evaluation we compare the distribution time and the aggregated bandwidth demand for SatTorrent and BitTorrent. The latter is equivalent to SatTorrent without any sat-enabled peers. Since we do not expect to have 100% of peers being sat-enabled in a real world scenario, we analyze the results for a file of 20MB being distributed to 1000 peers with $BT = 150$ under varying number of sat-enabled peers. In the simulation settings we can provide the *SatelliteSupportProbability* (SSP) which denominates the probability of a joining peer for being sat-enabled. Figure 1 shows the distribution time for SSP ranging from 0.0 to 1.0. Since the curve progression changes between SSP=0.9 and SSP=1.0, more fine grained steps are provided within this interval. What we

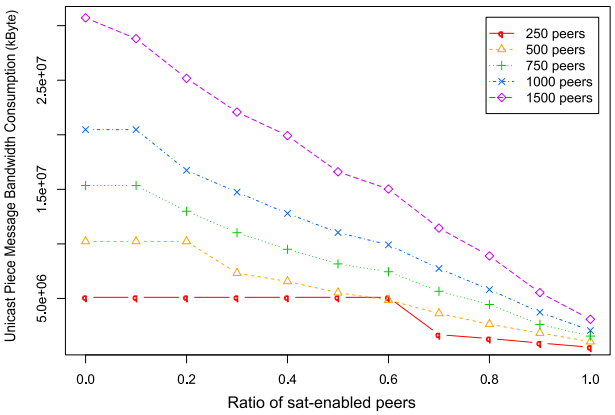

Fig. 3. Internet bandwidth consumption for different values of SSP

can see is a reduction of the distribution time for increasing ratios of sat-enabled peers except for settings where all or almost all peers are sat-enabled. This effect originates from the increased start delay for sat-enabled peers which have to wait longer for a tracker response on their get-requests. These metadata broadcasts are performed within fixed time intervals while non sat-enabled peers receive their answers immediately. This negative effect can be levelled out only as long as there is a reasonable number of non sat-enabled peers. However, it can probably be eliminated or at least be reduced by optimizing the tracker algorithm for handling get-requests from sat-enabled peers which is subject of future work. Another increase can be observed when the SSP changes from 0.0 to 0.1. The reason becomes clear by the results for the overall consumed satellite bandwidth shown in figure 2. For $SSP = 0.0$ there is obviously nothing broadcasted. The same applies for $SSP = 0.1$ since a sufficient number of sat-enabled peers is not reached in order to satisfy the condition given in equation 3. Thus only a small delay due to the metadata broadcasts which has been described above is introduced while the corresponding benefit—a reduced number of total unicast messages—is not reflected in these figures. At the same time, there are too little sat-enabled peers in order to take a considerable advantage of the metadata broadcasts. We will further discuss the characteristics of the satellite bandwidth demand under changing values of BT later when we make a comparison for different network sizes.

The major advantages of the payload broadcasts can be observed in figure 4 where the aggregated bandwidth consumption for the broadcasts and the unicast piece messages is shown. On the one hand we observe a monotonic decrease of total bandwidth demand for increasing values of SSP, on the other it manifests the high potential for reduction of unicast network traffic while at the same time allocating only marginal bandwidth on the broadcast network.

A further important aspect that must be analyzed is SatTorrent's performance for various sizes P2P networks, particularly smaller ones. Therefore the same file distribution has been analyzed for varying numbers of peers. In figure 3 and

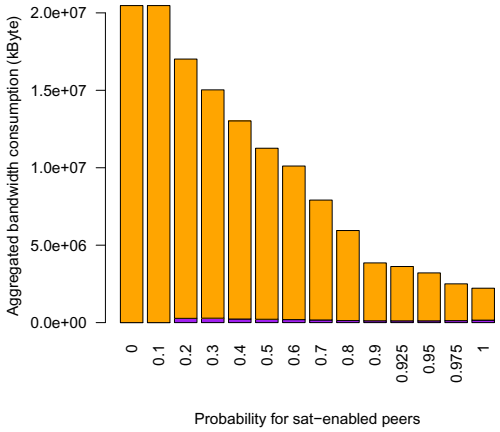

Fig. 4. Aggregated bandwidth consumption for varying proportions of sat-enabled peers

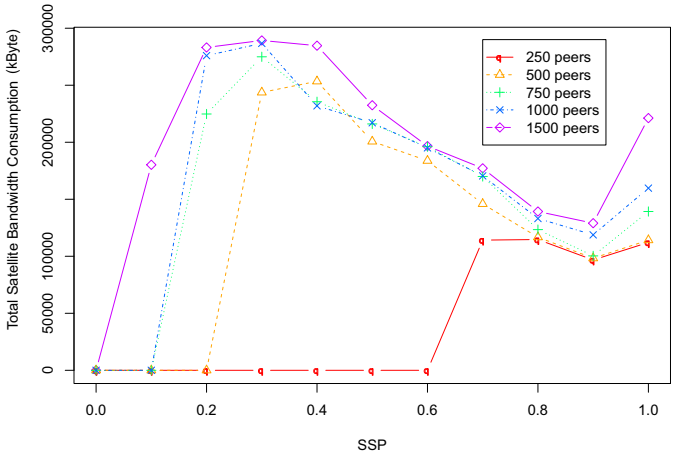

Fig. 5. Satellite bandwidth consumption for different values of SSP

5 we see the bandwidth consumption for different network sizes in the Internet respectively in the satellite network. The behavior with respect to the unicast messages (figure 3) is straightforward and satisfies our expectations: The bandwidth demand for payload delivery is continuously decreasing with the proportion of sat-enabled peers. The horizontal line segments in the plot reveal the only condition: The total number of sat-enabled peers must at least be equal or greater than the broadcast threshold, which is not surprising at all.

Even though the curves in figure 5 all exhibit a similar shape, their progression is by far less self-evident than the ones for Internet bandwidth consumption and

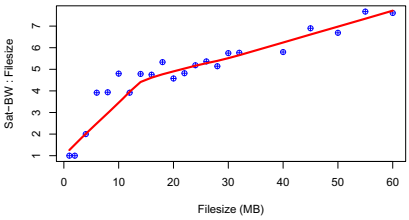

Fig. 6. Satellite bandwidth consumption relative to filesize

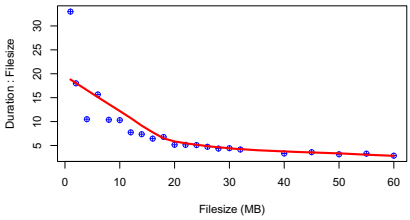

Fig. 7. Overall delivery duration in relation to filesize

takes a deeper investigation. First we observe a steep increase immediately after the SSP reaches a value that allows the number of sat-enabled peer to exceed the broadcast threshold BT. The fact that we observe a peak at $SSP = 0.3$ for network sizes of 750, 1000 and 1500 peers indicates that this high demand for satellite bandwidth is not depending on the absolute number of sat-enabled peers in relation to BT. The reason seems to be in the ratio between sat-enabled and non-sat-enabled peers. On the one hand peers that are able to receive pieces by broadcast don't wait idle for satellite transmissions but continuously exchange pieces with other peers in the network. On the other hand, the piece selection strategy leads to a uniform distribution of pieces at the peers. In consequence we might in many cases only scarcely fulfill the condition given in equation 3 even though the number of sat-enabled peers is twice or thrice as much as BT. With an increasing density of sat-enabled peers the probability that each piece broadcast is received by a larger number of peers that still need that specific part of the file grows, and thus the efficiency of the broadcast increases. The result are the decreasing curves we find after the peak.

This is true except for situations where all peers are sat-enabled. The main reason for this is the complete lost of non sat-enabled peers which are less restrictive in their behavior. Sat-enabled peers avoid connections to peers when they can not be sure about their usefulness. This leads to an increased time demand until the data has been completely delivered to all peers as we have already observed in figure 1. The positive aspect—which is not reflected in this figure—is that it also further reduces the unicast traffic. Whether this is desirable at this cost depends on the cost ratio between satellite and Internet bandwidth allocation and on the load situation on the satellite. However, there are two aspects that mitigate this undesired behavior. The first is that—as we discussed earlier—in a real life environment we will hardly ever reach a configuration where all peers are sat-enabled. Second, there is still room for optimizing the protocol parameters for $SSP = 1.0$ which will presumably reduce the bandwidth demand.

Next we investigate the impact of the file size on the performance of SatTorrent. For these measurements we simulated a distribution among 500 peers with $BT = 150$ and $SSP = 0.9$. The latter has been chosen since it delivered good results with respect to the time demand for the distribution as well as for the satellite bandwidth consumption. In general SatTorrent's performance can be

expected to increase with the size of the files being distributed since that also augments the probability to have many concurrent downloads. In consequence each broadcast can be received by a potentially higher number of peers which constitutes an elevated efficiency. By applying parameters that are nearly optimal also for smaller files we reduce the influence of other factors except file sizes in this measurement. The results can be seen in figures 6 and 7. The correlation between file size and the relative satellite bandwidth demand becomes obvious in figure 6. The decreasing gradient that we find here confirms our assumption of an increasing SatTorrent efficiency for larger files. The same applies for the relative distribution time that is decreasing with growing file sizes (see figure 7). At last SatTorrent has been analyzed under varying values of BT. The expectation that altering this parameter would have a significant effect on the distribution time and on the satellite bandwidth demand has not been confirmed. Evaluations show that the reduction in bandwidth demand at growing SSPs is rather small ($< 10\%$). However, we see great potential to achieve benefits from larger values for BT—adjusted relative to the file sizes—in conjunction with an improved piece selection strategy which is subject to future work. Further this might change in a competitive situation with several concurrent attempts to allocate satellite bandwidth.

5 Conclusion and Future Work

In this paper the payload broadcast feature of the SatTorrent protocol has been introduced. The evaluation that followed revealed its potential to reduce the traffic in the Internet by means of utilizing a comparatively small amount of satellite bandwidth. Further several aspects of SatTorrent have been observed which bear potential for improvement. The most important among these is the optimization of the piece selection strategy for sat-enabled peers and the further measures against the increasing satellite bandwidth demand for high ratios of sat-enabled peers. Besides that, the future work includes the study on how social network structures can be utilized to further improve the delivery. This includes file demand prediction as well as enhanced file exchange options that are based on the increased trust between nodes with small distances and strong connection in the social graph.

References

1. Backstrom, L., Sun, E., Marlow, C.: Find me if you can: improving geographical prediction with social and spatial proximity. In: WWW 2010 Proceedings of the 19th International Conference on World Wide Web, pp. 61–70. ACM, New York (2010)
2. Basher, N., Mahanti, A., Williamson, C., Arlitt, M.: A comparative analysis of web and peer-to-peer traffic. In: Proceeding of the 17th International Conference on World Wide Web, pp. 287–296. ACM (2008)

3. Brodersen, A.: YouTube Around the World: Geographic Popularity of Videos. In: WWW 2012 Proceedings of the 21st International Conference on World Wide Web, pp. 241–250. ACM, New York (2012)
4. Cha, M., Kwak, H., Rodriguez, P., Ahn, Y.-Y., Moon, S.: I tube, you tube, everybody tubes: analyzing the world's largest user generated content video system. In: Proceedings of the 7th ACM SIGCOMM Conference on Internet Measurement, pp. 1–14. ACM, New York (2007)
5. Cheng, X., Liu, J., Wang, H.: Accelerating YouTube with video correlation. In: Proceedings of the First SIGMM Workshop on Social Media - WSM 2009, p. 49. ACM Press, New York (2009)
6. Cho, K., Fukuda, K., Esaki, H., Kato, A.: The impact and implications of the growth in residential user-to-user traffic. In: Proceedings of the 2006 Conference on Applications, Technologies, Architectures, and Protocols for Computer Communications - SIGCOMM 2006, p. 207 (2006)
7. Cohen, B.: The BitTorrent Protocol Specification (2009)
8. Gill, P., Arlitt, M., Li, Z., Mahanti, A.: Youtube traffic characterization: a view from the edge. In: Proceedings of the 7th ACM SIGCOMM Conference on Internet Measurement, pp. 15–28. ACM (2007)
9. Klasen, B.: Efficient Content Distribution in Social-Aware Hybrid Networks. Journal of Computational Science (2011)
10. Klasen, B.: SatTorrent - Satellite-Aided P2P Content Distribution for Virtual Environments. In: Proceedings of the Fifth International Conference on Simulation Tools and Techniques. ACM, Desenzano (2012)
11. Leighton, T.: Improving Performance on the Internet. Queue 6(6), 20 (2008)
12. Maier, G., Feldmann, A., Paxson, V., Allman, M.: On dominant characteristics of residential broadband internet traffic. In: Proceedings of the 9th ACM SIGCOMM conference on Internet measurement conference, IMC 2009, vol. 9, p. 90. ACM Press, New York (2009)
13. Ramzan, N., Quacchio, E., Zgaljic, T., Asioli, S., Celetto, L., Izquierdo, E., Rovati, F.: Peer-to-peer streaming of scalable video in future Internet applications. IEEE Communications Magazine 49(3), 128–135 (2011)
14. Scellato, S., Mascolo, C., Musolesi, M., Crowcroft, J.: Track Globally, Deliver Locally: Improving Content Delivery Networks by Tracking Geographic Social Cascades Categories and Subject Descriptors. In: WWW 2011 Proceedings of the 20th International Conference on World Wide Web, pp. 457–466. ACM, New York (2011)
15. Choffnes, D.R., Bustamante, F.E.: Taming the Torrent: A Practical Approach to Reducing Cross-ISP Traffic in P2P Systems. ACM SIGCOMM Computer Communication Review 38(4), 363–374 (2008)
16. Theory.org Wiki contributors. Bittorrent Protocol Specification v1.0 (2013), `http://wiki.theory.org/BitTorrentSpecification`
17. Yin, H., Liu, X., Zhan, T., Sekar, V., Qiu, F., Lin, C., Zhang, H., Li, B.: Design and deployment of a hybrid CDN-P2P system for live video streaming. In: Proceedings of the Seventeen ACM International Conference on Multimedia - MM 2009, ACM Press, New York (2009)

Efficient Synchronization of Multiple Databases over Broadcast Networks

Muhammad Muhammad, Stefan Erl, and Matteo Berioli

German Aerospace Center (DLR)
Institute of Communications and Navigation
82234, Oberpfaffenhofen, Germany
{Muhammad.Muhammad,Stefan.Erl,Matteo.Berioli}@dlr.de

Abstract. This work deals with the problem of synchronizing multiple distributed databases over a broadcast network, such as satellite networks. The proposed method is based on introducing network coding techniques besides extending the well-known database reconciliation algorithm, the characteristic polynomial interpolation-based synchronization (CPISync). One key element is to elect a master node that manages the operations in a central manner. Performance is shown in terms of completion time for full synchronization, and average number of packets exchange. Compared to point-to-point and traditional broadcasting synchronization methods, the algorithm implementing network coding allows reaching the lower-bound for the number of packets exchange.

Keywords: multiple databases synchronization, network coding, broadcast channels, satellite communications.

1 Introduction

A database consists of an organized collection of related data. A distributed database system (DDBS) is a collection of multiple, logically interrelated databases. These distributed databases are physically spread over a computer network of multiple nodes, where any node can update its database at any time. A database management system (DBMS) consists of software that controls databases. The services provided include storage, access, security, backup and some other facilities. The DBMSs can be categorized according to the database model that they support such as relational databases, the type of computer they support, and the query language that accesses the database such as SQL. Some commonly used DBMSs are MySQL and PostgreSQL.

With the high demand on the usage of these DDBSs and due to the changes that may occur on one or many sites discarding the others, data synchronization algorithms have been deeply studied, see [1] and [2]. Additionally, several synchronization and replication applications, to harmonize information and to keep consistency of data among all points in the network managing these databases, have been developed for the different DDBSs currently available, such as Cybercluster and Maatkit.

R. Dhaou et al. (Eds.): PSATS 2013, LNICST 123, pp. 77–89, 2013.

In spite of the great effort done by the scientific community in the field of database synchronization, especially for CPISync, in terms of reducing the synchronization traffic, this method mainly operates in a point-to-point environment, which limits the applicability of synchronizing multiple databases. In this light, the aim of this work is to present a novel method for synchronizing multiple databases, namely, to make all datasets involved in the reconciliation process have local access to all the data with further minimized traffic load that is achieved by extending CPISync to multiple nodes, by applying network coding principles and by changing the network topology to a star network.

Network coding [3,5] has been also applied to solve the problem of distributed storage [10]. Distributed storage systems often introduce redundancy to increase reliability. When coding is used, the repair problem arises, which addresses the case if a node storing encoded information fails, then in order to maintain the same level of reliability, encoded information need to be created at a new node. A survey of network coding and distributed storage systems can be found in [13]. Some problems of distributed storage systems, like storage allocations, are addressed in [11,12]. However, our problem differs from that of the distributed storage systems in the sense that our proposal does not aim to provide data reliability in case of node failure, but to allow all involved nodes to acquire local access to the complete dataset at any given time.

This paper is organized as follows. The next section gives background information about the CPISync algorithm. Section 3 exploits different methods of differences discovery in database synchronization using CPISync. In Section 4 solutions for updating databases are given. The performance of the new methods is evaluated in Section 5. Finally, a conclusion follows in Section 6.

2 Background

Let us consider a network of nodes (distributed over a wide geographical area, but can be served by a single satellite beam), where each node in the system is maintaining a database. These datasets form a DDBS. The datasets may or may not have common entries. Whenever a synchronization is required; may be on demand, periodically, or after re-establishing the network connection in case of node or link failure, a bidirectional merge of the involved databases takes place. The operation of merging two databases can be separated in two subtasks: (i) the finding of the differences between the two databases, and (ii) the bidirectional data exchange to update the two databases and to guarantee that they are identical.

The former task requires an optimized algorithm for finding the differences. For the work in this paper, CPISync [6] is considered. The latter task may be non trivial in the case of a DDBS, but a lot of work has been done to provide efficient solutions; especially over broadcast networks, where the concepts of reliable multicast can be exploited. In this respect, this work will focus on Network Coding to perform the latter task. We will focus on a particular, yet simple, Network Coding scheme, namely Random Linear Network Coding (RLNC) [4],

which is representative of the general idea to exploit Network Coding for DDBS. The next subsection will introduce the basics of CPISync.

2.1 CPISync

The work in [6] shows that CPISync has close-to-optimum performance, it has a minimum comparison overhead that depends only on the amount of differences between the synchronizing datasets, but not on the dataset size itself. In [7] the authors tested CPISync and it was shown to be a promising solution for synchronizing databases over satellite narrowband links.

A record in a database is a row that is constructed of multiple related fields. In order to use CPISync, each record in the database can be represented by one unique integer, e.g. by means of a hash function. This allows to associate to each database A a set of integers $S_A = \{x_1, x_2, ..., x_n\}$, representing all records in the database A. The key point of the CPISync algorithm is the conversion of a database into a polynomial, which is called the characteristic polynomial of the database. The characteristic polynomial of database A is defined as follows:

$$X_{S_A}(Z) = (Z - x_1)(Z - x_2)(Z - x_3) \cdots (Z - x_n). \tag{1}$$

The idea is to manipulate these characteristic polynomials to discover the differences between two databases, and this is done as explained in the following.

Let us assume we have two databases A and B, for which we can define two characteristic polynomials as indicated in (1) above. Let us also define $\Delta_A = S_A \backslash S_B$, as the set of integers in A but not in B, and symmetrically $\Delta_B = S_B \backslash S_A$, as the set of integers in B but not in A. If we knew all elements of the two databases, we would be able to build the following rational function:

$$f(Z) = \frac{X_{S_A}(Z)}{X_{S_B}(Z)} = \frac{X_{S_A \cap S_B}(Z) \cdot X_{\Delta_A}(Z)}{X_{S_A \cap S_B}(Z) \cdot X_{\Delta_B}(Z)} = \frac{X_{\Delta_A}(Z)}{X_{\Delta_B}(Z)}. \tag{2}$$

This rational function has the interesting property that can be described by only means of the two sets Δ_A and Δ_B. So if it were possible to build this function without complete knowledge of the two databases, then it would be possible to discover the differences between the two databases. This is the core principle of CPISync. Curios readers are forwarded to [6] to find a detailed example on how CPISync works.

The upper bound ($\overline{m}$) of the actual symmetric differences is in reality difficult to know or predict in many applications. For that reason, an improved CPISync algorithm, called Partitioned-CPISync, was proposed in [8] to overcome this drawback. The value of $\overline{m}$ is fixed a priori by the two hosts, and the algorithm recursively divides each set into p partitions until the basic CPISync algorithm can succeed with the pre-agreed upper bound $\overline{m}$ on the number of differences in a single partition. In other words, the set S_A is partitioned into p non-intersecting subsets, and if the basic CPISync fails in a subset, the algorithm keeps dividing each subset into p subsubsets, and so on, until the differences can be discovered by the basic CPISync algorithm.

The complexity of the Partitioned-CPISync was analyzed in [8]. Worst-case bounds for communication and computation complexity are given there. When assuming hashed indexes of the set that are randomly and uniformly distributed, these worst-case bounds could be optimized to the following formulas for synchronizing two databases.

The expected number of rounds $\overline{r}$ needed by the Partitioned-CPISync algorithm for the reconciliation of two databases is at most:

$$\overline{r} = 2\log_p\left(\frac{m}{\overline{m}+1}\right) + \mathcal{O}(1), \tag{3}$$

with m denoting the actual number of differences between the two sets and p denoting the partition factor, representing the number of non-overlapping parts the set p is split up in each round. In one round several Basic-CPISync runs are performed, because the evaluation values of individual parts p of the same level do not depend on each other and can be generated and sent together.

The expected number of overall bits transmitted from one node to another in order to determine the differences is at most:

$$\overline{b} = 8emp(b+1) + \frac{8emkp(b+1)}{\overline{m}+1}, \tag{4}$$

with $e \approx 2.71828183$ being the Euler number. The parameter k is the number of additional evaluation values sent by the host to verify that the rational interpolation with the chosen $\overline{m}$ was correct. The parameter b is the length of the hash value of a row in the database, which is used to calculate the characteristic polynomial.

3 Phase I: Discovering the Differences

In this section, we propose, investigate, and compare different possibilities on how to exploit CPISync to discover the differences inside a DDBS.

Assume a network of N distributed nodes is maintaining a DDBS. Each endpoint is handling a single database. The goal of phase I is that the system knows which node is missing which packets and how all the nodes can be synchronized.

3.1 Solutions for Difference Discovery

Four solutions are proposed: one under the category of mesh network, and three under the category of star network.

Mesh Network. A fully meshed comparison between all nodes is the easiest way to run CPISync. In this scenario, every node is compared and synchronized with every other node in the system in order to achieve a complete system synchronization. There is no central coordination, to synchronize N databases in this scenario, every node has to synchronize (on its own) with all the other $(N-1)$ nodes. This will result in a complete synchronization of the system

after performing $\frac{N(N-1)}{2}$ synchronization procedures by all nodes. This technique considers the absence of a specific nodes set up, i.e., every node synchronizes its database with a randomly chosen another node, such that any synchronization process between any two nodes is performed only once. In this respect, the time required to run the algorithm and end up with a fully synchronized system is:

$$T_{\text{mesh}} = \frac{N\,(N-1)}{2}\,[\overline{r}\,(2T_{\text{s}} + T_{\text{eval}} + T_{\text{calc}}) + 2T_{\text{data}} + T_{\text{s}}]\,, \tag{5}$$

where T_{s} is the one-way signal delay between any two synchronizing nodes, T_{eval} is the time to receive the evaluations, and T_{data} is the time to receive the missing data. The time for the calculation is summarized in T_{calc}. T_{calc} mainly contains the time to perform the mathematical computations of the polynomial interpolation. T_{eval} depends on the chosen upper-bound $\overline{m}$, the length of the hash ID b and on the actual size $|d_i|$ of the differences set. For one complete run of CPISync, T_{eval} can be expressed in dependence of $\overline{b}$, the total number of bits transmitted.

In this scenario, phase I (difference discovery) and phase II (update of the differences) take place one after the other at each pairwise comparison, so they both take place $\frac{N(N-1)}{2}$ times.

Star Network. In a star network, one of the nodes is set to the role of the master node that takes care of the synchronization. In phase I, the master (with set S_0) gains the knowledge of its respective differences with S_i ($i = 1,...,N-1$); and receives the data d_i from the other nodes. In fact the operation of updating the master with the data d_i from all nodes, is already part of phase II; it will be mentioned in this section for the sake of understanding, but will not be considered in the performance evaluation of phase I presented at the end of this section. We present three methods on how to employ the CPISync algorithm within a multiple node environment. The more practical Partitioned-CPISync is used for our analysis as it is likely that several rounds of communication are used, which may drastically increase the time that is needed for discovering the differences between the nodes, especially for satellite networks with long round-trip time (RTT).

Round-Robin. The easiest and most straight-forward approach to obtain global view in the master node, since CPISync is originally suited for two sets, is a round-robin-like synchronization. The master discovers its differences to every node one after the other. After one full cycle, the differences between S_0 and each S_i are known. Combining these differences results in the global set ρ. This approach is shown in Figure 1(a). The figure shows the Partitioned-CPISync algorithm with taking two rounds of communication.

The master first sends its evaluations to the first node. This node tries to interpolate the missing data elements, but in this example, not enough evaluation values were sent. So it requests more evaluations from the master. After the interpolation was successful in the second round, the node knows its d_i and

sends it back to the master, including the request for the missing data (which would be d_0). In general, there are $\overline{r}$ rounds of communication between one node and the master. The same is also done with the remaining $N-2$ slaves. So the number of runs of the CPISync algorithm is $N-1$, and thus the complete number of transmitted bits, the complete amount of rounds needed, and the computation complexity for the CPISync in this scheme are multiplied by $N-1$.

The time to complete the algorithm can be derived from Figure 1(a). In each round, the evaluation values are sent to a node ($T_\mathrm{s} + T_\mathrm{eval}$) and a request is sent back to the master (T_s). In the last round, also the time for sending the data (T_data) is required. The time for the calculation is summarized in T_calc. The complete time results in:

$$T_\mathrm{rr} = (N-1)\left[\overline{r}(2T_\mathrm{s} + T_\mathrm{eval} + T_\mathrm{calc}) + T_\mathrm{data}\right]. \tag{6}$$

Central Calculation. In the central calculation approach, all the computation is moved from the nodes to the master. Here, the master requests evaluation values from all nodes. The computation for the first node can be started as soon as the evaluation values from the first node have been received. Figure 1(b) demonstrates this procedure. The request for the evaluation values is broadcast to the slave nodes. The first node starts transmitting, and the calculation is started as soon as the transmission is complete. Meanwhile the other nodes are sending their values. If the algorithm takes more rounds, a new request is sent to the corresponding node. After finishing the algorithm, the master has to request the missing data from all the nodes, because it only knows what data is missing, but it still does not have the data itself.

The transmitted bits, rounds and computation are the same like in the round-robin method, but since the single CPISync processes are more parallelized than in the previous method, the total time required to finish the algorithm will be shorter. Depending on the more time-intensive process, the interpolation or the reception of the evaluations, the total time for the algorithm is:

$$T_\mathrm{cc} = \begin{cases} 2\,T_\mathrm{s} + (N-1)(\overline{r}\,T_\mathrm{eval} + T_\mathrm{data}), & \text{if } T_\mathrm{eval} > T_\mathrm{calc} \\ 2\,T_\mathrm{s} + (N-1)(\overline{r}\,T_\mathrm{calc} + T_\mathrm{data}), & \text{if } T_\mathrm{calc} > T_\mathrm{eval} \end{cases} \tag{7}$$

The calculation for one node will be done while other nodes are still transmitting, or the reception is performed while other nodes' interpolations are still in progress, respectively.

Broadcast Evaluations. In contrast to the previous method, in this approach the evaluation values of the master's set are broadcast. Then each node does the interpolation on itself and discovers its differences to the master. Figure 1(c) shows this approach. Evaluation values needed for further rounds can be broadcast as soon as the first request arrives and following request for the same round can be ignored. Other nodes can buffer the further evaluations if their calculation is not yet finished. After the nodes finished their calculations, they send their additional data d_i and a request for the data they are missing to the master.

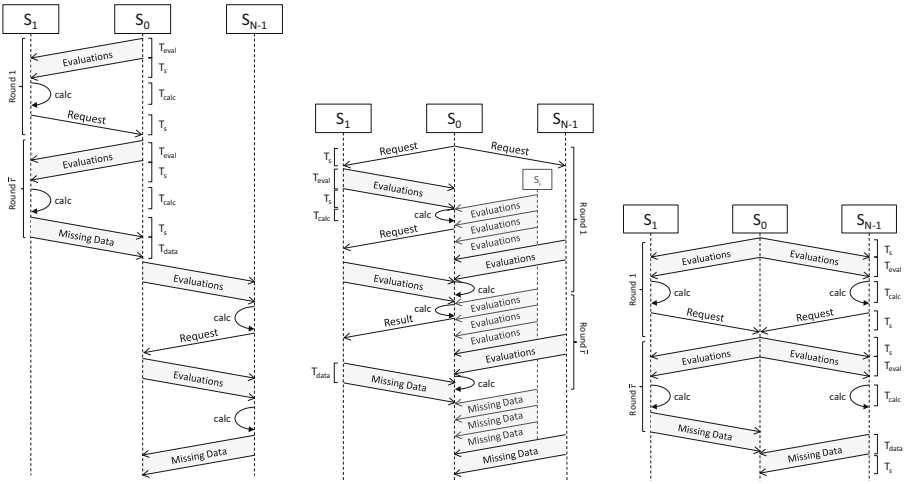

(a) Round-Robin-like deployment of CPISync. (b) Master computes differences centrally. (c) Evaluations are broadcast.

Fig. 1. Several techniques in obtaining differences in broadcast medium

Because the evaluation values are broadcast and the interpolation is done fully parallel across all nodes, the only parameter that depends on the number of nodes is the transmission time T_{data} when sending the missing data back to the master node. The total required time with this approach is then:

$$T_{\text{bc}} = \overline{r}(2\,T_{\text{s}} + (T_{\text{eval}} + T_{\text{calc}}) + (N-1)\,T_{\text{data}}). \tag{8}$$

3.2 Comparison

In this section, we provide lower and upper bounds on the number of CPISync processes to discover the complete differences between any two synchronizing databases. From the previously discussed methods, it is clear that the number of CPISync processes in master-slave mode ($P_{\text{M-S}}^{\text{CPISync}}$) is reduced due to the deployment of the star network. However, this will increase the complexity of the algorithm at the master node as the number of slaves increases. But, this difficulty will be linked only to the master end-point. Therefore, the number of CPISync processes is always: $(N-1)$.

Alternatively, when more and more nodes use CPISync in a mesh network, the complication will be on each device to track the changes occurring and the next node to connect to. This makes the number of CPISync processes grows up to: $\frac{N(N-1)}{2}$. So the number of CPISync calls grows with the square of the number of databases N, whereas for the master-slave approach it grows linearly with N. In addition, in the mesh-network approach also phase II (update of the differences) is called $\frac{N(N-1)}{2}$ times, whereas in the master-slave approach it can be performed just once and more efficiently, by exploiting network coding principles (this will be explained in the next section).

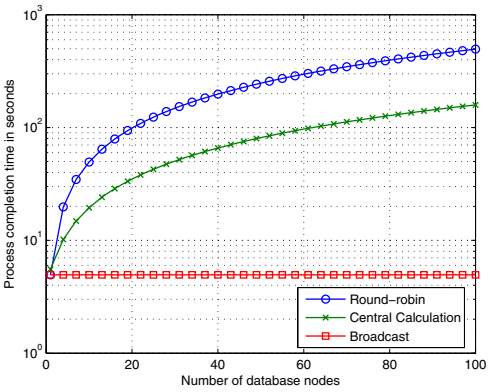

Fig. 2. Time for obtaining the differences using Star network topology

For these reasons the mesh-network approach can be discarded as it is the one with the highest complexity. Now we compare the three different methods for the star network, namely, *round-robin*, *central calculation*, and *broadcast evaluations*. We assume a satellite link with a signal delay $T_\mathrm{s} = 300\,\mathrm{ms}$ and a bit-rate of 1 Mbps. Each node has an additional data $|d_i| = 500$ rows, and each row has a size of 1 KB. The CPISync parameters are set to $b = 32$, $p = 4$, $k = 4$ and $\overline{m} = 50$, which results in an average number of $\overline{r} = 4$ rounds and $\overline{b} = 1.6\,\mathrm{Mbit}$. This results in $T_\mathrm{eval} = 1.6\,\mathrm{s}$. The calculation time is assumed with $T_\mathrm{calc} = 1\,\mathrm{s}$.

For sending and receiving data, a simple ideal channel model (i.e. with no packet error rate (PER)) with time slots is assumed. Only one node is allowed to send at each time slot, and the data sent from several nodes to one receiver arrives one after the other. For transmitting data no specific protocol is assumed and acknowledgments for each packet received or packet sizes are irrelevant.

Figure 2 shows the required time for the three methods with the above parameters as a function of the number of nodes N. Since all the methods include a transfer of the missing data to the master at the end of the algorithm, we ignored T_data in this graph, since this is in fact part of what we defined as phase II (update of the differences).

As expected, the round-robin method performs worst, as all nodes are synchronized serially, resulting in many rounds of communication and a long processing time. The central-calculation approach is a bit faster, because it is more parallelized and, depending on the properties of the channel and the master, either the channel or the processor in the master node are fully utilized. The best performance was given by the broadcast method, which can achieve a similar performance like a two-node synchronization, as the only time dependent on the number of nodes is the transmission of the data itself.

4 Phase II: Update of the Differences

Let us denote the complete set of the database records by $\rho = \{P_1, P_2, ..., P_K\}$, this is the set of packets (or records) that every node should have after synchronization, with $K = |\rho|$. Additionally, let us denote by ϕ_i the set of packets missed by node i. The set of records available at node i is S_i.

As mentioned previously, in a mesh network, the complexity will be at every node by monitoring the nodes to synchronize to; also, the processing power will be higher, because of the polynomial interpolation due to the one-to-one relationship.

For the synchronization process to take place, the nodes are re-arranged in a star network (i.e. Master-Slave). Otherwise, they can have a mesh network communication infrastructure. The rationale behind this topology is to allow network coding to reduce the bandwidth utilization and the delay and to minimize the complexity at the other nodes while keeping it at the central point.

Our algorithm allows to further reduce the traffic load related to the synchronization of multiple databases. This load is already minimized by CPISync for two synchronizing databases. Nevertheless, when harmonizing multiple databases, keeping the one-to-one relation introduces a large overhead, since synchronization will follow a mesh network topology. This overhead is reduced with our technique, which works as follows. First, one of the databases engaged in the synchronization process is selected as a master, say node 0 (whose set is S_0), to coordinate the overall reconciliation activity. The other nodes will be slaves. Secondly, the master will ask each slave to transmit the differences with its respective data by broadcasting its evaluation points to the other nodes, which is the fastest method according to Section 3. At this point, the master has a complete knowledge of what data every other database has and what it needs for a complete system synchronization. The master has now built the set ρ that is the complete database and he knows what every node is missing, i.e. he knows that node i is missing the set of records ϕ_i. The master builds the set of the records that are missed by at least one node, this set can be indicated as $\Psi = \rho \backslash \bigcap_{i=1}^{N-1} S_i$. Let $\Delta = |\Psi|$ be the number of records in this set. Finally, the master node linearly combines the packets required in the set Ψ using the RLNC technique and broadcast these coded packets to the slaves. In this way the number of packets that the master needs to send to update all slaves is drastically reduced; this will be shown in the next section.

5 Performance Evaluation

The performance of the proposed technique is analyzed in this section in terms of the average number of exchanged packets.

5.1 Average Number of Packets Exchange

In this section, the expected number of retransmissions ($\mathbb{E}[\mathcal{P}]$) will be evaluated according to two simulation schemes. In the first scheme (scheme A), the

databases to be synchronized have the same size (K) with a uniformly distributed set of differences. Scheme B, on the other hand, features the possibility that the synchronizing databases are of different sizes also having uniformly distributed differences. In the latter scheme, the different sizes will simulate the nodes being idle for some time.

In the two above mentioned schemes, the performance metric measure will be the expected number of packets exchange (i.e. the packets that have been interchanged during the synchronization process) in order to achieve a complete system harmonization. The simulations consider three techniques for synchronizing N datasets. The first one uses pure CPISync in a mesh network, where every node checks with all its peers about new information until all the nodes have the full set of packets (ρ). The average number of packets exchange grows with the square of the number of nodes (as previously explained):

$$\mathbb{E}\left[\mathcal{P}\right]_{\text{Mesh}} = \frac{\overline{d}}{1-\epsilon}\frac{N(N-1)}{2}, \tag{9}$$

where $\overline{d}$ is the average number of differences between any two synchronizing databases and ϵ is the PER.

The second method uses a star network, but without network coding, see 3.1. Instead, after the master pulls the differences from the other nodes, it broadcasts all the data packets (ρ) and each user will take or drop packets according to its need. The average number of packets exchange in this case is:

$$\mathbb{E}\left[\mathcal{P}\right]_{\text{BC}} = (N-1)\overline{d} + \frac{K}{1-\epsilon}. \tag{10}$$

Finally, applying network coding techniques in a star network only on packets that have not been correctly received by all slaves. The expected number of packets exchange can be evaluated using:

$$\mathbb{E}\left[\mathcal{P}\right]_{\text{NC}} = (N-1)\overline{d} + \left[\frac{\Delta}{1-\varepsilon}\right]\delta, \tag{11}$$

where Δ is the number of linear combinations with elements from a Galois field of $\mathbf{GF}\left(2^q\right)$ and δ is chosen as an optimal value of $\delta = \frac{1}{1-\epsilon}$ to overcome the link erasures. Additionally, a large $\mathbf{GF}\left(2^q\right)$ (with $q = 8$, i.e. a symbol = 8 bits) is chosen in order to reduce the probability of having linearly dependent equations and hence not ask for retransmissions, as proposed by [9]. Although it is very low, but there still exists a decoding failure probability (due to the linear dependency among the linear equations of the system), which is represented by ε.

Let us consider that $\hat{\varepsilon}$ is an upper-bound on ε, i.e., $\hat{\varepsilon} > \varepsilon$. This leads to identify an upper-bound on the average number of packets exchange for the network coding case of synchronizing N databases:

$$\mathbb{E}\left[\mathcal{P}\right]_{\text{NC}} \leq (N-1)\overline{d} + \frac{\Delta}{(1-\hat{\varepsilon})(1-\epsilon)} = \hat{\mathbb{E}}\left[\mathcal{P}\right]_{\text{NC}}. \tag{12}$$

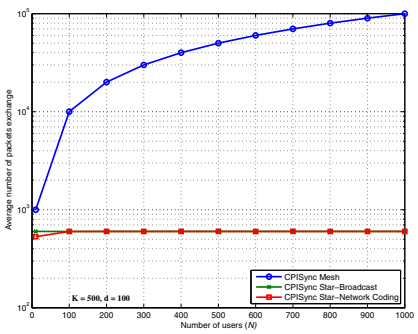

(a) Average number of packets exchange as a function of N

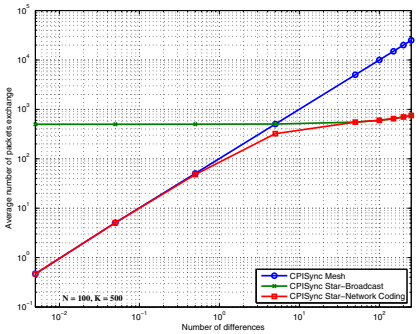

(b) Average number of packets exchange as a function of number of differences

Fig. 3. Average number of packets exchange versus N and PER

5.2 Results

The following results represent the average number of packets exchange for synchronizing multiple databases after 100 runs.

Figure 3(a) plots the simulation results of (9), (10) and (11) as a function of N using scheme A. The graph shows that for small values of N, the performance of network coding is slightly better than the broadcasting scenario. However, using a mesh network the expected number of packets exchange grows logarithmic with the number of users. The simulation used a database size $K = 500$ records with 100 uniformly distributed differences and PER $\epsilon = 0$.

The chart in Figure 3(b) also simulates scheme A. But here, the results are shown as a function of the number of differences. The number of users N is set to 100, the database size $K = 500$ and PER $\epsilon = 0$. As it can be realized, linearly combining packets in a star network forms a lower bound for all other techniques. Further, as the number of differences gets really low or very high, the number of packets exchange is the same for a mesh or broadcast scenarios, respectively.

The plots in Figure 4(a) represent the case when some (say 30 %) of the total $N = 100$ databases were off-line for a period of time. Therefore, they are missing relatively large amount of data in addition to the existence of few differences of the information they acquire with the other databases. It is clear the inefficiency of the point-to-point synchronization in terms of bandwidth utilization. Also, with the network coding approach, the packets exchange is very low for low-to-moderate differences values. However, as the latter value increases, the number of transmitted packets in a network coding scheme is similar to the simple broadcasting scenario. Nevertheless, this behavior is due to the fact that no packet erasures on the channel were considered.

In the last simulation, shown in Figure 4(b), a realistic scenario is implemented using scheme A, where packet erasures with probability ϵ occur on the downlink from the master node. For $N = 100$, $K = 500$ and number of differences of

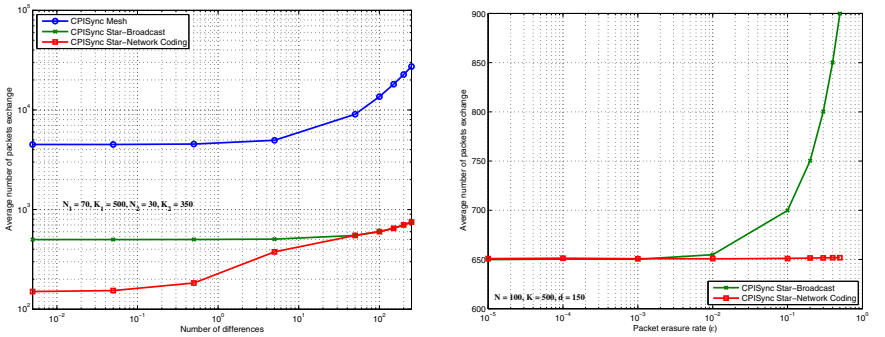

(a) Average number of packets exchange as a function of number of differences with different database sizes (K_1, K_2)

(b) Average number of packets exchange as a function of PER (ϵ)

Fig. 4. Average number of packets exchange versus number of differences and PER

150 with low-to-moderate PERs, both techniques (i.e. broadcasting and network coding) are comparable. However, for large values of ϵ, network coding is more appropriate and efficient because a single linear combination can reveal information about several missing native packets that have to be all retransmitted in case of simply broadcasting the information.

One last thing, by applying network coding, a coding delay ($D = D_e + D_d$) is added to the synchronization process. On the master side, the packets have to be encoded with delay denoted by D_e. Additionally, on the slave's side, a decoding delay D_d is realized due to the idle time the node has to wait to receive the coded block and to decode using Gaussian elimination techniques. However, compared to the RTT for requesting lost packets, the coding delay D is negligible. This is especially true for satellite networks with a high RTT. Further, it is shown in literature that the decoding complexity of RLNC is $\mathcal{O}\left(\Delta^3\right)$, which is applicable with nowadays technology.

6 Conclusions

In this work, a new approach to synchronize multiple databases was proposed based on network coding and an already state-of-the-art database synchronization mechanism, namely, CPISync. The newly recommended algorithm assumes that the master node, to coordinate the process of synchronizing all the databases involved, pulls from every slave node at a time its respective differences by using CPISync in a broadcast manner. Finally, when the big picture is clear, the master combines the packets that haven't been correctly received by all the users. As it has been clearly seen, using this approach, due to network coding lower capacity utilization was achieved. Further, because of the master-slave organization lesser CPISync processes were initiated, which could be accelerated by our broadcast method.

References

1. Tridgell, A.: Efficient Algorithms for Sorting and Synchronization, Ph.D. dissertation, The Australian National University (2000)
2. Agarwal, S., Starobinski, D., Trachtenberg, A.: On the Scalability of Data Synchronization Protocols for PDAs and Mobile Devices. IEEE Network 16(4), 22–28 (2002)
3. Fragouli, C., Le Boudec, J.-Y., Widmer, J.: Network Coding: An Instant Primer. SIGCOMM Comput. Commun. Rev. 36(1), 63–68 (2006)
4. Ho, T., Medard, M., Koetter, R., Karger, D., Effros, M., Shi, J., Leong, B.: A Random Linear Network Coding Approach to Multicast. IEEE Transactions on Information Theory 52(10), 4413–4430 (2006)
5. Ahlswede, R., Cai, N., Li, S.-Y., Yeung, R.: Network Information Flow. IEEE Transactions on Information Theory 46(4), 1204–1216 (2000)
6. Trachtenberg, A., Starobinski, D., Agarwal, S.: Fast PDA Synchronization Using Characteristic Polynomial Interpolation. In: Proceedings IEEE INFOCOM, New York City, NY, USA, vol. 3, pp. 1510–1519 (June 2002)
7. Tang, C., Donner, A., Chaves, J., Muhammad, M.: Performance of Database Synchronization Algorithms via Satellite. In: 2010 5th Advanced Satellite Multimedia Systems Conference (ASMS) and the 11th Signal Processing for Space Communications Workshop (SPSC), pp. 455–461 (September 2010)
8. Minsky, Y., Trachtenberg, A.: Practical Set Reconciliation, Boston University, Tech. Rep. (February 2002)
9. Liva, G., Paolini, E., Chiani, M.: Performance versus Overhead for Fountain codes over Fq. IEEE Communications Letters 14(2), 178–180 (2010)
10. Dimakis, A.G., Godfrey, P.B., Wu, Y., Wainwright, M., Ramchandran, K.: Network Coding for Distributed Storage Systems. IEEE Transactions on Information Theory 56(9) (September 2010)
11. Leong, D., Dimakis, A.G., Ho, T.: Distributed Storage Allocations for High Reliability. In: Proc. of the IEEE International Conference on Communications, ICC (2010)
12. Leong, D., Dimakis, A.G., Ho, T.: Distributed Storage Allocation Problems. In: Workshop on Network Coding Theory and Applications, NetCod (2009)
13. Dimakis, A.G., Ramchandran, K., Wu, Y., Suh, C.: A Survey on Network Codes for Distributed Storage. Proceedings of the IEEE 99(3) (March 2011)

Study on Research Challenges and Optimization for Internetworking of Hybrid MANET and Satellite Networks

Ye Miao, Zhili Sun, Fang Yao, Ning Wang, and Haitham S. Cruickshank

CCSR, University of Surrey
GU2 7XH, UK
{y.miao,z.sun,f.yao,n.wang,h.cruickshank}@surrey.ac.uk

Abstract. The integrated MANET and satellite network is a natural evolution in providing local and remote connectivity. The features of this integrated network, such as requiring no fixed infrastructure, ease of deployment and providing global ubiquitous communication, give advantages of its being popular. However, its unpredictable mobility of nodes, lack of central coordination and limited available resources emphasizes the challenges in networking. A large library of studies has been done in literature, yet some issues are still worth tackling, such as gateway selection mechanisms, satellite link management, resource management and so on. As a basic step of internetworking, the issue of gateway selection is studied specifically and corresponding optimization scheme for achieving load balancing is described.

Keywords: Internetworking, hybrid MANET-Satellite network, gateway selection, load balancing.

1 Introduction

The current trend of communication is shifting towards global ubiquitous networking and universal access for mobile users that wish to communicate with others through heterogeneous technologies (e.g. cellular networks, Wireless LANs and Satellite networks)[1][2]. The ultimate goal of wireless communication is to allow users to communicate reliably at anytime and anywhere. A mobile ad hoc network (MANET) is a self-configuring infrastructure-less network with mobile devices connected by wireless. Due to the cost-effective and ease of deployment, MANETs are widely used in military applications, emergency rescue operations and applications in infrastructure-less or remote areas for extending communications. Despite that MANETs are normally envisioned to operate as stand-alone networks, they can be extended by integrating with other networks (e.g. cellular networks and satellite networks). In order to achieve a real sense of worldwide communication, satellite, sometimes, is the only solution for MANET to communicate with other parts of the world [3] and bridge the digital divide [2]. In this regards, satellite is not only utilized as a component of an alternative routing path but also considered as part of integrated complete system. Convergence of satellite and terrestrial networks is becoming a key factor in forming the foundation for efficient global information infrastructure [3].

R. Dhaou et al. (Eds.): PSATS 2013, LNICST 123, pp. 90–101, 2013.

The integrated MANET and satellite network is therefore a natural evolution in providing local and remote connectivity in a highly mobile, dynamic and normally remote environment. Since both MANET and satellite networks possess their own unique characteristics, the integration work inevitably raises significant research challenges in terms of system architecture, overall routing protocol design, mobility management, resource allocation and management, and provisioning of Quality of Service (QoS) and Quality of Experience (QoE). On one hand, MANETs are characterized as dynamic network topology, unreliable channel share, self-configuration format and limited resources. On the other hand, satellite network is characterized as costly resources, long propagation delay, errors due to propagation and handovers and variable round trip time (RTT).

The rest of this paper is organized as follows: Section 2 presents the architecture of the integrated MANET-Satellite network. The relevant research challenges are discussed in Section 3. As one of the challenges, the issue of gateway selection for achieving load balancing is studied specifically in Section 4, and corresponding optimization schemes are described in Section 5. Section 6 explains the simulation setup and result analysis. Finally, conclusion comes in Section 7.

2 Architecture

Existing satellite systems can be geostationary earth orbit (GEO) systems and non-geostationary (NGEO), for example, low/medium earth orbit (LEO/MEO). Both of them can be the satellite constellation in integrated networks [4]. These two types share some issues when integrated with MANET, but also have their own particular problems. In this paper, we discuss not only the common issues, but also the issues mainly target to a certain satellite constellation type. A general architecture of the integrated network is depicted in Figure 1. A MANET cluster consists of a set of MANET nodes connecting to each other by appropriate wireless way (e.g. WiFi). A general MANET node (MN) is only equipped with WiFi interface and thus directly connect to other nodes as long as they are in wireless link range. Each cluster has at least one node with satellite interface capable of performing communications to a satellite. If the interface is activated, the node is a gateway node (GW). The internetworking related operations are also done in gateway nodes. The general node has all the services of a MANET node, including sending and receiving information without any specific task. A gateway node acts as a general node and also an entrance or exit to another network via satellite interface. It is used to forward traffic for external network (e.g. another MANET or satellite network), which means it is possible to communicate with different types of networks. That means the only way for a general mobile node to communicate with external networks is to communicate via a gateway node. Each MANET network has one or more gateway nodes capable of performing links to satellite network. When a node equipped with satellite interface is in de-active state, it is a potential gateway node (PGW). Under certain conditions, these nodes are activated to be gateway nodes to perform connections and allow MANET cluster to communicate with backoffice (BO) or other networks in remote area without direct link range and access information provided by other networks.

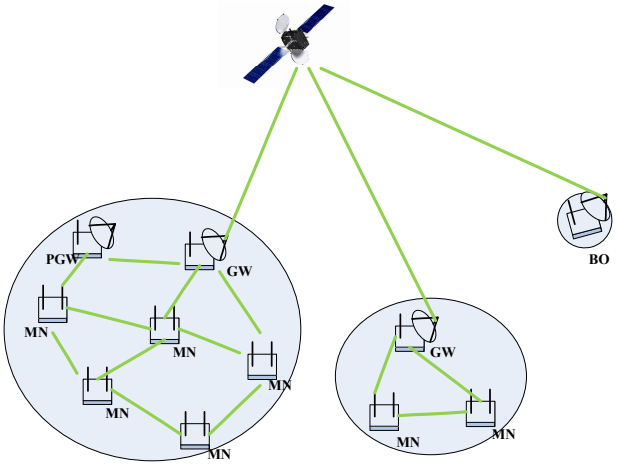

Fig. 1. Architecture of integrated network

The overall objective of integrating MANET with satellite network is to provide seamless broadband services to each node at any time in the network, overcome performance bottlenecks, and further optimize the usage of overall resources. In this regard, research issues should be considered at various aspects. Firstly, it is necessary to ensure the end-to-end communication. How to find a feasible route is always essential in a communication network. Based on the given criteria, different routing algorithms will be applied considering the link quality and QoS requirements. If there are two or more gateway nodes within the MANET, there should be an election process to select certain gateway(s) to perform the link to satellite. Secondly, as essential characteristics of MANET, mobility and scalability, require consideration when designing system. Ground segment handover and link layer handover are included in these issues. Another important aspect is to provide QoS guarantee which can be maintained by efficient resource management/allocation mechanisms. Load balancing is designed to balance load repartition and resource consumption over ground-part network. And CAC can be used to solve resource management issues especially in limited and costly resources network.

3 Challenges in Integrated Network

Since both MANET and satellite networks possess their own unique characteristics, the integration work inevitably raises significant research challenges in terms of system architecture, overall routing protocol design, mobility management, resource allocation and management, and provisioning of Quality of Service (QoS). In this section, four challenges will be discussed (routing interoperability, gateway selection mechanisms, satellite links' management and resource management) respectively.

To connect MANET with satellite networks, the routing interoperability, which means how to enable the routing protocols from both segments to understand each

other and work together seamlessly, is a challenge. The routing integration solutions can be divided into two groups. On one hand, the existing routing algorithms are adopted with proper access design for the other segment. That means one or several mechanisms can be implemented in the integrated system and adopted for both segments. For example, extension mechanism can be done in ad hoc routing protocol to support routing across the gateway to the other network. In this case, mobile nodes in MANETs can be capable of discovering and maintaining routes to the destination in different network domains. On the other hand, disparate routing strategies can be adopted in two segments. In this case, the interface between two sets of mechanisms must be defined carefully to translate the protocols for communications between different segments. The advantage is that only the characteristics of each segment need to be considered when come to disparate routing protocols design.

When a MANET is connected to a satellite, it is important for mobile nodes to detect available gateways providing access to the satellite segment. The key part of routing for hybrid networks is the gateway selection and normally, two approaches can be applied in the computation of the routing decision. One is to compute the best gateway(s) in terms of the parameters considered and afterwards the routing path. Another is to compute the routing paths and then weigh them by the parameters of the relevant gateways. Each MANET node should be registered in one gateway by three steps: gateway discovery, gateway selection and registration. Since the current MANET routing protocol does not exploit base stations, the gateway detection scheme, which could be done in three ways, should be implemented. The proactive gateway discovery is initiated by the gateways. The gateway periodically broadcast advertisement messages including the gateway information. The mobile nodes respond to these advertisements by requesting registration. The reactive discovery scheme allows the mobiles nodes to broadcast gateway solicitation message to find the proper gateways [6][7]. After the gateways send advertisements to reply these messages, the mobile nodes will reply by requesting registration. Hybrid approach uses combination of proactive and reactive approaches. Under certain conditions, proactive approach is used on some mobile nodes, whilst others use reactive scheme. Normally the hop number is considered: gateway broadcasts the advertisement periodically within the radius of n-hop, while for the nodes which are located n-hop away from the gateway, reactive approach is used.

Satellite link management, which is also known as gateway placement problem, may have major impact on network performance and power consumption of the satellite gateway nodes. A minimum number of gateways should be activated so to save terrestrial and satellite resources. There are several reasons that can trigger the turn on or off a satellite link in the integrated network. The premise for this mechanism design is that devices can provide the user with the capability to turn on or off link as they wish to do. The mechanisms can be implemented in related nodes instead of end users which reduce the time for end users to configure the network.

Efficient resource management/allocation mechanisms maximize the efficiency of transmission capacity, in order to better provide QoS guarantee. QoS is essential to ensure the end-users' satisfaction in the integrated network where different characteristics of networks coexist and as well as all different types of traffic. Data traffic can be large

data rate demanding, or time-sensitive and loss-sensitive. The purpose of QoS mechanisms is to ensure that network resources are appropriately used to provide relevant level of service to each type of traffic. Both satellite and ad hoc segments present some challenges in terms of QoS. Thus, in integrated networks, except for those, the coherency of QoS policies set up in two segments is equally important.

4 Load Balancing Based Gateway Selection Schemes

Gateway is the most important part in integrating Satellite and MANET networks, since quite a lot interworking operations are done in this part. Efficient and adaptive gateway selection reduces packet loss and delay due to the congestion on gateways or sudden unreachability of the gateway. Load balancing is a mechanism used in multiple links in order to balance load repartition and resource consumption over the network. In integrated MANET-Satellite network, all the MANET traffics are routed by the back office via satellite links which have limitation in terms of both amount and bandwidth. By using load balancing scheme, congestion in an overloaded gateway may be alleviated and data rate in an underused gateway may be increased [8][9]. In this case, it is possible to improve the overall throughput and reduce the delay caused by the congestion on gateways. What kinds of parameters should be considered to perform the load balancing mechanisms is still under study. It is hard to maintain absolute evenly traffic distribution because of the flapping problem caused by the synchronized rerouting. However, the optimal schemes can be considered to alleviate the flapping effect. Besides that, load balancing methods can also be integrated with multipath routing and gateway selection schemes in order to optimize the bandwidth utilization.

In the hybrid networks, gateways are always the bottleneck. There will be massive packets routed toward gateways to reach remote users. Selecting a proper gateway is the basic step for meeting QoS requirements. Among all the QoS considerations, load balancing is considered for evenly distributing traffic through the whole network in order to decrease the potential delay caused by congestions, and improve the resource utilization. As mentioned, efficient routing protocol dealing with node mobility should be considered. Since the available bandwidth of satellite is always the most valuable resource. Routing algorithms should take into account, first if a specific node is a satellite gateway and second, what are the specific characteristics of the satellite connection.

5 Proposed Scheme

As is mentioned, most of the current gateway selection methods use number of hops along the path and gateway queue length to select the particular gateway [10][11][12]. If all nodes select a gateway with the least hop count and traffic load, there will be congestions along the path to that gateway. So we propose a novel solution to intelligently select gateways in a balanced way by enable gateways to broadcast independent gateway message (GM), provided with information of traffic situation on their own. The whole procedure is depicted in Figure 2. Gateway nodes disseminate

gateway load information all over the network in a proactive manner, and normal nodes send local load information only to neighbors. When a node has data to be forwarded to a gateway, it checks if the selected gateway is overloaded in terms of the received gateway message. The node checks if the gateway switch is needed based on the combination of criteria and metrics set.

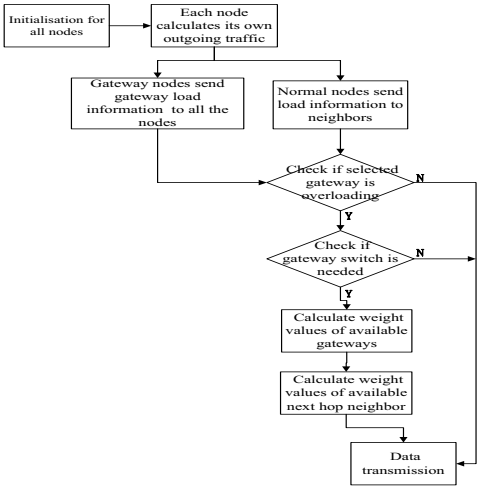

Fig. 2. Flow chat of proposed scheme procedure

Since the information of gateway state is disseminated periodically, different nodes may have different accurate information at the same time. That is to say, it can be possible that nodes close to gateways have a very good knowledge of gateways' state, but nodes farther away have poor information about that instead. In our proposed scheme, information of gateways' state is one aspect of routing path consideration. And another aspect is the traffic load situation of their neighbor nodes. They choose the least load neighbor node towards to the selected gateway. Then decisions of far-away nodes also help with distribute traffic among the overall network which alleviates traffic congestions in local nodes within MANET. In this case, the decisions made by near-gateway nodes and far-away gateway nodes cooperate to balance traffic in both terrestrial MANET and Satellite transmission links.

5.1 Gateway Discovery

By using the method of proactive gateway advertisement, the most accurate gateway information can be disseminated and mobile nodes can make proper estimation and decision thereby. Yet in this case, the larger network topology is, the higher overhead caused by control messages. How to manage the trade-off between control message overhead and information broadcast is the key point in proactive mechanisms.

In our design, the first step is to measure gateway traffic load and collect load information from each available gateway. By calculating the incoming packet number

and size, a gateway node is able to determine how much traffic it is suffering. The collected load information id will be inserted into gateway load message, and disseminated to all nodes in MANET along with the broadcasting mechanism in the employed proactive routing protocol (e.g. OLSR). After comparing with the defined capacity (i.e. the maximum capacity for a gateway to process data forwarding), the gateway node can recognize if it is to overload. If the gateway realizes that the critical value is to be reached, which means the current gateway is approaching its maximum capability, a mark label will be set up. The mark label is inserted into gateway message to indicate if the gateway is overloaded or not.

When a general MANET node receives the gateway advertisement, it records the gateway identity, load information, mark label, advertisement sequence number and advertisement lifetime. Based on its decision criteria, a suitable gateway will be worked out.

5.2 Gateway Selection

In our scheme, intermediate nodes are involved in gateway switching. If an intermediate node receives overloading alert from a gateway, and it is having data forwarding toward this gateway, it should make decision if gateway switching is applicable. This is the main part in gateway selection scheme and most of the previous algorithms consider the node number registered in the certain gateway, as the gateway load factor assumes that every node generates a similar traffic which is not realistic. In this algorithm, intermediate nodes are asked to record the traffic sent out locally. The decision is based on the traffic to the specified gateway. If the traffic previously sent from current intermediate node to the gateway issuing alert reaches certain point (e.g. a defined threshold), the gateway switching should be carried out where possible. Otherwise, the current intermediate node may choose to stay with existing gateway without changes.

Algorithm 1: Mn_receive(GW1_msg, GW2_msg)

Input: GW1_msg, GW2_msg, which are two messages from two gateways respectively.

Output: Gateway choice & next hop node.

begin

1. Abstract information about gateways.
2. Check if any gateway is overloading.
3. Calculate weight values of gateways.
4. Make decision about selected gateway.
5. Calculate weight values of neighbor nodes.
6. Choose next hop node.

return selected gateway, next hop node;

end

The gateway switching on intermediate nodes is based on the gateways' availability, which means if there is alternative gateway available, and if the load status on the alternative gateway is suitable to accept new traffic flow. Through receiving gateway load information from gateway message, each intermediate node can obtain such information. After receiving the gateway messages, the mobile nodes can choose their proper gateways for transmitting data in next time interval using the heuristic way, as specified in Algorithm 1.

Different gateways may have different threshold levels based on which gateways send overloading indication. And when it comes to decision making in intermediate nodes, in order to ensure the traffics are distributed as evenly as possible, we propose an adaptive overloading threshold based on current gateway traffics. T_{gw} is the proposed overloading threshold for gateways. L_{gw_n} is current traffic load of the n^{th} gateways. The function is shown below:

$$T_{gw} = \frac{1}{n} \sum_1^n L_{gw_n}$$

In addition to that, we use the stable interval based on current gateway traffics to evaluate if the switch is needed. That means the gateway switching won't be carried out if the current load is within the stable interval as shown below. In this case, routing flapping which is caused by simultaneously reroute can be alleviated.

$$[T_{gw} - m * \sum_1^n L_{gw_n},\ T_{gw} + k * \sum_1^n L_{gw_n}]$$

The main metric for evaluating gateway weight values (W_{gw}) is the weight value function for gateway. H_{gw_n} indicates the hop number of current local node to the n^{th} gateway node.

$$W_{gw} = \alpha \cdot \frac{H_{gw}}{\sum_1^n H_{gw_n}} + \beta \cdot \frac{L_{gw}}{\sum_1^n L_{gw_n}}$$

In order to balance traffic overall network, we consider not only the gateway load levels but also neighbor nodes'. W_{nb} represents the weight value of a certain neighbot node. H_{nb_n} and L_{nb_n} record the hop number of the neighbor node and the n^{th} gateway node and traffic load of the neighbor node, respectively. The weight value function of neighbor nodes is:

$$W_{nb} = \alpha_1 \cdot \frac{H_{nb}}{\sum_1^n H_{nb_n}} + \beta_1 \cdot \frac{L_{nb}}{\sum_1^n L_{nb_n}}$$

6 Simulation Setup and Result Analysis

6.1 Scenario Design and Parameters Setup

The scenario design for simulating gateway switching on intermediate nodes is shown in Figure 3. The MANET consists of 11 nodes communicating with each other through WiFi interface. Two out of them are equipped with satellite interfaces (GW1 and GW2). GEO satellite interface which has relatively stable latency compared with non-GEO is used in simulation. Gateway messages are disseminated across MANET. Nine general nodes are set as source nodes to issue UDP based CBR traffic towards the destination, backoffice. In order to evaluate the performance of the proposed scheme, the parameters are set for two stages (overall transmission rate is 64kb/s and 90kb/s, simulation lasts for 90s and 40s respectively).

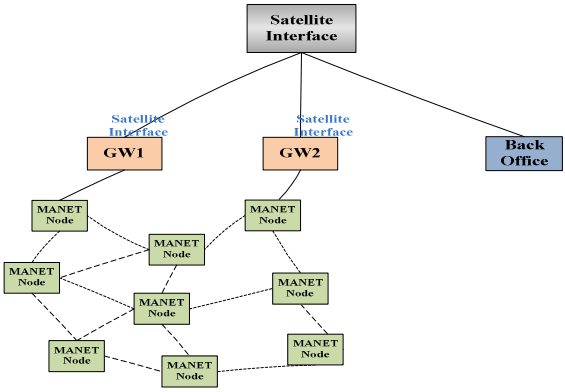

Fig. 3. Gateway selection scenario

The simulation software was implemented using NS-2. The proposed scheme is achieved on the basis of OLSR. The parameters are shown in following table 1.

Table 1. Parameters in simulation for load balanced multi-gateway selection

Parameters	Value
Simulation Area	600 x 600m
MAC type	IEEE802.11
Number of Gateway Nodes	2
Number of Mobile Nodes	9
Transmission Range	45m
Traffic Type	CBR
Packet Size	512bytes
Simulation Time	280s

6.2 Result Analysis

We use throughput as the performance metric for comparison. Throughput is defined as the total number of bits successfully delivered at the destination in a given period of time.

Figure 4 and 5 present the comparison of gateway throughput with the use of standard OLSR and modified OLSR with the proposed scheme. X axis denotes the simulation period and Y axis denotes the throughput of gateway. The throughput records on gateway 1 and 2 are shown by curves with cross and star respectively. The source nodes start to send packets from 150s and observation starts from 160s to eliminate the simulator issues. The first simulation period is from 160s to 230s and the nodes are sending traffic at a total rate of 64kb/s. Then traffics are increased to 90kb/s in total during the second period which lasts to 280s. Since shortest path criteria is the only metric used in standard OLSR, in Figure 4 we can see the throughput of two gateways are quite different and there is no cross for two curves. If transmission rate increases, it is possible that one gateway is overloaded and the other is underused which may cause serious packet loss and transmission congestion.

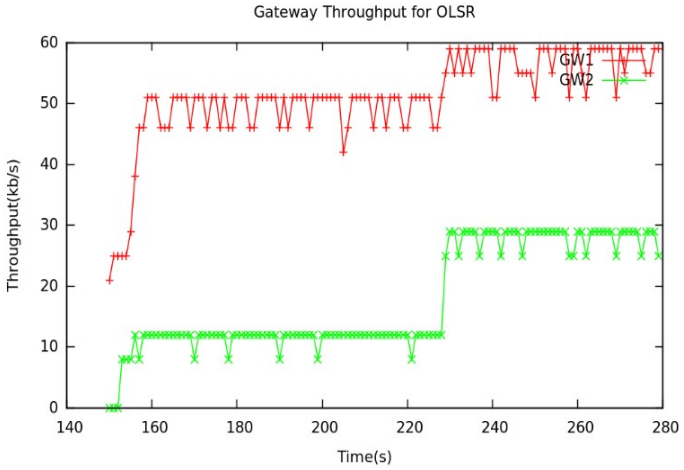

Fig. 4. Gateway throughput for OLSR

In Figure 5, gateway throughput changes and swings, and finally reaches stable and balanced. The blue and black lines marked as "T" are the thresholds for switch decision making. They are calculated based on overall gateway throughput at different stages. The aim of gateway switching is to evenly distribute traffic among gateways. That means the throughput level of gateways should be self-adaptive, and reach a stable level in proximity by which the network resource usage is balanced. In Figure 5 two curves cross each other. When a gateway is selected by MANET nodes, it is possible that another gateway is deselected. And thus throughput for the other gateway decreases accordingly. Since the gateway selection is independently implemented on MANET nodes, two gateways can be used simultaneously, and the final throughput levels will have chance to reach stable with balanced traffic distribution.

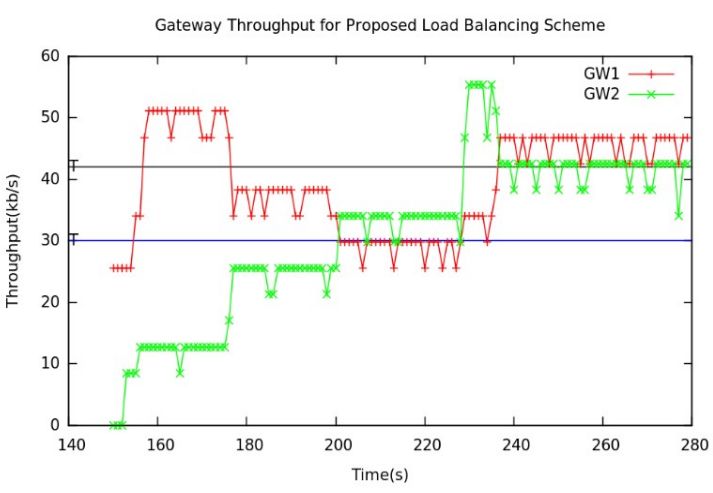

Fig. 5. Gateway throughput for proposed load balancing gateway selection scheme

Table 2 gives numerical comparison for two stages. It is shown that in both situations, the throughput can reach and maintain in an acceptable level.

Table 2. Throughput comparison for stage 1 and 2

		Throughput (OLSR)	Throughput (proposed scheme)
Stage 1	GW1	79.7%	46.9%
	GW2	20.3%	53.1%
Stage 2	GW1	37.8%	46.7%
	GW2	62.2%	53.3%

Apart from throughput, overall delay and packet loss rate are also used as performance metrics for comparison. Delay is defined as the delay for sending packets from source nodes to backoffice. And in our case, we calculate the average delay of all the packets delivered successfully. Packet loss rate is calculated by lost packets over overall sending packets. From the table, we can see the packet loss is high for using OLSR. The reason is congestions on general MANET nodes and gateways. Overall delay decreases because of the employment of feasible and uncongested paths.

Table 3. Performance comparison for two schemes

	Overall delay (ms)	Packet loss rate
OLSR	280.534	13/2567
Load balancing based OLSR	269.222	3/2567

From the simulation results, we can see that the load balancing scheme alleviate the gateway load at certain extent. The two gateways are simultaneously or alternatively used for traffic transmission. The simulation is executed with simple topology, and no mobility is introduced at this stage. Our purpose is to make a primary test to determine if enabling intermediate nodes to implement gateway switch is feasible. An interesting finding is that at some points, both of gateways are in operations for forwarding data. That is mainly because each intermediate node decides which gateway is to be selected based on its local traffic and overloading status on gateway. This feature will benefit to reduction of packet loss during gateway handover as not each intermediate node needs to switch gateway, which reduce the possibility of sudden unreachability to certain gateway. Comparing with the situation that the gateway switching is charged by source node and only happens when the overloading happens, our approach can take advantage of reacting with distributed manner.

Although the simulation test result proves the way of switching gateway on intermediate can be effective, there are still further details required to improve the load balancing scheme. For example, the corresponding routing protocol must take the factor of route loop into consideration, particularly when the issue of scalability is included. And the criteria to decide if a gateway is overloading might include multiple situations, e.g. unacceptable delay from gateway to satellite, energy consumption, and so on. As the same issue in proactive gateway discovery protocol, adaptive adjustment of gateway broadcasting time interval should be taken into consideration. Mobility of MANET nodes is also an important issue which affects packet loss rate and packet delivery delay, so must be carefully dealt with when improving load balancing scheme.

7 Conclusion

This paper first gives an introduction to the converged MANET-Satellite network. For realization of such integrated networks, a number of issues need to be addressed: routing interoperability, gateway selection mechanisms, satellite links' management and resource management. A large library of studies has been done in the literature, yet the issues are still worth tackling. Lots of interworking related operations can be done in gateways which makes gateway selection an essential part. We proposed a load balanced gateway selection scheme aims at alleviating congestion in overall network and distribute traffic as evenly as possible to achieve better network performance. The overall delay and packet loss rate can also be decreased. Resource management in integrated network is the key challenge which needs further study.

Acknowledgement. This paper is supported by FP7 Mission Project, by State Key Laboratory of Wireless Mobile Communication of China Academy of Telecommunication Technology (Project Number: 2007DQ305156) and by SatNExIII project.

References

1. Lera, A., Molinaro, A.: Designing the Interworking of Terrestrial and Satellite IP-Based Networks. IEEE Communications Magazine, 136–144 (February 2002)
2. Taleb, T., Hadjadj, Y., Ahmed, T.: Challenges, Opportunities, and Solutions for Converged Satellite and Terrestrial networks. IEEE Wireless Communications, 46–52 (February 2011)
3. Oliveira, A., Sun, Z., Monier, M., Boutry, P., Gimenez, D.: On Optimizing Hybrid Ad-hoc and Satellite Networks–the MONET Approach. In: Future Network and Mobile Summit 2010
4. Evans, B., et al.: Integration of Satellite and Terrestrial Systems in Future Multimedia Communications. IEEE Wireless Communications 12(5) (October 2005)
5. Le-Trung, Q., Engelstad, P.E., Pham, V., et al.: Providing Internet Connectivity and Mobility Management for MANETs. International Journal of Web Information Systems 5(2) (2009)
6. Jonsson, U., Alriksson, F., Larsson, T., et al.: MIPMANET-Mobile IP for Mobile Ad Hoc Networks. In: MobiHOC, pp. 75–85 (2000)
7. Zaman, R.U., Khan, K.-U.-R.: A review of gateway load balancing strategies in integrated internet-MANET. In: IEEE International Conference on Internet Multimedia Services Architecture and Applications (December 2009)
8. Shen, B., Shi, B., Li, B., Hu, Z.: Adaptive gateway discovery scheme for connecting mobile ad hoc networks to internet. In: Proc. Wireless Communications, Networking and Mobile Computing, vol. 2, pp. 7950–799 (2005)
9. Domingo, M.C.: Intergration of ad hoc networks with fixed networks using an adaptive gateway discovery protocol. In: Proc. 2nd IET International Conference on Intelligent Environments (July 2006)
10. Bouk, S.H., Sasase, I.: Multiple end-to-end QoS metrics gateway selection scheme in Mobile Ad hoc networks. In: International Conference on Emerging Technologies, pp. 446–451 (2009)
11. Manoharan, R., Mohanalakshmire, S.: A trust based gateway selection scheme for integration of MANET with Internet. In: IEEE-International Conference on Recent Trends in Information Technology, pp. 543–548 (June 2011)

Security Architecture for Satellite Services over Cryptographically Heterogeneous Networks

Yingli Sheng[1], Haitham S. Cruickshank[1], Martin Moseley[2], and John Ashworth[2]

[1] Centre for Communication Systems Research
University of Surrey
Guildford, United Kingdom
{Yingli.Sheng,H.Cruickshank}@surrey.ac.uk
[2] EADS Astrium
Portsmouth, United Kingdom
{Martin.Moseley,John.Ashworth}@astrium.eads.net

Abstract. The rapid growth in the demand for Internet services and many new applications has driven the development of satellite, which are the preferred delivery mechanism due to its wide area coverage, multicasting capacity and speed to deliver affordable future services. However, security has been one of the barriers for satellite services, especially for domains spanning over cryptographically heterogeneous networks. In this paper, a scalable and adaptable security architecture is specified to protect satellite services. Two major issues in the proposed security architecture, key management and policy provisioning, are presented and analyzed. And three scenarios, mobile network, fixed network and Delay Tolerant Network (DTN), are presented, with details on characteristics and security features.

Keywords: satellite, Heterogeneous network, policy, key management, mobile network, Delay Tolerant Network.

1 Introduction

Satellites will be an integral part of the Internet and next generation access technologies such as wireless, mobile and terrestrial broadband. As such, the broadcast nature of satellite coverage can be exploited, costs can be shared among large group of terminals providing a low-cost wide-area Internet multicast service. In addition, group-oriented applications are increasingly deployed over the Internet such as video conferencing, video on demand (VoD), TV over Internet and broadcasting stock quotes. A difficult barrier that prevents the wide exploitation of satellites and the group-oriented applications is the security provisioning for a large and cryptographically heterogeneous multicast group that span multiple domains.

It is proposed in the paper a scalable and adaptable security architecture that protects multicast data according to the cryptographic requirements of a variety of cryptographic domains. This work defines a new satellite multicast security architecture that addresses the specific obstacle that currently impedes development of large scale multicast security services that spans several cryptographically heterogeneous domains. By

R. Dhaou et al. (Eds.): PSATS 2013, LNICST 123, pp. 102–114, 2013.

introducing scalable key management and security policy mechanism, some of the security barriers that inhibit the integration of satellite networks with other network such as next generation mobile networks, would be removed. The major research issues in the security architecture are presented and analyzed, namely key management and security policy provisioning. Also, three sample scenarios are presented, including characteristics and security requirements for each of them.

2 Objectives

Future Internet will be a conglomerate of heterogeneous networks and systems such as satellite, next generation mobile, mobile adhoc and sensors nodes. It is envisaged that satellites will be part of broadband, mobile and Delay Tolerant Networking (DTN) service scenarios, which can span multiple security domains that are cryptographically heterogeneous. The concept of domains is used widely in the Internet. It is also applicable to group-key management to effect scalability, where members are divided (logically or physically) into domains or subgroups. In summary, at least two general types of domains are possible for secure group management:

- Domains according to data encryption: Here, the domains demarcate regions within which differing Traffic Encryption Key (TEK) are used to encrypt the group data.
- Domains according to key management: Here, the domains demarcate key management regions, where each region is associated with a different set of Key Encryption Keys (KEK) for the purpose of managing and disseminating the TEK, which is a common group data key.

Securing such service scenarios could be very challenging due to trust issues, key distribution, policy dissemination/management and multiple encryption/decryption across these domains.

The objective of the work is to specify a scalable and adaptable security architecture that is hierarchical and distributed, in order to protect unicast, multicast and broadcast data for a variety of cryptographically heterogeneous networks. The security architecture involves scalable key management and policy management entities. Such architecture should fit all the three scenarios mentioned above: mobile broadband, fixed network terminal and DTN.

3 System Architecture

It is presented in this section an innovative architecture for securing multicast services across heterogeneous security domains.

The architecture for securing multicast services across heterogeneous security domains is shown in Figure1. There are three novel concepts in this architecture:

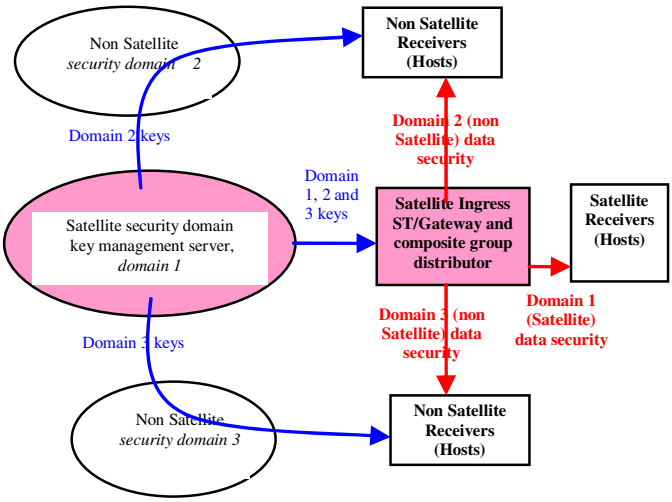

Fig. 1. Secure multicast service across heterogeneous security domains

- The first concept is the adaptive and scalable group key management. It will use adaptive grouping of members into encryption domains (subgroup) that use the same TEK. The partitioning will be made in a way that reduces both re-keying using KEKs and key translation overheads within the overall heterogeneous group. This concept promotes adaptability to changing membership dynamics in various domains.
- The second concept is the use of Data Distributors that disseminate the encrypted data with different keys for each domain. This will eliminate the need for encryption/decryption at security gateways at the ingress of each domain.
- The third concept is the use of security policies, especially for the distributed architecture to delegate trust and role to various entities in each domain. This will promote scalability and adaptability to changing security and threats situations. As such, policies can govern key dissemination, access control, re-keying of group-shared keys, and for the actions taken when certain keys are compromised.

The solution complements the existing link layer security solutions in satellite, digital video broadcasting (DVB), UMTS and WiMAX networks. However, it requires that data security should be implemented in a layer in the protocol stack that is common to all domains (e.g. satellite, UMTS and WiMAX), such as:

- IP network layer security (using IPSec);
- Transport layer security (TLS);
- Any application layer security.

4 Major Research Issues

There are several obstacles against the widespread deployment of multicasting services [1][2]. One of them is security. The security mechanisms for unicast are not adequate for the multicast scenario since multicast security mechanisms have scalability and efficiency constraints [3][4][5]. The work proposed in this paper aims to address gaps in secure multicast such as IP Multicast group key management and policies, with a particular focus on a group that spans many domains including a satellite network. Thus, there are two major research issues:

- Multicast key management in cryptographically heterogeneous domains
- IP multicast security policy provisioning

A Key Management

In a simple case, symmetric cryptography is used by the sender/source and the receivers/destinations, where the data is encrypted by the sender and decrypted by the receivers. The shared key is commonly referred to as the group-key or TEK, since only members of the multicast group are in possession of the key. The use of cryptography necessitates the delivery or dissemination of group keys. Group-oriented security, and more specifically the key management, has been researched for more than two decades. Most of the earlier work has focused on cryptographic approaches to manage keys for hierarchical organizations [6][7][8]. And satellite networks had their research on large scale secure multicast [9][10][11].

Rekeying in secure multicast is needed to preserve forward and backward secrecy whenever members join or leave. Thus rekeying overheads increases as the multicast group gets bigger. The concept of domains is also applicable to group-key management to effect scalability, where members can be divided (logically or physically) into domains (subgroups) [3][12]. However, a clash exists between re-keying overhead and computation overhead for key translation. Finding a trade-off between these two conflicting overheads is essential in the case of networks with resource constrained devices, such as sensors and Mobile Ad hoc NETworks (MANETs) and in the case of very large groups such as satellite multicast. At least two general types of domains are possible for secure multicast management:

- Domains according to data encryption: Here, the domains demarcate regions within which differing group-keys (data keys) are used to encrypt the multicast data. Thus, each domain is associated with a unique group-key, and "crypto-translations" (decryption using one key, followed by encryption using another key) must be carried out at the domain boundaries. Group-members residing within each domain would be in possession of a unique group-key (per domain).
- Domains according to key management: Here, the domains demarcate key management regions, where each region is associated with a different set of key management keys (KM-keys) for the purpose of disseminating the common group-key (TEK). Thus, each domain would manage its own km-keys (e.g., different rekey period for KM-keys), even though these are used to create safe passage for the common (group-wide) TEK from a key-source,

such as a key server, to each of the receivers residing in differing key management domains.

There exist a clash between re-keying overhead, and computation overhead: on one hand, using a single encryption domain increases the re-keying overhead and hence does not scale to large and highly dynamic groups, while it saves computation power which would have been spent in key translation. On the other hand, partitioning the group into different encryption areas reduces the re-keying overhead, but introduces additional computation overhead and delivery delays because of the requirement of key translation. The scalable key management scheme aims to find a good trade-off between these two conflicting overheads.

B Security Policy

Security policies provisioning is another focal point of the proposed architecture. Similar to other aspects of networking, the correct definition, implementation and maintenance of policies governing the various aspects of multicast security are important factors. Those which are directly related to multicast security include the policies for key dissemination, access control, re-keying of group-shared keys, and for the actions taken when certain keys are compromised [13]. The trust model is a critical issue for secure group communications, which can be established and managed using rule-based security policies. For large scale groups that span several security domains, security management might be delegated to group controllers (key managers) in each domain. Delegation of trust using policies allows the efficient working of distributed security management architecture [14][15]. Thus the use of such policies will help the security integration of satellite network with other networks. Through policies, a system may address the needs of all group participants in real time. The security policy could address the following requirements [16]:

- Identification - Each participant and group can be unambiguously identified.
- Authorization - A group policy can identify the entities allowed to perform protected actions. Group authorization partially determines the trust embodied by the group.
- Access control - Allowable access to group action can be stated by policy.
- Mechanism - Each policy can state how the security requirements of the group are to be addressed.
- Verification - Each policy can present evidence of its validity such as proof of its origin and integrity.

A Reference Framework has been defined and standardized and it addresses all problem areas mentioned above [12][17]. The framework presents a set of functional building blocks that should be tackled for any secure multicast architecture design. It also expresses the complex multicast security from the perspective of architecture (centralized/distributed), multicast group types (1-to-*N* and *M*-to-*N*), and classes of protocols (the exchanged messages) needed to secure multicast packets.

However, currently very little work exists on using security policies for distributed key management, particularly for satellite networks. As such, security policies should

be used to delegate trust to key managers and data distributors in various domains. If the multicast group membership is highly dynamic, then policies will also enable adaptive formation and deletion of data encryption domains depending on the subgroup membership dynamics. Security policies are used in the proposed architecture to promote scalability and adaptability in large heterogeneous multicast groups.

5 Scenarios

In this section, three scenarios are defined: mobile network scenario for the applications such as mobile broadband, fix network scenario for the applications such as SMART METER, broadband access and Delay Tolerant Network (DTN) scenario for the space applications such as Deep Space. The scenarios are described and the features are discussed in this section.

A Mobile Scenario

One typical application of mobile scenario is mobile broadband service, which includes web browsing and possibly video streams. Security, as one of the important features of mobile broadband, must be provided to essential signalling messages, but might not necessarily to the large amount of packet data.

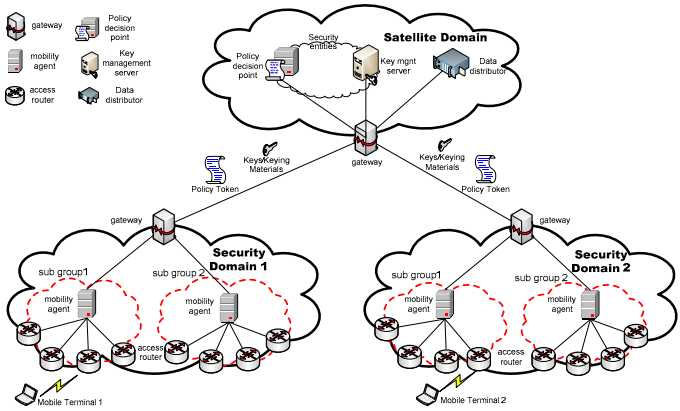

Fig. 2. Mobile scenario

As shown in Figure 2, three domains are involved in the mobile scenario: satellite domain, security domain 1 & 2. Security domain 1 &2 are assumed to be cryptographically separated. It is possible that different encryption/decryption algorithm, different key size are used to secure the signalling/traffic data in security domain 1 & 2. The satellite domain provides the ability for centralized key management and policy generation.

1) Satellite domain

a) Data distributor
Disseminate the encrypted data with different data keys for each domain. This entity eliminates the need for encryption/decryption at security gateways at the ingress of each domain.

b) Key management server
Dynamically generate different set of key management keys for different regions. The adaptive and scalable group key management is enabled by the use of key server. It uses adaptive grouping of member into encryption domains that use the same data key, therefore, it reduces re-keying and key translation overheads.

c) Policy decision point (PDP)
It acts as policy server which generates policy (such as policy token [18]) to delegate trust and defines different security mechanisms to various domains. Policy enables adaptable security solutions for changing security and threats situations. Therefore, the resilience to changing security environment is improved. Generally, policy can define key/keying materials dissemination, access control, re-keying conditions, actions taken when a key is compromised, and etc.

It should be noted that the centralized scenario is illustrated in Figure 2. In a centralised scenario, the policy decision point and key server are located in the satellite domain, and relevant security information is disseminated to various security domains. The policy enforcement point (PEP), which cooperates with PDP to enforce policy to the end terminals, can be collocated with entity in each security domain, such as the mobility agent. The PEP can issue policy request on behalf of the end user and handle policy response from the PDP. If distributed system is required, the PDP/key server should be available in each of the security domains, providing the ability to generate policy and set of keys locally within the particular security domain. And the local PDP/key server should be able to operate in a cooperative manner to achieve optimized performance.

2) Security domain1 & 2
In both of security domain 1& 2, the following entities are involved:

a) Gateway

It is the point of entry or exist for the security domain, providing connectivity to the satellite domain.

b) Mobility agent

It provides mobility management service to the mobile terminals, including location updates, forwarding traffic data, and etc.

c) Access router

It is a layer-3 router, providing network access to the mobile terminal. The access routers can be managed by the mobility agent.

d) Mobile terminal

It is the mobile user, who would like to use the network resources. It can perform micro-mobility handover within one mobility agent subgroup and can also perform macro-mobility handover across mobility agents/networks.

3) Characteristics

Some characteristics of mobile scenario are:

a) Moderate bandwidth availability
b) Limited number of security domains
c) Limited coverage areas

4) Security features

Some security features of mobile scenario are:

a) Specific key management requirements: multiple encryption/decryption domains are needed

b) Moderate data key updates due to moderate data rate in the forward link

c) For multicast services, moderate/fast changing group membership due to the nature of mobile services

d) Either centralized or distributed key/policy management architecture can be considered.

e) For the delay sensitive data in mobile applications, it is required to reduce the negative impact of security on delays by integrating security design with mobility protocols.

f) Due to the nature of valuable bandwidth resources, minimizing signalling overhead introduced by security mechanism is essential. The tradeoffs between strong security design which desired by the cryptography fans and the overhead introduced by security need to be considered.

B. Fixed Network Scenario

The fixed network scenario can be applied to broadband access in rural area, where DSL lines are not applicable, or specific application such as SMART METER/GRID.

As shown in Figure 3, three domains are involved in the fixed network scenario: satellite domain, security domain 1 & 2. Security domain 1 &2 are assumed to be cryptographically separated. The satellite domain remains the same as in the mobile scenario. While in each of security domain, instead of roaming mobile terminals, there are fixed terminals. The terminals can be broadband service terminals, or other devices, such as SMART METER device installed in the end users' home/office. All of the terminals are connected to the aggregation router, which provides the ability of

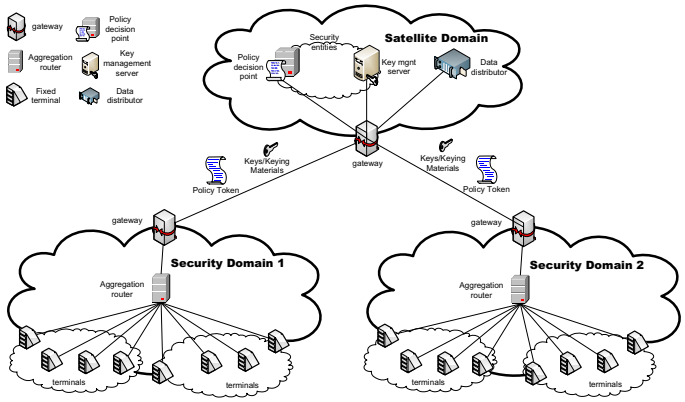

Fig. 3. Fixed network scenario

data aggregation. And the aggregation router is connected to the external network, via gateway. The fixed terminals (for a broadband service) can be connected directly to the aggregation router for the broadband service, and the aggregation router then connects to the satellite access gateway. If the SMART METER application is considered, the terminals are SMART METER devices installed at the end user's home/office to collect the electricity/gas/water meter information. Of all Smart Meter technologies, one critical technical problem is communication. Each meter, especially the sensitive user ID or billing related information, must be reliably and securely transferred to the central location. Considering the varying environments and locations where meters are found, that problem can be daunting. The existing solutions proposed are: the use of cell/pager networks, satellite, licensed radio, combination licensed and unlicensed radio, power line communication (PLC). Not only the medium used for communication purposes but the type of network used is also critical. Fixed wireless, mesh network or a combination of the two have been deployed for SMART METER application. There are several other potential network configurations possible, including the use of Wi-Fi and other internet related networks. No one solution seems to be optimal for all applications. Rural utilities have very different communication requirements from urban utilities or utilities located in difficult locations such as mountainous regions or areas ill-served by wireless and internet companies. Thus, providing SMART METER service using satellite is ideal for rural or difficult locations, and it is also possible to application in urban areas as well. There is a growing trend towards the use of TCP/IP technology as a common communication platform for Smart Meter applications, so that utilities can deploy multiple communication systems, while using IP technology as a common management platform.

1) Characteristics

Some characteristics of fixed network scenario are:

a) Higher bandwidth availability for forward link and limited bandwidth in the return link

b) Multiple security domains
c) Wider coverage area comparing to mobile scenario

2) Security features
Some security features of fixed network scenario are:

a) multiple encryption regions due to the multiple administrative domains
b) moderate/frequent data key updates might be necessary due to higher data rate in the forward link
c) For multicast services, slow/static group membership due to the nature of fixed network terminals
d) Centralised key/policy management architecture is the preferred solution.
e) Access control is one of the major concerns of SMART METER application. It is to ensure only devices authorised by the customer and energy supplier are allowed to interact with metering system.
f) How to manage and use the data key is essential. For the broadband services, the main types of communication that are supported by fixed network are voice, data transfer, video/images and web browsing. It might not be necessary to use data key to secure all of the traffic (such as large volumes of multimedia traffic). How to define the security level of different traffic becomes a challenge. For the SMART METER application, each meter, especially the sensitive user ID and billing related information, must be reliably and securely transferred to the central location.

C. DTN Scenario: Deep Space

Space exploration started in early sixties and since then the interest towards deep-space communication continuously increased especially from the scientific point view, thus paving the way for the Moon human exploration and then the Mars missions. More recently, the current advances and trends in technology have pushed the space agencies to a new and more futuristic concept of space exploration: the Solar System Internet. In fact, it consists in the deployment of a real Internet over the space, able to connect Earth centers to remote sites, located in possibly different places of the Solar System, such as Mars, Saturn, and Mercury. Consequently, it is immediate to think of a complex deep-space network (Figure 4), where data transaction and routing operations are performed seamlessly and autonomically, thus reducing the manual intervention to the least. The human assistance would be still needed to provide recovery to emergency situations that the implemented fault resilience model could not handle. Besides the attracting perspective, this future scenario may offer benefits in terms of scientific studies and possible revenues for the aerospace industries.

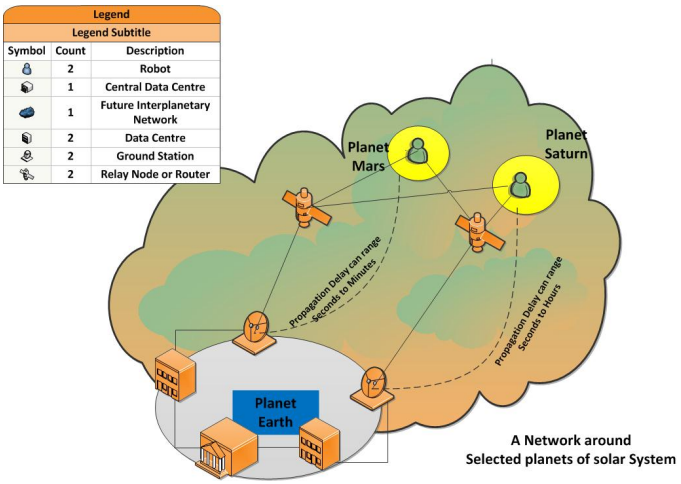

Fig. 4. DTN scenario: A Diagram showing a future network along planets of solar systems

1) Characteristics

Some characteristics of DTN scenario are:

a) Extremely limited bandwidth availability

b) Limited number of security domains.

c) Frequent disconnection/disruptions

d) Very large propagation delays. Depending on the specific addressed space mission, the propagation delay can range from a few seconds (e.g., Earth-Moon) to several minutes (e.g., Earth-Mars), to even hours (e.g., Earth-Saturn, Earth-Pluto).

e) Scarce and highly asymmetric link data rate. Because of the reduced spacecrafts' size, the deployed antenna can be only of reduced dimensions, thus implying small data rate available. In addition, most of part of data traffic flows though the downlink (e.g., measurement, image transfer), whereas the uplink is principally used for transmitting telecommand messages. As a result, strong asymmetry between data rates available on downlink and uplink respectively is experienced, being as high as 10000 to 1.

f) Limited storage availability. The limited dimensions of the space crafts pose additional constraints on the on-board storage, which plays some role for routing and buffering.

g) Degraded link quality. The long distances determine high free-space-loss to which also weather fading may add, occurring in case of Ka band transmission. Besides, in case of optical laser technology, additional quality impairments may take place, resulting in non negligible BER or PER.

h) Intermittent visibility between Earth and other remote planets, because of the relative movement around the Sun, resulting in tight transmission schedule to take advantage of the available resources. Finally, this leads to an overall reduced throughput measure, if compared to the total mission time. However, by using the

relay nodes or routers in the space, increased data rate and more communication opportunities can be achieved by using DTN store and forward mechanism

2) Security features
Some security features of DTN scenario are:

a) Limited number of encryption regions, due to the nature of space application
b) Slow data key updates
c) For multicast services, slow changing/static group membership
d) Distributed key/policy management architecture is the preferred solution, due to the sparse nature of space communications..

6 Conclusion

While the advantages of multicasting services over satellite networks are clear, security as one of the obstacles poses great challenges in terms of scalable key management and adaptable policy provisioning. An innovative security architecture is proposed in this paper to address the security challenges, with a particular focus on key management and security policy. The major issues on multicast key management/security policy are discussed. A brief literature review is provided and existing problems are highlighted. Also, three scenarios are defined for future implementation: mobile network scenario for the application such as mobile broadband, fixed network scenario for the application such as SMART METER/GRID and DTN scenario for the application of Deep Space. The characteristic of each scenario is analyzed and security requirements are also drawn.

Based on the security architecture, protocols between key managers, policy server and data distributor need to be defined in the future. Group Secure Association Key Management Protocol (GSAKMP) in [14] provides secure communications between group owner, key mangers, senders and receivers. Either GSAKMP-type protocol will be used to establish secure communications between data distributors the other entities or a new protocol will be developed, depending on the architecture requirements. If a new protocol is required, the proposed protocol will be analyzed and verified by model-checking or theorem-proving techniques.

References

[1] Brown, I., Crowcroft, J., et al.: Internet Multicast Tomorrow. Internet Protocol Journal 5(4) (2002)
[2] Diot, C., Levine, B.N., Layers, B., et al.: Deployment Issues for the IP Multicast Service and Architecture. IEEE Network 14, 10–20 (2000)
[3] Challal, Y., et al.: Adaptive clustering for Scalable Key Management in Dynamic Group Communications. International Journal of Security and Networks (2007) ISSN 1747-8413

[4] Rafaeli, S., Hutchison, D.: A Survey of Key Management for Secure Group Communication. ACM Computing Surveys 35(3), 309–329 (2003)
[5] Wittmann, R., Zitterbart, M.: Multicast communication: Protocols and applications. Morgan Kaufmann (2001) ISBN 1-55860-645-9
[6] Koyama, K., Ohta, K.: Identity based conference key distribution systems. In: Pomerance, C. (ed.) CRYPTO 1987. LNCS, vol. 293, pp. 175–184. Springer, Heidelberg (1988)
[7] Ballardie, A.: Scalable Multicast Key Distribution. RFC 1949, IETF (1996)
[8] Steiner, M., et al.: Diffie-Hellman key distribution extended to group communications. In: Proceedings of the 3rd ACM Conference on Computer and Communications Security. ACM (March 1996)
[9] Cruickshank, H., et al.: Securing multicast in DVB-RCS satellite systems. IEEE Wireless Communications, Special Issue on Key Technologies and Applications (October 2005)
[10] Ng, D., Cruickshank, H., Sun, Z., Howarth, M.P.: Dynamic Balanced Key Tree Management for Secure Multicast Communications. IEEE Transactions on Computers (2007)
[11] Zhang, Y.: A multilayer IP security protocol for TCP performance enhancement in wireless networks. IEEE Journal on Selected Areas in Cmmunications 22(4) (May 2004)
[12] Hardjono, T., et al.: The Multicast Group Security Architecture. RFC 3740 (2004)
[13] Harney, H., Harder, E.: Multicast Security Management Protocol (MSMP) Requirements and Policy. IETF, draft-harney-sparta-msmp-sec-00.txt (March 1999)
[14] Harney, H., et al.: GSAKMP: Group Secure Association Key Management Protocol. RFC 4535 (2006)
[15] Christian, T., Riguidel, M.: Distributed trust infrastructure and trust-security articulation: Application to heterogeneous networks. In: IEEE, Proceedings –20th International Conference on Advanced Information Networking and Applications, pp. 33–38 (2006)
[16] Harney, H., et al.: Principles of Policy in Secure Groups. In: Proceedings of Network and Distributed Systems Security 2001. Internet Society (2001)
[17] Baugher, M., et al.: Multicast Security Group Key Management Architecture. RFC 4046 (2005)
[18] Colegrove, A., Harney, H.: Group Security Policy Token v1, RFC 4534, IETF (June 2006)

Generalized Encoding CRDSA: Maximizing Throughput in Enhanced Random Access Schemes for Satellite

Manlio Bacco, Pietro Cassarà, Erina Ferro, and Alberto Gotta

National Research Council of Italy (CNR,
Institute of Information Science and Technologies (ISTI)
{manlio.bacco,pietro.cassara,
erina.ferro,alberto.gotta}@isti.cnr.it

Abstract. This work starts from the analysis of the literature about the Random Access protocols with contention resolution as Contention Resolution Diversity Slotted Aloha (CRDSA) and introduces a possible enhancement, named Generalized Contention Resolution Diversity Slotted Aloha (GE-CRDSA). The GE-CRDSA aims to improve the aggregated throughput when the system load is less than 50%, playing on the opportunity of transmitting an optimal combination of information and parity packets frame by frame.

Keywords: Satellite, Interference Cancellation, DVB-RCS2, CRDSA, Slotted Aloha.

1 Introduction

Many efforts have been made in the field of random access protocols for satellite communications, aiming to maximizing the aggregated throughput. Contention Resolution Diversity Slotted Aloha (CRDSA) [1] in the forthcoming DVB-RCS2 standard [2] and in general all the variants of Slotted Aloha (SA) protocols, which take advantage of contention resolution (CR), are clear examples of the strong interest in such results.

The advantage of this technique is represented by the increment of the performance in terms of throughput: in fact, CRDSA exhibits almost ideal performances (i.e low collision losses), up to 50-60% of the global access network load, in case of ideal power control [1]. Both CRDSA and SA assume the MAC frame duration equal to T_F, during which N_s slots are allocated. Then the time slot has duration $T_S = T_F/N_s$. Assuming that at each frame M users try to transmit data packets, each user transmits one or more replicas of the same packet in the current MAC frame. In each packet a pointer to the positions of its replicas is included. The pointer is used to locate its own other replicas into the frame and to remove the interfering ones in the collided slots. The contention resolution proceeds iteratively, by removing the decoded signals in the relative collided slots. At the end of the procedure the Packet Loss (P_L) due to the un-cancelled collisions is significantly reduced. By definition, the throughput is given by:

$$T = G(1 - P_L) \tag{1}$$

R. Dhaou et al. (Eds.): PSATS 2013, LNICST 123, pp. 115–122, 2013.

where for given number of stations M and number of time slots N_s, the constant $G = \frac{M}{N_s}$ is the average number of packet transmission attempts per frame, i.e., the average load of the system, when a single information packet is transmitted per station per frame. In the SA is the probability that no others attempts of transmission arises during a time slot. This value can be calculated through the Poisson distribution at $k = 0$:

$$P(k) = G^k \frac{e^{-G}}{k!} \xrightarrow{k=0} e^{-G}$$

Let G^* be the supremum of G such that, in the asymptotic setting $M \to \infty$, the throughput T fulfills $T = G$; therefore G^* is the asymptotic peak throughput. In the SA the maximum throughput $T_{SA}^{max} = G^* e^{-G^*} = \frac{1}{e}$ is achieved at $G^* = 1$. In CRDSA, reducing P_L at a given G value leads to a throughput gain with the respect to SA and its non-SIC variants[1]. This improvement is quantified in [1] as the normalized throughput $T_{CRDSA} \approx 0.55$, which is the probability of successful packet transmission per time slot, whereas the peak throughput for SA is $T_{SA} \approx \frac{1}{e}$. Further improvements can be achieved by exploiting the capture effect [4,5]. In [6] Irregular Repetition Slotted ALOHA (IRSA) was introduced to provide a further throughput gain over CRDSA. Higher throughput can be achieved by IRSA, allowing the satellite terminal (ST) to choose the number of replicas in a random way. As stated in [6], CRDSA and further improvements such as CRDSA++ can be considered as particular cases of IRSA where the repetition rate, frame by frame, is fixed. In [7] is shown that a variable repetition rate does not introduce significant improvements in terms of throughput, if N_s is limited to a few hundred of slots i.e., in the range foreseen in DVB-RCS2 standard [2]. $T_{IRSA} \leq 0.8$ is obtained in [6], when Ns is around 200. While CRDSA, CRDSA++ and IRSA are based on repetitions, Coded Slotted ALOHA (CSA) encodes the bursts of each user before transmitting [8].

All the methods presented above implicitly impose that the average load in the system is targeted around the G^* value, otherwise any improvement is appreciable. A centralised load control should reduce/increase Ns, according to the actual estimation of the average number of STs, which try to access to the channel. Since Ns in DVB-RCS2 standard is bounded between 64 and 128 slots [2], the satellite system may perform at G loads under the desired G^*, leading to the under-utilization of the available bandwidth. For example, according to (1), if P_L is negligible, it results that $T \approx G$. In CSA, the transmitted burst is made up of $k = 2$ information packets out of n transmitted packets. The others $r = n - k$ packets are generated by a packet-oriented binary linear block code.

This work aims at studying a generalized case of CSA, named Generalized Encoding CRDSA (GE-CRDSA), where each ST randomly sorts the $\{k, r\}$ pair, according to the relative probability distributions - described in the following - that generate the code (n, k). GE-CRDSA aims at optimizing CSA, by allowing each ST to transmit more than two information packets per frame, by reducing the queuing delay with the respect to those systems, which consider only a single information packet per frame.

[1] DSA [3] with two or more replicas for each information packet transmission.

2 System Overview

Let us consider a SA system, with a MAC frame duration of T_F, composed of N_s slots. Let be m_i a Poisson distributed r.v. of mean λ, which represents the number of active STs out of M terminals at frame i. Let us define:

$$G = \frac{\lambda\,\overline{k}}{N_s}$$

being G the system load and $\overline{k}$ the average number of information packets that STs transmit in a frame. Let $p_k\{\Omega_i\}$ be the probability distributions of the number of information packets k and $p_r\{\Psi_j\}$ the probability distributions of the number of parity packets r transmitted for a given frame, respectively. At any frame, a ST randomly sorts the $\{k, r\}$ pair, according to the probability distributions defined above. Hence, the number of information k and parity r packets sent by an active ST in a frame can be represented by the polynomials:

$$\Omega_k(x) \triangleq \sum_i \Omega_i x^i \tag{2}$$

$$\Psi_r(x) \triangleq \sum_j \Psi_j x^j \tag{3}$$

where the weights Ω_i and Ψ_j are the probability of having i information packets and j parity packets, respectively. From (2) and (3) the average information length $\overline{k}$ and the average parity length $\overline{r}$ are respectively given by the following equations:

$$\overline{k} = \sum_i i\Omega_i = \Omega'(1), \qquad \overline{r} = \sum_j j\Psi_j = \Psi'(1)$$

The Satellite Master Control Station shall account for monitoring the average system load and to communicate the weight vectors $\boldsymbol{\Omega} = \{\Omega_i\}$ and $\boldsymbol{\Psi} = \{\Psi_i\}$ at each load variation. The optimal choice of the load vectors $\boldsymbol{\Omega}$ and $\boldsymbol{\Psi}$ is not trivial and the optimization problem is not addressed in this manuscript. However, some considerations are presented in the section 4.

3 Numerical Results

In the previous section we have introduced the mathematical framework behind the GE-CRDSA. The algorithm allows the users to choose randomly the number of information packets as well as the number of parities from the probability distributions $p_k\{\Omega_i\}$ and $p_r\{\Psi_j\}$, respectively. In this section some simulation results are presented, showing how the choice of the $\{k, r\}$ pair affects the throughput and the packet loss at different

Table 1. Simulation parameters for the case study

Parameter	Value
Bandwidth	8 Mhz
Modulation	QPSK
Phy FEC	3GPP 1/3
Frame Duration	0.0202s
N_s (slots)	100÷1000
IC iterations[2]	20

G values. Matlab [9] has been used as simulation environment. System and simulation parameters are summarized in Table 1.

According to section 2, we estimated the aggregated throughput and the relative packet loss for each load G/k by changing exhaustively the coding rate, i.e. considering all the possible combinations of the couple $\{k, r\}$ up to $n_{max} = r + k <= 10$ that could be randomly extracted from the probability distributions $p_k\{\Omega_i\}$ and $p_r\{\Psi_j\}$, respectively.

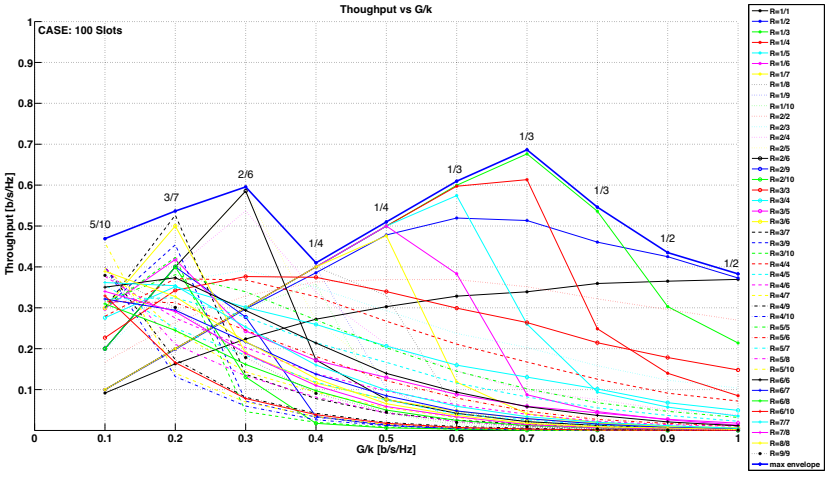

Fig. 1. Throughput vs G/k (N_s=100)

Figure 1 shows the throughput for all the different (n, k) pairs with respect to the ratio between the normalised offered load G and information length k. The most significant curve is the maximum envelope, which reports, for any G/k value, the k/n ratio

[2] The interference cancellation (IC) process performs several iterations in order to recover the maximum number of packets in each frame. A DSA is equivalent to a CRDSA using a single iteration [6]. Trivially, SA is for $k = n = 1$.

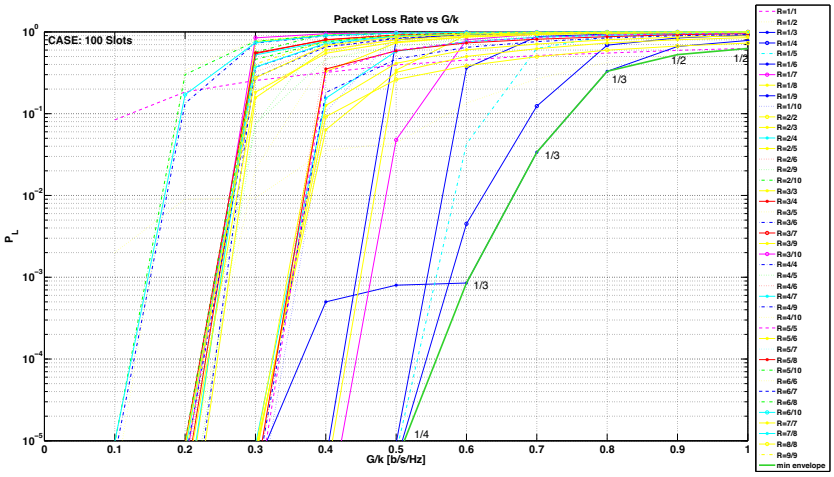

Fig. 2. Packet Loss Rate vs G/k (N_s=100)

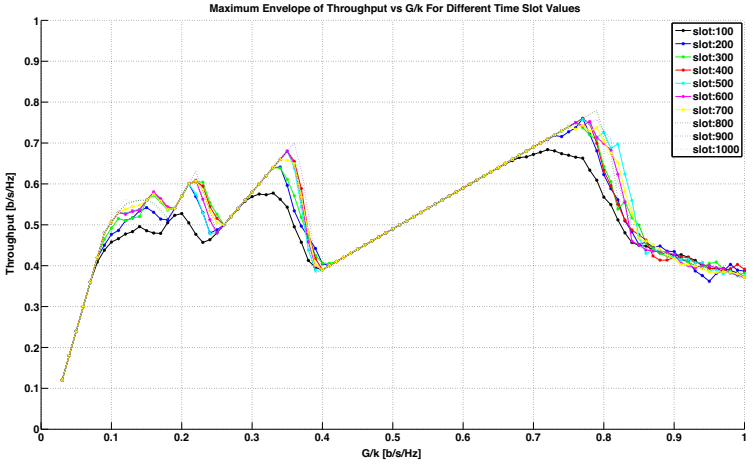

Fig. 3. Throughput vs G/k for different number of time slots

which maximises the overall system throughput. In other words, the means of distributions p_k and p_r should track the values on the maximum envelope in order to guarantee the highest throughput at every system load. In particular, GE-CRDSA reaches higher values of throughput than CRDSA *et alt.* for G/k lower than 0.4, imposing to transmit 2, 3 or more information packets per station per frame.

Figure 2 shows the packet loss rate for different (n, k) pairs used during the simulations, with respect to the ratio between the normalised offered load G and information length k. Dually, the figure also shows the minimum envelope of the packet loss rate

P_L^{min}, which corresponds to the (n, k) pair that maximises the throughput envelope in Figure 1.

According to the outcome in Figures 1 and 2, in Figure 3 we differently focus on the sole maximum envelope of the throughput, thus making N_s ranging in the interval $100 \div 1000$. The curves in Figure 3 show the expected trend, with maximum variation range that falls within 45%. Hence, changing N_s does not significantly affect the overall throughput and the k/n ratios on the max envelope remain almost the same. Therefore, the throughput can be enhanced choosing an appropriate (n, k) pair as well as the number of time slots N_s. Note that the choice of these parameters can be performed during the transmission according to a control flow policy that tracks the G^* value.

Figure 4 shows all the minimum envelopes of the packet loss rate vs. N_s.

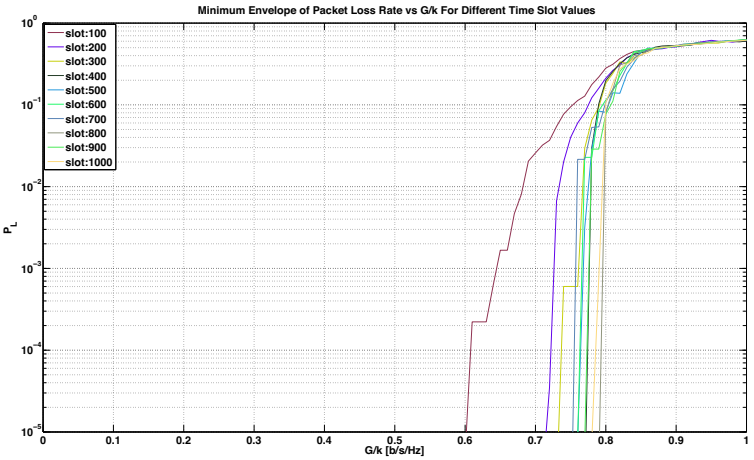

Fig. 4. Packets Loss Rate vs G/k for different number of time slots

4 Conclusions

Contention resolution algorithms have demonstrated to successfully reduce the collision probability in random access methods, renewing the application of random access for information delivery. We have shown that by increasing the mean number of information packets sent by a station at each frame, when the system load is poorly loaded, the system throughput can be significantly improved up to get the twice of that obtained with a standard CRDSA. Since this study only accounts for colliding packets with the same $SNIR$ (Signal-to-Noise plus Interference Ratio), further improvements in terms of optimal system load G^* and maximum achievable aggregated throughput can be obtained, by considering power unbalancing and capture effect. However, achieving higher loads thanks to capture effect does not impact on the rationale behind the proposed scheme and further improvements could be showed in terms of aggregated

throughput. GE-CRDSA does not neglect a load control system in order to track the optimal load correspondent to the maximum achievable throughput, but it relaxes the tracking constraints over a wider range of target loads, reducing the dynamic allocation of the pool of slots dedicated to random access. In our preliminary simulations, we have provided an exhaustive evaluation of all the possible combinations of k and r in order to achieve the maximum aggregated throughput. Future work foresees the definition of an optimisation problem, in order to define a control law to extract the $\{k, r\}$ pair for a given G that maximise the aggregated throughput and to evaluate the stability of the system in a dynamic context, i.e., when G is time variant. Assuming that any station at the frame t can randomly choose the $\{k, r\}$ pair, according to the probability distributions p_k and p_r, the throughput maximisation, over all the possible values of G, can be stated as in the following.

$$\begin{aligned} &\max\{T\}_{\{\Omega_1 \cdots \Omega_k\}} \\ &\qquad \text{s.t.} \\ &\qquad r = \mathcal{G}(P_L) \\ &\qquad k + r \leq n_{max} \end{aligned} \tag{4}$$

The solution of the optimization problem (4) is the probability distribution p_k, used by the user to extract the number of information packets to transmit at the frame t. This kind of problem can be addressed through both analytical or numerical solution [10], even if the first kind of solution gives much more information about the behavior of the system. The constraints of the optimization problem are the number of parity packets chosen according to the relation between the packet loss probability and the total number of transmitted packets, and the maximum number of transmitted packets n_{max}[3] per station per frame. Note that, $r = \mathcal{G}(P_L)$ is the probability distribution p_r, which can be estimated, given set of empirical data and few features assumptions, through nonparametric density estimation techniques such as the Generalized Cross Entropy Method (GCE) [11].

References

1. Casini, E., De Gaudenzi, R., Del Rio Herrero, O.: Contention resolution diversity slotted ALOHA (CRDSA): An enhanced random access scheme for satellite access packet networks. IEEE Trans. Wireless Commun. 6(4), 1408–1419 (2007)
2. Digital Video Broadcasting (DVB); Second Generation DVB Interactive Satellite System (RCS2); Part 2: Lower Layers for Satellite standard, Draft ETSI EN 301 545-2 V1.1.1 ed. (June 2011)
3. Choudhury, G., Rappaport, S.: Diversity ALOHA - a random access scheme for satellite communications. IEEE Trans. Commun. 31(3), 450–457 (1983)
4. Roberts, L.G.: Aloha packet systems with and without slots and capture. In: ARPANET System Note 8, NIC11290 (September 1972)
5. del Rio Herrero, O., Gaudenzi, R.D.: A high-performance mac protocol for consumer broadband satellite systems. In: Proc. of 27th AIAA Int. Communications Satellite Systems Conf., ICSSC (June 2009)

[3] Note that in case of a single terminal it would be possible at limit that $k \leq n_{max} \leq N_s$, i.e. the station occupies an entire frame.

6. Liva, G.: Graph-Based Analysis and Optimization of Contention Resolution Diversity Slotted ALOHA. IEEE Transactions on Communications 59(2) (2011)
7. Ferro, E., Gotta, A., Celandroni, N., Davoli, F.: Employing contention resolution random access schemes for elastic traffic on satellite channels. In: 18th Ka and Broadband Communications Navigation and Earth Observation Conference (June 2012)
8. Paolini, M.E., Liva, G.: High throughput random access via codes on graphs: Coded slotted aloha. In: ICC (2011)
9. Matlab, http://www.mathworks.com/products/matlab/
10. Boyd, S., Vandenberghe, L.: Convex Optimization. Cambridge University Press, New York (2004)
11. Botev, Z.I., Kroese, D.P.: The generalized cross entropy method, with applications to probability density estimation. University of Queensland's Institutional Digital Repository (2007)

Performance Evaluation of SPDY over High Latency Satellite Channels

Andrea Cardaci[2], Luca Caviglione[1], Alberto Gotta[2], and Nicola Tonellotto[2]

[1] Institute of Intelligent Systems for Automation (ISSIA)
National Research Council of Italy, Via de Marini 6, 16149, Genova
luca.caviglione@ge.issia.cnr.it
[2] Information Science and Technologies Institute (ISTI)
National Research Council of Italy, Via G. Moruzzi 1, 56124, Pisa
cyrus.and@gmail.com, {alberto.gotta,nicola.tonellotto}@isti.cnr.it

Abstract. Originally developed by Google, SPDY is an open protocol for reducing download times of content rich pages, as well as for managing channels characterized by large Round Trip Times (RTTs) and high packet losses. With such features, it could be an efficient solution to cope with performance degradations of Web 2.0 services used over satellite networks. In this perspective, this paper evaluates the SPDY protocol over a wireless access also exploiting a satellite link. To this aim, we implemented an experimental set-up, composed of an SPDY proxy, a wireless link emulator, and an instrumented Web browser. Results confirm that SPDY can enhance the performances in terms of throughput, and reduce the traffic fragmentation. Moreover, owing to its connection multiplexing architecture, it can also mitigate the transport layer complexity, which is critical when in presence of middleboxes deployed to isolate satellite trunks.

Keywords: networking protocol, satellite network, lossy channels, SPDY, HTTP, performance evaluation.

1 Introduction

Nowadays, services for sharing personal contents with a high degree of interactivity are considered new real killer applications of the Internet. This new paradigm has been mainly applied to the World Wide Web (WWW), which now approximates the *Social Web* initially envisaged by the World Wide Web Consortium (W3C). However, instead of a unified design, its implementation is based on heterogeneous sets of specific platforms, often with overlapped functionalities. We mention, among the others: blogs, wikis, Online Social Networks (OSNs), multimedia sharing platforms, and real-time collaboration frameworks.

In parallel, *legacy* websites have been enriched with such functionalities too. In fact, about the totality of *modern* webpages has some features to support interactivity or to provide dynamic contents. To this aim, one of the most popular approaches relies on the *mash-up* technique enabling to retrieve and merge data

R. Dhaou et al. (Eds.): PSATS 2013, LNICST 123, pp. 123–134, 2013.

from different remote providers (see, e.g., reference [1] for a paradigmatic example on the composition of mashable information). Moreover, the social vocation of the Web has been also ported to plain websites, e.g., via third party plug-ins directly embedded in the HTML. In order to be effective, interactivity needs a constant data exchange between the involved endpoints. A popular approach is to use the Asynchronous JavaScript and XML (AJAX) paradigm, which constantly transmits data between the server and the client over an indefinitely held HTTP connection. This also requires pages to embed proper scripts (e.g., the `XMLHTTPRequest` Javascript object), or additional software components to interact with remote services (often defined as plug-ins).

Such aspects lead to the so-called *Web 2.0* also accounting for mutations in the structure of pages, and characteristics of the related Internet traffic. In more details, a Web page is composed of many *objects*, which have to be retrieved to compose the whole content, i.e., the *main* object containing the HTML code, and (multiple) *in-line* objects(s) linked within the hypertext. The Web 2.0 heavily alters the characteristics of in-line objects, which can now embed additional services, such as for audio/video streaming, or to interact with an OSN [2]. Nevertheless, this enriched vision has not been limited only to contents, since it is now possible to deliver full-featured applications via a Web page. As an example, many Software-as-a-Service (SaaS) platforms [3] are based on interactive Graphical User Interfaces (GUIs) directly operated from the browser. Yet, to issue commands and provide feedbacks to users, they require a non-negligible amount of bandwidth and real-time constraints for assuring prompt data synchronization with a remote back-office. To summarize, the highly interactive nature of Web 2.0 reduces the accuracy of the *page-by-page* model.

Another important feature to comprehensively evaluate the modern Internet is its increased support of *mobility*. Thus, many network appliances also assure connectivity via wireless links, e.g., IEEE 802.11, the Universal Mobile Telecommunication System (UMTS), Long Term Evolution (LTE), and satellite channels. Yet, mobile nodes impose constraints clashing with the resource consuming nature of the Web 2.0. This is even truer in the case of satellite communications, potentially leading to additional hazards in terms of performances, for instance due to delays (see, e.g., reference [4] for a performance evaluation of an OSN accessed through a geostationary satellite facility). We point out that a satellite link is not only deployed to support mobile nodes, but it is also the main choice to grant access to the Internet in rural areas, or developing Countries.

Hence, the more aggressive behaviors of Web 2.0 applications also need proper adjustments in the protocol stack, especially for the case of the HTTP. In this perspective, a cutting-edge solution is SPDY [5], i.e., an enhanced HTTP supporting data compression and connections multiplexing. It can also mitigate the impact of channels with large Round Trip Times (RTTs) and high packet losses. According to reference [5], when used on wired links, SPDY can reduce download times in the range of 27-60%. With such premises, it could be a very suitable solution for improving performances when accessing the Web from a satellite network. Nevertheless, since SPDY uses a single transport connection, its deployment in

satellite networks can lead to further benefits. For instance, typical transport-layer enhancements like Performance Enhancing Proxies (PEPs) can experience a reduced workload, i.e., in terms of TCP connections to be handled to serve multiple Web sessions.

From the author's best knowledge, there are not any prior attempts to characterize SPDY over satellite channels. Thus, this paper evaluates the effectiveness of using SPDY in place of standard HTTP to increase performances of Web access over satellite networks. The contributions of this work are: *i*) to understand the most relevant behaviors of the SPDY protocol when used over heterogeneous wireless networks, especially those using large *delay* channels such as satellite one; *ii*) to showcase the creation of an ad-hoc testbed, which can be reused for similar investigations; *iii*) to provide an earlier comparison between HTTP and SPDY when used to access some popular websites.

The remainder of the paper is structured as follows: Section 2 compares HTTP and SPDY, while Section 3 showcases the testbed and some basic patterns of the protocol. Section 4 deals with the performance evaluation when in a worst case scenario, and Section 5 concludes the paper.

2 Evolving from HTTP to SPDY

As hinted, the growing complexity of Web 2.0 should be also properly addressed by the protocol architecture. Some issues have been partially resolved by amending the HTTP protocol specification, namely: *i*) to avoid performance degradations, the increased number of objects composing a page requires proper parallelization of the retrieval process; *ii*) the rising volume of data needs to increase the protocol efficiency, also by reducing overheads; *iii*) the "distributed" nature of many contents (i.e., data can be stored in different providers), jointly with the need of long-held connections for interactivity purposes, require more flexible policies. To partially fulfill requirements *i*) – *iii*), the HTTP/1.1 [6] relies on multiple connections for concurrency. Even so, this can introduce additional hazards, including: supplementary round trips for completing the connection setup/teardown phases, delays in the slow-start phase of the TCP, as well as connection rationing by the client, e.g., when it tries to avoid opening too many connections over a single server. HTTP/1.1 also uses pipelining to send multiple requests over a single TCP connection without waiting for a response. This technique limits the offered load in terms of TCP Protocol Data Units (PDUs), and can also reduce the loading times of pages. Potential benefits are greater over high latency connections, such as satellite Internet connections [7]. Figure 1 shows how pipelining reduces the connection time with the respect to sequential HTTP requests.

However, the gains of pipelining are limited by the HTTP/1.1 protocol specification, since the server must generate responses ordered as the requests were received. Thus, the entire flow of information belonging to a connection is ruled according to a first-in-first-out policy. In turns, this can lead to performance

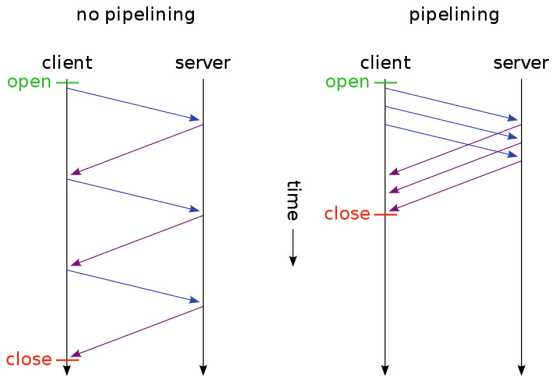

Fig. 1. Example of pipelined HTTP requests

degradation due to Head of Line (HOL) blocking[1] phenomena. Unfortunately, HTTP pipelining requires to be implemented both within the client and the server. As today, it is not widely available into existing browsers.

To prevent similar issues, SPDY introduces a specific *framing layer* (also named session layer) [5] for multiplexing concurrent streams atop a single persistent[2] TCP connection, as well as any other reliable transport service. Furthermore, it is optimized for HTTP-like request-response conversations, and also guarantees full backward compatibility with the plain HTTP.

In more details, SPDY offers *four* major additional improvements to the network behavior of HTTP:

1. *multiplexed requests*: to increase possible gains, the SPDY protocol specification does not impose any limits to the number of concurrent requests that can be sent over a single connection;
2. *prioritized requests*: to avoid congestion phenomena due to scarce resources at the network level, clients can indicate resources to be delivered first. This can enhance the Quality of Experience (QoE) of a service, even in presence of incomplete pages;
3. *compressed headers*: modern Web applications force the browser to send a significant amount of redundant data in the form of HTTP headers. Since each Web page may require up to 100 sub-requests, the benefit in term of data reduction could be relevant;

[1] HOL blocking is a performance-limiting event occurring when a trail of PDUs is held-up by the first packet. This can happen when in presence of network switches with buffered inputs, protocols supporting out-of-order delivery, or multiple requests as in the case of HTTP pipelining.

[2] An HTTP persistent connection, or HTTP keep-alive, uses a single TCP stream to move multiple HTTP requests/responses, instead of opening a new connection for each single request/response pair.

4. *server pushed streams*: this feature enables content to be pushed from servers to clients without additional requests.

Though, mechanisms 1) – 4) are somewhat analogous to HTTP pipelining, thus leading to potential transport level HOLs. This is even truer when in presence of packet losses, which could invalidate compression and prioritization as a consequence of TCP error recovery strategies. For such reasons, SPDY needs a proper comprehension when in jointly used with error prone links.

For what concerns all the protocol resources (e.g., documentation and software), they are provided by the SPDY Google Developer Group. In addition, performance evaluations in real-world use cases have been by the Chromium Projects[3], which spawned the "*Let's make the Web faster*" initiative[4]. The preliminary results were focused on comparing SPDY against HTTP. The reference testbed has been developed by simulating a user population browsing, from a Small Office Home Office (SOHO) Internet access, a selected set of reference Web sites called the "*top 100*". Additionally, different packet losses have been considered, i.e., in the range of $0 - 1\%$. The main outcome is that SPDY reduces the average page load times, for 25 websites of $27 - 60\%$ when using the TCP without the Secure Socket Layer (SSL), and $39 - 55\%$ when SSL is in place. A similar set of trials, also devoted to quantify the impact of SPDY over mobile terminals, has been proposed in reference [8], where the authors ran experiments on Chrome for Android[5], in order to have a draft 2 version of the protocol. Also in this case, SPDY outperformed HTTP by assuring an average reduction of the 23% in terms of loading times of pages.

Yet, literature still lacks of a thorough performance analysis of SPDY, both in terms of precisely quantifying the benefits for each feature introduced, and over a wide variety of network scenarios. Despite that, we decide to focus on the multiplexing ability of SPDY when used over a satellite channel. On one hand, this effort emphasizes benefits of exchanging data within a single SPDY stream tunneled within a TCP connection. On the other hand, the trials underline the impact of header compression when juxtaposed over a network having high access delays and packets losses. Additional benefits, compared with the current state-of-the-art literature, are the increased understanding of the HOL/error relationship, as well as the consequences of large propagation delays over the congestion control of the TCP.

3 Testbed Creation and Measurement Methodology

As said, our goal is to comprehend and evaluate the basic behaviors of SPDY when used in a satellite environment. In order to assure a fair approach, we test the protocol against a subset of the "top 100 websites" list compiled by Google. To this aim, we implemented a testbed composed by: an SPDY-enabled

[3] `http://www.chromium.org/chromium-projects`
[4] `http://www.chromium.org/spdy/spdy-whitepaper`
[5] `http://www.google.com/intl/en/chrome/android/`

browser (i.e., Google Chrome), which has been properly scripted for automating the content retrieval, as well as data collection; an emulated satellite link; a proxy for accessing non-SPDY sites; additional tools, such as a traffic sniffer.

To emulate the satellite access, we used `netem`[6], which is part of the native Linux queuing discipline. It permits to easily superimpose wide area network characteristics, e.g., the delay and the packet error rate, over standard routing strategies. Since `netem` can only process inbound packets, as a quick workaround, we created a new Intermediate Functional Block (IFB) pseudo device, in order to handle the emulation discipline also to incoming packets. Another possible solution would be using `netem` both in the satellite gateway and terminal. As regards the proxy, it has been deployed to cope with the scarcity of SPDY enabled websites on the Web. Hence, we used a `node.js` SPDY server[7], which has been configured to act as a Web proxy, as depicted in Figure 2.

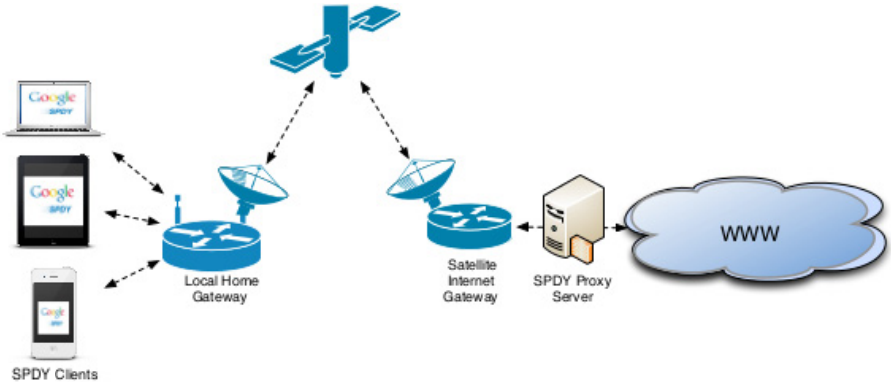

Fig. 2. Reference architecture of the adopted tested

3.1 Testbed Validation and Basic Protocol Understanding

As a consequence of a lack of thorough past investigations on the SPDY protocol, this initial round of tests has been performed to comprehend some of its core behaviors, also to understand wether SPDY could really outperform HTTP when used over a satellite link. Therefore, we focus on a GEO satellite system, that has been emulated by imposing a round trip time (RTT) of 720 ms (according to real measurements performed on the Skyplex Platform as discussed in reference [9]), and by limiting the bandwidths to 1 Mbit/s and 256 kbit/s, in the forward and return links, respectively. To have a controlled environment, in this first run of tests we assumed the channel as error-free.

The first analysis compares HTTP against SPDY in terms of used transport connections. This metric is a rough "complexity" indicator, which quantifies the perspective reduction of overheads for enhancing/splitting TCP flows, for instance by using a PEP machine. Table 1 summarizes the number of transport

[6] `http://swik.net/netem`
[7] `https://github.com/igrigorik/node-spdyproxy`

Table 1. Number of TCP connections per site when using standard HTTP

Site name	# of connections
Flickr	14
Huffington Post	173
Reddit	41
Microsoft	58
Slashdot	50
Wikipedia	17
BBC	88

connections required to download the contents of the selected sites when using standard HTTP. As reported, the presence of an extremely high amount of TCP conversations is mainly due to the content-richness nature of Web 2.0 applications, as well as the need of retrieving a composite set of objects, e.g., plug-ins or multi providers mash-ups. Yet, Table 1 underlines that not all sites present such extreme characteristics. This is the case of Wikipedia, which is mainly delivered through a text-based layout without any additional service embedded (e.g., advertisements, Facebook plug-ins or location widgets à-la Google Maps).

On the contrary, when pages are retrieved through the SPDY proxy, the amount of required TCP connections always reduces to *four*. This is a consequence of the multiplexing architecture of the protocol. Besides. we underline that only *one* connection is strictly related to SPDY traffic, while others are initiated by the browser to perform navigation statistics, or to fetch data for remote services (e.g., to provide users search suggestions/completions). Unfortunately we were not able to inhibit such process. Yet, we were able to precisely quantify the resulting overhead as to avoid "noise" in the collected results. Specifically, despite the adopted protocol, only one connection generates traffic and produces less than 100 kbyte of data. The other two connections simply perform a `SYN/FIN` exchange, probably to enable some kind of viewing time profiling. Thus, we solely focus on the transport connection devoted to transfer the Web page, which can be always correctly identified. As a consequence, the adoption of SPDY leads to a very minimal load in terms of connection to be managed, also accounting for a reduced complexity. Since satellite networks often use some kind of middleboxes (e.g., PEPs) for increasing the throughput of transport layer protocols, SPDY has to be considered a very interesting option to shift overheads at the borders of the network.

Another benefit is given by the compression of data via the `gzip` algorithm accounting for relevant gains when in presence of textual information, e.g., large headers. To better quantify this improvement, Figure 3 shows the Cumulative Density Function (CDF) of the HTTP PDUs produced when using HTTP and SPDY, when accessing two popular websites. Since both the client and the SPDY proxy operate on the same virtual machine in loopback, the maximum allotted PDU can benefit of a Maximum Transmission Unit (MTU) up to 64KB.

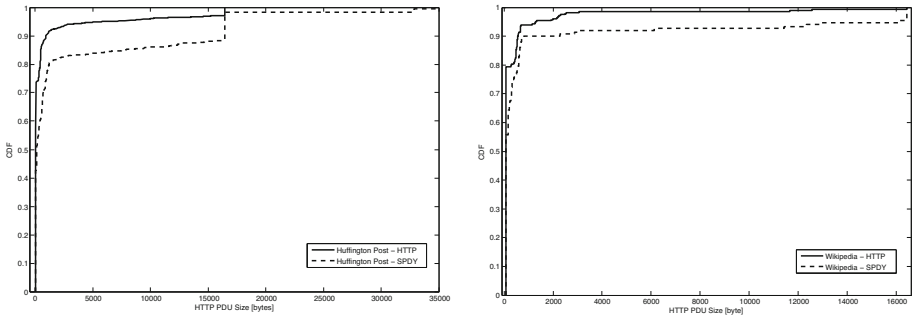

(a) CDFs of Huff-Post PDUs. (b) CDFs of Wikipedia PDUs.

Fig. 3. CDF of the HTTP and SPDY PDUs for two reference Websites

As depicted, SPDY optimizes the PDU size, with the acceptation that small packets are fewer than in the HTTP case. Consequently, the traffic is less fragmented, thus reducing the performance issues related to the TCP throughput. Similar results are observable when accessing a text-based service likes Wikipedia. For such a reason, the behavior of CDFs are different than when in presence of content-rich sites, but inspecting the throughput will reveal enhancements also in this case.

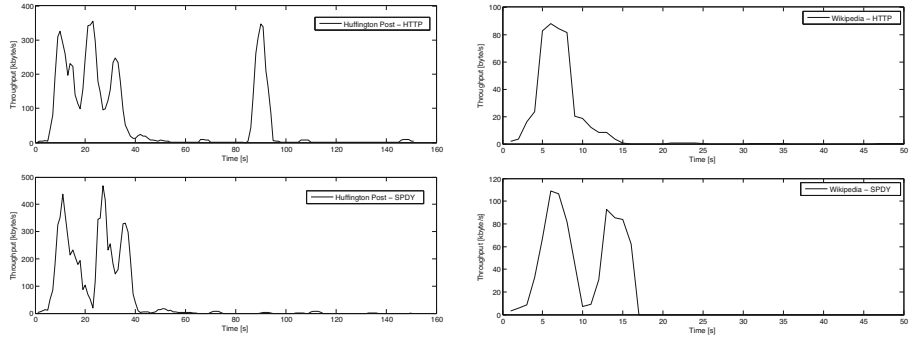

(a) Throughputs for the Huff-Post. (b) Throughputs for Wikipedia.

Fig. 4. Throughput when retrieving the Huffington Post and Wikipedia homepages with and without SPDY

Figure 4 shows improvements in terms of throughput, leading to a significant reduction of the downloading time. We point out that traffic spikes are periodically generated even when the page has been completely received for updating in a real-time manner some portion of the page (i.e., it represents exchanges due to AJAX-like techniques). Instead, for the case of Wikipedia the gain is less obvious, primarily due to effect of the aggressive compression performed by `gzip` over

the textual components composing the page. Yet, apart from a small amount of data transmitted in the $20 - 25$ s range, the largest part of the information is received almost faster when in presence of HTTP.

4 Performance Evaluation over Satellite Accesses

In this section, we evaluate the robustness of SPDY into account a worst-case scenario, i.e., we want to analyze some "macro" effects revealed by extreme conditions like a high Bit Error Rate (BER). We point out that we do not assume the presence of a TCP splitting architecture to isolate the satellite portion of the network. In fact, we are interested into understand wether SPDY can be used as a standalone workaround. According to Figure 1 the client connects to the satellite gateway through an IEEE 802.11 wireless link. To this aim, we used `netem` to emulate a bi-stable wireless channel, as depicted in Figure 5. The model is implemented via a 2-state Markov process, which is characterized by the transition probabilities p and q. Specifically, p is the probability of passing from the error-free state `0`, to the error-prone state `1`, while q quantifies the vice-versa. According to a past measurement campaign (see reference [10] for further details), we set $p = 0.54$ and $q = 0.78$, as to characterize a wireless indoor channel with an average packet loss (defined as *ploss* in the following) of 6.8%.

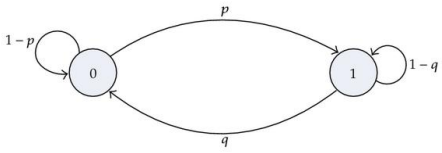

Fig. 5. Model of an on-off bi-stable channel

To conduct the evaluation, we used eight reference sites, which have been repeatedly accessed more than 20 times, as to have steady results. The same usage-pattern has been applied both for the cases of HTTP and SPDY. Figure 6 shows the distributions of load page failures for each protocol. For what concerns relative percentages, we experienced that SPDY fails 22 times, i.e. the 12.5%, while the HTTP only fails once, i.e., the 0.57%. Hence, SPDY appears to be more fragile when in presence of errors. To better elaborate on this point, we discovered that page failures mainly happens when the browser cannot correctly receive the `index.html` (with the acceptation of the main HTML body). This is a consequence of SPDY transmitting the whole content via a single TCP connection, rather than using multiple streams as the HTTP. Therefore, a single connection failure (even in the set-up phase) could block the page request transaction in its entirety.

Collected traffic traces reveal some duplicated `SYN-ACKs` received by the client side, eventually causing the conversation fail. In this perspective, Figure 7 reports a paradigmatic example. Another point to be remarked is that a `SYN` packet is

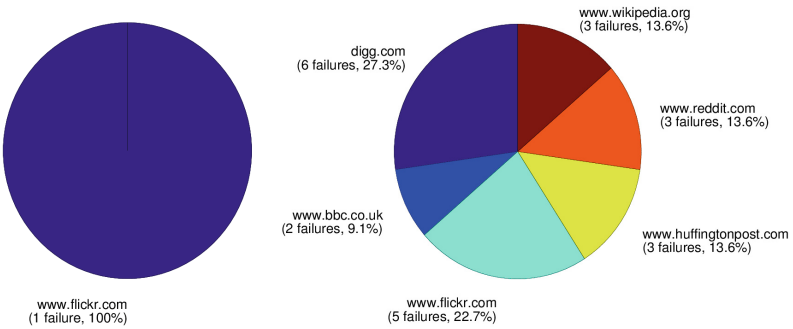

(a) HTTP (b) SPDY

Fig. 6. Failures when retrieving a page with a $ploss = 5\%$

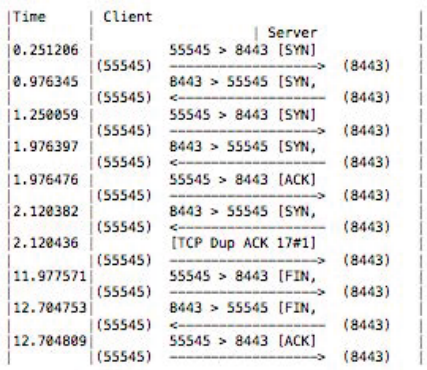

Fig. 7. Example of a failed TCP conversation

sent twice after the expiration of the Retransmission Time Out (RTO) which is set to 1s. This is an outcome of having the average RTT set to 720 ms, as not the unique delay imposed by the network. In fact, it does not include timings due to internal data processing/percolation for each element composing the network, as well as TCP buffering traversal. Thus, the overall delay could be greater than the RTO threshold. However, even though HTTP seems to be more robust against errors than SPDY, such behavior is almost uninfluential. In fact, failures cannot be able to capture implications on the perceived user experience, thus they must be compared against loading times. In this vein, Table 2 and 3 showcase collected timing statistics, both for HTTP and SPDY. According to data, on the average, SPDY seems to slightly outperform HTTP. Even if HTTP fails in less occasions than SPDY, the times to retrieve a content are excessive. As a consequence, a user would close the browser (i.e., abandon the session) before the complete reception of the page. Therefore, paying a price in terms of failed receptions would lead to a better QoE, rather than waiting for too long periods for accessing a content.

Table 2. HTTP loading time

Site name	min	max	avg
Flickr	26.15	372.48	160.94
Huffington Post	120.64	637.29	351.11
Reddit	49.84	584.11	261.59
Microsoft	143.63	552.00	298.38
Slashdot	107.52	544.95	286.66
Wikipedia	38.28	344.54	135.36
BBC.co.uk	137.07	769.17	382.40

Table 3. SPDY loading time

Site name	min	max	avg
Flickr	52.89	258.08	141.89
Huffington Post	263.54	669.49	362.00
Reddit	41.69	332.26	124.83
Microsoft	144.43	593.04	296.25
Slashdot	148.43	364.40	211.00
Wikipedia	13.38	184.10	48.98
BBC.co.uk	175.93	468.78	270.60

To clarify the QoE perception, we would recall the worst-case nature of the test. SPDY could lead to a barely satisfactory experience when accessing the Web, even in presence of an unacceptable average *ploss*. SPDY is more robust against high BERs and allows slightly reduced loading times, as it can be observed by comparing Table 2 and 3. Nevertheless, quantifying only loading times could be misleading, since with SPDY a page could be almost readable after ∼30 s, even if its completion could happen in many minutes.

5 Conclusions and Future Work

In this paper we investigated the use of SPDY to enhance performances when retrieving Web contents over an heterogeneous wireless scenario composed by an error-prone IEEE 802.11 access and a satellite link. Then, we showcased the creation of an ad-hoc testbed, and we also provided a basic understanding of the SPDY protocol compared to HTTP when jointly used with a satellite link. We investigated the effect of the packet loss on the overall performance, especially in terms of page loading time, and loading failures. As a result, SPDY is a promising protocols, since it outperformed HTTP in our tests, while reducing the complexity in terms of number of transport connections.

Future work aims at enriching the experimental results, also by testing SPDY with a more complete variety of channel conditions. Besides, part of our ongoing research deals with the creation of a more precise emulated environment. In

particular, to test SPDY when the satellite links is implemented through a DAMA systems as the one discussed in reference [9].

Acknowledgment. This work has been partially funded by the European Space Agency (ESA) within the framework of the Satellite Network of Experts (SatNex-III), CoO3, Task3, ESA Contract N. 23089/10/NL/CLP.

References

1. Zhang, J., Karim, M., Akula, K., Ariga, R.K.R.: Design and development of a university-oriented personalizable web 2.0 mashup portal. In: Proceedings of the 2008 IEEE International Conference on Web Services, ICWS 2008, pp. 417–424. IEEE Computer Society, Washington, DC (2008)
2. Caviglione, L.: Extending http models to web 2.0 applications: The case of social networks. In: Proceedings of the 2011 Fourth IEEE International Conference on Utility and Cloud Computing, UCC 2011, pp. 361–365. IEEE Computer Society, Washington, DC (2011)
3. Knorr, E.: Software as a Service: The Next Big Thing (2009), http://www.infoworld.com/article/06/03/20/7610312FEsaas1.html
4. Caviglione, L.: Can satellites face trends? The case of web 2.0. In: Int. Workshop on Satellite and Space Communications, IWSSC 2009, pp. 446–450 (2009)
5. Belshe, M., Peon, R.: SPDY protocol - draft 3 (2012), http://www.chromium.org/spdy/spdy-protocol/spdy-protocol-draft3
6. Fielding, R., Gettys, J., Mogul, J., Frystyk, H., Masinter, L., Leach, P., Berners-Lee, T.: RFC 2616, Hypertext Transfer Protocol – HTTP/1.1 (1999), http://www.rfc.net/rfc2616.html
7. Nielsen, H.F., Gettys, J., Baird-Smith, A., Prud'hommeaux, E., Lie, H.W., Lilley, C.: Network performance effects of HTTP/1.1, CSS1, and PNG. SIGCOMM Comput. Commun. Rev. 27, 155–166 (1997)
8. Welsh, M., Greenstein, B., Piatek, M.: SPDY performance on mobile networks (2012), https://developers.google.com/speed/articles/spdy-for-mobile
9. Gotta, A., Potorti, F., Secchi, R.: An analysis of tcp startup over an experimental dvb-rcs platform. In: 2006 International Workshop on Satellite and Space Communications, pp. 176–180 (2006)
10. Barsocchi, P., Bertossi, A.A., Pinotti, M.C., Potorti, F.: Allocating data for broadcasting over wireless channels subject to transmission errors. Wireless Networks 16, 355–365 (2010)

Fuzzy Based CRRM for Load Balancing in Heterogeneous Wireless Networks

Muhammad Ali, Prashant Pillai, Yim Fun Hu,
Kai J. Xu, Yongqiang Cheng, and Anju Pillai

School of Engineering Design and Technology
University of Bradford, UK
{m.ali70,p.pillai,y.f.hu}@bradford.ac.uk

Abstract. The ever increasing user QoS demands and emergence of new user applications make job of network operators and manufacturers more challenging for efficiently optimisation and managing radio resources in radio the radio resources pools of different wireless networks. A group of strategies or mechanisms which are collectively responsible for efficient utilisation of radio resources available within the Radio Access Technologies (RAT) are termed as Radio Resource Management (RRM). The traditional RRM strategies are implemented independently in each RAT, as each RRM strategy considers attributes of a particular access technology. Therefore traditional RRM strategies are not suitable for heterogeneous wireless networks. Common Radio Resource Management (CRRM) or joint radio resource management (JRRM) strategies are proposed for coordinating radio resource management between multiple RATs in an improved manner. In this paper a fuzzy algorithm based CRRM strategy is presented to efficiently utilise the available radio resources in heterogeneous wireless networks. The proposed CRRM strategy balances the load in heterogeneous wireless networks and avoids the unwanted congestion situation. The results such as load distribution, packet drop rate and average throughput at mobile nodes are used to demonstrate the benefits of load balancing in heterogeneous wireless networks using proposed strategy.

Keywords: CRRM, Load balancing, radio resource management, heterogeneous wireless networks, load balancing in wireless networks, vertical handovers, satellite-terrestrial wireless networks load balancing.

1 Introduction

In wireless communication networks, the increasing number of mobile subscribers and dynamic change in number of active mobile nodes is a real challenge for the network providers as it incurs in real time load variations in the network. This dynamic change in load on network is due to many reasons like peak hours at hot spots or motorways, special events like football match, exhibition or a festival celebration. The network performance gets significantly degraded at the time when network gets heavily loaded. In the urban areas it is common on most places that multiple networks provide coverage over the same geographically located area. For

R. Dhaou et al. (Eds.): PSATS 2013, LNICST 123, pp. 135–145, 2013.

example a busy town market area may possess coverage of WLAN, cellular networks like WiMax and UMTS and coverage of satellite networks. In this context while one of the available networks in particular area gets overloaded, other networks covering the same geographical area may remain lightly loaded. This results in poor utilisation of available wireless resources and poor network performance thereby poor user experience. While network operators considered users' population density and mobility patterns for planning network deployment, each service provider would be required to have large infrastructure in place to cater to the needs of their users in these densely populated areas. Hence the different networks of heterogeneous wireless networks, whose coverage areas overlap experience imbalance of radio resource utilization and performance degradation due to the unbalanced load across the different wireless networks.

This paper presents a novel fuzzy based CRRM strategy which uniformly distributes the network load between co-located heterogeneous wireless networks. It utilizes IEEE 802.21 Media Independent Handover (MIH) [1] to seamlessly handover mobile nodes between heterogeneous wireless networks for load balancing purpose. The advantage of this approach is that it minimizes the call blocking and dropping probabilities, number of packet drop/lost and delays during the handover process and enhances the network utilization by continuously balancing the load in co-located networks. The proposed load balancing approach monitors and controls the network load from both side (mobile node and network side), and addresses the most important problem of efficiently utilising radio resources in heterogeneous wireless networks. The rest of the paper is organized as follows; section 2 describes the literature review of CRRM strategies, section 3 briefly describes the proposed load aware RAT selection framework. Simulation topology and results are discussed in section 4, which is followed by the conclusion.

2 CRRM Strategies

In heterogeneous wireless networks the main challenge is the efficient CRRM [2, 3] strategy which can competently manage the resources of different access technologies in heterogeneous wireless networks. The concept of CRRM is based on a two tier RRM model [4, 5] as shown in the Figure 1 below. The lower tier is the local RRM entity which manages and allocates the resources in the local network, whereas the CRRM is the upper tier of the model which is responsible for managing all the resource in multiple networks. The CRRM entity in the two tier architecture controls the RRM entities and can also communicate with other CRRM entities. The users can always be assigned to the most suitable networks using CRRM which improves the performance by efficiently utilising the available resource from different networks. From a network topology point of view, the CRRM functionality can be implemented in various different ways such as CRRM server approach [6, 7], integrated CRRM approach [8], hierarchical CRRM approach [9], CRRM functions in User Terminal (UT) approach [10] and a hybrid approach which can be combination of these approaches. While in the CRRM server approach, a separate CRRM server is added in the core network, in the integrated CRRM approach, the CRRM functionality is added within an existing network entity like the basestation (BS), the Radio Network Controller (RNC) or the Access Point (AP).

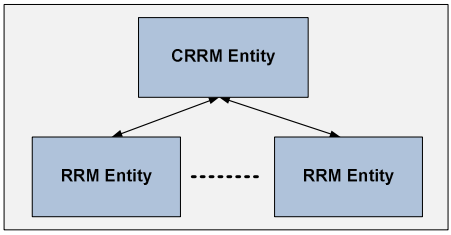

Fig. 1. Two tier model [5]

The CRRM server is a centralised approach due to which it attains high scalability. The integrated CRRM requires minimum infrastructure changes and also reduced the communication delays between the local RRM and CRRM entities. However this approach is distributed and scale well due to the large number of connection between the various local RRM entities. The hierarchical CRRM approach divides the problem into various layers and each layer is managed by a dedicated management entity. This approach adds further complexities due to a number of new entities additions in the architecture infrastructure. The final approach the CRRM functions are present in the end user terminal. This approach allows the mobile node to make decision for suitable RAT selection. In this case, the network needs to provide enough information to the mobile nodes, but this would require extra signalling.

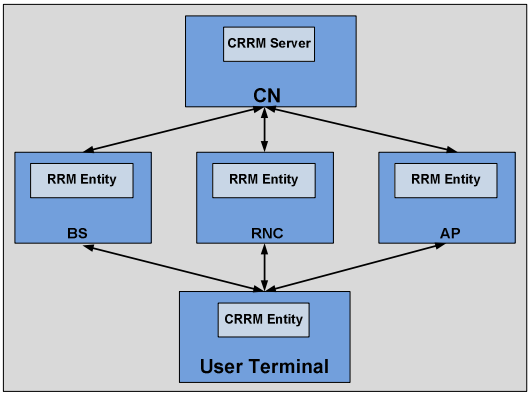

Fig. 2. Proposed CRRM approach

In this paper a hybrid of CRRM server and CRRM functions at the user terminal approach is applied to get advantages of both centralised and distributed approaches. Figure 2 represents the proposed CRRM approach. The CRRM architecture shown in Figure 2 is composed of three layers namely, the Core Network (CN), the access network entities and the UT. For the load balancing purpose each of these layer are equipped with MIH components i.e. CRRM server acts as Media Independent Information Server (MIIS) and similarly the CRRM entity in the mobile node or UT communicate with the RRM entities in the network side using IEEE 802.21 MIH reference model.

3 Load-Aware RAT Selection Framework

3.1 Network Architecture

Figure 3 presents the target network architecture considered in this research. It shows an MIH enabled multi-interface mobile node which can use any of the four available wireless access networks (Satellite, WiMax, WLAN and UMTS) [11] supported by its interfaces. It is assumed that a single operator is controlling all the wireless networks hence all four wireless networks share a common core network. The core network is in turn connected to the Internet. The mobile node can communicate with a correspondent node over the internet, using any available wireless network which it supports. On-going sessions would be handed over to another available network without losing any connectivity if the mobile node moves out of its current network coverage and enters into another network.

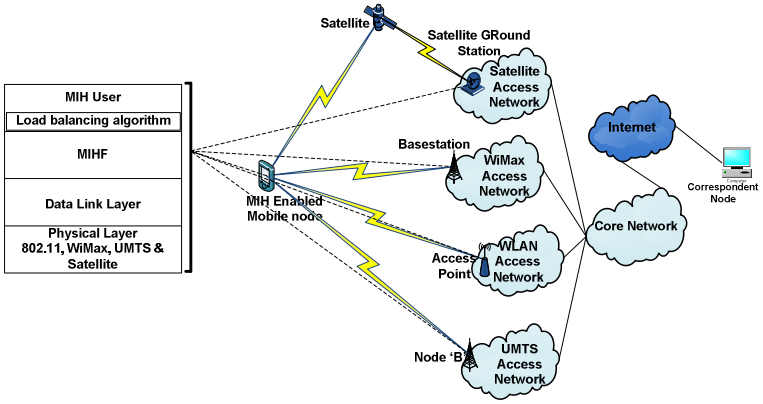

Fig. 3. Load balancing architecture design

The key phenomenon in the MIH reference model is the introduction of Media Independent Handover Function (MIHF) between layer 2 and layer 3 of the OSI layer model. The MIHF receives and transmits the information about the network condition and configurations of the access networks around the mobile node, regardless of the MIHF location such as mobile node or network elements. The information handled by the MIHF originates at different layers of protocol stack in mobile node or in network elements. The MIHF is composed of a set of handover enabling functions which provide service continuity while a MN traverses between heterogeneous wireless access link layer technologies. In the MIH Reference model [1]. The MIH user makes use of the MIHF function to support seamless handovers. Hence as shown in Figure 3, the load balancing module acts as the MIH user. The following sub-sections describe in general the proposed framework of the load balancing algorithms that are running at the mobile node and the network entities.

3.2 Load Balancing Algorithms

The flow chart shown in Figure 4 summarises the load aware RAT selection algorithm which runs at the mobile node. The mobile node side algorithm can also be seen as different phases of a handover process: handover initiation, handover decision and handover execution. In the handover initiation phase, a mobile node detects new network or existing link getting weak. In this phase the process of load aware handover is initiated using MIH event signalling. The second phase is handover decision in which the mobile node compares all the considered parameters from available network and decides the target network for handover. The second phase also comprises of an important component which is the load aware RAT selection algorithm. The last phase is the handover execution in which the mobile node performs the load aware handover and moves all the active connections to the target network.

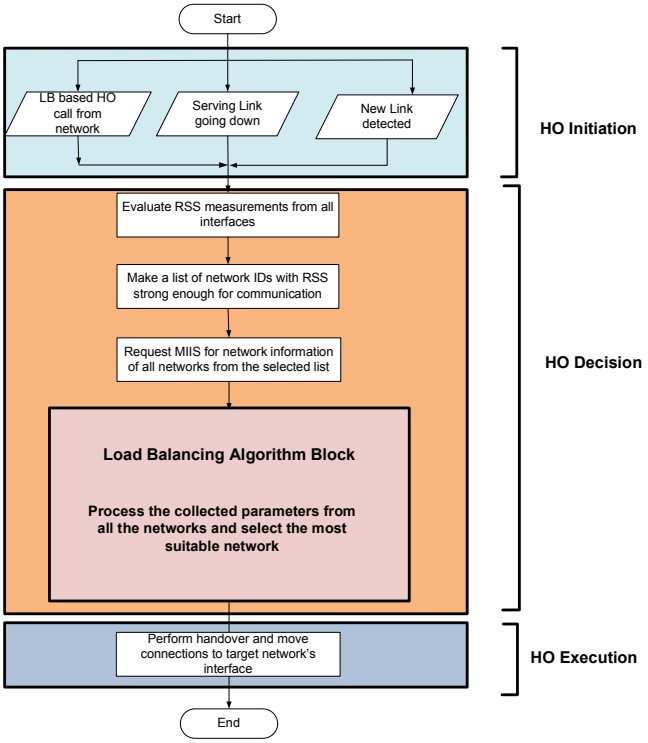

Fig. 4. Load-aware RAT selection algorithm

The mobile node compares the load conditions of the new available networks and the one to which it is currently connected. A list of networks IDs is generated for those networks which are visible to the mobile node such that the received signal strength from those networks is higher than the minimum threshold for basic communication. In the next step load, cost, offered QoS and other network related

information of each network in the list is obtained from MIIS. This information is then forwarded to the load balancing algorithm block which applies different algorithms to select the most suitable network. One of the two different algorithms, namely, baseline (least loaded) and Fuzzy algorithm [12, 13] are applied to select the most suitable network. In case of baseline or non-cognitive algorithm the most preferred network from the generated list is the one with lowest load and highest offered data rate, whereas for the fuzzy algorithm all the parameters such as signal strength, load, offered data rate of network, cost of network, coverage area of the network, speed of mobile node, user preferred network and required data rate of mobile node are considered. The Figure 5 shown below represents the fuzzy logic controller used for balancing the load in this paper. All the values obtained from different parameters are first fuzzified and then passed on to the fuzzy inference system. The fuzzy inference system then uses the fuzzy rule base and defuzzification modules to generate the decision factor for each network. At the end the network with highest decision factor is selected as the target network for load balancing based handover.

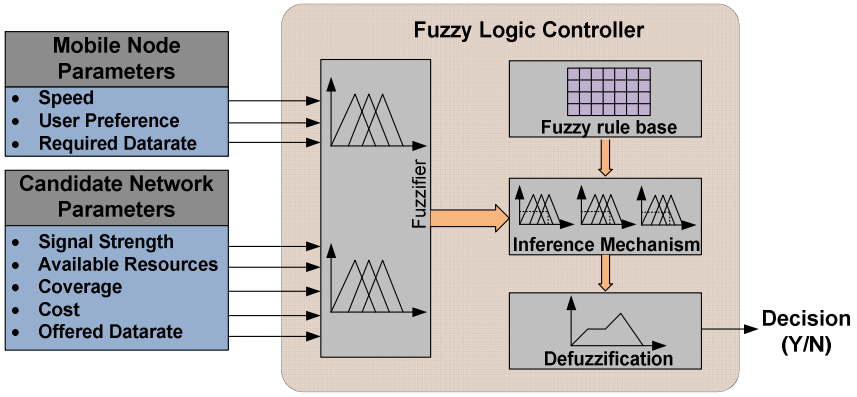

Fig. 5. Fuzzy logic controller for load aware RAT selection

4 Simulation Topology and Results

4.1 Simulation Topology

Figure 6 presents the simulation topology considered in this paper. Purpose for considering particular topology for simulation is to observe the effects of load balancing in most ideal scenarios where mobile nodes can see maximum overlapped coverage areas from different networks. Each mobile node maintains a TCP connection with the TCP source shown in Figure 6 throughout the simulation such that effects of load balancing on active connections can be measured.

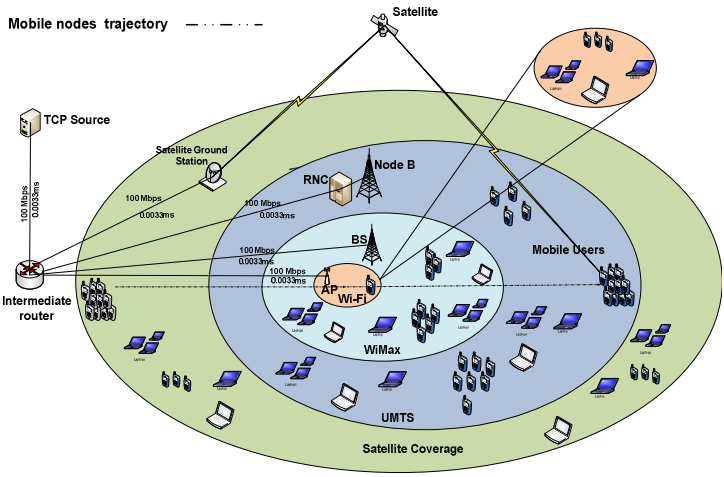

Fig. 6. Network topology for simulation

The scenarios considered in this paper consist of a group of mobile nodes which travel across the coverage areas of all four networks such as Satellite, UMTS, WiMax and Wi-Fi as shown in Figure 6. The Table 1 shown below represents the simulation parameters used in the target simulation scenarios.

Table 1. Simulation parameters

Simulation parameters	**Values**
Satellite coverage radius	4000 meters
UMTS coverage radius	1000 meters
WiMax coverage radius	500 meters
WLAN radius	100 meters
Satellite data rate (per user)	492 kbps
UMTS data rate (per user)	384 kbps
WiMax data rate	45 Mbps
WLAN data rate	11 Mbps
Wired links capacity	100 Mbps
Propagation delays wired links	0.0033 ms
Propagation delay satellite	250ms
Application type	TCP
Application data rate	2 kB/s
Number of mobile nodes	50, 100
Speed of mobile nodes	25m/s

4.2 Results

The simulation scenario discussed in the previous section is simulated using both load balancing and non-load balancing algorithms using the network simulator NS2 [14]. Results of packets drop rate, handover latencies and load distribution at different networks such as satellite, UMTS, WiMax and Wi-Fi networks are described in this section.

a) Handover Latencies Comparison

Table 2 represents the mean value of the total handover latencies observed by each mobile node in different scenarios using baseline and fuzzy load balancing algorithms. In comparison scenario A and B the fuzzy load balancing algorithm has the least handover latency values. This means that the fuzzy load balancing algorithm minimizes the total number of handovers hence results into low handover latencies and still manages to balance the load between different co-located networks.

Table 2. Handover latencies

Scenarios	No. of MNs	Algorithm	HOL (second)
A	50	Baseline	0.502643
		Fuzzy	0.485328
B	100	Baseline	0.684761
		Fuzzy	0.555694

b) Load Distribution Comparison

The load distribution in scenarios with 100 mobile nodes is shown in the following graphs in Figure 7 to Figure 9. Point 1 in these graphs represents the time in simulation where only satellite coverage is available, point 2, 6 & 7 show the time when mobile nodes are under the coverage of UMTS and satellite, point 3 & 6 represent the time when mobile nodes are under common coverage are of satellite, UMTS and WiMax and point 4 represents the time in simulation when mobile nodes are under common coverage areas of all the networks. The load distribution using load balancing algorithm is far better as compared to the no load balancing scenario. The results obtained from baseline load balancing algorithm are slightly different from fuzzy load balancing algorithm as baseline algorithm uses Wi-Fi and fuzzy does not use it. The fuzzy algorithm intelligently detects that mobile nodes are moving with high speed and decides that it is not suitable to handover mobile nodes to Wi-Fi as they would not remain there for long enough. The load distribution in fuzzy algorithm shows very minor variations but in fuzzy this variation controls the total number of handovers and minimizes the total handover latencies. The performance of fuzzy algorithm for load distribution is dominant due to the limited number of handovers.

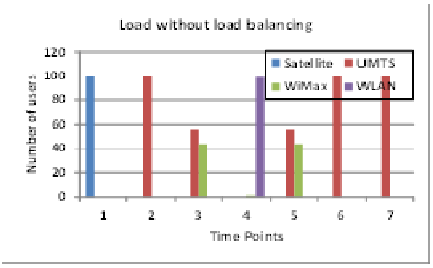

Fig. 7. Load distribution without load balancing using 25m/s

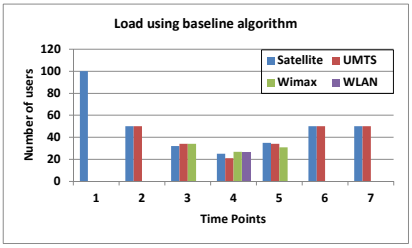

Fig. 8. Load distribution with baseline load balancing using 25m/s

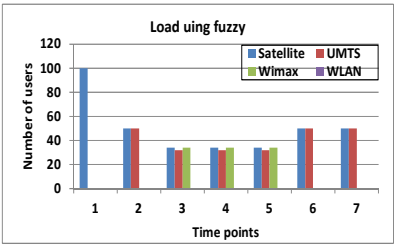

Fig. 9. Load distribution with fuzzy load balancing using 25m/s

c) Packet Drops Comparison

The comparison of packet drop rate for proposed load balancing algorithms is shown in the graphs in Figure 10 and Figure 11.

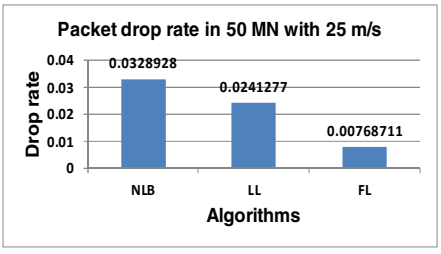

Fig. 10. Packets drop rate with 50 MN

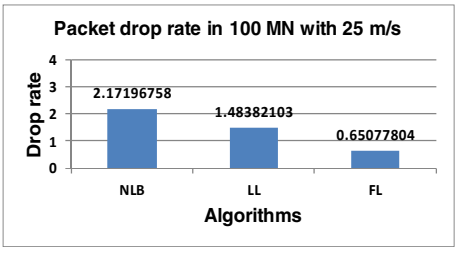

Fig. 11. Packets drop rate with 100 MN

The comparison of the different approaches shown in the graphs below for packet drop rate shows that fuzzy have lowest drop rates. One reason for less number of drops in fuzzy is that it reduces the total number of handovers which results into less packet drops as compared to baseline algorithm. The fuzzy approach has one more advantage that it encompasses lowest handover latencies for average mobile node in all scenarios as shown in Table 2. Therefore the fuzzy load balancing algorithm is considered as the most dominant approach overall.

5 Conclusion

In this paper a fuzzy based CRRM strategy is presented for balancing the load in heterogeneous wireless networks. The comparison of results generated by simulation scenarios using load balancing algorithms and without load balancing is presented to show the sovereignty of proposed algorithms. Considered attributes for observation are handover latencies, packet drop rate and load distribution on each of the network such as satellite, UMTS, WiMax and Wi-Fi. The results showed that with load balancing all parameters showed improvement in the target heterogeneous wireless network architecture. The baseline and fuzzy load balancing algorithms assured the fair load distribution between the overlapping networks whereas without load balancing different networks show abrupt load variations which decrease the performance with high congestion, high call dropping probability and blocking probability at overloaded network. The benefit of using fuzzy over baseline load balancing algorithm is that it reduces the total number of handovers and hence suffers from low handover latencies and fewer packets drops. The fuzzy algorithm also intelligently detects the speed of mobile nodes and does not allow mobile nodes with high speed to handover to Wi-Fi as they would not remain there for enough time. The Load balancing approach utilizes the available radio resources efficiently. Handover latencies are minimized, as it does not require all the mobile nodes to handover when load balancing algorithms are used. Hence the load aware RAT selection is a better approach as it offers high radio resource utilization with minimum number of handovers and hence low handover delays and ability to maximize the network availability with uniformly distribution of load in co-located networks.

References

1. IEEE Std. 802.21, Media Independent Handover Services (2009)
2. Wu, L., Sandrasegaran, K.: A Study on Radio Access Technology, Selection Algorithms. SpringerBriefs in Electrical and Computer Engineering (2012), doi:10.1007/978-3-642-29399-3_2
3. Tolli, A., Hakalin, P.: Adaptive load balancing between multiple cell layers. In: Proc. on Vehicular Technology Conference, vol. 3, pp. 1691–1695 (Fall 2002)
4. Passas, N., Paskalis, S., Kaloxylos, A., Bader, F., Narcisi, R., Tsontsis, E., Jahan, A.S., Aghvami, H., O'Droma, M., Ganchev, I.: Enabling technologies for the always best connected concept. Wireless Communication & Mobile Computing 6, 523–540 (2006)
5. Wu, L., Sandrasegaran, K.: A Survey on Common Radio Resource Management. In: The 2nd International Conference on Wireless Broadband and Ultra Wideband Communications, AusWireless 2007 (2007)
6. Pérez-Romero, J., Sallent, O., Agustí, R.: On Evaluating beyond 3G radio access networks: architectures, approaches and tools. In: IEEE 61st Vehicular Technology Conference, Stockholm, Sweden, pp. 2964–2968 (May-June 2005)
7. 3GPP TR v5.0.0, Improvement of RRM across RNS and RNS/BSS, Release 5 (2001)
8. Casadevall, F., Karlsson, P., Sallent, O., Gonzalez, H., Barbaresi, A., Dohler, M.: Overview of the EVEREST Project. In: 13th IST Mobile & Wireless Communications Summit, Lion, France (2004)

9. Cui, Y., Xue, Y., Shang, H., Sha, X., Ding, Z.: A novel scheme and access architecture for joint radio resource management in heterogeneous networks. In: International Forum on Information Technology and Applications, (IFITA 2009), Chengdu, China, pp. 24–27 (May 2009)
10. Magnusson, P., Lundsjö, J., Sachs, J., Wallentin, P.: Radio resource management distribution in a beyond 3G multi-radio access architecture. In: IEEE Global Telecommunication Conference, pp. 3472–3477 (2004)
11. Ali, M., Pillai, P., Hu, Y.F.: Load-aware radio access selection in future generation wireless networks. In: Pillai, P., Shorey, R., Ferro, E. (eds.) PSATS 2012. LNICST, vol. 52, pp. 104–112. Springer, Heidelberg (2013)
12. Espinosa, J.J., Vandewalle, J.P.L., Wertz, V.: Fuzzy Logic, Identification and Predictive Control. Springer verlag London limited (2005) ISBN: 1-85233-828-8
13. Hines, J.W.: Fuzzy and Neural Approaches in Engineering MATLAB Supplement. John Wiley and Sons, New York (1997)
14. `http://www.isi.edu/nsnam/ns/index.html` (accessed November 26, 2012)

Flexible QoS Support in DVB-RCS2

Ziaul Hossain, Arjuna Sathiaseelan, Raffaello Secchi, and Gorry Fairhurst

Electronics Research Group, School of Engineering, University of Aberdeen,
Fraser Noble Building, King's College, Aberdeen AB24 3UE, UK
{ziaul.hossain,a.sathiaseelan,r.secchi,g.fairhurst}@abdn.ac.uk

Abstract. Satellite is considered a vital technology for enabling ubiquitous access to broadband services in many countries. This paper explores provision of IP-based broadband satellite access with Quality of Service (QoS). It analyses a set of example scenarios, based on the recently published DVB-RCS2 standard involving web and voice traffic. It specifically explores the interaction between Bandwidth-on-Demand (BoD) and QoS, showing that this interaction offers the flexibility required for satellite Internet service operators to manage the bandwidth of broadband users in a multi-service access network.

Keywords: QoS, BoD, DVB-RCS2, VoIP.

1 Introduction

Satellite systems can provide broadband access that is not dependent on the cable infrastructure. The advances in satellite technology in recent years have significantly increased the capacity available to customers, enabling satellite to become a strong contender for providing fast broadband to places that cannot be covered by other technologies due to physical, technical or economical limitations.

The second generation Digital Video Broadcast Return Channel Satellite (DVB-RCS2) [1] is the only open IP-based next-generation multivendor standard for broadband satellite access. This specifies IP QoS functions at layer 3 that can ensure appropriate traffic classification and prioritisation, essential for a satellite Internet Service Provider (ISP) to guarantee application performance. Bandwidth-on-Demand (BoD) methods, defined at Layer 2, are vital components to maximise the capacity utilization of satellite resources. The Quality of Service (QoS) architecture in DVB-RCS2 is sufficiently flexible to implement policies for specific classes of traffic/application and can be associated with different BoD methods.

QoS support in satellite networks is an important topic that has been explored extensively in the past. Examples of frameworks to support QoS and bandwidth allocation are provided in [2] [3] considering the first generation standard DVB-RCS. [4] and [5] analysed the behaviour of applications: web, VoIP, bulk file transfer etc. with BoD methods. Applications differ in their QoS requirements and a possible mapping of applications to BoD methods is presented in [6].

This paper examines the interaction between the Layer 2 and Layer 3 and implications of BoD methods on application performance through simulations. Our results illustrate the flexibility offered in DVB-RCS2 by tuning the BoD methods to support multiple network services, each of which can be customised to meet the

R. Dhaou et al. (Eds.): PSATS 2013, LNICST 123, pp. 146–155, 2013.

requirements of a particular traffic class. The analysis considers both VoIP and web traffic separately and simultaneously.

2 BoD in DVB-RCS2

BoD allows multiple Return Channel Satellite Terminals (RCSTs) to share Return Link (RL) satellite capacity. RCSTs transmit explicit Capacity Requests (CRs) to the Network Control Centre (NCC) in order to notify their instantaneous capacity requirements. The NCC uses the CRs to generate a burst-time plan (BTP) that contains RCSTs allocations. The BTP is broadcast periodically on the Forward Link (FL).

DVB-RCS2 permits an RCST to use a range of BoD mechanisms to request capacity, including Continuous Rate Assignment (CRA), Rate Based Dynamic Capacity (RBDC), Volume Based Dynamic Capacity (VBDC), Absolute VBDC (AVBDC) or Free Capacity Assignment (FCA). Some of these depend on the CRs made by the terminals while some of them are based on the Service-Level-Agreement (SLA) between the RCST and NCC.

Table 1. BoD methods

Method	Request Type	Set by
CRA	Rate	SLA or Control plane
RBDC	Rate	Explicit Capacity Request
VBDC	Volume	Explicit Capacity Request
AVBDC	Volume	Explicit Capacity Request
FCA	Volume	SLA or Control plane

These methods may be used alone or in combinations to form the basis of a bandwidth allocation strategy, known as a Request Class (RC). In DVB-RCS2, RCs can be mapped to particular traffic classes to satisfy the capacity requirement of a specific type of traffic. When multiple mechanisms are combined in an RC, DVB-RCS2 mandates not to request more than 110% of the resources needed [1].

3 Simulation Setup and Traffic Description

Simulations were performed to study the interaction between BoD and QoS for a set of services. Our DVB-RCS2 simulator [7] implemented IP-based QoS with priority queuing. An RCS Terminal (RCST) was configured with traffic classes to differentiate VoIP and Web flows using the IP Diffserv code-point assigned by the application.

Our experiments considered two key request methods: RBDC and VBDC. An RBDC Capacity Request (CR) reflected the rate of incoming traffic, averaged over the past request period. The following formula was used in the simulator to calculate the RBDC requested rate (R_{now}) in the terminal:

$$R_{now} = \alpha \times R_{prev} + (1 - \alpha) \times X \quad (1)$$

where α is the smoothing factor between 0 and 1, R_{prev} is the capacity requested in the previous request interval, X is the incoming traffic rate. This method (with a high α value) prevents the system against the high fluctuations of the RBDC burstiness which was described in [14]. A VBDC CR reflected the estimated volume of incoming traffic in an allocation period. This included all the capacity requested and not allocated at the time the CR was issued.

We considered two types of service with different traffic patterns: web and VoIP. Our web model [8] simulated a web page download comprising several Hyper-Text-Transfer-Protocol (HTTP) request/response exchanges. Each web page consisted of several objects distributed on multiple servers. The HTTP client opens multiple parallel connections to the servers and reuses a connection for multiple object requests. VoIP traffic consists of fixed-size packets of 76 B (with TCP/IP headers) and constant inter-transmission time of 40 ms. The voice encoder generates data with a media rate of 8 kb/s resulting in a constant flow of 15.2 kb/s including TCP/IP overhead.

Table 2. Key Simulation Parameters

Network	
Internet delay (sat. gateway and servers)	50ms
FL capacity	2 Mb/s
FL encapsulation	GSE
Max RL capacity	512 kb/s
RL encapsulation	RLE
Request interval	100 ms
Superframe period (one frame/superframe)	26.5ms
Min RBDC request	16 kb/s, 32 kb/s
Web page model	
Number of servers	4
Number of objects	40
Obj. avg. size	7 KB
Obj. size distribution	Pareto; shape=1.2
Max no. of persistent connections	6
HTTP request size	320 B
VoIP Model	
Packet size (IP/RTP/media)	76B
Inter-transmission time (without VAD)	40ms
Traffic rate	15.2 kb/s
VoIP/VAD Model	
Packet size (IP/RTP/media)	76B
Inter-transmission time (without VAD)	40ms
Peak Traffic rate	15.2 kb/s
Average codec rate	8 kb/s
Avg. burst duration (exp. distributed)	0.46 s
Avg. idle duration (exp. distributed)	0.54 s

When VAD was enabled, voice activity was modeled as a two state ON/OFF Markov chain [9]. The generation of comfort noise packets was ignored, since these packets are small and infrequent and produce negligible effects on the return link. The packet inter-arrival time and VAD design follows guidance in G.729 Annex B [10].

The performance of HTTP traffic was evaluated by performing 500 simulation runs and plotting the 90 percentile of the transfer duration (the time between issuing an HTTP request and download all the requested objects). The performance of VoIP traffic was evaluated by calculating a Mean Opinion Score (MOS) derived from the R-score [11] using an empirical mapping. This provided an objective perceived-quality measurement with a range from 1 to 5, where 1 is the poorest perceived quality and 5 the best. The allocation efficiency provided a metric for the effectiveness of the requestor/allocator in predicting the capacity required for the traffic. This was the ratio between the used slots and the total allocated slots.

Table 2 identifies the key simulation parameters. There are several additional delays with the request-allocation mechanism besides the satellite Round-Trip-Time (RTT), such as CR submission delay, NCC processing delay, waiting time for the allocated superframe, etc. For simplicity, only the effect of RTT was introduced between a request and the corresponding allocation and it was assumed that the NCC was always able to grant the requested amount. There was no L2 congestion at the satellite Network Control Centre, NCC, (i.e., capacity was always available).

4 Experiments and Results

This section investigates the suitability of specific RCs for web and VoIP traffic. The experiments demonstrate that the performance of different traffic classes is significantly impacted by the choice of RC parameters.

4.1 Web Performance Tuning with Different RCs

Web flow performance was evaluated across a range of RCs. We define RC1 using RBDC and VBDC, where the estimated input rate and queue size in the RBDC and VBDC CR are multiplied by p and $(1-p)$ respectively. Thus, the total amount of capacity requested per request period (in bytes) C_{REQ} is:

$$C_{REQ} = p \times C_{RBDC} \times RP + (1 - p) \times C_{VBDC} \quad (2)$$

where C_{RBDC} (B/s) is the RBDC request calculated according to (1), RP (sec.) is the request period, and C_{VBDC} (bytes) is the VBDC request as described in Section 3. This way, C_{REQ} remains below the 110% threshold described in Section 2. Simulations varied p in the range [0,1]. When $p=1$ and $p=0$, RC1 respectively corresponds to RBDC and VBDC. Fig. 1 shows the page download time and efficiency versus the number of objects on the webpage. The results confirm the findings in [3]: An increase of p increases the allocation efficiency, but also increases the completion time. Indeed, as p varies between 0 and 1, the completion time curve moves upwards maintaining a quasi linear behaviour. The case $p=0.2$ can be regarded as a good compromise between performance and efficiency for web.

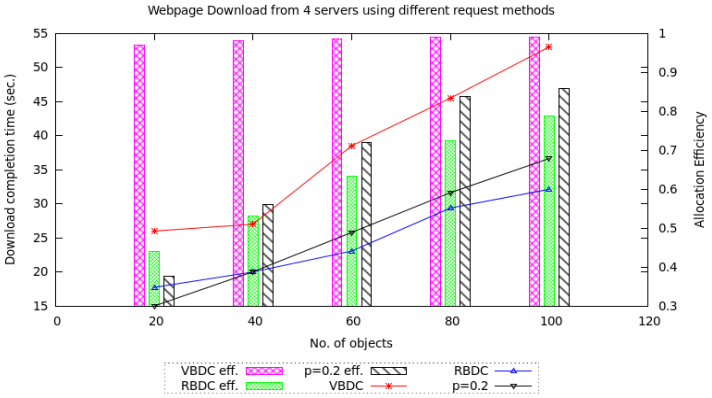

Fig. 1. Webpage download time as a function of the no. of objects in the webpage; download time and allocation efficiency increases with the no. of objects and they depend on the 'p' value

This analysis suggests that a satellite ISP can select a suitable RC for any traffic by varying the parameter to weight the different CR components. This allows an operator to trade efficiency and performance.

4.2 RC Tuning for VoIP Traffic

VoIP (not using VAD) flows result in constant bitrate traffic (Table 2). Hence, an RC using the simple RBDC method (defined by Equation 1) can support this kind of traffic and it was named RC2 in our simulations. In contrast, VoIP flows that use VAD, result in a traffic flow that continuously varies its rate. RC2 requests reflect the average traffic rate. These were unable to make appropriate CRs for this variable traffic and resulted in reduced performance.

One way to mitigate this problem would be to use a request/allocation method that predicts the capacity using an algorithm tailored to the VoIP/VAD traffic characteristics. We defined RC3 so that it allocates extra capacity over the average rate to accommodate the burstiness of the VoIP/VAD traffic. RC3 is implemented by measuring the input rate each second and using a high smoothing factor ($\alpha = 0.9$ in equation (1)) for RBDC. The NCC allocates capacity to the RCSTs by multiplying RC3 CRs with a constant factor.

Fig. 2 plots the MOS against the allocated capacity divided by the average rate for combinations of VoIP flows. This shows that good performance (around MOS 3) can be achieved for VoIP (with VAD enabled) traffic when the allocation is substantially higher than the average rate. It can be noted that multiple flows of VoIP with VAD requires less allocation on average than a single flow to achieve a good performance level. Multiplexing of several flows reduces the rate variation in the traffic [12], reducing the need for extra capacity to compensate for rate fluctuations. RC3 outperformed RC2 in the presence of multiple flows. It can also be noted that increasing the ratio of allocated capacity to average rate beyond a certain point does not offer any better performance than a certain level. This defines the upper-bound of the performance that can be observed in satellite network. For example, 1.5 for 4 VoIP flows - allocating more than this not bring any significant performance improvement.

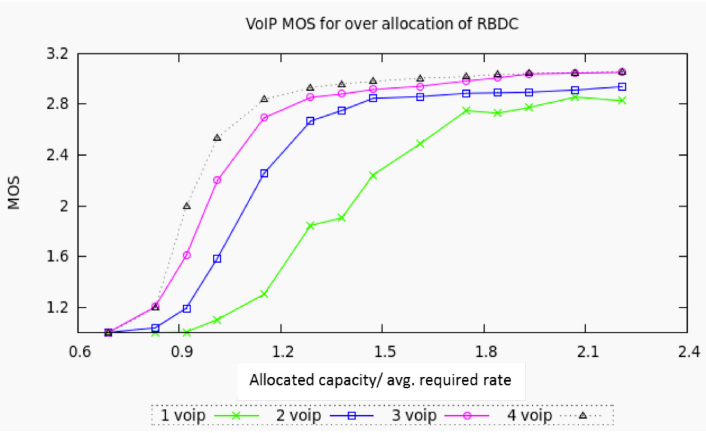

Fig. 2. MOS for VoIP traffic as a function of the allocated capacity per flow normalised to the flow peak rate assigned using RC3

4.3 Simultaneous Multiple Web and VoIP Flows

The previous sections illustrated how the performance of an application depends on the strategy implemented by the RC. In this section, we focus on the performance of a traffic mix in a multi-service scenario. In particular, we show that performance and efficiency gains are possible when different traffic share the allocated capacity.

Simulations considered traffic with a varying number of parallel running web and VAD-enabled VoIP flows. Web and VoIP flows were respectively assigned to RC1 and RC3. Moreover, the VoIP traffic was given priority over web, as recommended in [13]. Fig. 3 shows the webpage download time in this mixed traffic scenario as a function of the number of competing web and VoIP flows. The webpage download

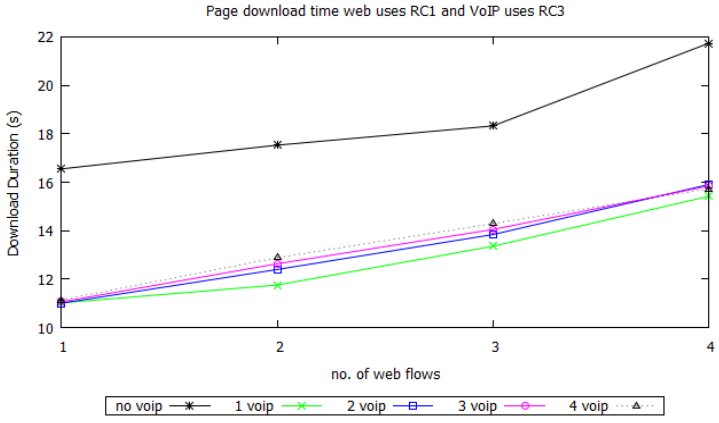

Fig. 3. Excess capacity from VoIP flows benefits web flows when downloading web pages

time in absence of VoIP (labelled 'no voip') ranged from 16 to 22 seconds as the number of web flows varied between 1 and 4. The download time increased almost linearly as the number of web flows increased. Indeed, the burstiness of web traffic caused a transient backlog of ACKs at the RCST buffer, which increased as the number of web flows increased.

Fig. 3 shows a significant reduction in the latency of webpage download time - independent of the number of web flows. The introduction of competing VoIP traffic had a beneficial effect on web performance. It takes less time to download a page when at least 1 VoIP is present. Since each VoIP/VAD flow had an ON/OFF behaviour, the VoIP aggregate left some of the allocated capacity unused. Web traffic could use this capacity to clear any backlog at the RCST, avoiding the need for additional CRs. This reduced the time for the download. The addition of more VoIP flows had only a small impact of web performance.

RC3 was suited to support multiple VoIP flows also in a mixed traffic scenario. Fig. 4 shows that the MOS was fair (around 3) and it did not deteriorate significantly when the number of VoIP flows increased.

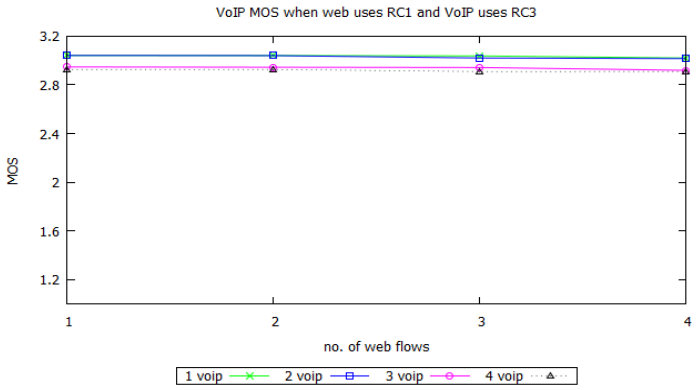

Fig. 4. VoIP MOS for multiple flows with multiple Web flows; the web flows have negligible effect on the VoIP performance level

We also report the efficiency of a broadband resource sharing scheme. Resource sharing is an important metric for commercial operation. This metric (Fig. 5) can be used to determine whether the resource distribution can be improved. Any unused capacity may be made available to support additional users or new services. The efficiency for one or two VoIP (with VAD enabled) flows was low (around 25% and 50% respectively). This poor efficiency was dominated by predictive over-allocation, required to ensure VoIP flows did not experience jitter, but exceeded the average capacity required for a few VoIP flows. Efficiency increased with the number of flows (VoIP or web).

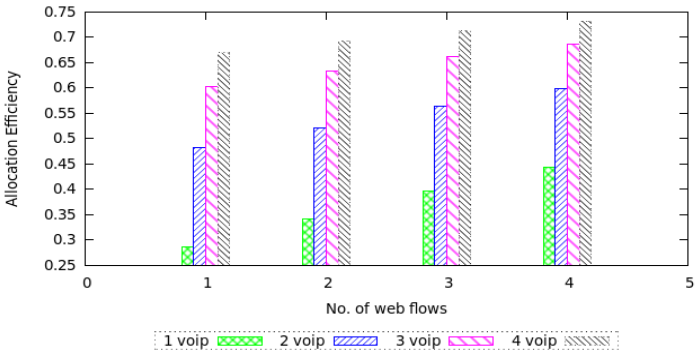

Fig. 5. Allocation efficiency as a function of number of simultaneous web and VoIP flows; higher number of flows contribute to better efficiency

5 Discussion

Resource sharing is important in all types of commercial access networks. In cabled services, an operator typically needs to consider contention in the backhaul since all downstream users share the resource of this backhaul. To avoid degrading the user performance, the decision to add a new user must consider whether the backhaul resources will become saturated. Contention ratios of 10:1, 20:1 or 50:1 are not uncommon, with smaller ratios for premium services.

A satellite access network has a similar need to share the resource of the return link capacity. However, the resource pool is typically much larger than that of cabled systems, where a satellite operator may share available resource among a large number (~1000s) of active users. The larger pool size allows an operator more flexibility in the way that the resources are assigned. Appropriate assignment can then be used as a tool to ensure economic system operation – assigning more capacity than needed incurs unnecessary cost to an ISP, allocating less than needed impacts the user performance.

The first two sets of experiments provided examples of ways to tune the performance and efficiency by choosing an RC with appropriate BoD mechanisms. RCs can be further customized to satisfy the service needs of a specific application.

The third set of experiments presented the performance and system efficiency when used to support multiple concurrent web and VoIP sessions, each supported by the RC best suited to the corresponding application. These results illustrate the advantage of selecting appropriate BoD methods and QoS parameters. We did not find a single optimum RC that could support the entire range of traffic in a multi-service network. Different applications have different traffic profile and delay requirements (Table 3).

It was also shown that a combination of RCs can provide the flexibility needed for bandwidth management by allowing an operator to tune the BoD to achieve a particular set of QoS classes (i.e. to meet a customer service level agreement –SLA). RCs can be designed combining RBDC and VBDC requests with different weights to meet these varying requirements.

Table 3. Traffic profile and delay requirements for different applications

Application	Traffic Profile	Delay Requirements
Web	Variable rate (Bursty)	Moderately delay sensitive
VoIP	Fixed rate	Real-time
VoIP/VAD	ON/OFF between 0 and fixed rate	Real-time
Video-conferencing	Fixed rate (based on encoder)	Real-time
Web Video	Variable rate/ Bursty	Low delay and jitter
Instant messaging	Very short interactive transfer	Medium delay, low jitter
File Transfer	Bulk transfer	Medium delay
Email	Short transaction	Medium delay

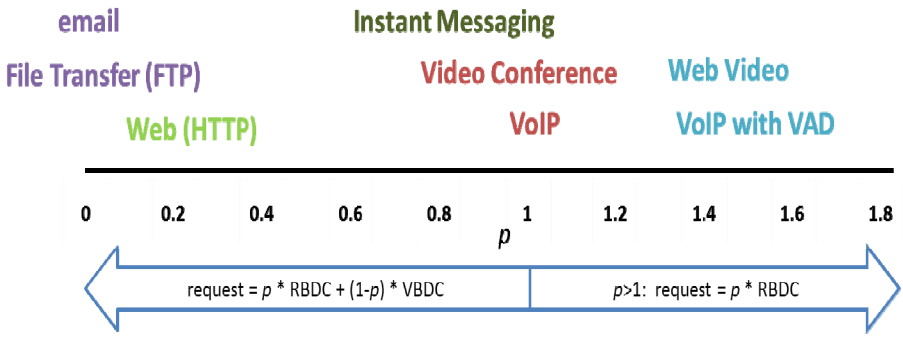

Fig. 6. A possible mapping of different applications to different RCs varying the value '*p*'

Fig. 6 shows a possible mapping of different applications to RCs. In our experiments, we considered two different request strategies: one combines RBDC and VBDC requests with a weighted value *'p'* ($p<1$), while the other multiplies the RBDC requested amount with *'p'* for allocation ($p>1$). Our results showed that application performance (for web and VoIP) varied greatly on the values of *'p'* and an RC can be designed with a particular value of *'p'* matching the application requirement. Other applications can also use the same allocation strategy, but certainly requires a suitable *'p'* value. Based on the traffic profile and delay requirements, an RCST running different applications may possibly follow the mapping in Fig. 6. However, the satellite operator has the full flexibility in selecting the appropriate value of *'p'* for different applications based on the factors like SLA, number of users etc.

6 Conclusion

This paper explored the interaction between BoD and QoS for multi-service support in an IP-based DVB-RCS2 system. Simulation results evaluated BoD methods for tuning the QoS. A combination of RCs can provide the flexibility needed for

bandwidth management by allowing an operator to tune the BoD to achieve the set of QoS classes. This offers functions for the satellite that are similar to those used to provide a cabled broadband service. As a result, satellite broadband can be an effective complimentary access technology to enable universal broadband roll-out.

Acknowledgement. The research described here is supported by the award made by the RCUK Digital Economy program to the dot.rural Digital Economy Hub; reference: EP/G066051/1.

References

1. ETSI EN 101 545, Second Generation DVB Interactive Satellite System; Part 2: Lower Layers for Satellite Broadband (March 2011)
2. Iuoras, N., et al.: An IP-based satellite communications system architecture for interactive multimedia services. International Journal of Satellite Communications and Networking 21(4-5), 401–426 (2003)
3. Skinnemoen, H., et al.: VoIP over DVB-RCS with QoS and Bandwidth on Demand. IEEE Wireless Communications 12(5), 46–53 (2005)
4. Lexow, H., Navekvien, T., Paxal, V.: Satellite resource management combining distributed cooperative methods and central control using BoD variants of DVB-RCS. In: 11th Ka-Band Communications Conference, Rome (September 2005)
5. Kalama, M., et al.: VoIP over DVB-RCS satellite systems: a novel capacity request mechanism for improved voice activity detection. In: IEEE Vehicular Technology Conference, Singapore, pp. 2957–2961 (May 2008)
6. Chini, P., Giambene, G., Hadzic, S.: Broadband satellite multimedia networks. In: Cranley, N., Murphy, L. (eds.) Wireless Multimedia: Quality of Service and Solutions, pp. 377–398. IGI Global (2009)
7. Secchi, R.: DVB-RCS(2) for ns2 (September 11, 2012), `http://homepages.abdn.ac.uk/r.secchi/pages/dvbrcs_ns2.htm`
8. Secchi, R., Sathiaseelan, A., Fairhurst, G.: Evaluating web traffic performance over DVB-RCS2. In: Pillai, P., Shorey, R., Ferro, E. (eds.) PSATS 2012. LNICST, vol. 52, pp. 148–155. Springer, Heidelberg (2013)
9. Adas, A.: Traffic Models in Broadband Networks. IEEE Communications Magazine, 82–89 (July 1997)
10. ITU-T: G.729 Annex B: A silence compression scheme for G.729 optimized for terminals conforming to Recommendation (October 1996)
11. Cole, R., Rosenbluth, J.: Voice over IP performance monitoring. ACM Computer Comm. Review 31(2), 9–24 (2001)
12. Castro, V., et al.: Quality of Service of VoIP over DVB-RCS. In: 6th Workshop on Signal Processing in Communications, Baiona (September 2003)
13. Sathiaseelan, A., Fairhurst, G.: Multimedia congestion control for broadband wireless networks. IST Mobile Summit, Budapest (2007)
14. Adami, D., Giordano, S., Pagano, M., Secchi, R.: Modeling the Behavior of a DVB-RCS Satellite Network: an Empirical Validation. In: Proceedings of Performance Modelling and Evaluation of Heterogeneous Networks (HET-NET's 2005), Ilkley, UK (July 2005)

Impact of the Railway Centerline Geometry Uncertainties on the Train Velocity Estimation by GPS

Guoliang Zhu[1,⋆], Lionel Fillatre[2], and Igor Nikiforov[1]

[1] ICD - LM2S - UTT, UMR STMR - CNRS, Troyes, France
{guoliang.zhu,igor.nikiforov}@utt.fr
[2] Laboratoire I3S, UMR7271 - UNS CNRS, Sophia-Antipolis, France
lionel.fillatre@i3s.unice.fr

Abstract. The railway centerline is defined by a polygonal line with some level of uncertainty in the train onboard database. The goal of this paper is to estimate the train speed by GPS and to study the impact of railway centerline uncertainty on the speed estimation. The equations for first two moments of the estimated speed are obtained and compared with the results of Monte-Carlo simulations.

Keywords: GPS train positioning, Train track model, Least square method, Model nonlinearity.

1 Introduction and Motivation

The estimation of train speed and distance to target plays an important role in the management of modern railways. For safe and efficient railway operations, these parameters should be estimated with a high level of accuracy [1,2] and integrity [3].

This paper is devoted to the GPS train positioning by using a low-cost receiver. Two limit cases of the train speed estimation can be considered. The first approach is based on the exactly known three-dimensional train-track model (this is so-called one-dimensional navigation). The second approach does not use any information about the train track (hence, it is the classical two or three-dimensional navigation). The first case provides the user with the best precision but it is unrealistic because the exact three-dimensional train-track model needs an enormous effort of geodesic measuring and the onboard train database preparation. The second case is rather pessimistic, some information about the train track is always available, at least by using electronic maps for large public. A crucially important question is the impact of such a map imprecision on the estimation of train speed and distance to target.

This paper is organized as follows. Section 2 is devoted to the problem statement. Section 3 provides the geometric model of railway track, the train dynamical model and the method of train speed estimation. The impact of train-track model imprecision on the speed estimation is discussed in section 4. Simulation results are shown in section 5. Finally, some conclusions are drawn in section 6.

⋆ The authors would like to thank the China Scholarship Council and the University of Technology of Troyes (UTT), France, for supporting their research.

R. Dhaou et al. (Eds.): PSATS 2013, LNICST 123, pp. 156–161, 2013.

2 Problem Statement and Contribution

Let us consider that the train runs along the track with a constant (unknown) speed. The goal of this paper is twofold : first, to calculate the train speed by using GPS and an imprecise geometric model of the railway centerline; second, to estimate a negative impact of the railway centerline uncertainty on the mean error and on the second order moment of the estimated speed. The equations for first two moments of the estimated speed are obtained and compared with the results of Monte-Carlo simulations.

3 Description of Models

3.1 Train Track Model

Let us assume that the railway centerline is approximated by a polygonal line (piecewise linear curve), which represents a connected series of line segments in the Earth-centered, Earth-fixed coordinates. More formally, the railway centerline is defined by a sequence of vertices $Z_0, Z_1, Z_2, \ldots, Z_n$, $Z_i \in \mathbb{R}^3$, so that the curve consists of the line segments connecting the consecutive vertices. It is assumed that the errors related with such an approximation of the vector function $\ell \mapsto X(\ell)$, $\ell \in \mathbb{R}$, $X \in \mathbb{R}^3$, defining the railway centerline is negligible for our study. Here and in the rest of the paper, ℓ denotes the curvilinear abscissa, or the covered distance, and $m = \|Z_{j+1} - Z_j\|_2 = \text{const}$ is the distance between two adjacent vertices, respectively. Unfortunately, the on-board database uses an

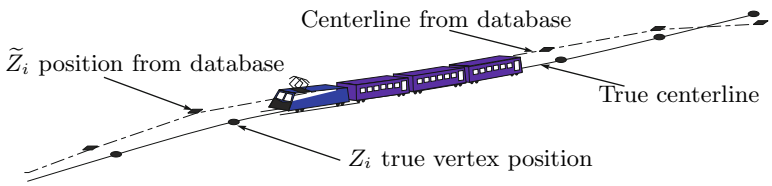

Fig. 1. Train track model

imprecise information about the positions of vertices, namely : $\widetilde{Z}_0, \widetilde{Z}_1, \widetilde{Z}_2, \ldots, \widetilde{Z}_n$. The quantity $\xi_i = Z_i - \widetilde{Z}_i$ defines the knowledge uncertainty concerning the train track. This situation is illustrated by Fig. 1. To simplify the presentation, a two-dimensional train trajectory is considered.

3.2 Train Dynamical Model

Traditionally, the train dynamical model is described by an equation formulated in term of the covered distance, speed and acceleration. To simplify the estimation problem, it is assumed for this study that the acceleration is negligible for

some short periods. Let us suppose that the train runs along the above railway track with an unknown constant speed v. Hence, the true train position is defined as follows: $X_k = X_{k-1} + A_{j(k)} \cdot v \cdot \Delta t$, $k = 1, 2, \ldots$, where $X_k = (x_k, y_k, z_k)^T$ is the train position at the k-th GPS measurement (GPS epoch), t_k denotes the instant of the k-th measurement, $\Delta t = t_k - t_{k-1}$ represents the GPS sampling interval, $A_j = (a_x^j, a_y^j, a_z^j)^T = \dfrac{1}{m}(Z_{j+1} - Z_j)$ is the directional vector corresponding to the segment number j, $\|A_j\|_2 = 1$. The current segment number $j = j(k)$ is calculated as a function of k by using the following equation

$$j(k) = \min\left\{j \in \mathbb{N} | j \geq \lfloor (v \cdot \Delta t \cdot k)/m \rfloor\right\}, \tag{1}$$

where $\mathbb{N}$ is the set of natural numbers. The train position X_k can be rewritten as

$$X_k = X_0 + v\Delta t \sum_{t=1}^{k} A_{j(t)} \tag{2}$$

where $X_0 = (x_0, y_0, z_0)^T$ is the starting point.

3.3 Exact and Imprecise Pseudo-range Measurement Model

Suppose that there are n satellites located at the known positions $X_i^s = (x_i, y_i, z_i)^T$, $i = 1, \ldots, n$. The pseudo-range r_i from the satellite i to the train can be written as:

$$r_i^k = d_i^k + cb_r^k + \varepsilon_i^k = \left\| X_0 + v\Delta t \sum_{t=1}^{k} A_{j(t)} - X_i^s \right\|_2 + cb_r^k + \varepsilon_i^k, \;\; \varepsilon_i^k \sim \mathcal{N}(0, \sigma^2),$$

where b_r^k is a user clock bias, $c \simeq 2.9979 \cdot 10^8 m/s$ is the speed of light and ε_i^k is a pseudo-range noise. By linearizing the pseudo-range equation around the working point $V_0 = (v_0, cb_0)^T$, we get

$$r_i^k - r_{i,0}^k \simeq h_{i,0}^k (v - v_0) + c(b_r^k - b_0) + \varepsilon_i^k, \;\; i = 1, \ldots, n, \tag{3}$$

where $r_{i0}^k = d_{i0}^k + cb_0$, $d_{i0}^k = \left\| X_0 + \left(\sum_{t=1}^{k} A_{\widehat{\jmath}(t)} \right) \cdot v_0 \Delta t - X_i^s \right\|_2$ and

$$h_{i0}^k = \frac{1}{d_{i0}^k} \left[X_0 + \left(\sum_{t=1}^{k} A_{\widehat{\jmath}(t)} \right) \cdot v_0 \Delta t - X_i^s \right]^T \left(\sum_{t=1}^{k} A_{\widehat{\jmath}(t)} \right) \Delta t.$$

Because the true train speed v is unknown, the current segment number $\widehat{\jmath} = \widehat{\jmath}(t)$ is calculated as a function of the previously calculated speed $\widehat{v}_t$ by using (1) with $v = \widehat{v}_t$. The above mentioned linearized measurement equation (3) can be rewritten in the following matrix form

$$R^k - R_0^k \simeq H_0^k \cdot (V_k - V_0) + \Xi^k, \tag{4}$$

where $V_k = (v, cb_r^k)^T$ and the working point at step k is equal to the previously calculated estimation : $V_0 = \widehat{V}_{k-1}$.

Let us discuss now an unprecise measurement model. Since the true vertex position Z_j is unknown and only its imprecise estimation $\widetilde{Z}_j$ is available, the linearized measurement equation (4) cannot be used to compute the train speed. To estimate the impact of this uncertainty, let us define the directional vector $\widetilde{A}_j = A_j + \delta_j$, where the random vector $\delta_j = (\delta_x^j, \delta_y^j, \delta_z^j)^T$ is assumed to be uniformly distributed in the cube $[-b, b]^3$ with $b > 0$. Finally, the pseudo-range measurement model (4) is defined for the imprecise directional vectors $\widetilde{A}_j$ in the following manner

$$R^k - \widetilde{R}_0^k \simeq \widetilde{H}_0^k \cdot (V_k - V_0) + \Xi^k \tag{5}$$

where $\widetilde{R}_0^k$ and $\widetilde{H}_0^k$ are calculated exactly as in equation (3) but with the vector $\widetilde{A}_j$ instead of A_j.

4 The Impact of Track Uncertainty on the LS Estimator

The goal of this section is to study the impact of the train track uncertainty δ_j on the first and second moments of the least square (LS) estimator $\widehat{v}_k$. To seek simplicity, let us assume that the track entirely belongs to the local tangent plane. We follow here the analysis of the regression model uncertainties and their impact on the LS estimators developed in [4]. First, the measurement equation (5) can be rewritten as follows:

$$Y^k + \Delta Y^k \simeq (H_0^k + \Delta H^k) \cdot \beta_k + \Xi^k \tag{6}$$

where $Y^k = R^k - R_0^k$, $\Delta Y^k = R_0^k - \widetilde{R}_0^k$, $\Delta H^k = \widetilde{H}_0^k - H_0^k$ and $\beta_k = V_k - V_0$. It is assumed that the second column of ΔH^k is equal to zero because the impact on the clock bias estimation is of no interest for this study. The LS estimator is given by

$$\widehat{\beta}_k = \left[\left(H_0^k + \Delta H^k\right)^T \left(H_0^k + \Delta H^k\right) \right]^{-1} \left(H_0^k + \Delta H^k\right)^T \left(Y^k + \Delta Y^k\right). \tag{7}$$

After expanding $\left[\left(H_0^k + \Delta H^k\right)^T \left(H_0^k + \Delta H^k\right) \right]^{-1}$ around H_0^k (see appendix of [4]) and computing the expectation of equation (7), the mean error is

$$\mathbb{E}(\widehat{V}_k - V) = B_0^{-1} \left[(H_0^k)^T \Sigma_H C - F + G \right] \beta \tag{8}$$

where Σ_H denotes the covariance matrix of ΔH^k, $F = \begin{pmatrix} \mathrm{tr}(\Sigma_H) & 0 \\ 0 & 0 \end{pmatrix}$, $G = \begin{pmatrix} \mathrm{tr}\left[H_0^k B_0^{-1} (H_0^k)^T \Sigma_H\right] & 0 \\ 0 & 0 \end{pmatrix}$, $B_0 = \left(H_0^k\right)^T H_0^k$, the first column of a $(n \times 2)$ matrix C is equal to the first column of $H_0^k B_0^{-T}$ and its second column is equal to zero.

Since the random vector ΔY^k acts in the same way as the pseudo-range noise Ξ^k, the two errors can be considered together. After expanding and ignoring

the terms of order $\left(\Delta H^k\right)^2$ and under the assumption that the errors ΔH^k are reasonably small, the second order moment of $\widehat{V}_k - V$ is given by

$$\mathbb{E}(\widehat{V}_k - V)(\widehat{V}_k - V)^T = B_0^{-1}(H_0^k)^T\left[\sigma^2 I_n + \Sigma_Y - \beta_1(\Sigma_{HY} + \Sigma_{YH}) + \beta_1^2 \Sigma_H\right] H_0^k B_0^{-1}, \quad (9)$$

where $\beta_1 = v - v_0$, Σ_Y denotes the covariance matrix of ΔY^k, $\Sigma_{HY} = \mathbb{E}\left[\Delta H^k (\Delta Y^k)^T\right]$ and $\Sigma_{YH} = \Sigma_{HY}^T$. When the expectation (8) of $\widehat{V}_k - V$ is almost zero, this second order moment corresponds to the variance of $\widehat{V}_k$.

5 Numerical Simulations

The comparison of the theoretical mean error and second order moment given by (8) and (9), respectively, with the results of a 10^4-repetition Monte-Carlo simulation, is shown in Fig. 2-7. The standard GPS constellation has been used with $n = 6$ visible satellites and $\sigma = 2$ (m). The distance between two adjacent vertices has been chosen $m = 50$ (m). Different values of railway centerline

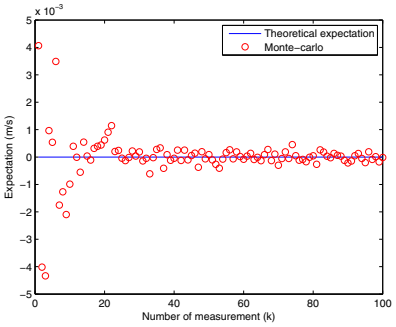

Fig. 2. The estimated speed mean error for $\delta_j = 0$

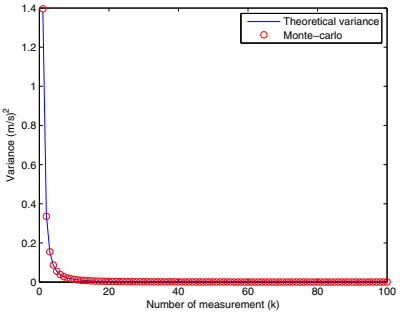

Fig. 3. The estimated speed second order moment for $\delta_j = 0$

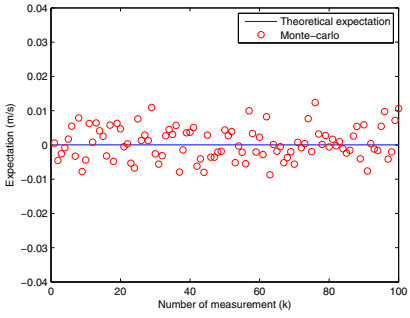

Fig. 4. The estimated speed mean error for $\delta_j \in [-0.01, 0.01]^2$

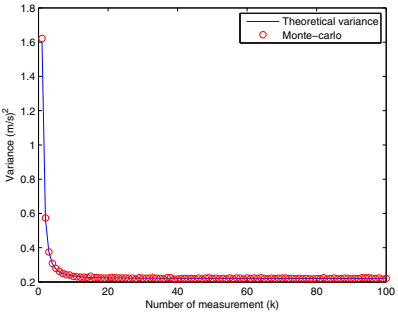

Fig. 5. The estimated speed second order moment for $\delta_j \in [-0.01, 0.01]^2$

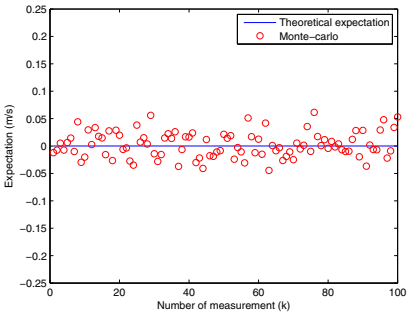

Fig. 6. The estimated speed mean error for $\delta_j \in [-0.05, 0.05]^2$

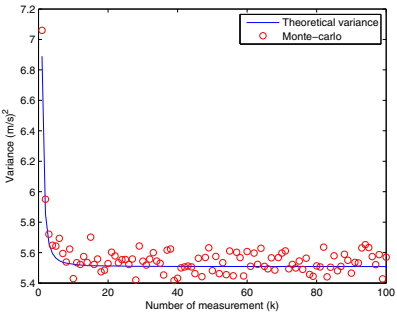

Fig. 7. The estimated speed second order moment for $\delta_j \in [-0.05, 0.05]^2$

uncertainty have been tested : $b = 0$ (no uncertainty); $b = 0.01$ (uncertainty $\simeq \pm 0.5$ (m)); $b = 0.05$ (uncertainty $\simeq \pm 2.5$ (m)).

6 Conclusions

The comparison of the train speed estimation by GPS with an imprecise geometric model of the railway centerline and by using odometric measurements [1,2] shows that the second order moments of the estimated speed are comparable but the speed mean error obtained by GPS is better. It is practically unbiased, even with an imprecise geometric model of the railway centerline. A hybrid estimation connecting the odometer, accelerometer and GPS measurements seems to be very promising for the train speed estimation.

References

1. Malvezzi, M., Allotta, B., Rinchi, M., Bruzzo, M., De Bernardi, P.: Odometric Estimation for Automatic Train Protection and Control Systems. In: 8th World Congress on Railway Research, Korea (2008)
2. Malvezzi, M., Allotta, B., Rinchi, M.: Odometric Estimation for Automatic Train Protection and Control Systems. Vehicle System Dynamics 49(5), 723–739 (2011)
3. Nikiforov, I.V., Choquette, F.: Integrity Equations for Safe Train Positioning Using GNSS. Istituto Italiano di Navigazione 171, 52–77 (2003)
4. Hodges, S.D., Moore, P.G.: Data Uncertainties and Least Squares Regression. JRSS, Series C (Applied Statistics) 21, 185–195 (1972)

A Satellite Radio Interface Compatible with Terrestrial 3GPP LTE System

Hee Wook Kim*, Taechul Hong, Kunseok Kang, and Bon-Jun Ku

Electronics and Telecommunications Research Institute,
305-350 Gajeong-dong Yuseong-gu Daejeion, Korea
{prince304,taechori,kskang,bjkoo}@etri.re.kr

Abstract. In this paper, a candidate satellite radio interface, satellite orthogonal frequency division multiplexing (SAT-OFDM), for the satellite component of IMT-Advanced is presented. The SAT-OFDM is based on long term evolution (LTE) terrestrial radio interface for maximum commonality with IMT-Advanced terrestrial radio interface. This paper deals with the configuration and performance of the 3GPP LTE based satellite radio interface. And then, as an enhancement of the satellite-specific radio interface, it addresses the possible adaptation of 3GPP LTE to the satellite in order to maximize the performance over satellite link.

Keywords: mobile satellite system, OFDM, LTE, radio interface.

1 Introduction

Considering cost-effective, in a future IMT-Advanced satellite system, a satellite radio interface needs to be compatible with a maximum degree of commonality with emerging terrestrial standards. Therefore, the techniques adopted for the satellite system have to be similar to or even the same as those of the terrestrial system. The adaptation of a compatible radio interface with maximum commonality will result in possibility to reuse terrestrial component technology to minimize the change of user equipment (UE) chipset and network equipment for low cost and fast implementation.

As emerging terrestrial radio interfaces, the third generation partnership project (3GPP) long term evolution (LTE) and the institute of electrical and electronics engineers (IEEE) mobile worldwide interoperability for microwave access (WiMAX) radio interfaces are being considered [1]. Both two radio interfaces adopted orthogonal frequency division multiplexing (OFDM) scheme, which is intrinsically able to manage the most typical radio frequency distortion without the help of complex equalization techniques and has scalability easily to fit different bandwidth [2]. There had not been much attention to the study on OFDM based satellite radio interfaces because of severe peak to average power ratio (PAPR) problems, considering a high cost power amplifier in satellite systems. Nevertheless, recent study results reported the

* This work was also supported by the 2012 new R&D program of KCC/KCA, [Optimized utilization technology development of 2.1 GHz satellite frequency band for mobile communications].

R. Dhaou et al. (Eds.): PSATS 2013, LNICST 123, pp. 162–173, 2013.

adaption of OFDM technique in the satellite systems to give benefits such as capability of high data rate transmission and commonalities with the terrestrial systems.

In this regards, the satellite orthogonal frequency division multiplexing (SAT-OFDM) is being developed as a candidate satellite radio interface to provide various IMT services over satellite environments. The radio interface can be applied for Geo-stationary earth orbit (GEO) satellite for the provision of global IMT service. It adopts orthogonal frequency division multiple access (OFDMA) for downlink and single carrier frequency division multiple access (SC-FDMA) for uplink. The radio interface has a high degree of commonality with the terrestrial radio specifications, 3GPP long term evolution (LTE) technology for IMT-Advanced services, but it also has many different features. Those features are inevitable to consider the satellite-specific characteristics such as long round trip delay and slow fading satellite channel, and are implemented in the form of random access, interleaving, power control and so on. Furthermore, the radio interface has two operational modes which are expressed as normal and enhancing modes. The normal mode is fully compatible with 3GPP LTE Release 8, while the enhancing mode provides performance enhancement by incorporating new satellite-specific features. The satellite radio access network (RAN) should support both modes while the UE can support either the normal mode only or both modes.

This paper first address brief IMT-Advanced system description using the SAT-OFDM radio interface in Section 2. A detail introduction of the SAT-OFDM is presented in Section 3. Then some satellite-specific features defined in the enhancing mode of SAT-OFDM are introduced as the possible further enhancements to its normal mode. In Section 4, we demonstrate performance of the SAT-OFDM in normal mode in order to validate the feasibility of 3GPP LTE as a satellite radio interface. Finally, we will draw conclusions in Section 5.

2 Satellite IMT-Advanced System Using the SAT-OFDM

2.1 Architectural Description

Figure 1 describes an overall system architecture using the SAT-OFDM. The satellite will provide various mobile services similar to those of terrestrial IMT systems outside terrestrial and complementary ground component (CGC) coverage under the intrinsic limitations induced by transmit power and long round trip delay constraints. On the other hands, the CGC can be deployed in regions where satellite signal is hard to be received, particularly in urban areas in order to provide mobile satellite broadcasting/multicasting services. It can be collocated with terrestrial base station sites for the cost-effective deployment. The satellite component can provide voice and data communication service in regions outside terrestrial coverage. The areas not adequately covered by terrestrial component include physically isolated regions, gap of terrestrial component and areas where terrestrial component permanently, or temporarily, collapses due to disaster.

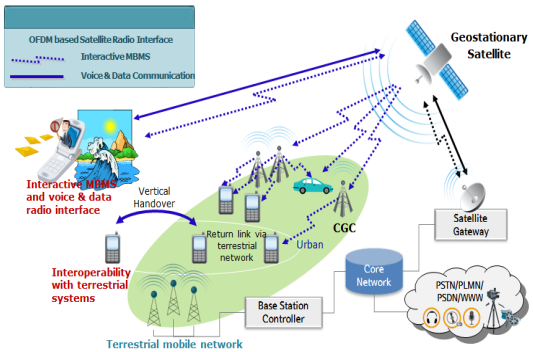

Fig. 1. IMT-Advanced system concept using SAT-OFDM

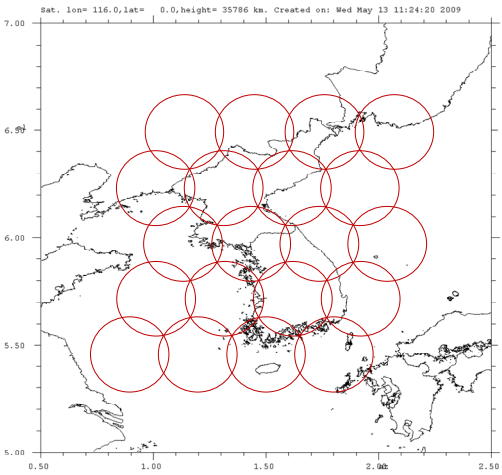

Fig. 2. Multi-beam configuration example with a 24m satellite antenna

The two way communication scenario is regarded as coverage extension and service continuity of the terrestrial part. In the scenario, handover technique with terrestrial part would be most importantly considered. For the cost-effective interworking, future satellite radio interfaces should be compatible as well as have maximum common functionality with an envisaged LTE based terrestrial radio system. Also, terrestrial part technology can be reused to decrease user equipment (UE) chipset and network device for fast and low-cost development. In addition, the SAT-OFDM can be used to provide efficient interactive multimedia broadcasting services since the envisaged terrestrial mobile radio interfaces can handle services for broadcast as well as a bi-directional communications in a cellular system. Indeed, the satellite component has an advantage of efficiently delivering the same content over worldwide geographical area.

This interface is able to deal with several satellite constellation types, i.e. low earth orbit (LEO), medium earth orbit (MEO), GEO or highly elliptical orbit (HEO). It is

noted, however, descriptions in the following sections are mostly based on the GEO constellation type. Several architectures are envisaged depending on throughput requirements e.g. global beam, multi-beam, and multi-satellite configurations. The example in Fig. 2 assume multi-beam configuration over Korean coverage.

2.2 System Description

The SAT-OFDM based on the key technical characteristics listed in Table 1 could provide a wide range of telecommunication services in ITU-R Recommendation M.1822 to mobile users [3]. Quality of service (QoS) for various telecommunication services supported by the radio interface would be different from that in the terrestrial component of IMT-Advanced due to inherent satellite features such as long round trip delay. In this interface, maximum transfer delay of one way of the real time services at the bearer transport level could be less than 400 ms in the range of values $1x10^{-2}$ to $1x10^{-7}$ of bit error rate (BER).

The user equipment may be of various types: handheld, portable, vehicular, transportable or aeronautical. The data rate and mobility restriction for each type of terminal are described in Table 3. For the maximum capacity assessment it is necessary to distinguish data rates for the downlink from those of the uplink.

The SAT-OFDM will support handover of communications from one satellite radio channel to another. The handover strategy is mobile-assisted network-decided handover and only hard handover is supported. The SAT-OFDM system can support beam handover, inter-satellite handover, inter-frequency handover.

Table 1. Key characteristics of SAT-OFDM

Multiple access method	OFDMA (downlink) SC-FDMA (uplink)
Duplex	Frequency division duplexing (FDD)
Chip rate	A multiple or submultiple of 3.84 Mcps
subcarrier spacing	15 kHz
Carrier spacing	1.3, 3, 5, 10 15, 20 MHz
Frame length	10 ms
Inter-spot synchronization	No accurate synchronization needed (Accurate synchronization needed for inter-beam coordination)
Multi-rate/Variable-rate scheme	Variable modulations and coding rates + multi-layer
Channel coding scheme	Convolutional coding 1/3 Turbo coding 1/3
Multiple-access scheme	OFDMA (downlink), SC-FDMA (uplink)

3 SAT-OFDM Radio Interface

3.1 Multiple Access

Overall uplink transmission of the SAT-OFDM is described in Figure 3. The SAT-OFDM has basically the same transmission blocks with 3GPP LTE Release 8 radio interface for commonality but can also modify some blocks or add new blocks in order to adopt satellite-specific features. Its downlink transmission is same as uplink transmission except DFT and IDFT blocks.

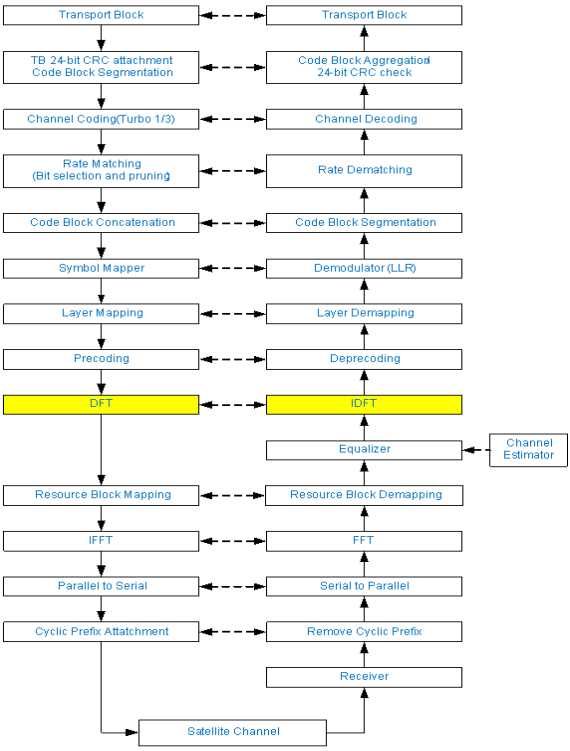

Fig. 3. Uplink transmission in the SAT-OFDM

Multiple input and multiple output antennas (MIMO) transmissions is supported with two or four satellites or two polarizations and two or four received antennas in the downlink. The MIMO transmission supports multi-layer with up to four data streams. Multi-user MIMO, in which different streams are allocated to different users, is also supported in uplink as well as downlink.

For the SAT-OFDM physical layer, the multiple access method in downlink is based on OFDM with a cyclic prefix (CP) while that in uplink is based on SC-FDMA with a CP. In addition, frequency division duplex is supported in order to support transmission in paired S-band spectrum. The bandwidth agnostic physical layer is defined based on resource block concept which allows the SAT-OFDM physical layer to adjust to various bandwidth allocations. One resource block consists of either twelve

subcarriers with a subcarrier bandwidth of 15 kHz or twenty four subcarriers with a subcarrier bandwidth of 7.5kHz each during a slot interval of 0.5ms. The FDD radio frame structure consists of twenty slots with a slot interval of 0.5ms and has a frame duration of 10ms. A subframe of 1ms length is formed by two adjacent slots.

The physical channels are defined in the SAT-OFDM as followings.

- Downlink physical channels for transmission of user data and control, information
  - PDSCH (Physical Downlink Shared Channel)
  - PMCH (Physical Multicast Channel)
  - PDCCH (Physical Downlink Control Channel)
  - PBCH (Physical Broadcast Channel)
  - PCFICH (Physical Control Format Indicator Channel)
  - PHICH (Physical Hybrid ARQ Indicator Channel)
- Downlink physical signals for cell search and channel estimation
  - RS (Reference Signal)
  - SCH (Synchronization signal)

Uplink

- Uplink physical channels for transmission of user data and control information
  - PUSCH (Physical Uplink Shared Channel)
  - PUCCH (Physical Uplink Control Channel)
  - PSRACH (Physical Satellite Random Access Channel)
- Physical signals for channel estimation
  - RS (Reference Signal)

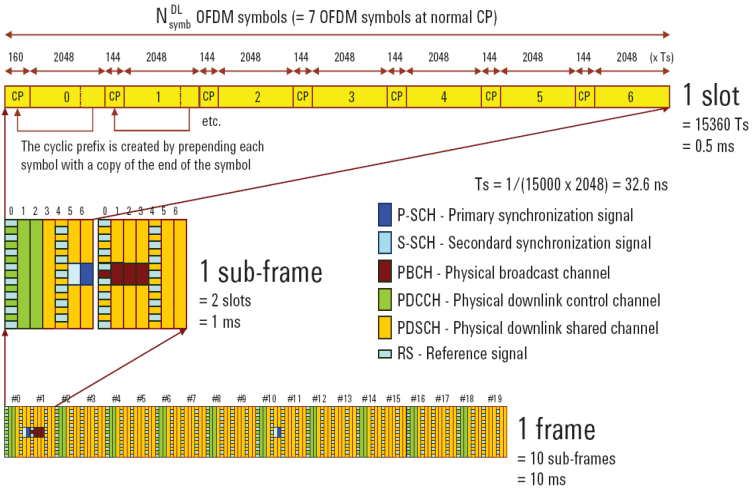

Fig. 4. Downlink frame structure of the SAT-OFDM

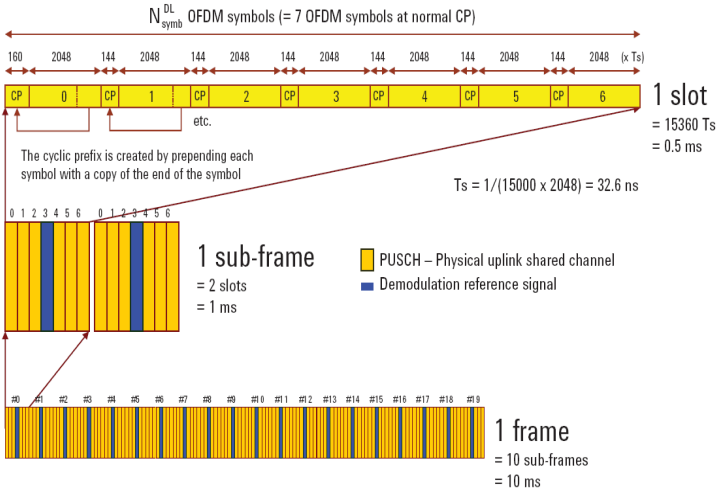

Fig. 5. Uplink frame structure of the SAT-OFDM

Figure 4 and 5 show downlink and uplink frame structure of the SAT-OFDM including whole physical channels. The smallest resource unit in both uplink and downlink transmissions is denoted as a resource element (RE). A physical channel is relevant to a set of the REs carrying information generating from higher layers. On the other hands, a physical signal is used only for the physical layer but does not accomplish information generating from higher layers.

4 Some Candidate Satellite-Specific Features for Performance Enhancement

The SAT-OFDM has a high degree of commonality with the terrestrial radio specifications based on 3GPP long term evolution (LTE) technology for IMT-Advanced services but it also has many different features. Those features are required in order to consider the satellite-specific characteristics such as long round trip delay and slow fading satellite channel. For this purpose, the following techniques can be included for enhancing mode operation.

4.1 AMC Scheme Combined with Long-Term Interleaving

This scheme can be used for an efficient adaptive modulation and coding (AMC) operation in satellite environment [4]. Adaptive transmission techniques such as AMC are applied in order to satisfy the required transmission speed and QoS. Because of a long RTD in the GEO satellite systems, the adaptive transmission technique for the satellite systems should be different from that for the terrestrial radio interface. Considering the RTD of a GEO system, the updating interval of the AMC scheme should be an order of a second, and thus the AMC of the satellite systems cannot effectively counteract to short term fading. A long time interleaving technique is used in conjunction with AMC, and it is also used to compensate the short term fading.

4.2 Cooperative Transmission between a Satellite and CGCs

This scheme is used for performance enhancement in an integrated satellite/CGC configuration [5]. The concept of system model where a cooperative diversity technique is employed is as following. The satellite transmits data to the user terminals and all ground components. In order to achieve diversity gains via utilization of space-time coding (STC) schemes, each of the ground components must convert the received signals into a pre-defined encoded signal format, and then retransmit them to the UE. The CGCs and satellite can be cooperated in order to transmit space-time coded signals. For this, the CGCs can encode the transmitted satellite signal rather than serving as simple repeaters. A UE can receive the STC-encoded signals. If the UE receives the multiple signals from CGCs as well as the satellite, then it can get STC diversity gains by using these signals. In addition, a delay compensation algorithm is needed in the cooperative scheme. Since we can estimate processing delay to convert to a pre-defined STC encoded format at the CGCs as well as propagation delay difference between the links from the satellite and CGCs, the delay compensation for the signal transmitted from the CGCs can carry out successful synchronization at the UE. A coarse and fine compensation can be made at the satellite gateway and each ground component, respectively.

4.3 Narrowband PUSCH Transmission

In satellite systems the available bandwidth is constrained due to power limited environments, particularly in uplink. This means that the bandwidth that can be dedicated to one transport block also should be constrained. The constraint can be in the constitution of fewer subcarriers. Because the transport block size for narrowband transmission should be maintained for no modification on terrestrial LTE MAC layer, the data in the transport block is better inserted in such a way that it occupies a larger number of symbols compared to the terrestrial LTE system. For this, LTE physical layer should be modified in order to reduce the size of resource block (RB) and increase of the length of transmission time interval (TTI) of terrestrial LTE. In terrestrial LTE, 1 ms of TTI is considered in order to reduce latency of service delivery and make fast resource adaptations. However, considering a satellite system has already a few hundred miliseconds of very long round trip delay and mainly suffers from slow channel fading effects, the 1ms of short TTI doesn't give any advantages in the mobile satellite systems and prevents to get a time diversity gain to compensate slow channel fading effects. Therefore, the increase of the length of TTI in the satellite system will be under a reasonable adaptation of terrestrial LTE to satellite environment [7].

5 Performance Evaluations

Satellite and UE characteristics considered in performance evaluation are summarized in Table 2 and 3, respectively. Furthermore, the Fontan's static model for the land mobile satellite (LMS) channel is considered for the link and system level simulation. This model is competent to describe both narrow- and wideband conditions. Model parameters obtained from a complete experimental data base are also given for many elevation angles and environments at around 1.5GHz and 2GHz [8]. For evaluation, the LMS 3-state Markov chain model based on the measurements parameters for open environment at 40^{o} elevation in S-band is adopted.

Table 2. Satellite multi-beam with 24m satellite antenna

Number of spot beams	20
Downlink (satellite to UE) Frequency (satellite to UE) (MHz) Polarisation On board e.i.r.p. per carrier (dBW)	 2170~2200 LHCP or RHCP 73
Uplink Frequency (UE to satellite) (MHz) Polarisation Rx Antenna gain (dB)	 1980~2010 LHCP or RHCP ~ 30

Table 3. UE maximum transmit power, antenna gain and eirp

UE type	**Max. transmit power**	**Ref. antenna gain**	**Max. EIRP**	**Antenna temp.**	**G/T (dB/K)**
Handset Class 1 Class 2 Class 3	 2W 500mW 250mW	0dBi	 3dBW -3dBW -6dBW	290K	-33.6
Portable	2W	3dBi	5dBW	200K	-26
Vehicular	8W	4dBi	13dBW	250K	-25
Transport.	2W	14dBi	17dBW	200K	-14

Baseline configuration parameters are listed in Table 4 for simulation assessment of the SAT-OFDM. Evaluation is performed in open environment defined in ITU-R Report M.2176, which identifies visions and requirements for the satellite component of IMT-Advanced [8]. We assumed that UEs are randomly distributed over whole coverage and are located outdoor with the mobility of 3km/h. For assessment of beam spectral efficiency, beam spectral efficiency is defined in ITU-R Report M.2176 as the aggregate throughput of all users divided by the channel bandwidth as well as the number of satellite beams. Aggregate throughput means the number of correctly received bits, i.e. the number of bits contained in the service data units (SDUs) delivered to Layer 3. Also, full buffer best effort service profile is considered. VoIP capacity is drawn assuming a 12.2 kbps codec with a 50% activity factor such that outage percentage of users is less than 2%, where it is assumed that a user experience a voice outage if less than 98% of the VoIP packets is delivered successfully to the user within a one-way propagations delay about of 400 ms, considering maximum transfer delay of one way for the real-time services in the satellite component.

Table 4. Baseline evaluation configuration parameters

Parameters	Values used for evaluation
Deployment scenario	Open environment, GEO satellite
Duplex method and bandwidths	FDD: 5(Up) + 5(Down) MHz, 2.1 GHz carrier frequency
Frequency reuse plan	Reuse factor 6
Number of beams	20 (3dB of beam edge loss)
Transmission scheme	SISO
Scheduler	Channel dependent
Power control	None (allocate full power)
Link adaptation	Non-ideal based on delayed SRS-based measurements: MCS based on LTE transport formats and SRS period and bandwidths according to LTE Rel-8
HARQ scheme	Incremental redundancy or Chase combining None for VoIP traffic
Receiver type	MMSE
Satellite antenna	ITU-R Recommendation S.672, 50dBi gain
UE antenna	Omnidirectional, 0dBi gain
UE transmit power	250 mW
Channel estimation	Non-ideal
Feedback and control channel errors	None
HARQ/ARQ interaction	HARQ/ARQ interaction scheme for full buffer traffic.
MAC/RLC header overhead	Assume minimum size of specification
Layout	Hexagonal grid
Inter-site distance	180 km
Satellite system noise temperature	450 K
G/T	23.47 dB/K
Target packet error rate	1 %
Path loss	189.5 (LoS) + 2.5 (fading margin) dB

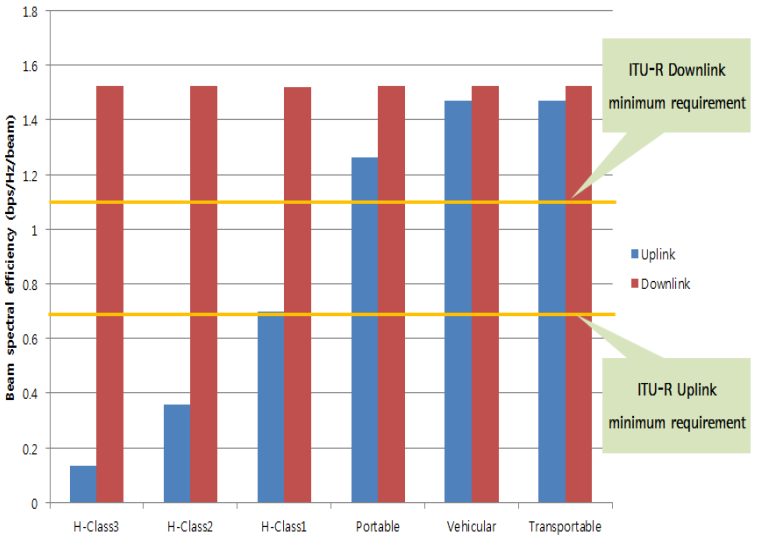

Fig. 6. Beam spectral efficiency (bps/Hz/beam)

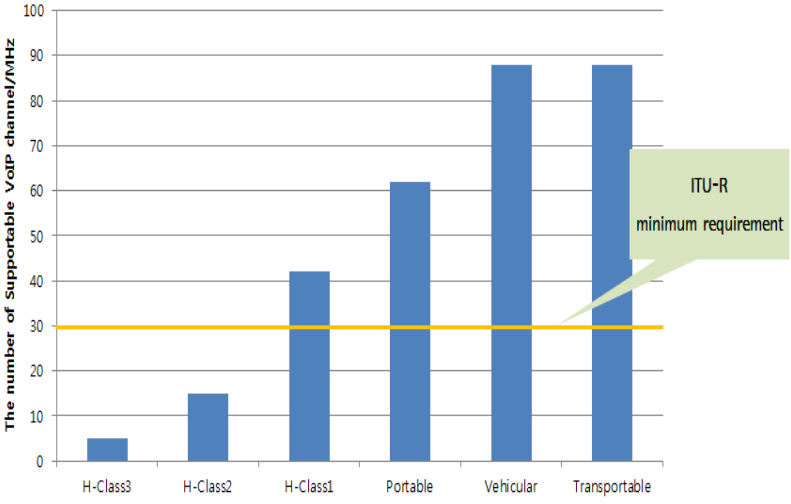

Fig. 7. Beam spectral efficiency (bps/Hz/beam)

Figure 6 and 7 show system level simulation results with respect to average beam spectral efficiency and VoIP capacity, respectively. As seen in the figures, the normal mode of the SAT-OFDM satisfies ITU-R minimum requirement for the satellite component of IMT-Advanced from the handheld class 3 UE to the transportable UE. Here, ITU-R minimum requirements are beam spectral efficiency of 1.1 in downlink and 0.7 bps/Hz/beam in uplink and the number of supported VoIP users of 30 active

users/beam/MHz. On the other hands, the handheld classes 1 and 2 UEs don't provide EIRP enough to satisfy ITU-R minimum requirement. However, those UEs with low transmit power also can make performance increased in the enhancing mode of the SAT-OFDM such as narrowband PUSCH transmission [7].

6 Conclusions

In this paper, we presented the SAT-OFDM as a satellite radio interface for IMT-Advanced. It has a great degree of commonality with the 3GPP LTE based terrestrial radio interface for IMT-Advanced. With the SAT-OFDM satellite radio interface, IMT equipments realizing 3GPP LTE radio interface with widen agility in the satellite IMT frequencies can operate over satellite environments with reasonable performance. This paper also highlighted candidate enhancing features of the radio interface to improve the satellite link performance at the expenditure of a restricted change to the UE chipset. Therefore, the SAT-OFDM satellite radio interface can decrease the cost impact on satellite-enabled terrestrial UEs as well as still make sure interoperability with 3GPP cellular networks. It is expected to accelerate the smoother convergence between mobile satellite systems and terrestrial mobile systems.

References

1. Hwang, S.Y., et al.: Design and implementation of a latency efficient encoder for LTE systems. ETRI Journal 32(4) (August 2010)
2. Shamsan, Z.A., et al.: Coexistence of OFDM-based IMT-Advanced and FM brodcasting systems. ETRI Journal 33(2) (April 2011)
3. ITU-R Recommendation M.1822, Framework for services supported by IMT (June 2010)
4. Kim, H.W., et al.: Applicability of OFDMA in satellite communication. In: IEEE VTC 2011 Spring Conference (May 2008)
5. Kota, S., et al.: "Satellite component of NGN" Integrated and hybrid networks. IJSCN 29(3), 191–208 (2011)
6. Kim, H.W., et al.: Narrowband uplink transmission in LTE based satellite radio interface. In: Accepted at SPACOMM 2012 Conference (2012)
7. ITU-R Report M.2176, Visions and requirements for the satellite component of IMT-Advanced (January 2011)

Physical Channel Access (PCA): Time and Frequency Access Methods Simulation in NS-2

Nicolas Kuhn[1,2], Olivier Mehani[1], Huyen-Chi Bui[2],
Jérôme Lacan[2], José Radzik[2], and Emmanuel Lochin[2]

[1] NICTA, Sydney, Australia
firstname.lastname@nicta.com.au
[2] University of Toulouse, ISAE, TeSA, France
firstname.lastname@isae.fr

Abstract. We present an NS-2 module, Physical Channel Access (PCA), to simulate different access methods on a link shared with Multi-Frequency Time Division Multiple Access (MF-TDMA). This technique is widely used in various network technologies, such as satellite communication. In this context, different access methods at the gateway induce different queuing delays and available capacities, which strongly impact transport layer performance. Depending on QoS requirements, design of new congestion and flow control mechanisms and/or access methods requires evaluation through simulations.

PCA module emulates the delays that packets will experience using the shared link, based on descriptive parameters of lower layers characteristics. Though PCA has been developed with DVB-RCS2 considerations in mind (for which we present a use case), other MF-TDMA-based applications can easily be simulated by adapting input parameters. Moreover, the presented implementation details highlight the main methods that might need modifications to implement more specific functionality or emulate other similar access methods (*e.g.*, OFDMA).

Keywords: simulation, physical channel access, time and frequency access methods.

1 Introduction

When the medium needs to be shared between multiple active users, the resource is fairly distributed with multiple access techniques, such as Multi-Frequency Time Division Multiple Access (MF-TDMA) or Orthogonal Frequency-Division Multiple Access (OFDMA). OFMDA is used in 4G/LTE and WiMAX/802.16 whilst MF-TDMA is used in Digital Video Broadcasting (DVB). Considering recent deployments of such multiple access networks, it is important to study the interactions of these access methods (PHY/MAC) with the rest of the network protocols (transport layer) in order to ensure optimal experience for the end user. This can be achieved through large simulations studies.

Several modules simulating OFDMA or MF-TDMA techniques for NS-2 [1] already exist. In the context of OFDMA, WiMAX has seen a lot of interest [2,3].

R. Dhaou et al. (Eds.): PSATS 2013, LNICST 123, pp. 174–185, 2013.

The current DVB-S2/RCS specifications have also been implemented with MF-TDMA characteristics [4,5]. These modules attempt to be as close as possible to the real systems and the layout of their components, which make them unsuitable to assess proposed changes to the DVB-S2/RCS architecture (*e.g.*, access methods strategies), nor to extend their work to other MF-TDMA networks. Moreover, this level of realism might not be necessary for the study of high layer behaviours. Indeed, Gurtov and Floyd claim that a better trade-off between generality, realism and accurate modeling can be found to improve transport protocol performance evaluation [6].

We therefore propose an NS-2 module, Physical Channel Access (PCA), which emulates packet delays at the access point based on specific access methods parameters. This module allows to integrate channel access considerations within NS-2 and assess their impact on upper layers performance. We follow the idea of [6] by emulating the characteristics of various physical channel access techniques rather than extending MAC/PHY simulation models. This therefore allows to conveniently study a wider range of scenarios than the modules presented in [4,5]:

- experimental channel access strategies for MF-TDMA based systems (*e.g.*, current drafts);
- generic time-frequency multiplexing architectures;
- adaptive access methods.

PCA is well suited for current needs in the extension of the DVB specifications: it is based on the currently standardized parameters but allows to depart from them for further investigations. For example, it allows to consider experimental access methods and capacity allocation processes which are under discussion to support transmission of home user data on the satellite return channel (RCS), so far reserved to signaling.

The rest of the paper is organized as follows. In Section 2, we present the general concepts behind MF-TDMA and notations relevant to the rest of this paper. We describe the implementation of PCA in Section 3. We document the internal parameters and present a use case in the context of DVB-RCS2 in Section 4. We conclude and discuss future work in Section 5.

2 MF-TDMA Networks

On an MF-TDMA link, the capacity is shared at the *Access Point*: it is dynamically distributed on times × frequency blocks (denoted "frame" in this article). The access point (the NS-2 node where the module we present in Section 3 is introduced) forwards traffic from one or more users to one or more receivers over the shared medium, therefore covering both up and down link scenarios.

Before presenting in details our NS-2 module, we provide some definitions of the terms used in this paper:

- Flow: data transfer at the transport layer;
- Datagram: network layer segment of a flow;
- Link Layer Data Unit (LLDU): N_{data} bytes of a fragmented datagram;

- Physical Layer Data Unit (PLDU): LLDU with an optional N_{repair} recovery bytes ($N = N_{\text{data}} + N_{\text{repair}}$);
- Block: PLDUs can be further split into N_{block} blocks if the access method requires;
- Slots: element of a frame where a block can be scheduled.

2.1 Access Methods

In the context of MF-TDMA networks, two classes of access methods can be introduced: dedicated and random access methods.

Dedicated access. When a new flow arrives at the access point, parts of the channel have to be reserved for it. This induces a delay resulting from the reservation negotiation process. The reservation ensures that capacity is fairly distributed: if there are 40 slots available and 10 users, each user can transmit data on 4 slots.

Random access. No reservation is needed and data can be transmitted without additional delay. However several users can unknowingly use the same slot and data risks not to be recovered. Stronger error codes are introduced at the physical layer and each user can transmit a reduced N_{data} useful bytes: N_{repair} redundancy bytes are added to the N_{data} bytes to form a code word of $N = N_{\text{data}} + N_{\text{repair}}$ bytes that are split into N_{block} blocks. N_{ra} slots form a *Random Access* block (RA block) on which erasure codes are introduced. Each transmitter randomly spreads its N_{block} blocks across the N_{ra} slots of the RA block for spectral diversity.

Performance of random access methods can be described by the probability that a receiver decodes its N_{data} useful bytes depending on the number of users that transmit data on the RA block. Table 1 shows a generic example of such a description where $P_{i,j}$ is the probability that a packet cannot be recovered by the receiver when there are $N_U \in [NbUser_j; NbUser_{j+1}]$ users on the RA block and and the signal-to-noise ratio of the channel is $Es/N0_i$.

Table 1. Random access method performance

0	$NbUser_1$	$NbUser_2$	$NbUser_3$	...	$NbUser_{26}$	0
$Es/N0_1$	$P_{1,1}$	$P_{1,2}$	$P_{1,3}$	...	$P_{1,26}$	0
$Es/N0_2$	$P_{2,1}$	$P_{2,2}$	$P_{2,3}$	...	$P_{2,26}$	0
...	...	...	...	...	...	...
$Es/N0_X$	$P_{X,1}$	$P_{X,2}$	$P_{X,3}$	...	$P_{X,26}$	0

2.2 Frame Structure

The capacity is dynamically distributed between the different users on the time $\times$ frequency frame which structure is detailed in Figure 1. At the access point, transmission of a frame is scheduled every T_F. We denote by N_S the number of

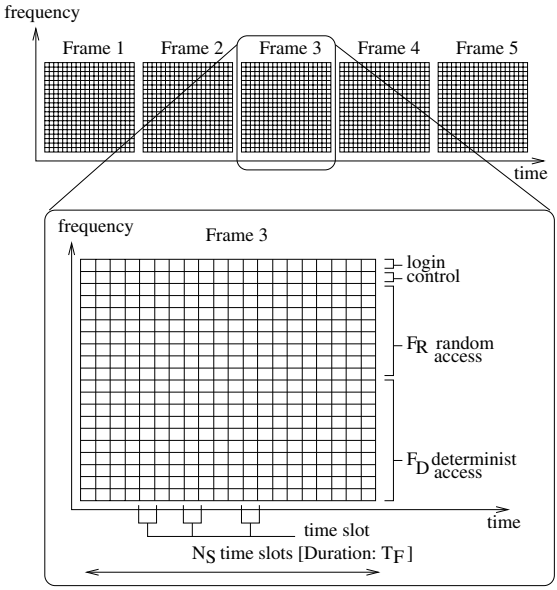

Fig. 1. Times × Frequency block description

time slots available per frequency. The frequencies on which data is transmitted can be divided depending on the access method: F_R frequencies are dedicated to the random access methods and F_D are reserved to the dedicated access methods. In total, a frame can carry $N_S \times (F_R + F_D)$ slots.

2.3 Antenna Limitations

It is possible that some transmitters cannot send data on different frequencies at once. This limitation has to be considered when determining the maximum number of slots that a user is allowed to occupy on each frame. This is highly linked to the frame structure, and in this case, a flow can only use N_S slots whatever the number of available frequencies.

As an example, if $N_S = 40$ slots and:

- $F_R = 0$ & $F_D > 1$ (dedicated access): a unique user can exploit $N_S = 40$ slots;
- $F_R = 1$ & $F_D = 0$ (random access), $N_{\text{block}} = 3$, $N_{\text{ra}} = 40$: a unique user can exploit $\lfloor N_S / N_{\text{block}} \rfloor = 13$ slots.

3 Implementation Details

In order to control delays, PCA is implemented as a queueing delay. We inherit from the `DropTail` queue management scheme, of which our PCA sub-class

redefines the methods used to process the packets. Each node uses the `enque()` and `deque()` methods to add and remove packets from the queue.

In Figure 2, we compare the `enque()` and `deque()` methods of `DropTail` and `DropTail/PCA`. With `DropTail`, when the `enque()` method adds packet P_{N+1}, it is added at the end of the sending buffer and transmitted when $P_1, \ldots, P_N$ have been transmitted with the `deque()` method. With `DropTail/PCA`, when a packet is `enque()`ed, it is also added to the sending buffer. However, depending on the access method introduced, only a subset of the datagram is considered sent with each frame. When the last byte of a datagram has been transmitted, `deque()`, which is called every T_F, removes the packets from the sending buffer and passes it along.

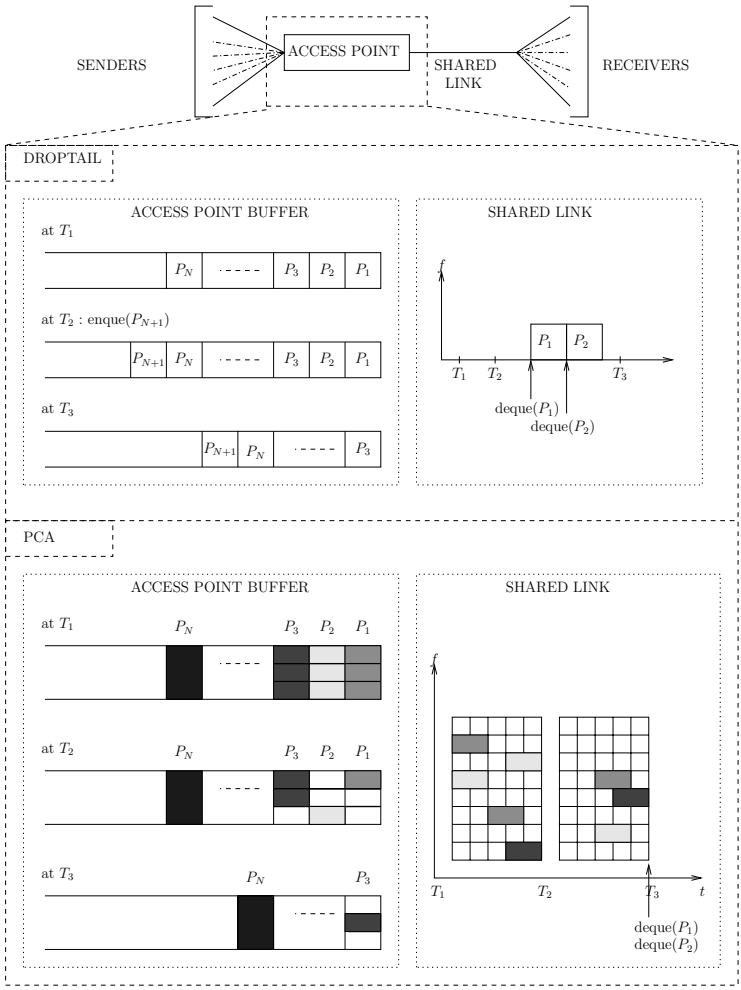

Fig. 2. Capacity allocation: `enque()` and `deque()`

The `DropTail/PCA` queuing policy is implemented in two files (`pca.cc` and `pca.h`) located in the `queue/` sub-directory of the NS-2 source. We detail the content of these files here.

3.1 Data Structures

Our module implements linked-lists in order to store information about the current flows and their packets.

Packets list The packet list contains information about the different packets that have reached the access point node but have not been fully transmitted yet. Each packet is defined by:

- `appl_id`: identifier of the flow;
- `pkt_seqno`: sequence number in the flow;
- `frame_in`: emulated frame number after which the data of the packet start to be transmitted;
- `frame_out`: frame number at which the last bit of the packet must be transmitted;
- `bool_first_frame`: boolean to specify if the connection needs to be established (first packet of the current application);
- `bool_lost`: boolean specifying whether the packet is lost;
- `bool_rand`: boolean specified if the access method is random (`bool_rand`=1) or dedicated (`bool_rand`=0);
- `bits_to_send`: actual number of bits of the datagram that have not been sent yet;
- `bits_next_frame`: number of bits that will be sent at the next frame;
- `remaining_slot_frame_appl_det`: number of dedicated slots that remain for this packet's flow;
- `remaining_slot_frame_appl_rnd`: number of random slots that remains for the flow of the packet;
- `used_slot_frame_appl_rnd`: number of slots that the packet's flow will use in the next frame.

Applications list. This linked list is used to collect information relative to the currently active applications. It tracks all the open connections and maintains information about the last transmitted datagrams.

- `appl_id`: identifier of the application;
- `pkt_seq`: sequence number of the last packet transmitted;
- `last_time_out`: time when the last packet of the given application has been sent.

3.2 `enque(Packet *p)` Method

The `enque()` method is called when the network layer passes a packet down to PCA. It registers the packet and its attributes for consideration in the capacity distribution process. Figure 3 summarises the operation of this function.

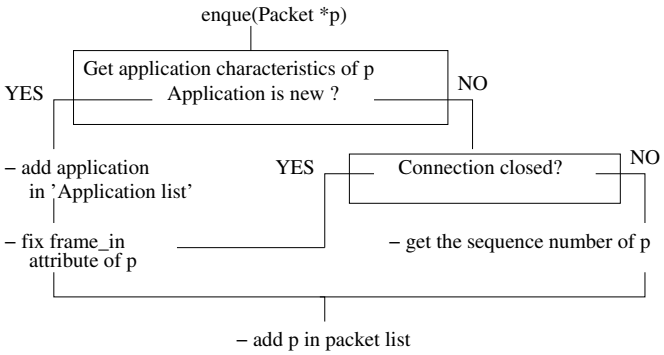

Fig. 3. `enque()` method flowchart

Before enqueuing a packet, it verifies whether the connection needs to be established and the application added in the applications list. If the application is not new, it checks whether the connection is still open. It then adds the packet with its characteristics to the packets list. If `pkt_seqno`=0, it sets the `frame_in` attribute of the packet (first frame where data from this packet starts being transmitted) depending on the access method. `frame_out` is initially set to ∞, and later updated by the `adaptBitNextFrame()` method described in the next section.

3.3 `deque()` Method

The `deque()` method emulates arrival of a new frame at the receiver. It is called by a timer every T_F. It loops over the packet list, forwards the packet for which `frame_out` is the current frame to the receiving node and updates the transmission progress of the other datagrams by adjusting their attributes. Figure 4 details how the number of bits to transmit on the next frame is calculated in the `adaptBitNextFrame()` function. This process has been introduced to take care of:

- fair distribution of the capacity with dedicated access methods;
- determination of erasure probability with random access methods (depending on the load of the link and methods performance as detailed in Table 1);
- adaptation of the packet transmission to ensure that flows send their packets in the order they have been received.

To do so, `adaptBitNextFrame()` updates the values of `bits_next_frame`, `used_slot_frame_appl_rnd` and `frame_out` as follows. At frame F, for each packet where `frame_in`$< F$, we compute $B_{\text{remaining}}$=`bits_to_send-bits_next_frame`, which corresponds to the data which remains to be transmitted. If $B_{\text{remaining}} > 0$, the packet is left in the queue; `bits_next_frame`, which corresponds to the data that will be transmitted at frame $F+1$, is determined depending on the access method (as well as the number of slots which it

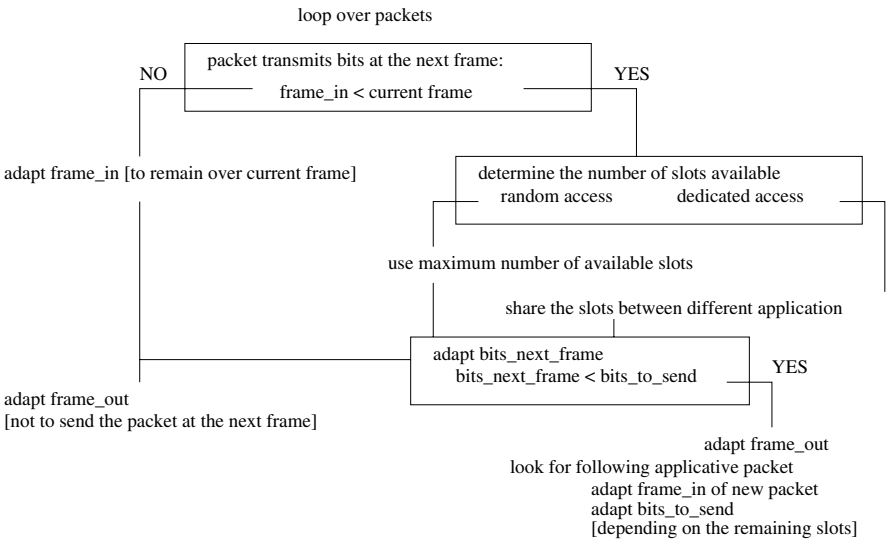

Fig. 4. `adaptBitNextFrame()` method flowchart

will use, `used_slot_frame_appl_rnd`) and `bits_to_send` is set to $B_{\text{remaining}}$. If $B_{\text{remaining}} \leq 0$, `frame_out` is set to $F + 1$; the next packet for that application is then found in the packet list, its `frame_in` is set to F and $B_{\text{remaining}}$ is subtracted from its `bits_to_send`.

3.4 Limitations and Extensions

PCA can be used to conduct large studies on (MF-)TDMA schemes, however it has some limitations. First, the performance of random access methods depends on the signal-to-noise ratio of the specific link between one receiver and the access point. It is currently assumed that this value is the same for all receivers, but this can be easily lifted by adapting the receiver-to-SNR mapping code. Second, PCA does not consider prioritization between flows. Nonetheless, this could be achieved by flagging packets at higher layers and inspecting these flags in `deque()` and `adaptBitNextFrame()` functions.

The development of this module has been driven by (MF-)TDMA specifications. However, it can easily be extended for other similar access methods (time and/or frequency multiplexing) by adapting the `adaptBitNextFrame()` method to reflect the specific data scheduling scheme of the desired technique. Also, in the current implementation, it was considered that one flow could only send a limited amount of data per RA block. This quantity can be adjusted in the simulation parameters (through `sizeSlotRandom_` and `nbSlotRndFreqGroup_`).

4 Use Case Example

In this section, we detail the principal parameters of the `DropTail/PCA` queuing policy and illustrate them with an example in the context of DVB-RCS2.

4.1 Parameters

The parameters are set following the standard NS-2 fashion:

```
Queue/DropTail/PCA set <PARAMETER> <VALUE>
```

The following parameters have to be specified prior to starting a simulation:

- `cutConnect_`: time after which the connection between the gateway and the user is closed (in seconds);
- `esNO_`: signal-to-noise ratio of the channel in dB (for random access methods performance);
- `switchAleaDet_`: sequence number at which the access method switches from random to dedicated;
- `frameDuration_` (T_F): duration of a frame;
- `nbSlotPerFreq_` (N_S): number of time slots per frequency;
- `sizeSlotRandom_` (N_{data}): useful number of bits that can be sent on one RA block (*i.e.*, where random access methods are introduced);
- `sizeSlotDeter_` (N_{data}): useful number of bits for each time slots where dedicated access methods are introduced;
- `rtt_`: two-way link delay (in seconds);
- `freqRandom_` (F_R): number of frequencies used for random access;
- `nbFreqPerRand_` ($(F_R \times N_S)/N_{\text{ra}}$): number of frequencies comprised in an RA block;
- `freqDeter_` (F_D): number of frequencies used for dedicated access;
- `maxThroughtput_`: maximum authorized throughput for one given flow (in Mbps);
- `nbSlotRndFreqGroup_` (N_{block}): number of blocks a PLDU is split into for distribution in one RA block;
- `boolAntennaLimit_`: boolean whether one transmitter has one or $F_R + F_D$ antennas.

In order to introduce PCA, the link between two nodes N1 and N2 (N1 is the access point node) can then be defined as:

```
$ns simplex-link $N1 $N2 $bandwidth [$rtt_ / 2]  \
    DropTail/PCA $random_access_file_performance
```

where `$random_access_file_performance` is the name of the file containing information about random access performance laid out as in Table 1.

4.2 Use Case in the Context of DVB-RCS2

We illustrate the results obtained with this PCA module in the context of DVB-RCS2. DVB-RCS2 is the return link on which the home user transmits data to the satellite gateway: the satellite link is shared between the different users. There is a recent interest in enabling the home user to transmit data (*e.g.* for web browsing or email exchange) through this channel. However, there is contention about which access method is best suited for this use. PCA allows to provide insight on this question by evaluating transport layer performance with various access method proposals.

We consider three different cases: (1) a dedicated access method and random access methods ((2) CRDSA [7] and (3) MuSCA [8]). We use input for each random access method that follows the format illustrated in Section 2. We base the choice of parameters on specifications defined in [9] and present them in Table 2.

Table 2. Use case simulation parameters

Parameters	Access method		
	Dedicated	Random (CRDSA)	Random (MUSCA)
`cutConnect_`	3	3	3
`esNO_`	5	5	5
`switchAleaDet_`	0	∞	∞
`frameDuration_`	0.045	0.045	0.045
`nbSlotPerFreq_`	40	40	40
`sizeSlotRandom_`	xx	613	680
`sizeSlotDeter_`	920	xx	xx
`rtt_`	0.5	0.5	0.5
`freqRandom_`	0	100	100
`nbFreqPerRand_`	2.5	2.5	2.5
`freqDeter_`	100	0	0
`maxThroughtput_`	1 Mbps	1 Mbps	1 Mbps
`nbSlotRndFreqGroup_`	xx	3	3
`boolAntennaLimit_`	1	1	1

We consider two nodes in NS-2. The first node transmits a various number of FTP flows to the second node. This allows to study the transport layer performance (no data-starved sender). The size of IP packets is 1500 bytes, and the queue at the sender is large enough not to be overflowed. We use the Linux implementation of TCP Reno, with SACK options. The simulation time is 20 seconds.

In Figure 5, we show the total achievable throughput measured on the shared link level. This shows that dedicated access methods support more load on the network whereas random access methods, which PCA allows us to study, experience lower throughput with increasing loads.

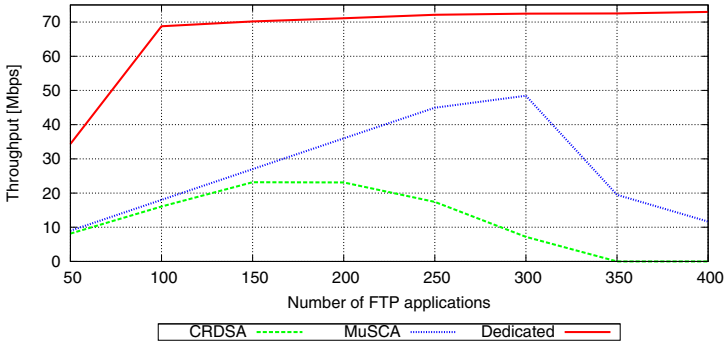

Fig. 5. Throughput depending on the load of the network

Figure 6 illustrates the evolution of the packet sequence numbers of one given FTP application during the first seconds of the simulation. We only show the results with MuSCA as the random access method; the performance with CRDSA is qualitatively similar. Contrary to the previous metrics, random access methods seem to perform better. Indeed, thanks to a faster connection establishment, random access methods transmit the first packets faster than dedicated access methods. However, with dedicated access, the time needed to effectively transmit one packet is smaller: as detailed in Table 2, more bits can be sent on one slot (*i.e.*, `sizeSlotDeter_>sizeSlotRandom_`).

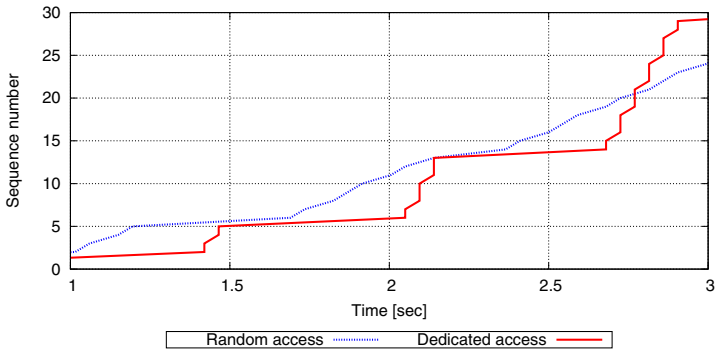

Fig. 6. Sequence number evolution

These preliminary simulations present a first evaluations of the impact of access methods on TCP performance in the context of DVB-RCS2. We expect to explore and analyze this use case further.

5 Conclusion and Future Work

In this article, we presented PCA, a module for NS-2 that enables to emulate channel access methods for the evaluation of the interaction with transport protocol mechanisms. This module considers time and/or frequency multiplexing access methods and can be used in contexts where the capacity of the channel is shared among multiple users. We detailed the main components and their operation as well as the parameters required to configure the module.

PCA is useful to assess the impact of medium access strategies on transport performance, especially for satellite links. It was initially developed with MF-TDMA specifications in mind, however we also indicated where extensions should be made to accommodate other similar technologies (*e.g.*, OFDMA).

We are currently using this module to investigate random access performance in the context of DVB-RCS2. Also, we plan to release the module as open source soon on ISAE webpage.

Acknowledgments. This work presented in this article documents part of the simulation scenarios and results obtained in a study funded by CNES in which TéSA and Thales Alenia Space took part.

References

1. Fall, K., Varadhan, K.: The ns Manual (formerly ns Notes and Documentation). VINT Project (2009)
2. The Network Simulator NS-2 — NIST add-on — IEEE 802.16 model (MAC/PHY). Technical Report. NIST (2009)
3. Wu, P., Tsai, T., Kao, Y., Hwang, J., Lee, C.: An NS2 Simulation Module for Multicast and OFDMA of IEEE 802.16e Mobile WiMAX, `http://edith.cse.nsysu.edu.tw/wimax/wimax.htm`
4. Gayraud, T., Bertaux, L., Berthou, P.: A NS-2 Simulation model of DVB-S2/RCS Satellite network. In: 15th Ka Band Conference (2009)
5. Secchi, R.: DVB-RCS(2) for ns-2, `http://homepages.abdn.ac.uk/r.secchi/pages/dvbrcs_ns2.htm` (last accessed November 12, 2012)
6. Gurtov, A., Floyd, S.: Modeling Wireless Links for Transport Protocols. ACM Computer Communication Review (CCR) 34(2), 85–96 (2004)
7. Casini, E., De Gaudenzi, R., del Rio Herrero, O.: Contention Resolution Diversity Slotted ALOHA (CRDSA): An Enhanced Random Access Schemefor Satellite Access Packet Networks. IEEE Transactions on Wireless Communications (2007)
8. Bui, H.-C., Lacan, J., Boucheret, M.-L.: An Enhanced Multiple Random Access Scheme for Satellite Communications. In: Wireless Telecommunications Symposium (WTS 2012) (2012)
9. Digital Video Broadcasting (DVB); Second Generation DVB Interactive Satellite System; Part 2: Lower Layers for Satellite standard. Draft ETSI EN 101 545-2 V1.1.1 (2011)

Spatial Filtering for Underlay Cognitive SatComs

Shree Krishna Sharma, Symeon Chatzinotas, and Björn Ottersten

SnT - securityandtrust.lu, University of Luxembourg, L-2721, Luxembourg
{shree.sharma,symeon.chatzinotas,bjorn.ottersten}@uni.lu

Abstract. Herein, we study an underlay beamforming technique for the coexistence scenario of satellite and terrestrial networks with the satellite return link as primary and the terrestrial uplink as secondary. Since satellite terminals are unique in that they always point towards the geostationary satellite, interference received by the terrestrial Base Station (BS) is concentrated in a specific angular sector. The priori knowledge that all the geostationary satellite terminals are facing south for the European coverage can be used in designing a beamformer at the terrestrial BS. Based on this concept, we propose a receive beamformer at the BS to maximize the Signal to Interference plus Noise Ratio (SINR) towards the desired user and to mitigate the interference coming from the interfering satellite terminals. The performances of Minimum Variance Distortionless (MVDR) and Linear Constrained Minimum Variance (LCMV) beamformers are compared for our considered scenario. It is shown that LCMV beamformer is better suited in rejecting interference even in case of Direction of Arrival (DoA) uncertainty of interfering satellite terminals as long as DoA range of the interfering sector is known to the beamformer. Furthermore, it is noted that MVDR beamformer is suitable for a large number of interferers.

Keywords: Spatial Filtering, Underlay, Satellite-terrestrial Coexistence, Interference Mitigation.

1 Introduction

Recently, cognitive communication has been considered a promising technology for allowing the coexistence of different wireless networks within the same spectrum. Wireless networks may exist within the same spectrum in different ways such as two terrestrial networks or two satellite networks or satellite-terrestrial networks. The most common cognitive techniques in the literature can be categorized into interweave or Spectrum Sensing (SS), underlay, overlay and database related techniques [1]. In SS only techniques, Secondary Users (SUs) are allowed to transmit whenever Primary Users (PUs) do not use a specific band, whereas in underlay techniques, SUs are allowed to transmit as long as they meet the interference constraint of the PUs.

Existing spectrum sharing techniques mostly consider three signal dimensions i.e., frequency, time and area for sharing the available spectrum between primary

R. Dhaou et al. (Eds.): PSATS 2013, LNICST 123, pp. 186–198, 2013.

and secondary systems. However, due to advancement in smart antennas and beamforming techniques, multiple users can be multiplexed into the same channel at the same time and in the same geographical area [2]. In cognitive scenarios, the knowledge of propagation characteristics of the PUs can be used to mitigate interference from Cognitive Radio (CR) transmitter towards the PUs and to mitigate interference from the PUs towards the CR receiver. In this context, angular dimension or directional dimension of spectral space can be considered as more efficient way of exploiting the underutilized primary spectrum for the SUs. To exploit the angular dimension, multi-antenna transceivers are needed. Recently, the spatial dimension for spectrum sharing purpose has received important attention in the literature [2, 3, 4, 5]. In [3], the angular dimension of spectral space is used to detect the presence of a PU and to estimate the Direction of Arrival (DoA) of the PU signal. In [4], propagation characteristics of the rays arriving in clusters is exploited for SS purpose. In [5], a directional SS using a single radio switched beam antenna structure is proposed to enhance the sensing efficiency of a CR.

Beamforming is a signal processing technique used in antenna arrays with the advantages of spatial discrimination and spatial filtering capabilities [6]. Multi-antenna beamforming is an effective means to mitigate co-channel interference and has been widely used in traditional fixed spectrum based wireless systems. In the context of a CR, beamforming techniques have been investigated for the secondary network for various objectives such as controlling interference [7], capacity maximization [8], SINR balancing [9]. The beamforming design problem in the context of an underlay CR is challenging since the underlay technique requires the interference caused by the SUs to be below the interference threshold level required by the PUs. According to author's knowledge, beamforming techniques have been considered for various objectives mostly in the coexistence scenario of two terrestrial networks in the existing CR literature. In the context of cognitive satellite communications, SS techniques for dual polarized channels have been proposed in [10, 11]. In [12], interference alignment technique has been proposed for spectral coexistence of monobeam and multibeam satellite systems. In [13], different transmit beamforming techniques have been proposed for spectral coexistence of satellite and terrestrial networks. In this paper, we apply beamforming technique for spatial filtering in the spectral coexistence scenario of satellite and terrestrial networks with the satellite return link as primary and the terrestrial uplink as secondary. The main difference is that although interference is concentrated in an angular sector, we do not specifically know the number of interferers and the DoA of their signals.

Geostationary (GEO) satellites are located in the geosynchronous orbit above the equator and therefore transmit in a northerly direction if we consider the European continent. The GEO satellite terminals have therefore the special propagation characteristic to always point towards the GEO satellites (south). While considering the coexistence of a satellite network with the terrestrial cellular network, the interference received by the terrestrial Base Station (BS) is concentrated in a specific angular sector. Furthermore, this interference becomes more

prominent as we move towards the polar region from the equator due to reduction in the elevation angles of the satellite terminals [1]. Similar scenario was considered in [14] while reusing the satellite broadcast spectrum for terrestrially broadcast signals in the United States and the use of different directional antennas at the user location was proposed to allow the spectrum reuse. In this paper, we propose a receive beamforming technique at the BS to maximize the SINR towards the desired terrestrial user and to mitigate the interference coming from interfering satellite terminals. The prior knowledge that all the ground satellite terminals are pointing south is the cognition that we exploit in this study. Since this is an inherent characteristic of SatComs, no interaction is needed between primary and secondary systems. In this context, we apply widely used Linear Constrained Minimum Variance (LCMV) and Minimum Variance Distortionless (MVDR) beamformers for our scenario and analyze their performances in terms of pattern response and output SINR. Furthermore, we consider link budget analysis of satellite and terrestrial link considering the path loss between satellite terminals and the BS and between terrestrial terminals and the BS.

The paper is structured as follows: Section 2 presents the considered system and signal models. Section 3 provides the theoretical analysis of LCMV and MVDR techniques in the context of our proposed scenario. The proposed spatial filtering technique is presented in Section 4. Section 5 describes the simulation environment and evaluates the performance of the beamformers with the help of numerical results. Section 6 resumes the conclusions.

2 System and Signal Model

2.1 System Model

We consider a practical coexistence scenario of satellite and terrestrial networks with both networks operating in normal return mode as shown in Fig. 1. The satellite link is considered as primary and the terrestrial link as secondary i.e., satellite terminals are PUs and terrestrial terminals are SUs. In this context, we consider a Fixed Satellite System (FSS) with fixed ground terminals (i.e., dishes) operating in the C-band. Furthermore, a terrestrial WiMax network is considered providing broadband services to the fixed users within the same spectrum. The interference from terrestrial terminals to the satellite is assumed to be negligible due to large distance as well as low elevation angles of the terrestrial terminals while the interference from satellite terminals to the terrestrial BS should be taken into account [1]. Due to unique propagation characteristic of GEO satellite terminals, the interference received by the BS is concentrated in a specific angular sector and the BS receives interference due to geostationary satellite terminals from its northern sector. In this scenario, we consider the satellite coverage over Europe (not the regions which are near to the equator). In this context, we apply a receive beamforming technique at the BS to maximize SINR towards the desired user, which is located in the south and to mitigate the interference coming from the northern sector as illustrated in the layout (Fig. 2). Furthermore, the

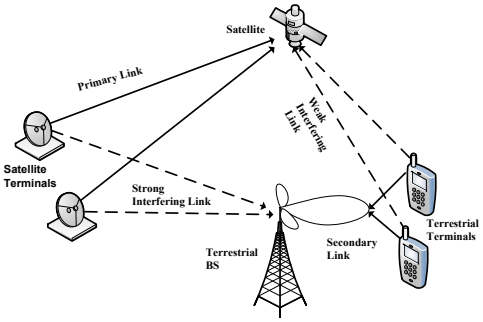

Fig. 1. Satellite-terrestrial coexistence scenario

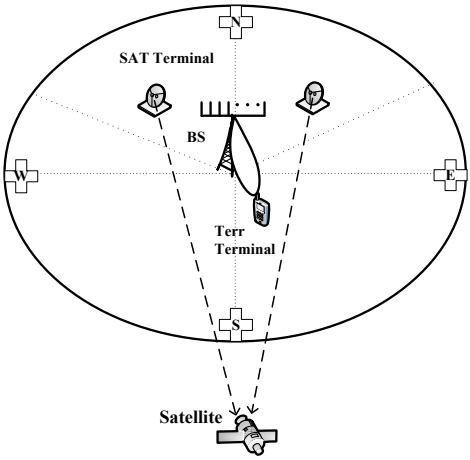

Fig. 2. Layout of the considered scenario (N,W,S and E denote North, West, South and East)

exact locations and the number of the interfering satellite terminals are unknown to the beamformer in our considered scenario.

2.2 Signal Model

Let M be the number of antennas in the BS antenna array and K be the number of total users in the considered system including both the PUs and SUs. In the uplink, each user can be viewed as a transmit antenna in a point to point Multiple Input Multiple Output (MIMO) system and the same receiver architecture can be used at the BS to separate each user's data by applying a receive beamforming technique. The received signal vector $\mathbf{y}$ at the BS can be written as:

$$\mathbf{y} = \sum_{k=1}^{K} h_k \mathbf{a}(\theta_k) s_k + \mathbf{z}, \tag{1}$$

where h_k represents the channel gain for k-th user and it is assumed that it remains constant for all antennas in the array assuming that there is strong line of sight between the array antenna and user antennas, s_k is the transmitted symbol by k-th user, $\mathbf{a}(\theta_k)$ is the $M \times 1$ array response vector, θ_k being the angle of arrival for k-th user, $\mathbf{z}$ is $M \times 1$ independent and identically distributed (i.i.d.) Gaussian noise vector. The array response vector $\mathbf{a}(\theta_k)$ can be written as [15]:

$$\mathbf{a}(\theta_k) = \left[1, e^{\frac{-j2\pi d sin(\theta_k)}{\lambda}}, ..., e^{\frac{-j2\pi(M-1)dsin(\theta_k)}{\lambda}}\right]^T, \tag{2}$$

where d is the inter-element spacing of the antennas at the BS array, λ represents the wavelength of radio frequency signal. The receiver at the BS can separate signals transmitted from different users because of their different spatial signatures on the received antenna array. Consider that there is only one desired user [1] i.e., single SU and $(K-1)$ interfering users i.e., PUs. Then (1) can be expressed as:

$$\mathbf{y} = h_1\mathbf{a}(\theta_1)s_1 + \mathbf{q}, \tag{3}$$

where h_1 is the channel towards the desired user, $\mathbf{a}(\theta_1)$ is the array response vector for the desired user, s_1 is desired user's transmitted symbol and $\mathbf{q} = \sum_{k=2}^{K} h_k\mathbf{a}(\theta_k)s_k + \mathbf{z}$. For the purpose of receive beamforming, the received signal vector $\mathbf{y}$ is then linearly combined through a complex weight vector $\mathbf{w} \in \mathcal{C}^N$ to yield the array output $\hat{s}_1$ as:

$$\hat{s}_1 = \mathbf{w}^H\mathbf{y}. \tag{4}$$

The weight vector $\mathbf{w}$ should be chosen in such a way that the first term of (3) is maximized and the second term is minimized.

3 Beamforming Techniques

Several array signal processing techniques have been presented in the literature [16, 17, 7]. Beamformers can be classified into data independent or statistically optimum depending on how the combining weights are chosen [6]. The later technique can be divided into different categories such as Multiple Side-lobe Canceler (MSC), MVDR and LCMV beamformers. In this section, we review the most widely used MVDR and LCMV beamformers from the literature for their use in our scenario [17].

3.1 MVDR Technique

The received signal at the BS antenna array from (1) can also be written as:

$$\mathbf{y} = \mathbf{A}\mathbf{s} + \mathbf{z}, \tag{5}$$

where $\mathbf{A} = [\mathbf{a}(\theta_1), \mathbf{a}(\theta_2), ..., \mathbf{a}(\theta_K)]$ is called the Signal Direction Matrix (SDM), $\mathbf{s} = [s_1, s_2, ..., s_K]^T$, each s_k being the symbol associated with the k-th user.

[1] Multiple desired users can be supported by using some form of scheduling techniques.

The beamformer response to the desired user at an angle θ_d can be denoted by $\mathbf{w}^H\mathbf{a}(\theta_d)$. Let us consider that noise over each element of the array is white with variance σ^2. Then the SINR for user k can be written as:

$$SINR_k = \frac{\gamma|\mathbf{w}^H\mathbf{a}(\theta_d)|^2}{\mathbf{w}^H(\sum_{i=1,i\neq k}^{K}\mathbf{R}_i + \sigma^2)\mathbf{w}} = \frac{\gamma|\mathbf{w}^H\mathbf{a}(\theta_d)|^2}{\mathbf{w}^H\mathbf{R}_{i+n}\mathbf{w}}, \tag{6}$$

where γ is the SNR of the desired incoming signal, $\mathbf{R}_{i+n}$ is the covariance matrix of interference plus noise. The optimization problem for MVDR beamformer can be written as:

$$\begin{aligned} &\min_{\mathbf{w}} \mathbf{w}^H\mathbf{R}_{i+n}\mathbf{w} \\ &\text{subject to } \mathbf{w}^H\mathbf{a}(\theta_d) = 1. \end{aligned} \tag{7}$$

Since in practical scenarios, $\mathbf{R}_{i+n}$ is unavailable and only sample covariance matrix $\mathbf{R}_y$ is available, which can be expressed as:

$$\mathbf{R}_y = \frac{1}{N}\sum_{i=1}^{N}\mathbf{y}(n)\mathbf{y}^H(n). \tag{8}$$

Using $\mathbf{R}_y$ instead of $\mathbf{R}_{i+n}$, the optimization problem for MVDR beamformer can be written as:

$$\begin{aligned} &\min_{\mathbf{w}} \mathbf{w}^H\mathbf{R}_y\mathbf{w} \\ &\text{subject to } \mathbf{w}^H\mathbf{a}(\theta_d) = 1. \end{aligned} \tag{9}$$

When the desired signal is uncorrelated to the interference, minimization problem in (9) is same as the minimization problem in (7) [18]. The solution of constrained optimization problem (9) using Lagrange multipliers is obtained as:

$$\mathbf{w} = \frac{\mathbf{R}_y^{-1}\mathbf{a}(\theta_d)}{\mathbf{a}^H(\theta_d)\mathbf{R}_y^{-1}\mathbf{a}(\theta_d)}. \tag{10}$$

3.2 LCMV Technique

In this beamformer, the weights are chosen to minimize the output variance or power subject to the response constraints. To allow any desired signal coming from an angle θ with response g, the weight vector can be linearly constrained in such a way that $\mathbf{w}^H\mathbf{a}(\theta) = g$, where g is a complex constant [6]. Similarly, the contributions of signals coming from the interfering sector to the array output can be minimized by choosing the weights in such a way that the output power or variance $\mathbb{E}[|\mathbf{w}^H\mathbf{y}|^2] = \mathbf{w}^H\mathbf{R}_y\mathbf{w}$ is minimized. The LCMV problem for choosing the weights can be written as:

$$\begin{aligned} &\min_{\mathbf{w}} \mathbf{w}^H\mathbf{R}_y\mathbf{w} \\ &\text{subject to } \mathbf{w}^H\mathbf{a}(\theta) = g, \end{aligned} \tag{11}$$

where $\mathbf{w}^H\mathbf{a}(\theta) = g$ is a single linear constraint. Using Lagrange multiplier as in the above subsection, (11) can be solved to yield the following [6]:

$$\mathbf{w} = g\frac{\mathbf{R}_y^{-1}\mathbf{a}(\theta)}{\mathbf{a}^H(\theta)\mathbf{R}_y^{-1}\mathbf{a}(\theta)}. \tag{12}$$

To include the multiple constraints in the above single constraint problem, the following constraint equation can be written:

$$\mathbf{C}^H\mathbf{w} = \mathbf{f}, \tag{13}$$

where $\mathbf{C}$ is a $M \times L$ constraint matrix and $\mathbf{f}$ is $L \times 1$ response vector, $L = K$ is the number of constraints. We consider the following constraint equation in our scenario:

$$\begin{bmatrix} \mathbf{a}^H(\theta_1) \\ \mathbf{a}^H(\theta_2) \\ \vdots \\ \mathbf{a}^H(\theta_K) \end{bmatrix}^H \mathbf{w} = \begin{bmatrix} 1 \\ 0 \\ \vdots \\ 0 \end{bmatrix}. \tag{14}$$

Then the LCMV beamforming problem can be written as:

$$\begin{aligned} &\min_{\mathbf{w}} \mathbf{w}^H\mathbf{R}_y\mathbf{w} \\ &\text{subject to } \mathbf{C}^H\mathbf{w} = \mathbf{f}. \end{aligned} \tag{15}$$

The solution of above problem can be written as [17]:

$$\mathbf{w} = \mathbf{R}_y^{-1}\mathbf{C}(\mathbf{C}^H\mathbf{R}_y^{-1}\mathbf{C})^{-1}\mathbf{f}. \tag{16}$$

4 Proposed Spatial Filtering Technique

We assume that BS antenna array is oriented horizontally i.e., East-West direction as shown in Fig. 2. We consider a desired user to be located at angle θ_d at the south of the BS. Due to special propagation characteristic of satellite terminal antennas looking towards the GEO satellite (south), the angular sector in which interfering satellite terminals are located is known to the beamformer beforehand. Then we design a receive beamformer at the BS to mitigate the interference coming from the interfering sector i.e., from northern sector of the BS and to maximize the SINR towards the desired user. Following assumptions are made during the analysis:

- The DoA of the desired user is known. [2]
- The incident wave arrives at the array in the horizontal plane $\phi = \pi/2$ so that azimuthal direction completely determines the DoA.
- The distance between the BS and the user is large enough to be user at the far field region so that spherical waves approximate the plane waves.

[2] In practice, the DoA of the desired user can be estimated by using some DoA estimation algorithms such as MUSIC algorithm.

Furthermore, we consider that only the angular sector in which interfering terminals are located is known to the BS while the number of interfering terminals and their exact locations are unknown. Let us define DoA range for the interfering signals from the satellite terminals to lie in the range $[\theta_{min}\ \theta_{max}]$. The values of θ_{max} and θ_{min} at a particular geographical location can be calculated by geometric analysis of a GEO satellite link [1]. To design a beamformer, we uniformly sample this range in the interval of $\theta_i = \Delta/(K-1)$, where $\Delta = \theta_{max} - \theta_{min}$.

We consider the arrival angle along the array axis as 0° and the arrival angle along broadside direction as 90°. The position of satellite terminals are generated randomly with uniform distribution in the angular sector from 0° to 180°. Based on the received signal at the BS, we calculate the received signal's covariance matrix and based on this, weights for MVDR and LCMV beamformer are calculated using (10) and (16) respectively. These weights are then used for calculating SINRs in the considered scenario. If the received SINR at the BS is above the target SINR, the desired user can be served by that particular BS. If the received SINR is less than the target SINR, the desired user can not be served by that particular BS and some other nearby BS should be involved to serve that user [3]. The performance of a beamformer can be specified in the form of its response pattern and the output SINR. The response pattern specifies the response of the beamformer to an incoming signal as a function of DoA and frequency. The response pattern in θ direction can be calculated as:

$$\mathrm{G}(dB) = 20\log_{10}(|\mathbf{w}^H\mathbf{a}(\theta)|). \tag{17}$$

In the considered scenario, the actual array response vector for the interfering users differ from the array response vector used in the design of the beamformers since the user positions have been generated randomly. Therefore, there occurs uncertainty in the interference response vectors. In this context, firstly, we calculate the beamformer weights considering one interferer in each quantized angle and based on the assumption that the array response vectors for the desired user and interfering users are exactly known. Then we apply these weights to the considered scenario to evaluate the performance of these LCMV and MVDR beamformers. For a particular beamformer, we calculate the average SINR by considering several Monte-Carlo simulations as:

$$\overline{SINR} = \frac{1}{N_s}\sum_{n=1}^{N_s}\frac{\gamma|\mathbf{w}^H\mathbf{a}(\theta_d)|^2}{\mathbf{w}^H\mathbf{R}_{i+n}\mathbf{w}}, \tag{18}$$

where N_s is the number of Monte-Carlo simulations. Using Friss transmission formula, the received power (P_r) at the BS from the satellite/terrestrial terminal located at a distance r is calculated as:

$$P_r = \frac{P_t G_t G_r}{(4\pi r/\lambda)^2} = P_t G_t G_r L_p^{-1}, \tag{19}$$

[3] This would be the responsibility of the scheduling algorithm.

where G_t and G_r are gains of transmit and receive antennas respectively, P_t is the transmitted power and the term $L_p = (4\pi r/\lambda)^2$ represents the free space path loss. Let us define the β_k be the path loss coefficient of the link between k-th user and the terrestrial BS. Then we modify the SDM in the following form to take into account of the path loss and we assume the path loss to be same for all the antennas in the array.

$$\mathbf{A}^T = \boldsymbol{\beta} \odot \begin{bmatrix} \mathbf{a}(\theta_1) \\ \mathbf{a}(\theta_2) \\ \vdots \\ \mathbf{a}(\theta_K) \end{bmatrix}, \tag{20}$$

where $\boldsymbol{\beta} = [\,\beta_1\ \beta_2 \cdots \beta_K\,]^T$.

5 Numerical Results

1) Simulation Environment: Let us consider that all the satellite terminals are seen at azimuth angle range of 10° to 85° from the BS. We consider a single desired user at an angle of −30° and a Uniform Linear Array (ULA) at the BS with the layout shown in Fig. 1. The simulation and link budget parameters for both the links (i.e., link between SAT terminal and the BS and the link between terrestrial terminal and the BS) are provided in Table 1. To design a LCMV beamformer, we need DoAs of the interfering users. For this purpose, we quantize the considered interfering sector in the interval of 5° and consider one terminal in each quantized angle. It can be noted that the pattern generated in 0° to 90° quarter is repeated in another quarter 90° to 180° due to symmetric nature of ULA pattern. Therefore, the response pattern generated within the region 10° to 85° is repeated over the region 170° to 95°.
2) Results: Figure 3 shows the array response versus azimuth angles plot for MVDR and LCMV beamformers. The number of interferers considered was 16 and the transmit power for each interfering terminal was considered to be 30 dBm. From the figure, it can be observed that by considering the interfering range from 10° to 85°, we can create the array response about −50 dB to −110 dB down the desired response for MVDR beamformer and about −80 to −200 dB down the desired response for LCMV beamformer. Figure 4 shows the SINR versus azimuth angles plot of LCMV and MVDR beamformers for $M = 20$ and $K = 17$ in the considered simulation environment in which the random interfering users have been generated with uniform distribution and the interfering power at the BS from these terminals is different due to different DoAs and distances to the BS. From the figure, it can be observed that the LCMV beamformer provides similar SINR as that of MVDR beamformer towards the desired user and can provide very low SINR towards the interfering sector than the MVDR beamformer. From this result, it can be concluded that LCMV beamformer can reject the interference more effectively than MVDR beamformer in the considered scenario.

Table 1. Simulation & Link Budget Parameters

Parameter	**Value**
Satellite longitude	28.2^o E
Considered latitude range	35^o to 70^o
Considered longitude range	-10^o to 45^o
Elevation angle range [1]	7.07^o to 49.40^o
Carrier frequency	4 GHz
SAT terminal to BS link	
SAT Terminal Tx power	30 dBm
SAT Terminal Gain range	20 to -9.5047 dB
SAT Terminal EIRP range	50 to 21.50 dBm
Distance bet SAT terminal and BS	0.5 km to 10 km
Path loss range $\propto r^{-2}$	98.47 to 124.49 dB
BS antenna Gain	10 dB
Noise power @ 8 MHz	-104.96 dBm
INR range at BS	10.97 to 66.49 dB
Terrestrial terminal to BS link	
Terrestrial terminal Tx power	20 dBm
Terrestrial terminal antenna gain	10 dB
Distance bet desired terminal and BS	0.05 km to 5 km
Path loss range $\propto r^{-2}$	78.46 to 118.48 dB
BS antenna Gain	10 dB
Noise power @ 8 MHz	-104.96 dBm
SNR range for desired signal at BS	26.48 to 66.5 dB

Figure 5 shows the SINR versus number of interferers for $M = 18$ and $K = 17$. The SINR for both beamformers decreases as the number of interfering users increases in the considered interfering sector. From the figure, it can be noted that the LCMV beamformer shows better performance compared to MVDR for low number of interferers (< 9 in Fig. 5) and for higher number interferers, MVDR shows better performance than the LCMV beamformer. Figure 6 shows the SINR versus mismatch azimuth angles of the desired user for the considered scenario with $M = 18$ and $K = 17$. From the figure, it can be noted that up to 3° mismatch, MVDR beamformer's performance is slightly better than LCMV beamformer's performance. When the mismatch angle increases beyond the 3°, MVDR beamformer's SINR performance becomes worse than the that of LCMV beamformer.

3) Discussion: In our considered scenario, the DoA of the desired user and the range in which interferers are located is known while the exact locations of the interferers are unknown to the beamformer. Simulation results show that performance of both the beamformers is similar in the desired direction while the performance of the LCMV beamformer is much better in terms of rejecting the interference coming from the interfering sector. Mathematically, the LCMV beamformer places unit response constraint in the desired direction and zero response constraints in the interfering regions while the MVDR beamformer places only unit response constraint in the desired direction and tries to minimize total

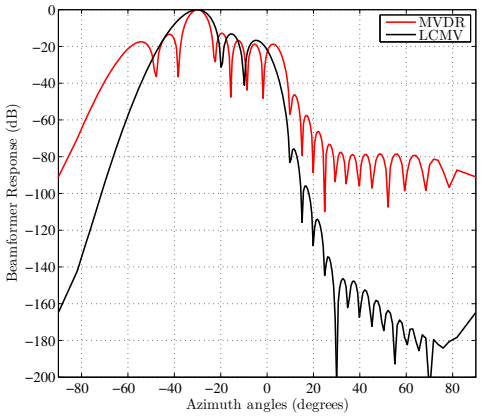

Fig. 3. Response versus azimuth angle for LCMV and MVDR beamformers, $M = 20$, $K = 17$

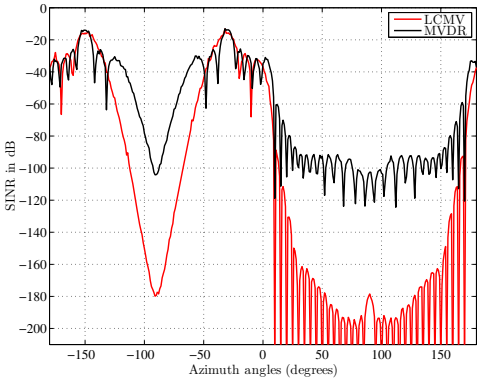

Fig. 4. SINR versus Azimuth angles plot of LCMV and MVDR beamformers for the considered scenario, M=20, K=17

interference plus noise. Furthermore, it has been noted from the results that even in case of uncertainty of exact locations of the interfering users, the LCMV beamformer is capable of creating low response towards the considered interfering region. In practical situations, exact DoA of the desired signal may deviate from the estimated one causing DoA mismatch of the desired signal. The response of the LCMV beamformer in case of angular mismatch can be maximized by placing multiple unit response directional constraints while the performance of MVDR beamformer becomes worse in this case. However, the performance of the LCMV beamformer becomes worse for a large number of interferers and it deteriorates rapidly when the number of antennas becomes less than the number of interferers while the performance of the MVDR beamformer is better than that of the LCMV in this condition. Therefore, the LCMV beamformer is suitable in terms of rejecting interference effectively for a small number of interferers and the MVDR beamformer is suitable for a large number of interferers.

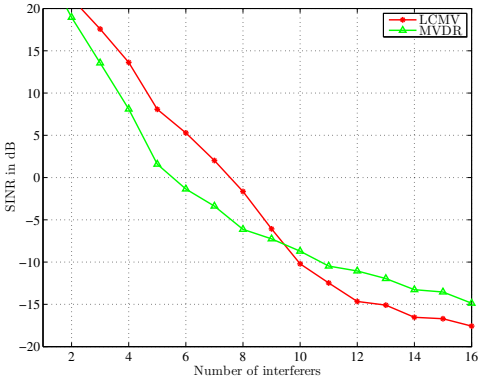

Fig. 5. SINR versus number of interferers for proposed scenario with beamformers designed for $M = 18$, $K = 17$

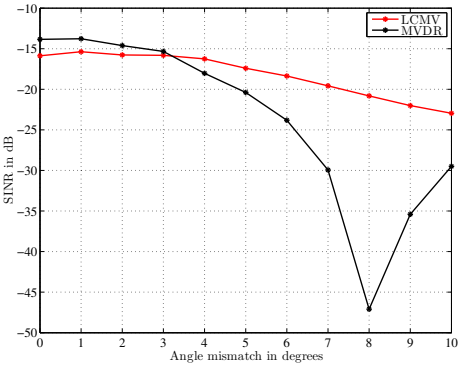

Fig. 6. SINR versus angular mismatch for the desired user

6 Conclusion

In this work, an underlay beamforming technique has been proposed for the spectral coexistence scenario of satellite and terrestrial networks. By using the priori knowledge about the interfering sector which arises due to special propagation characteristics of the satellite terminals, we have porposed a receive beamformer at the terrestrial BS to maximize the SINR towards the desired user and to mitigate the interference from the interfering satellite terminals. In this context, the performances of MVDR and LCMV beamformers have been compared. It has been shown that LCMV beamformer is better suited in terms of rejecting interference even in case of DoA uncertainty of the interfering signals as long as the sector in which interfering users are located is known to the beamformer. Furthermore, it can be concluded that the MVDR beamformer is better suited for a large number of interfering terminals. In our future work, we plan to investigate the robustness on the proposed methods as well as to apply other beamforming techniques for the proposed scenario.

Acknowledgement. This work was supported by the National Research Fund, Luxembourg under AFR (Aids Training-Research) grant for PhD project (Reference 3069102) under the CORE project "CO2SAT: Cooperative and Cognitive Architectures for Satellite Networks".

References

[1] Sharma, S.K., Chatzinotas, S., Ottersten, B.: Satellite cognitive communications: Interference modeling and techniques selection. In: 6th ASMS/SPSC Conf. (2012)
[2] Sarvanko, H., et al.: Exploiting spatial dimension in cognitive radios and networks. In: 6th Int. Conf. CROWNCOM, pp. 360–364 (2011)
[3] Xie, J., Fu, Z., Xian, H.: Spectrum sensing based on estimation of direction of arrival. In: Proc. ICCP, pp. 39–42 (2010)
[4] Lu, J., Lu, I.T.: Propagation based spectrum sensing: A novel beamforming detection method. In: 6th Int. Conf. CROWNCOM, pp. 11–15 (2011)
[5] Tsakalaki, E., et al.: Spectrum sensing using single-radio switched-beam antenna systems. In: 7th Int. Conf. CROWNCOM (2012)
[6] Van Veen, B., Buckley, K.: Beamforming: a versatile approach to spatial filtering. IEEE ASSP Magazine 5(2), 4–24 (1988)
[7] Yiu, S., Vu, M., Tarokh, V.: Interference and noise reduction by beamforming in cognitive networks. IEEE Trans. Commun. 57(10), 3144–3153 (2009)
[8] Luan, T., Gao, F., Zhang, X.D., Li, J., Lei, M.: Rate maximization and beamforming design for relay-aided multiuser cognitive networks. IEEE Trans. Veh. Technol. 61(4), 1940–1945 (2012)
[9] Cumanan, K., et al.: SINR balancing technique for downlink beamforming in cognitive radio networks. IEEE Signal Process. Lett. 17(2), 133–136 (2010)
[10] Sharma, S.K., Chatzinotas, S., Ottersten, B.: Exploiting polarization for spectrum sensing in cognitive SatComs. In: Proc. 7th Int. Conf. CROWNCOM (2012)
[11] Sharma, S.K., Chatzinotas, S., Ottersten, B.: Spectrum sensing in dual polarized fading channels for cognitive SatComs. In: Proc. IEEE Globecom Conf. (2012)
[12] Sharma, S.K., Chatzinotas, S., Ottersten, B.: Interference alignment for spectral coexistence of heterogeneous networks. EURASIP Journal on Wireless Communications and Networking 46 (2013)
[13] Sharma, S.K., Chatzinotas, S., Ottersten, B.: Transmit beamforming for spectral coexistence of satellite and terrestrial networks. In: Int. Conf. CROWNCOM (2013)
[14] Bryson: Northpoint Technology Ltd. v. MDS america. Inc. and MDS International S.A.R.L. (Fed. Cir. June 28, 2005), `http://caselaw.findlaw.com/us-federal-circuit/1369005.html`
[15] Katkovnik, V., et al.: Performance study of the minimax robust phased array for wireless communications. IEEE Trans. Commun. 54(4), 608–613 (2006)
[16] Wang, X., Poor, H.: Robust adaptive array for wireless communications. IEEE J. Sel. Areas Commun. 16(8), 1352–1366 (1998)
[17] Lorenz, R., Boyd, S.: Robust minimum variance beamforming. IEEE Trans. Signal Process. 53(5), 1684–1696 (2005)
[18] Santos, E., Zoltowski, M., Rangaswamy, M.: Indirect dominant mode rejection: A solution to low sample support beamforming. IEEE Trans. Signal Process. 55(7), 3283–3293 (2007)

Network Coding Advantage over MDS Codes for Multimedia Transmission via Erasure Satellite Channels

Paresh Saxena and M.A. Vázquez-Castro

Universitat Autònoma de Barcelona, Spain
{paresh.saxena,angeles.vazquez}@uab.es

Abstract. In this paper, we focus on the performance analysis of packet-level Forward Error Correction (FEC) codes based on Systematic Random Linear Network Coding (SRNC) for multimedia transmission via erasure satellite channels. A performance comparison is presented against maximum distance separable (MDS) codes currently used in state-of-the-art satellite transmission air interfaces, specifically Reed Solomon (RS) codes. Firstly, a theoretical analysis is presented for which we first develop a matricial erasure channel model. The theoretical analysis shows that both the RS and SRNC have, as expected, similar error correction performance over different packet erasure lengths for commonly used size fields. Secondly, we present an on-the-fly progressive algorithm for SRNC, which takes advantage of the inherent randomness of SRNC encoding. Thirdly, a performance comparison is presented for two different satellite scenarios: 1) DVB-S2/RCS railway scenario and 2) Broadband Global Area Network (BGAN) mobile scenario. We use real channel parameters for the first scenario and channel traces of video streaming sessions for the second scenario. Our simulation results confirm that both the RS codes and SNRC have the same packet recovery capabilities. However, for low coding rates, SRNC is shown to achieve up to 71% delay gain as compared to RS codes.

Keywords: Network Coding, Erasure Channel, Forward Error Correction, MDS codes.

1 Introduction

The demands for satellite services are growing for wide range of applications such as land-mobile, emergency, disaster relief, etc. However, the performance over the satellite systems is usually limited by the erasures caused by fading events, blockage, congestion due to transmission over best effort channels etc. To recover from the erasure events, satellite services specifications like Digital Video Broadcasting (DVB) [1] – [3] has adopted an link layer (LL) LL-FEC. In general, the requirements for FEC codes are MDS encoding if possible and low latency. However, due to the advancement in the FEC codes, it is important to investigate their performance for multimedia transmission via erasure satellite channels. In this work we leave out complexity issues and focus on performance.

R. Dhaou et al. (Eds.): PSATS 2013, LNICST 123, pp. 199–210, 2013.

In this work, we focus on the FEC based on SRNC [4] – [6] for multimedia transmission. SRNC provides proactive random retransmissions without the prior knowledge of lost packets over the network. The decoding can be done progressively at the receiver due to the inherent random structure of the code. Hence, the delay in the delivery time of recover packets can be substantially reduced.

The remainder of this paper is organized as follows. In Section 2, we introduce the system model. In Section 3, we present the theoretical performance analysis of the SRNC codes. Section 4 presents the numerical results and Section 5 concludes the paper.

Notations: Let $\mathbb{F}_q$ be a finite field. We denote $\mathbb{F}_q^{a_1 \times a_2}$ the set of all $a_1 \times a_2$ matrices with entries in $\mathbb{F}_q$, and $\mathbb{F}_q^{a_1}$ as the set of all column vectors with a_1 entries in $\mathbb{F}_q$. We will use boldface uppercase letters to denote matrices and boldface letters to denote column vectors. $\mathbf{I}_a$ is used to denote $a \times a$ identity matrix. We use the notation $\cup \mathbf{I}_a^{a \times a_1}$ to represent the set that contains a_1 distinct columns of identity matrix $\mathbf{I}_a$.

2 System Model

We consider a satellite scenario for the multimedia transmission where the sender transmits data packets via satellite. The receiver of interest could be a mobile receiver either within the satellite network or in a terrestrial network in the case of a hybrid architecture.

Let us assume that the time is slotted and source injects K source packets at time slot t. We assume that the source input can be modeled as an input unit $\mathbf{S}(t) \in \mathbb{F}_q^{M \times K}$ where each packet is a column vector of M symbols. We denote the encoding function by $\mathcal{E}_t : \mathbb{F}_q^{M \times K} \rightarrow \mathbb{F}_q^{M \times N}$, that maps the K source packets to N encoded packets. The coding rate is given by $R = K/N$.

These N encoded packets are represented by $\mathbf{X}(t) \in \mathbb{F}_q^{M \times N}$ where each encoded packet is a column vector of M symbols. These encoded packets are the function of source packets, given by $\mathbf{X}(t) = \mathcal{E}(\mathbf{S}(t))$. In our case, the encoding model is linear where $\mathbf{X}(t) = \mathcal{E}_t(\mathbf{S}(t)) = \mathbf{S}(t)\mathbf{G}(t)$ with generator matrix $\mathbf{G}(t) \in \mathbb{F}_q^{K \times N}$.

We consider an additive-multiplicative erasure-error channel model where the channel can 1) erase the transmitted packet or 2) introduce additive errors within the transmitted packet. Let us denote the channel function $\mathcal{H}_t : \mathbb{F}_q^{M \times N} \rightarrow \mathbb{F}_q^{M \times N_r(t)}$, that maps the N encoded packets to $N_r(t)$ received packets. We denote the received unit by the matrix $\mathbf{Y}(t) \in \mathbb{F}_q^{M \times N_r(t)}$ such that each received packet is a column vector of M symbols. In our case, the channel model is linear and we have,

$$\mathbf{Y}(t) = \mathcal{H}_t(\mathbf{X}(t)) = \mathbf{X}(t)\mathbf{H}(t) + \mathbf{Z}(t) = \mathbf{S}(t)\mathbf{G}(t)\mathbf{H}(t) + \mathbf{Z}(t) \tag{1}$$

with $\mathbf{H}(t) \in \cup \mathbf{I}_N^{N \times N_r(t)}$ and $\mathbf{Z}(t) \in \mathbb{F}_q^{M \times N_r(t)}$. The matrix $\mathbf{H}(t)$ is used to represent the erasure events, where $\mathbf{H}(t)$ consists of all the columns of $\mathbf{I}_N$ except

the columns $i \in \{1, 2, , ..., N\}$ if the i^{th} column/packet is erased by the channel and the matrix $\mathbf{Z}(t)$ represents the additive errors.

In this work, we will focus only on the erasure events such that with (1) we have,

$$\mathbf{Y}(t) = \mathbf{X}(t)\mathbf{H}(t) = \mathbf{S}(t)\mathbf{G}(t)\mathbf{H}(t) \tag{2}$$

We also denote $E(t) = N - N_r(t)$ as the total number of packets erased by the channel for the time slot t.

In particular, our matricial erasure channel model can be used for channel encoding for any packet-level erasure channel. Specifically, in this work, we compare the SRNC and the RS codes.

For, the RS codes, generator matrix is given by $\mathbf{G}^{RS}(t) = \left[\mathbf{I}_K | \mathbf{C}^{RS}(t)\right]$ where $\mathbf{C}^{RS}(t) \in \mathbb{F}_q^{K \times N-K}$. An explicit formula for the $\mathbf{C}^{RS}$ can be found in [7]. Using (2), with RS codes, we have,

$$\mathbf{Y}^{RS}(t) = \mathbf{X}^{RS}(t)\mathbf{H}(t) = \mathbf{S}(t)\mathbf{G}^{RS}(t)\mathbf{H}(t) \tag{3}$$

For, the SRNC, generator matrix is given by $\mathbf{G}^{SRNC}(t) = \left[\mathbf{I}_K | \mathbf{C}^{SRNC}(t)\right]$ where $\mathbf{C}^{SRNC}(t) \in \mathbb{F}_q^{K \times N-K}$ and each symbol of $\mathbf{C}^{SRNC}(t)$ is chosen independently and equiprobably from $\mathbb{F}_q$. Using (2), with SRNC, we have,

$$\mathbf{Y}^{SRNC}(t) = \mathbf{X}^{SRNC}(t)\mathbf{H}(t) = \mathbf{S}(t)\mathbf{G}^{SRNC}(t)\mathbf{H}(t) \tag{4}$$

Usually, each column of K symbols from $\mathbf{G}^{SRNC}(t)$, also known as coding coefficients, is attached with the corresponding column/packet of $\mathbf{X}^{SRNC}(t)$. These coding coefficients are used at the receiver for decoding [4]. This introduces an extra overhead of $K \log(q)$ bits, therefore several other approaches [8]-[9] have been proposed to reduce such kind of overhead. However, this particular aspect is out of the scope of the paper and hence, we assume that the coding coefficients are known at the receiving ends. At the receiver side, we denote $\hat{\mathbf{G}}^{SRNC}(t) \in \mathbb{F}_q^{K \times N_r(t)}$ as the matrix with columns as coding coefficients (locally retrieved) corresponding to the received packets.

3 Theoretical Performance Analysis

In this Section, we compare the SRNC and the RS codes based on their theoretical erasure correction performance. We also discuss the delay in the delivery time for both of these schemes. For the simplicity in showing our results, we drop the index t in this section.

3.1 RS: Probability of Successful Decoding (p^{RS})

RS codes are the class of MDS codes that operate on $GF(q)$. In particular, $RS(N, K)$ codes can correct up to $d_{MDS} - 1 = N - K$ erasures where d_{MDS} is the minimum distance of the RS codes. Let us denote the probability of successful

decoding of K source packets using RS codes by p^{RS}. Hence, if the number of packet erasures over the coding window of N packets are less than d_{MDS}; i.e., $E \leq d_{MDS} - 1$, then $p^{RS} = 1$ and if $E > d_{MDS}$, then $p^{RS} = 0$.

3.2 SRNC: Probability of Successful Decoding (p^{SRNC})

To evaluate the erasure correction performance of SRNC, let us first denote the probability of successful decoding of K source packets using $SRNC(N, K)$ codes by p^{SRNC}. Note that for the systematic coding, first K source packets are transmitted in the systematic phase and then $N-K$ encoded packets are transmitted in the non-systematic phase. To decode the K source packets successfully, the receiver should receive at least K independent packets out of N_r received packets, which means, that the rank of the locally retrieved coefficient matrix $\hat{\mathbf{G}}^{SRNC}(t)$ corresponding to the received packets should be K [4]. Therefore, to recover the K source packets successfully, following conditions should be satisfied:

1. L packets should be received from the first K transmissions of the systematic phase. The coding coefficients, corresponding to these L packets, are always independent as they belong to the columns of the identity matrix (4).
2. $J = N_r - L$ packets should be received from the next $N-K$ encoded packets of the non-systematic phase.
3. The coefficient matrix $\hat{\mathbf{G}}^{SRNC}$ of dimensions $K \times N_r$ should have full rank K given that L columns are independent.

Given these three conditions, we have

$$p^{SRNC} = \frac{1}{K} \sum_{L=1}^{K} p_{\hat{G}}(J, L, K) \tag{5}$$

where from [10] using urn model, we can obtain

$$p_{\hat{G}}(J, L, K) = \prod_{F=0}^{K-L-1} (1 - q^{F-J}) \tag{6}$$

where $p_{\hat{G}}(J, L, K)$ is the probability of condition 3 to be satisfied. In the Fig. 1-Fig. 3, we show the values of $1 - p^{SRNC}$ for different values of K, N and q. Firstly, these results show that the exact MDS like performance; i.e., the probability to correct exactly $d_{MDS} - 1 = N - K$ erasures is limited by the use of the field size. For example, for any combination of (N, K), we have $1 - p^{SRNC}$ equals to around 0.25, 10^{-2} and 10^{-3} for $q = 4$, $q = 64$ and $q = 256$ respectively. It shows that with the use of high finite field size, we can acheive very close to exact MDS like performance, for example, with $q = 256$ and $E = N - K$, we have $p^{SRNC} = 1 - 10^{-3}$ approaching to 1. Moreover, as the total number of erasures decreases, p^{SRNC} increases and $1 - p^{SRNC}$ decreases significantly. For e.g., in Fig. 3., for $RS(255, 127)$ and $SRNC(255, 127)$ codes, if there are $E = 61$ erasures in the coding window, RS will correct these erasures with $p^{RS} = 1$ $(N - K > E)$ and SRNC will correct these erasures with $p^{SRNC} = 1 - 10^{-10}$

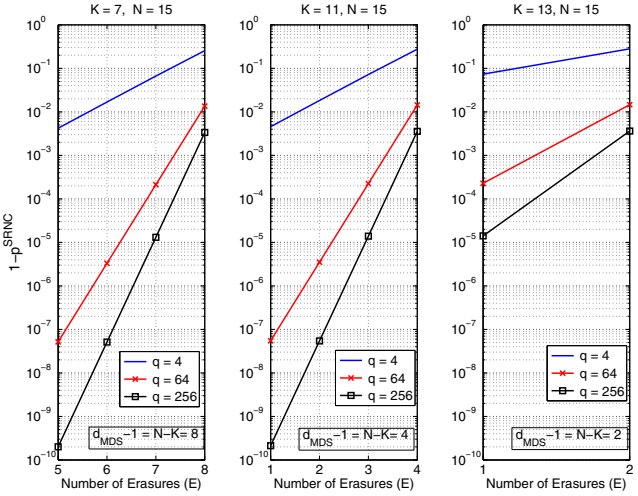

Fig. 1. $1 - p^{SRNC}$ for different K, E, q and $N = 15$

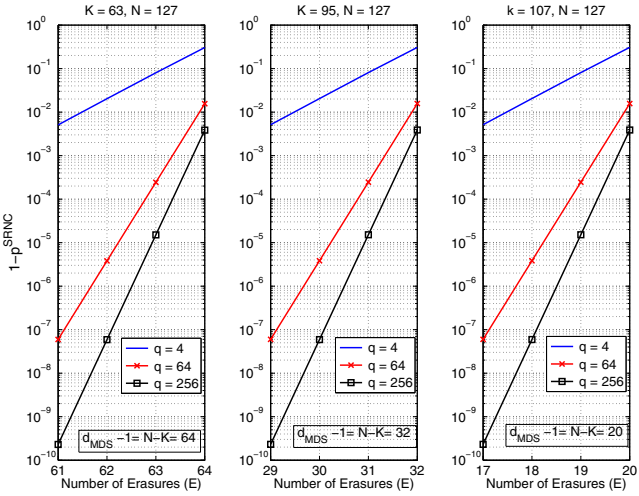

Fig. 2. $1 - p^{SRNC}$ for different K, E, q and $N = 127$

which is almost equal to 1. In fact, as the value of E decreases, the difference between p^{RS} and p^{SRNC} will approach to almost zero. So, we can conclude that both the RS and the SRNC have similar correction performance over the erasure channels.

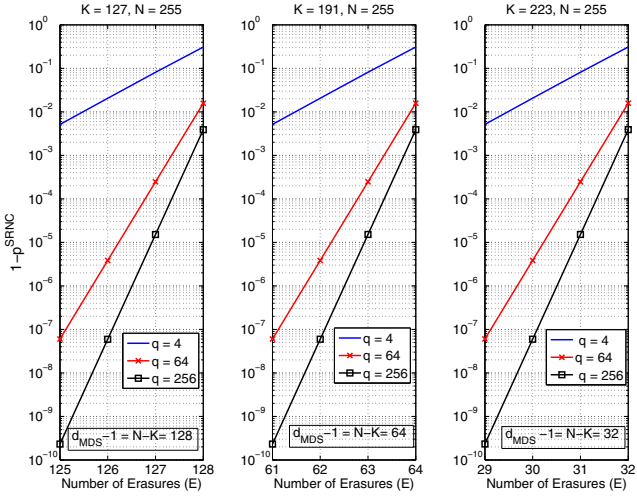

Fig. 3. $1 - p^{SRNC}$ for different K, E, q and $N = 255$

3.3 RS vs SRNC: Delay in the Delivery Time

Delivery time is the time that receiver has to spend until it is able to recover the packets. Note that transmission delay is assumed to be constant and same for both the schemes. Hence, in this work, we do not consider the transmission delay. For the RS systematic codes, first uncoded packets corresponding to systematic phase are transmitted and then the encoded packets are transmitted. The packets received by the receiver from the systematic phase are recovered without any delay. However, to recover the lost packets, receiver has to wait to receive all the unerased packets of the non-systematic phase. For $RS(N, K)$ with constant N, if coding rate R decreases which means when K decreases, delivery time increases due to the increase in size of the non-systematic phase $(N - K)$.

In SRNC, we perform decoding progressively using on-the-fly Gauss Jordan algorithm [11]. The decoding procedure is illustrated in Fig. 4. In the progressive decoding, receiver starts decoding as soon as it receives the first packet. Hence, it does not wait for all the packets to arrive. We show in the simulations that due to the progressive decoding, average delay in the delivery time for the packets obtained in the non-systematic phase is significantly reduced using SRNC.

4 Numerical Results

4.1 DVB-S2/RCS Railway Scenario

For the recovery from the erasure events, DVB has adopted an link layer (LL) LL-FEC. In particular, there can exist different frameworks for the LL-FEC mainly known as MPE-FEC, MPE-IFEC and extended MPE-FEC [12]. In this

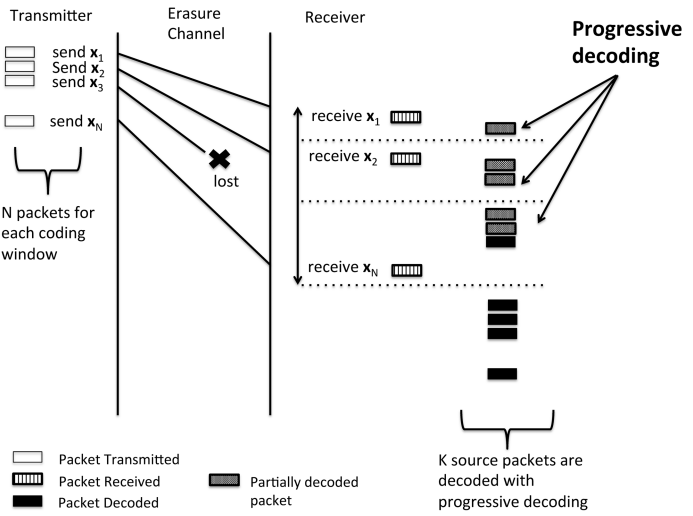

Fig. 4. Illustration of the progressive decoding over the erasure channel

work, we consider only the MPE-FEC framework. In particular, the size of the MPE-FEC frame is limited to 2 Mbits [13]. Following our system model, the encoded packets should form the columns of the MPE-FEC frame and each column of MPE-FEC frame should consists of M symbols. We keep field size $q = 256$ such that each symbol is equivalent to 1 byte. As the size of the MPE-FEC frame is limited to 2 Mbits, we have $N \times M \leq 2 \times 10^6$. With the packet size of $M = 1500 \times 8$ bits, we have the number of encoded packets limited to $N \leq 166$.

Now let us denote B_s as the physical layer symbol rate in baud/s, ς is the modulation constellation and r_{phy} is the physical coding rate where the bit rate is given by $B_s \varsigma r_{phy}$ bits/sec. For each packet we have $M = 1500 \times 8$ bits/packet, therefore we can define the packet rate as $B_p = \frac{B_s \varsigma r_{phy}}{M}$ packets/s. If more than $N - K$ packets are lost, then the decoding of K source packets is not possible. Hence, we are interested in the transmission time of $N - K$ packets, denoted as, $T_{N-K} = (N - K) \times \frac{1}{B_P}$.

Specifically, we analyze the performance over the railway scenario with line of sight, together with the effect of power arches. The presence of PAs in the railway environment can be modeled as a erasure channel where the packets are considered to be erased whenever there is a presence of PA. Let us denote l_{PA} as the width of the power arches (PA) and velocity of the train as v_{train}. During the time when the train passes through the PA, there is an erasure event. Let us denote this time as $T_{erasure} = l_{PA}/v_{train}$. We are able to obtain all the source K packets only when $T_{erasure} \leq T_{N-K}$.

In Fig. 5., we compare T_{N-K} and $T_{erasure}$ for different values of l_{PA} and v_{train}. Note that T_{N-K} does not have any dependency on l_{PA} and v_{train}. To vary T_{N-K} we consider two cases where $(N, K, R) = (166, 83, 0.5)$ and

$(N, K, R) = (166, 141, 0.85)$. We choose $N = 166$, as it is the maximum value availaible due to limited size of MPE-FEC frame. From [12], using $B_s = 27.5M\ bauds/s$, $\varsigma = 2$ and $r_{phy} = 1/2$, we get $T_{N-K} = .0362$ seconds for $(N, K, R) = (166, 83, 0.5)$ and $T_{N-K} = .012$ seconds for $(N, K, R) = (166, 141, 0.85)$.

From Fig. 5, we can see the MPE-FEC framework is only useful for $l_{PA} = 0.5$, when $l_{PA} \geq 0.5$, $T_{erasure}$ is always greater than T_{N-K}. This means that we will loose more than $N - K$ packets due to the PA and hence recovery of all the K source packets is not feasible. Therefore, we wil only focus for the case where $l_{PA} = 0.5$. For the cases where $l_{PA} \geq 0.5$, other frameworks should be followed, for which MDS-like performance of SRNC shall hold true as in the assessed framework. For the case $l_{PA} = 0.5$, $SRNC(166, 83)$ is sufficient to recover the source packets from the erasure events as from (5), p^{SRNC} approaches to 1.

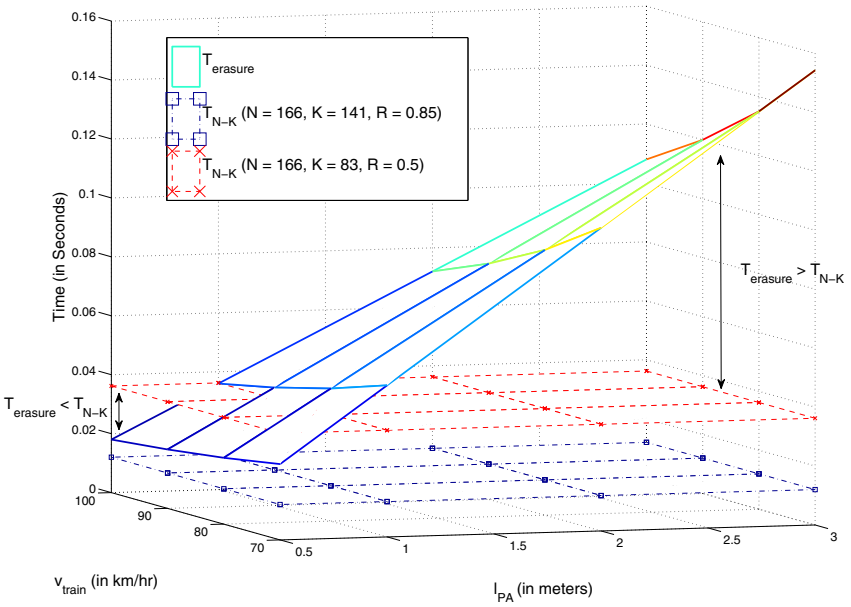

Fig. 5. 3-d mesh graph for comparison of $T_{erasure}$ and T_{N-K} over different values of l_{PA} and v_{train}

4.2 Broadband Global Area Network (BGAN) Mobile Scenario

For the second result, we consider real network traces over the BGAN mobile scenario. These traces are obtained from the video streaming sessions through a Inmarsat's Broadband Global Area Network (BGAN) mobile satellite network. The streaming session, which is over the best effort channel, suffers from the packet losses due to the network congestion. One way to control this congestion is by adapting the video codec rate [14]. However, adapting the video codec rate

requires the cross layer feedback. Moreover, diminishing the video codec rate, may cause the degradation in Quality-of-Service (QoE). Hence, in this work, without adapting the video rate, we use the channel coding to counter these packet losses due to the congestion.

In the video streaming session, source/uncoded packets are transmitted and traces are recorded. First, let us denote the total number of transmitted encoded packets by $n_{encoded}$. For the given code (N, K), the encoding is performed over $|t| = \lceil \frac{n_{encoded}}{N} \rceil$ coding windows. Therefore, total number of source packets transmitted are given by $n_{source} = |t| \times K$. At the receiver, after recovery, if the total number of source packets lost is n_{lost}, we have the total source packets lost in percentage given by $p_{lost} = \frac{n_{lost}}{n_{source}} \times 100$. Using these parameters, we compare SRNC and RS codes with different encoding parameters for the recorded channel traces.

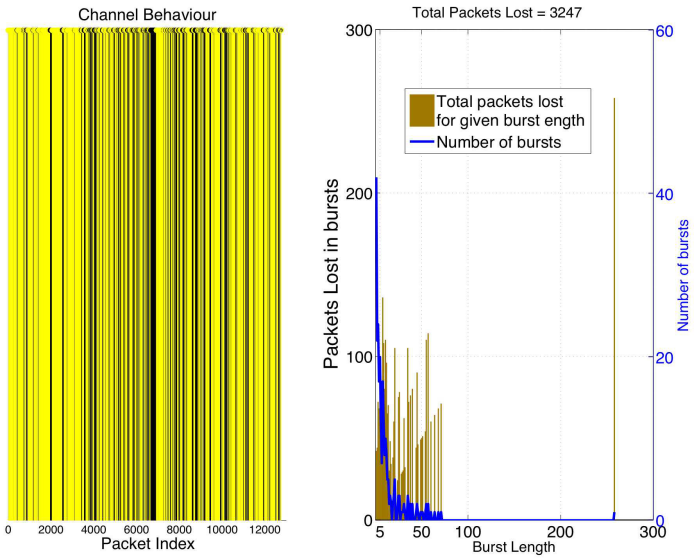

Fig. 6. Channel Traces: Channel behavior for the video transmission over the BGAN mobile satellite network. Lost packets are shown by black shades and received packets by yellow. In the left side, channel characteristics are shown with the number of bursty errors present in the channel.

The recorded channel traces is shown in Fig. 6. To obtain these traces, transmission is done without coding, and total $n_{encoded} = n_{source} = 12760$ source packets are transmitted where $n_{lost} = 3247$ source packets are lost such that $p_{lost} = 25.44\%$. In Fig. 6, channel behavior is shown where packets lost are represented by black shades and packets received by yellow corresponding to their packet index. In the right side of the figure, channel characteristic are shown in terms of burst lengths and the packets lost in those bursts. It is clear that the channel is bursty with different burst error lengths.

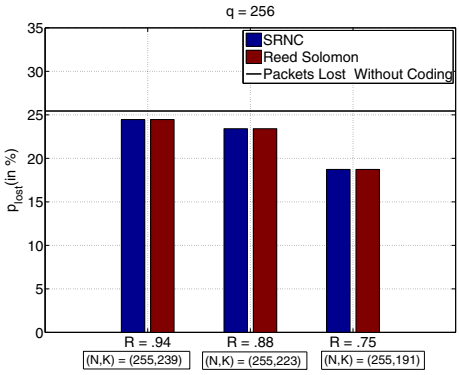

Fig. 7. Packets Lost for RS(N, K) and SRNC(N, K) for the traces shown in Fig. 6

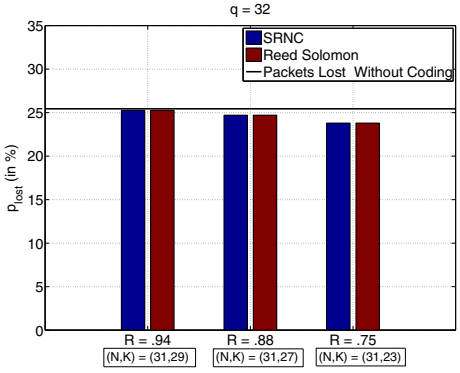

Fig. 8. Packets Lost for RS(N, K) and SRNC(N, K) for the traces shown in Fig. 6

As illustrated in Section 3, theoretically, RS codes and SRNC have similar erasure correction performance. This result is verified by simulations for recorded traces. Both $RS(N, K)$ and $SRNC(N, K)$ are compared with different values of K, N and q in Fig. 7. and Fig. 8. In all the cases, RS and SRNC are having the same erasure correction performance. In case of the RS codes, N is limited by $N < q$. This means that there is also an additional advantage while choosing SRNC because there is no limitation on N with respect to the field size for SRNC. However, in these simulations, to show the fair comparison we choose the same parameters for both the schemes. Due to the higher code length N, and higher redundancy $N - K$, p_{lost} decreases as the code length increases for the same coding rate R. Our results also illustrate that the field sizes ranging from $q = 256$ to $q = 32$ are sufficient for the SRNC, with the given channel traces, to give the same performance as the RS codes.

To illustrate the delay gain of SRNC, we consider delay in the per packet delivery time that receiver has to spend until is it able to recover the packet.

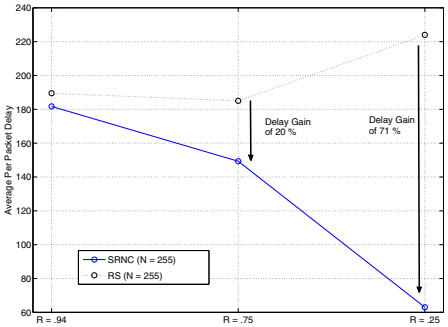

Fig. 9. Average per packet delay in the delivery time

As mentioned before, we are not considering delay due to the transmission time from the sender to the receiver as it should be constant and same for both the coding schemes. Note that the packets received from the systematic phase for both the schemes are recovered without any delay. Hence, we focus on the average per packet delay for the packets which are lost in the systematic phase and recover with the help of coded packets in the non-systematic phase. Fig. 9. shows the per packet delay performance for both the schemes. For the RS code, receiver has to wait for all the packets received from the non-systematic phase to recover the lost packets. In particular, for RS(N, K) with constant N, if code rate $R = K/N$ decreases, delivery time increases due to the increase in the size of the non-systematic phase. However, for SRNC, as progressive decoding is done, lost packets can be recovered progressively without waiting for rest of the packets. In fact, for the low coding gain, when the non-systematic phase is longer, the SRNC performs better as the average is done for all the packets recovered in the non-systematic phase. Specifically, as shown in the figure, up to 71% gain in the delivery time could be achieved with the use of SRNC coding.

5 Conclusions

In this work, we present the systematic random network coding for the multimedia transmission over the erasure satellite channels. We show the analytical analysis of the SRNC with the matricial erasure channel model. Theoretical expressions illustrate the similarity in the erasure correction performance of the SRNC and commonly used RS codes. We compare both these codes for the real traces obtained over the mobile satellite channel. Simulation results show that both the coding schemes have same packet recovery capabilities. Finally, we have illustrated the delay gain in the delivery time for the SRNC due to the early recovery of lost packets by progressive decoding.

References

[1] ETSI EN 301 709 V1.5.1; Digital Video Broadcasting (DVB); Interaction channel for satellite distribution systems; ETSI (2009)
[2] ETSI EN 302 307, Digital Video Broadcasting (DVB); Second Generation Framing Structure, Channel Coding and Modulation Systems for Broadcasting, Interactive Services, News Gathering and Other Broadband Satellite applications, ETSI European Standard, v.1.1 (March 2005)
[3] ETSI EN 301 790, Digital Video Broadcasting (DVB); Interaction Channel for Satellite Distribution Systems, ETSI European Standard, 2000, v. 1.3.1 (March 2003)
[4] Chou, P.A., Wu, Y., Jain, K.: Practical network coding. In: Proc. 2003 Allerton Conf. Communications, Control and Computing, pp. 40–49 (2003)
[5] Xiao, M., Aulin, T., Medard, M.: Systematic binary deterministic rateless codes. In: Proceedings IEEE ISIT, pp. 2066–2070 (2008)
[6] Lucani, D.E., Medard, M., Stojanovic, M.: Systematic network coding for time-division duplexing. In: Proc. of IEEE ISIT, pp. 2403–2407 (2010)
[7] Versfeld, D.J.J., Ridley, J.N., Ferreira, H.C., Helberg, A.S.J.: On Systematic Generator Matrices for Reed-Solomon Codes. IEEE Trans. Information Theory 56(6) (June 2010)
[8] Heide, J., Pedersen, M., Fitzek, F., Medard, M.: On code parameters and coding vector representation for practical RLNC. In: Proc. IEEE ICC, Kyoto, Japan, pp. 1–5 (June 2011)
[9] Chao, C.-C., Chou, C.-C., Wei, H.-Y.: Pseudo random network coding design for IEEE 802.16m enhanced multicast and broadcast service. In: Proc. IEEE VTC, Taipei, Taiwan, pp. 1–5 (May 2010)
[10] Trullols-Cruces, O., Barcelo-Ordinas, J., Fiore, M.: Exact decoding probability under random linear network coding. IEEE Commun. Lett. 15(1), 67–69 (2011)
[11] Meyer, C.D.: Matrix Analysis and Applied Linear Algebra. SIAM, PA (2001)
[12] Lei, J., Vazquez-Castro, M.A., Stockhammer, T., Vieira, F.: Link-Layer FEC and Cross-Layer Architecture for DVB-S2 Transmission With QoS in Railway Scenarios. IEEE Trans. on Vehicular Technology 58(8) (June 2009)
[13] ETSI EN 301 192 v1.4.1, Digital Video Broadcasting (DVB): DVB Specification for Data Broadcasting (November 2004)
[14] Pimentel-Niño, M.A., Vazquez-Castro, M.A., Skinnemoen, H.: Optimized AS-MIRA Advanced QoE Video Streaming for Mobile Satellite Communications Systems. In: 30th AIAA International Communications Satellite Systems Conference (2012)

Author Index